AIR VOID CLUSTERING IN CONCRETE

by

JAN VOSAHLIK

B.S., Czech Technical University in Prague, Czech Republic, 2012

A THESIS

submitted in partial fulfillment of the requirements for the degree

MASTER OF SCIENCE

Department of Civil Engineering
College of Engineering

KANSAS STATE UNIVERSITY
Manhattan, Kansas

2014

Approved by:

Major Professor
Kyle A. Riding

Abstract

Air void clustering around coarse aggregate in concrete has been identified as a potential source of low strengths in concrete mixes by several Departments of Transportation around the country. Research was carried out to (1) develop a quantitative measure of air void clustering around aggregates, (2) investigate whether air void clustering can be reproduced in a laboratory environment, (3) determine if air void clustering can blamed for lower compressive strengths in concrete mixes, (4) and identify potential factors that may cause clustering.

Five types of coarse aggregate and five different air entraining agents were included in the laboratory study to see if aggregate type or chemical composition of air entraining agent directly relates to air void clustering. A total of 65 mixes were made, implementing the frequently used technique of retempering that has been previously associated with air void clustering around aggregates. Compressive strength specimens as well as samples for hardened void analysis were made. Compressive strength at 7 and 28 days was determined and the automated hardened void analysis (including a new method of clustering evaluation) was performed on all samples.

It was found that it is possible to reproduce air void clustering in laboratory conditions. However, the results have shown that retempering does not always cause air void clustering. It was also observed that air void clustering is not responsible for a decrease in compressive strength of retempered concrete as neither aggregate type nor chemical composition of air entraining agent had a significant impact on severity of void clustering around coarse aggregate particles. It was also found that the total air content and an inhomogeneous microstructure and not air void clustering were responsible for lower strengths.

Table of Contents

List of Figures

List of Tables

Acknowledgements

I would like to thank to Dr. Kyle Riding for the opportunity to work on this project and his guidance through it as well as to Dr. Asad Esmaeily for his encouragement to pursue the master's degree at Kansas State University and his help on the software development. I also would like to acknowledge the Kansas Department of Transportation for research funding provided for the study through its K-TRAN program.

I surely appreciate all the help provided by undergraduate and graduate students who collaborated on various tasks performed in this project. Without their support I would not have been able to complete this research. Big thank you belongs to Ryan Benteman, K-State Department of Civil Engineering Research Technologist, for his help with laboratory equipment and tools.

Finally, I would like to thank to my parents Jana and Radek for always supporting me during my studies and encouraging me to pursue my dreams.

Chapter 1 - Introduction

1.1 Research Background

Discovery of air entrainment was arguably one of the most significant milestones in the history of the concrete industry. In use since the 1930s, small air voids allow concrete structures and pavements to reduce the impact of aggressive environments, especially in cold climates. Since 1970s, concerns have arisen regarding air void clustering around coarse aggregate particles. Clusters of entrained air bubbles were observed primarily during the summer construction season (May – August) in retempered mixes or mixes that use a non-organic air entraining admixture. Air void clustering has been blamed for low compressive strengths in pavement concrete (Cross, Duke, Kellar, & Johnston, 2000; Distlehorst, 2009).

1.2 Scope of Research

From July 2013 to July 2014 a laboratory study was conducted in the Department of Civil Engineering at Kansas State University, Manhattan, Kansas, to answer questions related to air void clustering. Extensive testing was conducted in order to answer the following questions:

(1) Is air void clustering reproducible under laboratory conditions using materials frequently utilized on pavement construction projects in Kansas?

(2) What effect does concrete mix retempering have on air void clustering?

(3) Is air void clustering directly associated with loss of compressive strength in retempered concrete?

(4) How does the chemical composition of air entraining agents (AEA) affect air void clustering?

(5) How does the aggregate type affect air void clustering?

(6) What is the effect of aggregate cleanness on air void clustering?

Chapter 2 - Literature Review

2.1 Air Entrainment

Similar to other breakthroughs in the concrete industry (such a reinforced concrete), air entrained concrete was discovered accidently. In the mid-1930s, a beef tallow was used as a grinding aid in cement production in New York State (Torrans & Ivey, 1968). Concrete made from this cement showed significantly improved resistance to freezing and thawing when exposed to water. Subsequent research attributed improved freeze-thaw performance to the incorporation of a fine air void system in the cement paste.

Currently, air-entrained concrete is required in cold climates or environments that include freezing water (Kosmatka, Kerkhoff, & Panarese, 2003). However, entrained air voids are not the only air bubbles found in concrete. T. C. Powers and his colleagues (1953), pioneers in the research of air-entrained concrete, defined three groups of voids in concrete:

Gel pores. These are the smallest pores that can be found in cement paste (0.5 nm – 10 nm) and water in these pores usually does not freeze. Gel pores represent approximately 28% of the total volume of hydration products (Pigeon & Pleau, 1995).

Capillary pores. The size of these pores varies from 50nm to 10 μm (Pigeon & Pleau, 1995). Capillary pores fill spaces between cement grains and hydration products originally occupied by water. Gel and capillary pores are randomly distributed over the concrete mass, separated with cement hydration products so water can move through pores with changes in ambient conditions.

Air entrained voids. These voids are larger by order of magnitude than the gel or capillary pores. Entrained air voids size typically ranges between 10 to 1000 microns (Kosmatka, Kerkhoff, & Panarese, 2003; Walker, Lane, & Paul, 2006). Air bubbles, defined as entrained air voids, are "artificially" stabilized in concrete by adding air entraining admixtures (AEAs) to the concrete mix.

In addition to these three main groups of pores, two other types of air voids can be found in hardened concrete: entrapped voids (pores formed by air with radii bigger than 1000 micrometers) and water voids (irregularly shaped air voids primarily formed by water). These two void types weaken the concrete instead of offering benefits (Walker, Lane, & Paul, 2006).

2.2 Freeze-Thaw Resistance

A quality air void system in hardened concrete significantly improves its frost resistance. Several theories explaining the principle how air entrained concrete improve frost durability have been developed. The first theory adopted the basic explanation of water behavior under freezing conditions, i.e., expansion of water volume when transforming from liquid to solid phase. Unfortunately, this theory did not account for the micro scale of concrete air system, thereby neglecting some important factors (such as void size, capillary effects or air void distribution in cement paste). Consequently, Powers (1949) introduced his hydraulic pressure theory. According to this theory, when water presented in capillary pores freezes and saturates the pores, remaining water forced from the pores must move to available free spaces in the cement paste: air voids. Hydraulic pressure drives this motion, thereby obeying water flow rules of Darcy's law. When distance to the next available pore is too long or the freezing rate is too fast, hydraulic pressure within the cement paste may exceed available tensile strength, causing tensile crack formation in the paste. This theory was the first to provide a mathematical relationship between paste properties, freezing rate, and air void spacing (Pigeon & Pleau, 1995).

Power's original theory, however, was found to be inconsistent with experimental data, so a modified theory known as the osmotic pressure theory was introduced (Powers & Helmuth, 1953). This theory accounts for the effect of dissolved alkalis in water in pores. Because these ions are present in the solution and the capillary pores are very small (50nm to 10 μm), the freezing point of water in these pores is lower than 32°F (0°C). During freezing, the concentration of dissolved chemicals in water increases, freezing stops, and the moment of water's melting point (reduced due to alkali presence) becomes equal to the ambient temperature. In other words, equilibrium between the ice and water solution is reached at that temperature. Considering the effect of pore size on freezing temperature (the lower the pore size, the lower the freezing temperature of water in the pore), the balanced temperature level is lower in smaller pores and, therefore, equilibrium is not preserved. Thus, water from smaller pores (including gel pores) moves to larger pores in order to reestablish a balanced state; this motion creates internal pressure that may cause cracking in the cement paste. If a sufficient air void system is created in concrete, ice formed in these voids more readily attracts water than capillary pores and protects the paste from damage.

Litvan (1973) elaborates on the assumption that water cannot freeze inside capillary pores due to changes in vapor pressure, and states that water must travel through the paste to the external surface in order to freeze. Therefore, if it requires longer period of time for water to travel from an air void to the external surface than to freeze in the pore, internal pressure can cause damage.

One of the newest theories (Chatterji, 2003) questions many assumptions made by previous explanations and adds several factors that have not been considered previously, such as the effect of chemical composition of the air entraining agent used. However, despite the large number of hypotheses explaining air void action in concrete during a freeze-thaw event, a comprehensive theory clarifying the entire phenomena is still lacking.

2.3 Air-Void System Characterization

Spacing factor and total air void content are the two parameters used to describe the air-void system. Spacing factor was developed by Powers as part of his hydraulic pressure theory (Powers & Willis, 1949). Two formulas, each developed using a specific idealized system, calculate the spacing factor. The first formula, given by Eq. (2-1), is valid for values of p/A smaller than 4.342, while the second formula, defined by Eq. (2-2), is valid for values of p/A greater or equal to 4.342 (Garboczi, et al., 2014).

$$L = \frac{p}{\alpha A} \tag{2-1}$$

$$L = \frac{3}{\alpha}\left[1.4\left(\frac{p}{A} + 1\right)^{\frac{1}{3}} - 1\right] \tag{2-2}$$

Where:

	L	spacing factor,
	p	paste volume,
	A	air void volume,
	α	specific surface area of voids.

The first idealized system (small values of p/A ratio) is composed of air voids uniformly covered with a thick layer of paste; the layer thickness (or shell) is the spacing factor. The second system utilizes the cubic lattice approach in which mono-sized air voids are distributed in the space at vertices of a cubic array, each with a specific surface area equal to the bulk value. Lattice spacing is chosen in such a way that air content equals bulk. The spacing factor then represents the distance from the center of a unit cell to the nearest air void surface (Garboczi, et al., 2014; Peterson, 2008).

Freeze-thaw resistance clearly increases with lower spacing factors. Typically, spacing factor of 200 microns (0.008 in) and specific surface of 25 mm^2/ mm^3 (600 sq. in. per cubic inch) are considered acceptable values for freeze-thaw resistant air entrained concrete (Pigeon & Pleau, 1995). In order to calculate spacing factor, analysis of hardened concrete sample must be conducted. For air volume, 5-8% air content by volume of concrete is typically required for freeze-thaw durable concrete design (Chatterji, 2003; Chatterji, 2003; Kansas Department of Transportation, 2007). Air content in concrete can be determined on a fresh concrete sample or hardened concrete sample (ASTM C457, 2012) by utilizing one of the Pressure Method (ASTM C231, 2010), Volumetric Method (ASTM C173, 2014), or Gravimetric Method (ASTM C138, 2012).

Fresh concrete air content, possibly the most common air void characteristic utilized daily in field applications, is often used as a prompt indicator of air system quality. However, total air content is not always the most accurate parameter of freeze-thaw resistance because research has shown that total volume of air void and other parameters, such as uniform distribution of air voids in the cement matrix, are equally important factor in freeze-thaw resistant concrete (Whiting & Nagi, 1998).

2.4 Mechanism of Air Entrainment

To achieve required air entrainment in concrete, AEAs are added to concrete mix. Chemicals which can be utilized as AEAs are often byproducts of various chemical industries. Pigeon & Pleau (1995) classified AEAs into four groups:

1) sodium salts of wood resin
2) salts of fatty acids
3) salts of sulphonated hydrocarbon
4) alkyl-benzyl sulphonates

Classification system provided by Kosmatka et al. (2003) (adapted from Naranjo, 2007) is shown in Table 2-1.

Table 2-1: Air Entraining Agents

Classification	Performance Characteristics
Wood resin and rosin	Quick air generation. Minor air gain with initial mixing. Air loss with prolonged mixing. Mid-size air bubbles formed. Compatible with most other admixtures.
Tall oil	Slower air generation. Air may increase with prolonged mixing. Smallest air bubbles of all agents. Compatible with most other admixtures
Synthetic detergents	Quick air generation. Minor air loss with mixing. Coarser bubbles. May be incompatible with some high range water reducing admixtures. Also applicable to cellular concretes.
Vegetable oil acids	Slower air generation than wood rosins. Moderate air loss with mixing. Coarser air bubbles relative to wood rosin. Compatible with most other admixtures.

Note. Adapted from Clustering of Air Voids Around Aggregates in Air Entrained Concrete, p. 7, by A. Naranjo, 2007, Austin: UT at Austin.

Every AEA is a mixture of surfactants (substances reducing fluid surface tension) that must be soluble in water. Most modern AEAs are anionic, although cationic, nonionic, or amphoteric agents can also be used (Du & Folliard, 2005).

The process of air generation in concrete is complex, but two partial sub-processes can be easily distinguished: air bubble formation and air bubble stabilization. Two primary processes to generate air voids in concrete have been proposed (Ramachandran, 1997):

(1) Folding of air by a vortex action (similar action to stirring a liquid),

(2) Three-dimensional screen formed by fine aggregates when mass falls and cascades onto itself during mixing.

Concrete mixing is a living process in which air bubbles come into existence and simultaneously vanish unless stabilized. Three fundamental mechanisms may lead to the collapse of air bubbles (Du & Folliard, 2005):

(1) Diffusion of air from a small bubble (high internal pressure) to a larger one (lower internal pressure)

(2) Bubble coalescence due to capillary flow, leading to rupture of lamellar film between adjacent bubbles (typically slower than Mechanism 1, occurring even in stabilized systems). This mechanism often occurs in fresh concrete due to vibration.

(3) Rapid hydrodynamic drainage of liquid between bubbles, leading to rapid collapse. This mechanism is not likely to occur in fresh concrete because air bubbles are immersed in fresh concrete.

AEA molecules are responsible for various tasks during the mixing process, as symbolically introduced in Eq. (2-3) and described as follows (Du & Folliard, 2005):

(1) Because AEA molecules are typically composed of a hydrophilic head on one end and hydrophobic tail (usually negatively charged) on the other end, portion of AEA dosage is absorbed or adsorbed by solid surfaces of cement particles, primarily due to electric attraction to hydrophobic tail of surfactant.

(2) Another portion of AEA molecules dissolved in the bulk liquid phase has a primary purpose to reduce surface tension of water (Pigeon & Pleau, 1995). Surface tension acts as an energy barrier against the stabilization of air bubbles; therefore, the surface tension reduction is necessary. Reduction allows for breakdown of large voids into smaller voids.

(3) Once generated, air voids must be stabilized in the cement matrix. AEA concentrates at the liquid/air interfaces and forms elastic film around air bubbles, thereby protecting bubbles against collapse.

$$A = A_s + A_l + A_b \tag{2-3}$$

Where:

A	AEA dosage
A_s	portion of AEA adsorbed or absorbed on solid surfaces
A_l	portion of AEA in the bulk liquid phase
A_b	portion of AEA in the liquid/air interface

2.5 Factors Affecting Air Entrainment in Concrete

Many factors affect AEA performance, the air entrainment process, and the quality of air void system in concrete. Development of the air system is a complex process that has been studied for decades and is still not fully understood.

2.5.1 Cement

As the fineness of cement particles increases, the total surface area required to react with AEA increases. Therefore, the amount of available surfactants in the system is reduced (as shown in Eq. (2-3)) and, consequently, the level of air entrainment is reduced (Kosmatka, Kerkhoff, & Panarese, 2003). A low-alkali cement may require 20% - 40% more AEA dosage than a high-alkali cement in order to achieve equivalent air content because air content typically increases as cement alkali level increases (Pomeroy, 1989; Whiting & Nagi, 1998).

2.5.2 Supplementary Cementitious Materials

In general, increased AEA dosage is required to achieve targeted air content when any supplementary cementitious material (SCM) is used due to its finesses and increased surface area of particles absorbing AEA molecules (Kosmatka, Kerkhoff, & Panarese, 2003).

2.5.3 Admixtures

Research has shown that use of additional concrete admixtures to AEA, such as water reducers, retarders, or super-plasticizers, can improve air entrainment and increase total air content. However, increased spacing factor has been associated with usage of specific types of admixtures (Kosmatka, Kerkhoff, & Panarese, 2003).

2.5.4 Aggregate

If the amount of fine aggregates increases, the total amount of air content typically decreases because sand particles provide reduced shear action due to their smaller size compared to particles that are of larger size (Du & Folliard, 2005). However, aggregate particles with sizes ranging from 0.0234 in to 0.0059 in (sieves #30 and #100, respectively) help with the persistence of small air bubbles. In addition, the aggregate manufacturing process (natural or crushed) is important as well as crushed rock provides increased shear action, thereby generates smaller air bubbles and higher air content than natural rock (Du & Folliard, 2005).

2.5.5 Water

Air content increases with higher water-to-cement (w/c) ratio (Kosmatka, Kerkhoff, & Panarese, 2003). Research has shown that increasing w/c from 0.4 to 0.8 leads to an approximate 3% increase of air content (Whiting & Nagi, 1998).

Mixing water quality can also significantly impact the quality of air entraining systems; in order to reduce mix cost, some contractors reuse mixing water (i.e., wash water from mixing trucks). This reuse can result in decreased air content and decreased air void system quality. In addition, hard water can decrease air content (Kosmatka, Kerkhoff, & Panarese, 2003; Whiting & Nagi, 1998).

2.5.6 Concrete Workability and Slump

Yield stress of fresh concrete is closely related to slump: An increase in slump reduces yield stress. As discussed, internal stress and viscosity acts as an energy barrier to air void creation. Therefore, increased slump results in an increase of the total amount of air voids in the system, and vice versa (Du & Folliard, 2005). Whiting and Nagi (1998) suggested that slump increase of 1 in leads to approximately 0.5% increase in air content.

2.5.7 Mixing Procedures

The order of added materials also significantly affects the total amount of air content. Simultaneous batching provides less air content than batching of cement prior to adding AEA (Whiting & Nagi, 1998). Highest air content is typically achieved when maximum mixer capacity is used since small loads in the mixer cause less stirring and larger blade impact. However, exceeding allowable mixer capacity causes air content loss (Whiting & Nagi, 1998; Kosmatka, Kerkhoff, & Panarese, 2003).

Short mixing periods can also reduce air content; the minimal recommended mixing time is 75 seconds. If truck mixers are used, air content rises during the first 15 minutes of mixing (Whiting & Nagi, 1998). Optimal mixing speed is approximately 20 rotations per minute (rpm). At higher mixing speeds, air content may decrease due to stronger impact of the mixing blades (Kosmatka, Kerkhoff, & Panarese, 2003).

Other properties of the mixing system, such as mixing system age, total power of the mixer, and blade quality, strongly influence efficiency of the air void system generation (Du & Folliard, 2005).

2.5.8 Transport, Construction Techniques, and Field Conditions

Usually 1% - 2% of air content loss can be contributed to transport. Mixes with high air content (above 6%) experience even greater loss of air while being transported from the ready-mix plant to the construction site (Whiting & Nagi, 1998). Use of belt conveyors reduces air content by an average of 1%, and loss in air due to pumping is approximately 2% - 3% (Kosmatka, Kerkhoff, & Panarese, 2003).

Over-vibration can cause damage to the air void system. If excessive finishing is used, air content in the surface layer can decrease (Whiting & Nagi, 1998).

Retempering (i.e., withholding mixing water in the plant and adding it on site) is a common practice used by contractors to meet prescribed performance specification (typically slump or air void content). Outside temperatures can rise high above 90 °F during the summer construction season (May to August in the USA), typically leading to loss of concrete workability and decreased air content. Research has shown that the loss of workability is primarily caused by evaporation, absorption of water by aggregates, or hydration during transportation (Naranjo, 2007). To prevent this workability loss, concrete suppliers sometimes withhold portion of the mixing water and add that water back to the mix prior to placing (and sampling) the mix. Retempering is thought to have no effect on spacing factor (Kosmatka, Kerkhoff, & Panarese, 2003). AEAs are occasionally used in addition to water while retempering, despite the fact that higher dosages of AEA may be needed for jobsite admixture additions (Whiting & Nagi, 1998). The suggestion has been made (Kozikowski, David, Peter, & Steven, 2005; Naranjo, 2007; Walker, Lane, & Paul, 2006) that retempering can also affect air void clustering and subsequently compressive strength; this issue is discussed later in this review.

In general, higher temperatures result in lower air void content. Du and Folliard (2005) offered the following explanations:

(1) Higher temperature leads higher viscosity of the entire system. Higher viscosity requires more energy to form air voids; therefore, the total amount of generated air in the mix is reduced.

(2) Polyvalent cations, such as Ca2+, Al3+, react with AEAs containing alkali salts or wood rosin and form insoluble salts that help stabilize entrained air. Rising temperatures cause these salts to coagulate and precipitate; therefore, the foaming ability of AEA is reduced. In addition, significant amounts of electrolytes in the solution reduce air bubble stability by reducing repulsion acting between layers formed around air bubble surfaces.

(3) Higher ambient temperatures accelerate the cement hydration process; therefore, more solid surfaces areas in the solution are generated. These surfaces absorb or adsorb part of the surfactant dosage, thereby reducing the amount of available surfactants in the system. Therefore, the amount of created air content is also reduced, as demonstrated in Eq. (2-3).

(4) Increased temperature decreases the amount of air that is able to solute in water. Vaporing air joins existing air bubbles and they together form larger air bubbles. These large bubbles are susceptible to destruction during the mixing process. Therefore, under high temperature conditions, the amount of entrained air content is lowered and larger air bubbles are formed.

2.6 Effects of Air Entrainment on Concrete Properties

Air entrainment in concrete positively and negatively affects concrete properties. In addition to improved freeze-thaw resistance, air entrainment in concrete increases slump and subsequent workability because small air bubbles in concrete act as a lubricant and reduce friction between cement particles and aggregate. Research has shown that an increased air content of 0.5% - 1% can increase slump by approximately 1 in (Whiting & Nagi, 1998). Concrete with entrained air also demonstrates improved resistance to bleeding and segregation, and less vibration time is required to consolidate air entrained concrete (Kosmatka, Kerkhoff, & Panarese, 2003).

Compressive strength of air entrained concrete is typically expected to be less than strength of corresponding concrete (with identical w/c ratio) without air. For low w/c ratios, loss in strength is typically higher compared to concretes higher w/c values. Loss in compressive strength ranges from 2% - 6% for every percent increase in air content. Similarly, flexural strength decreases by 2% - 4% for every percent of air in concrete (Whiting & Nagi, 1998).

2.7 Air Void Clustering In Entrained Concrete

Air void clustering around coarse aggregate particles in air entrained concrete and related loss in concrete compressive strength has recently been identified in the concrete industry community but not fully investigated. Clustering was observed in pavement projects and reported by Departments of Transportation (DOTs) in Delaware, Michigan, New Jersey, Virginia, and South Dakota (Cross, Duke, Kellar, & Johnston, 2000), as well as by the Kansas Department of Transportation (KDOT) (Distlehorst, 2009).

An extensive examination of air void clustering was conducted by the South Dakota Department of Transportation (SSDOT) (Cross, Duke, Kellar, & Johnston, 2000). During the summer construction season of 1997, SDDOT experienced unusual failing of concrete cylinders in compressive strength tests. Detailed investigation was performed and investigators concluded that low compressive strength could be attributed to a weak bond between cement paste and aggregate particles and could be associated with formation of air void clusters around those particles. Air void clustering was observed in mixes that utilized synthetic AEA. Foam tests of AEA showed difference in foaming performance of synthetic AEAs and vinsol (non-synthetic) resin agents. Results proved that synthetic AEAs drain faster than natural admixtures, resulting in thinner bubble walls and low quality cement paste on aggregate surfaces. Researchers hypothesized these factors led to lowered compressive strength of concrete cylinders (Cross, Duke, Kellar, & Johnston, 2000).

KDOT has reported similar issues with the compressive strength of concrete cylinders in pavement concrete on a new pavement project on US Highway 56 in Meade, Kan. Some of the cylinders that were sampled in 2006 and 2007 failed to meet the required minimum strength of 20 MPa (2900 psi) at 28 days. Further investigation showed that failed samples had higher air content (in average 14.4%) than cylinders that passed the strength requirement (average air content 8.5%). Air void clustering in all tested samples was quantified using the method developed by Kozikowski et al. (2005). Failed cylinders experienced higher clustering index than samples that did not fail. However, compressive strength loss caused directly by air void clustering has not been proven (Distlehorst, 2009).

An extensive research study regarding clustering was carried out in 2004 in Portland Cement Association laboratories (Kozikowski, David, Peter, & Steven, 2005). A wide range of variables was investigated and several conclusions were made:

(1) Similar to (Cross, Duke, Kellar, & Johnston, 2000), no air void clustering was observed in concrete mixes in which vinsol (organic) resin admixtures were used.

(2) It was reported that clustering likely occurs in concrete mixes with late addition of water (i.e., retempering), especially when synthetic agents are used.

(3) Total mixing time of retempered concrete was found to be another significant factor affecting clustering rate; severity of air-void clustering increased with increased mixing time.

(4) Aggregate shape/mineralogy may also significantly impact strength loss due to clustering.

A rating system was developed to describe the extent of air void clustering. Each coarse aggregate greater than 6 mm was assigned to one of four categories, depending on the visual rating of clustering (no clustering, minor clustering, moderate clustering, and severe clustering). Then the number of aggregates in the category was multiplied by the category number (0-3) and totals from each category were averaged over the number of examined particles. Results indicated that for ratings greater than 1.0 air void clustering may negatively affect compressive strength of concrete although experimental data did not provide strong evidence for ratings ranging from 1.0 to 1.5.

Both previously discussed research programs (SSDOT and PCA) independently concluded that use of synthetic AEAs may lead to increased rate of air void clustering and air void clustering could possibly reduce compressive strength of concrete.

However, a recent research project in this field (Naranjo, 2007) questioned the influence of air void clustering on concrete strength reduction. Laboratory experiments and field concrete tests were conducted; reduction in concrete strength discovered in laboratory tests was attributed to increased air content due to retempering. Clusters of air void were also observed in field concrete tests, but due to lack of data, whether or not a correlation existed between clustering and concrete strength was impossible to establish. Nevertheless, similar to projects discussed, results indicated that late addition of water in concrete significantly impacts rate of air void clustering.

Since lower compressive strength was initially reported during the construction summer season, it is possible that temperature may be a key factor to clustering issues. To the authors' knowledge, no research has been conducted considering temperature effects.

Chapter 3 - Materials

3.1 Cementitious Materials

ASTM C150 Type I cement, obtained from a local construction materials supplier and produced by the Monarch Cement Company in Humbolt, Kan., was used. Due to the complexity of laboratory testing, three loads of cement were received: June 2013 (Cement A), March 2014 (Cement B), and May 2014 (Cement C). Once received, cement was removed from original packaging and stored in sealed, 55-galon plastic barrels under room temperature conditions (72°F). Cement composition was analyzed by X-ray fluorescence by KDOT Material and Research Center in July 2014, and results are presented in Table 3-1. Analysis showed that the samples had very similar composition. Table 3-2 shows adjusted potential phase composition calculated according to ASTM C150.

Table 3-1: Cement Chemical Composition - XRF

Component	Cement A	Cement B	Cement C
SiO_2 (%)	21.9	21.4	21.2
Al_2O_3 (%)	4.2	4.3	4.3
Fe_2O_3 (%)	3.3	3.4	3.4
CaO (%)	63.7	63.6	63.5
MgO (%)	1.8	2.1	2.2
SO_3 (%)	2.6	2.6	2.6
Loss on Ignition (%)	1.09	1.40	1.38
Na_2O (%)	0.15	0.14	0.14
K_2O (%)	0.50	0.47	0.47
Insoluble Residue (%)	0.10	0.08	0.06

Table 3-2: Compound Calculations – ASTM C150

Component	Cement I	Cement II	Cement III
Al_2O_3 / Fe_2O_3	1.3	1.3	1.3
C3S	52.5	55.8	56.3
C23	22.9	19.2	18.3
C3A	5.5	5.5	5.5
$C_3S + C_3A$	58.0	61.3	61.8
Total Alkali as Na_2O_{eq}	0.48	0.45	0.45

3.2 Aggregate

Four types of coarse aggregate identified as frequently used on Kansas projects by KDOT and listed on their prequalified material list (Kansas Department of Transportation, 2014), were used in this study: (1) Lincoln Quartzite (APAC – Shears, Lincoln, Kan.), (2) Granite (Martin Marietta Materials Raleigh, N.D.), (3) Limestone (Bayer Construction, Manhattan, Kan.), and (4) South Dakota Quartzite (L.G. Everist, Sioux Falls, S.D.). Concerns arose regarding the performance of unwashed Lincoln Quartzite because KDOT had experienced unexpected behavior of this material. Therefore, laboratory testing was performed on mixes containing washed and non-washed Lincoln Quartzite. To determine gradation, specific gravity, and water absorption, each aggregate was sampled and tested in KSU laboratories following procedures specified in ASTM C127 and ASTM C136. Aggregate gradation curves are shown in Figure 3-1 and other properties are summarized in Table 3-3.

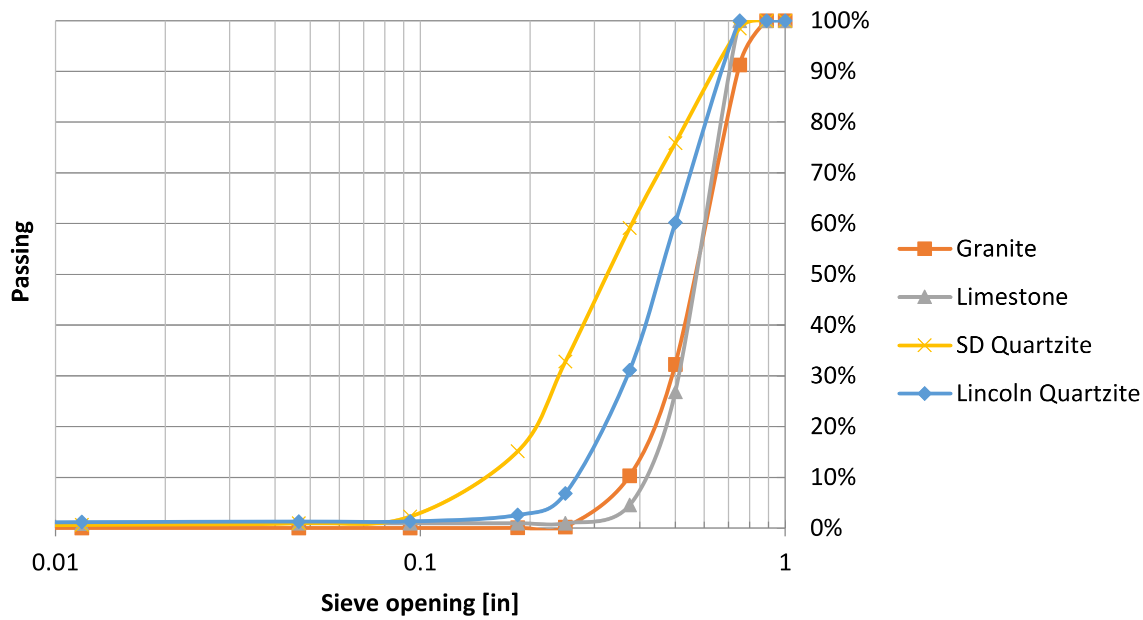

Figure 3-1: Aggregate Gradation

Table 3-3: Coarse Aggregate Properties

Component	Granite	Limestone	SD Quartzite	Lincoln Quartzite
Bulk Specific Gravity	2.69	2.54	2.63	2.60
Bulk Specific Gravity (SSD)	2.69	2.60	2.64	2.63
Apparent Specific Gravity	2.70	2.70	2.65	2.68
Water Absorption (%)	1.10	2.30	0.27	1.25

Local sand (Midwest Concrete Materials, Manhattan, Kan.) which met ASTM C33 FA and KDOT FA-A specifications was used in all mixes as fine aggregate. Sand was sampled and tested following ASTM C136 and ASTM C128 procedures. Gradation curve is presented in Figure 3-2 and other material properties are shown in Table 3-4.

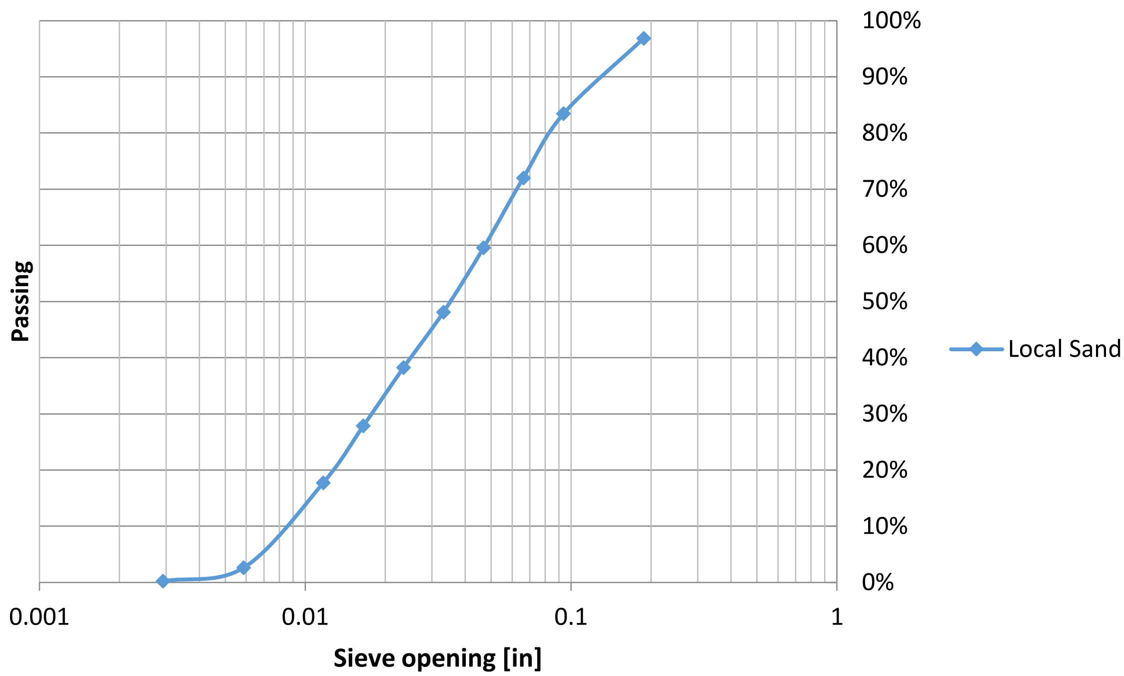

Figure 3-2: Fine Aggregate Gradation

Table 3-4: Fine Aggregate Properties

Component	Sand
Bulk Specific Gravity	2.65
Bulk Specific Gravity (SSD)	2.67
Apparent Specific Gravity	2.67
Water Absorption (%)	0.70

3.3 Air Entraining Admixtures

In July 2013, an email survey was conducted among KDOT districts to determine AEAs used on public projects in Kansas. Consequently, five AEAs were selected for use in this laboratory study. However, in addition to frequent occurrence of the admixture in KDOT projects being a factor for agent selection, the chemical nature of a given admixture was also considered, with the objective to encompass a wide range of AEAs in terms of chemical composition. Using classification of AEAs developed by Whiting & Nagi (1998), selected AEAs are presented in Table 3-5.

Table 3-5: Air Entraining Agents

Classification	Chemical description	Selected AEA	Manufacturer
Vinsol® resin	Alkali or alkanolamine salt of a mixture of tricyclic acids, phenolics, and terpenes	Daravair M	WR Grace
Wood rosin	Alkali or alkanolamine salt of tricyclic acids – major components	Daravair 1000	WR Grace
Tall oil	Alkali or alkanolamine salt of fatty acids - major component	Darex II	WR Grace
Vegetable oil acids	Coconut fatty acids, alkanolamine salt	Polychem SA-50	General Resource Technology
Synthetic detergents	Alkyl-aryl sulfonates and sulfates	AEA-92S	Euclid Chemicals

3.4 Testing Matrix

Five AEAs and four coarse aggregates were chosen to be used in the study. Based on selected materials, a testing matrix was established which contained a total of 50 mixes (25 mixes with no retempering and 25 retempered mixes) and 15 control mixes. Control mixes were mixes with identical w/c ratios as retempered mixes and were included in the matrix to investigate the effect retempering may have on clustering and compressive strength.

In order to maintain organization of the testing process, a labeling system was developed and implemented. Each sample used in the study was labeled following a two or three letter mask (e.g., 2-V, 2-V-R, or 2-V-C). The Arabic numeral refers to aggregate used in a given mix while the Roman numeral represents the AEA, as shown in Table 3-6. A letter "R" that occurs at the end of a label indicates that the mixture was retempered, and a letter "C" indicates a control mix. Therefore, 2-V-R stands for retempred mix with washed Lincoln Quartzite and Darex II.

Table 3-6: Labeling System

Aggregate	**Denotation**	**Admixture**	**Denotation**
Non-washed Lincoln Quartzite	1	Daravair 1000	I
Washed Lincoln Quartzite	2	AEA-92s	II
Granite	3	Daravair M	III
Limestone	4	Polychem SA-50	IV
SD Quartzite	5	Darex II	V

The complete testing matrix is presented in

Table 3-7 and Table 3-8.

Table 3-7: Testing Matrix

Mix ID		AEA Type	Coarse Aggregate
1	I	Daravair 1000	Lincoln Quartzite - Non-Washed
1	II	AEA-92s	Lincoln Quartzite - Non-Washed
1	III	Daravair M	Lincoln Quartzite - Non-Washed
1	IV	Polychem SA-50	Lincoln Quartzite - Non-Washed
1	V	Darex II	Lincoln Quartzite - Non-Washed
2	I	Daravair 1000	Lincoln Quartzite - Washed
2	II	AEA-92s	Lincoln Quartzite - Washed
2	III	Daravair M	Lincoln Quartzite - Washed
2	IV	Polychem SA-50	Lincoln Quartzite - Washed
2	V	Darex II	Lincoln Quartzite - Washed
3	I	Daravair 1000	Granite
3	II	AEA-92s	Granite
3	III	Daravair M	Granite
3	IV	Polychem SA-50	Granite
3	V	Darex II	Granite
4	I	Daravair 1000	Limestone
4	II	AEA-92s	Limestone
4	III	Daravair M	Limestone
4	IV	Polychem SA-50	Limestone
4	V	Darex II	Limestone
5	I	Daravair 1000	SD Quartzite
5	II	AEA-92s	SD Quartzite
5	III	Daravair M	SD Quartzite
5	IV	Polychem SA-50	SD Quartzite
5	V	Darex II	SD Quartzite

Table 3-8: Testing Matrix – Control Mixes

Mix ID		AEA Type	Coarse Aggregate
1	I-C	Daravair 1000	Lincoln Quartzite - Non-Washed
1	II-C	AEA-92s	Lincoln Quartzite - Non-Washed
1	III-C	Daravair M	Lincoln Quartzite - Non-Washed
1	IV-C	Polychem SA-50	Lincoln Quartzite - Non-Washed
1	V-C	Darex II	Lincoln Quartzite - Non-Washed
2	I-C	Daravair 1000	Lincoln Quartzite - Washed
2	II-C	AEA-92s	Lincoln Quartzite - Washed
2	III-C	Daravair M	Lincoln Quartzite - Washed
2	IV-C	Polychem SA-50	Lincoln Quartzite - Washed
2	V-C	Darex II	Lincoln Quartzite - Washed
3	I-C	Daravair 1000	Granite
3	II-C	AEA-92s	Granite
3	III-C	Daravair M	Granite
3	IV-C	Polychem SA-50	Granite
3	V-C	Darex II	Granite

3.5 Mix Design

Two mix designs that varied in w/c ratios were adopted in this study. Batches with Lincoln Quartzite were initially mixed utilizing w/c ratio of 0.40 and later retempered to increase the w/c to 0.43. All other mixtures had w/c of 0.43 which increased to 0.45 after late water addition. The target air content for all mixes before retempering was 6.5% ± 1.5% in accordance with current KDOT requirements (Kansas Department of Transportation, 2007). The target slump range was 1 - 3 in. Mixes before retempering are referred to as “original” in this report, while mixture after water addition is referred to as “retempered.”

To investigate the effect of air void clustering and retempering on compressive strength, an additional 15 mixtures with w/c of retempered mixes (0.43 and 0.45) were mixed. Their target air content corresponded to air content of retempered mixes (with 0.5% tolerance). Those mixes are referred to as “control” mixes.

All mixes contained 580 lbs of cement per cubic yard and 65:35 ratio of coarse to fine aggregate. The total weight of aggregates in each mix was adjusted to account for specific gravities of each type of coarse aggregate. The dosage of AEAs also varied among mixes; the required dosage of a given AEA (i.e. the dosage that resulted in 6.5% ± 1% of air fresh air content) for each mix was determined by trial-and-error. In general, approximately 0.5 to 1.5 fl oz per 100 lbs of cement was required to achieve targeted air content. Mix designs are presented in Table 3-9 and dosages of AEA used are presented in Table 3-10.

Table 3-9: Mix Designs

Aggregate / Concrete Component	Lincoln Quartzite	Granite	Limestone	SD Quartzite
Cement (lbs/yd³)	580	580	580	580
Coarse Aggregate (lbs/yd³)	1951	2008	1939	1961
Fine Aggregate (lbs/yd³)	1078	1068	1068	1068
Water (lbs/yd³)	249	244	244	244
Original w/c	0.40	0.42	0.42	0.42
Retempered w/c	0.43	0.45	0.45	0.45

Table 3-10: AEA Dosages (fl oz per 100 lbs of cement)

Aggregate / AEA	Non-Washed Lincoln Quartzite	Washed Lincoln Quartzite	Granite	Limestone	SD Quartzite
Daravair 1000	1.2	1.0	1.1	2.8	1.0
AEA 92s	0.9	0.9	0.9	1.1	0.8
Daravair M	0.9	0.8	0.6	1.4	0.9
Polychem SA-50	1.2	1.1	1.0	1.2	1.0
Darex II	0.9	0.9	1.1	1.8	1.1

Chapter 4 - Laboratory Study

4.1 Mixing Procedure

Valid ASTM standards for making and testing concrete in laboratory were followed for this study: C138 (2012), C143 (2012), C172 (2010), C192 (2013), and C213 (2010).

Prior to mixing, all materials were moved into the mixing laboratory to ensure they were at room temperature (72 °F) at the moment of mixing. In addition, all aggregates were placed in the oven (200 °F) and dried to constant mass before placing in the mixing laboratory to cool to room temperature. This procedure allowed identification of the volume of water that had to be added to the w/c ratio-calculated mixing water due to aggregates' absorption capability.

A Lancaster shear mixer (Figure 4-1) was used to perform mixing. With its maximum capacity of 2 cubic ft, the volume of all regular mixes was designed to be 1.8 ft^3, while the control mixes were 1.05 ft^3 (1.05 ft^3 corresponds to the volume of concrete left in the mixer after the Phase 1 of mixing).

Figure 4-1: Lancaster Shear Mixer

A simplified version of the procedure described by Naranjo (2007) was used in this study. The procedure consisted of two mixing phases, as illustrated in Figure 4-2.

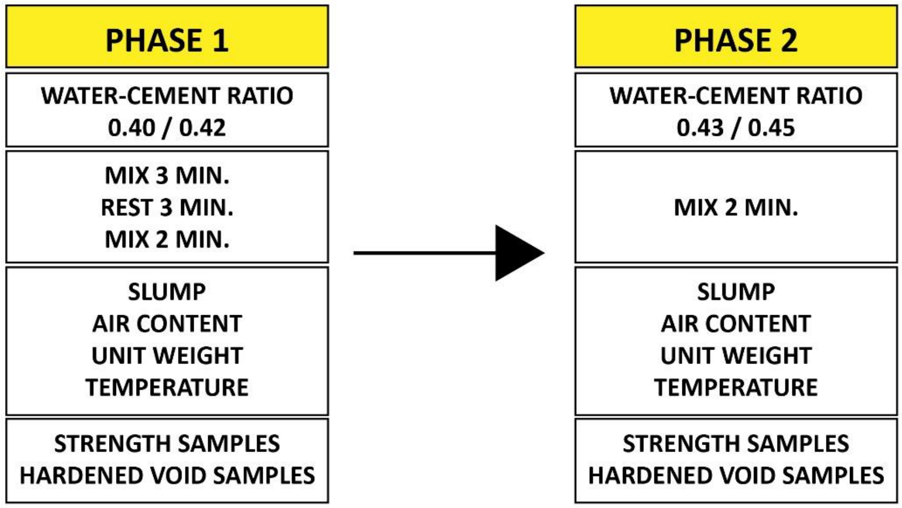

Figure 4-2: Mixing Procedure

Phase 1 - Fine and coarse aggregate were placed in the mixing pan with approximately half of the mixing water containing added dispersed AEA. Aggregates with water and AEA were then mixed until blended and then cement and the remainder of the mixing water was added to the mix. As prescribed by current standards (ASTM C192, 2013), the concrete was mixed for 3 minutes, followed by a 3-minute resting period, followed by an additional 2 minutes of mixing. After mixing was complete, 105 lbs of concrete were removed from the mixing pan while the remaining concrete was covered with plastic wrap to prevent moisture loss. The removed concrete was then used to measure slump, fresh air content, unit weight, and temperature. Once all required tests were performed, six 4 x 8 in cylinders and two food boxes were cast in order to obtain specimens for future testing: cylinders for compressive strength (three strength at 7 days, three for 28-day strength) and two Chinese food boxes for hardened void analysis.

Phase 2 - The second phase typically occurred 30-45 minutes after the initial stage once all test were completed and specimens cast. At the beginning of this stage, additional water was added to the mix, the mixer was turned on, and the concrete was mixed for another 2 minutes. Tests similar to the first stage were then run and six 4 x 8 in cylinders and two food boxes were cast again. The second stage was typically completed within 20-30 minutes from initiation.

Control mixes were mixed following only the Phase 1 procedure (with corresponding w/c ratios – 0.43 or 0.45).

Casted samples were labeled and left undisturbed in the laboratory. After an initial 24-hour period, compressive strength specimens were unmolded and moved to a room with constant temperature of 72 °F and relative humidity of 99% (“fog room”). Hardened void samples were removed from paper molds, labeled, and stored on shelves in the cement laboratory at K-State. (Figure 4-3).

Figure 4-3: Stored Hardened Void Samples

4.2 Material Testing and Evaluation Methods

4.2.1 Fresh Concrete Properties Testing

Slump, air content, unit weight, and temperature were four fresh concrete properties measured for each mix. Provisions of ASTM C 138 (2012) and ASTM C 143 (2012) standards were obeyed. Because a two-stage mixing procedure was adopted for most mixtures in this study, concrete properties were always determined for both the original and retempered mix. Standard testing equipment which met the requirements of both ASTM C 138 (2012) and ASTM C 143 (2012) was used, including Oakton Templog thermometer (Serial Number 502399).

4.2.2 Compressive Strength

ASTM C39 (2012), ASTM C192 (2013), and ASTM C1231 (2014) were followed to perform all tasks associated with concrete compressive strength testing. Standard 4x8-in plastic molds (Deslauriers Inc) were used to make concrete specimens. Cylinders were covered with plastic lids immediately after they were formed and left undisturbed in the laboratory under constant temperature (72 °F) for the first 24 hours. Cylinders were then removed from plastic molds using compressed air, labeled, and stored in the curing room (73 °F, 50% relative humidity).

Specimens were tested for compressive strength at 7 and 28 days after casting. Steel retaining cups, rubber compression pads, and Forney compression machine were utilized for the testing. Test setup is shown in Figure 4-4. Each tested set of cylinders was composed of three samples, and total compressive strength was calculated as an average of obtained values.

Figure 4-4: Compressive Strength Setup

4.2.3 Air Void Analysis of Hardened Concrete

Samples for air void analysis of hardened concrete were cast into paper boxes typically used as food containers (Figure 4-5). Compared to rounded cylinders typically used for hardened void analysis, cutting and other operations with specimens were easier and more convenient when rectangular molds were used. A total of four specimens were made for each mix from the main testing matrix: two with original concrete mix, two with retempered mix, and two food boxes were cast for each control mix.

Once cast, samples were left undisturbed for a 24-hour period and then removed from paper molds, labeled, and stored. Since air void structure is formed during the mixing period and does not change after concrete sets, samples were not stored under any specific conditions.

An automatic method of air void system investigation using a flatbed scanner was implemented to carry out analysis of all hardened concrete samples. The method introduced by Peterson (2008) was implemented with several modifications to adjust its usability. Analysis was carried out following subsequent steps.

Figure 4-5: Hardened Air Void Analysis Mold

4.3 Cutting of Specimens

Samples were cut using a Covington Engineering concrete saw shown in Figure 4-6 (a). Upon completion of the cutting process, concrete slices of uniform thickness, approximately 1 in, were prepared (Figure 4-6 (b)). Once cut, all samples were washed using water and compressed air to remove all cutting residues.

(a) (b)

Figure 4-6: (a) Cutting Setup, (b) Cut Sample

4.4 Surface Polishing

A horizontal polishing table (ASW Diamond SW-1800), equipped with diamond nickel-plated disks (ASW Diamond NT-80, NT-100) and flexible resin processing disks (ASW Diamond PP360, PP600), was used to polish all samples. Disks are shown in Figure 4-7. The polishing table presented in Figure 4-8 was adjusted with a custom-made mounting setup (including two Fischer Scientific DynaMix electric motors), allowing four samples to be polished simultaneously and ensuring that expected polished surface quality was achieved. Polishing procedure was derived from procedure developed by Ley (2007).

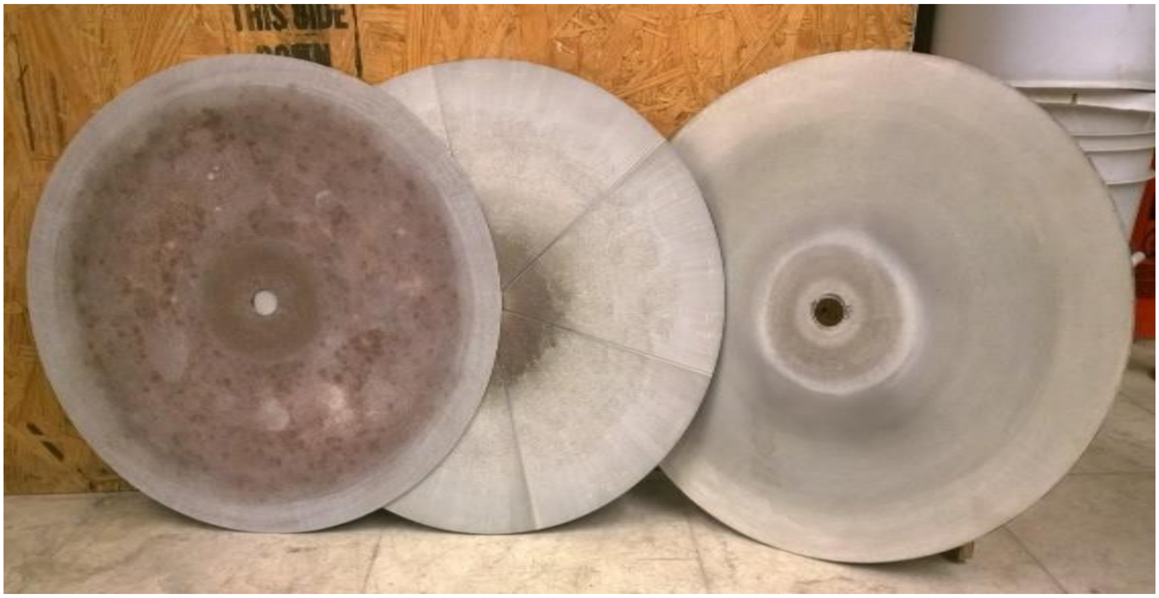

Figure 4-7: Polishing Disks

Figure 4-8: Polishing Setup

Cut and washed samples were attached to plastic cylinders (5.5 in diameter, 2 in height) using a hot glue gun. Cylinders were designed to hold samples on the lapping wheel. Once the glue dried, a 60:40 solution of acetone and clear lacquer was applied to the sample surface to stabilize the cement paste during polishing. The surface was allowed to dry. Water with a small amount of dish soap (approximately 0.15 fl oz per 5 gallons) was used to lubricate samples and disks during polishing; the amount of water applied to the disk depended on its fineness and was determined by the operator.

Samples were first polished using the nickel-plated disk with 80 grid, followed by the disk 100 grit. The primary purpose of the two disks was to completely flatten the sample; flatness was ensured by (a) drawing an orthogonal grid with construction crayon to determine whether the sample was polished uniformly, (b) performing a flatness check using a machinist rule (Figure 4-9).

(a) (b)

Figure 4-9: (a) Orthogonal Grid, (b) Machinist Rule Flatness Check

As soon as all specimens passed the flatness check, brown and red polymer disks with 1200 and 2200 mesh, respectively, were mounted on the polishing table. The brown disk was responsible for removing all scratches produced on the sample during previous processing while the red disk was used to complete the entire polishing procedure. Every time the polishing disk was changed, samples were cleaned with water to remove the polishing residues left on the sample. Once all samples were polished to shine like a sheet of glass, they were removed from the plastic cylinders, thoroughly cleaned with water, and dried. Specimens were then placed in plastic bags to protect from further scratching and stored in a desiccator to prevent surface carbonation.

4.5 Scanning

Immediately prior to scanning, specimens were submerged in an acetone bath for 3-5 minutes to remove lacquer from all voids if present. Samples were then dried using a hairdryer.

Scanning was carried out by EPSON Perfection V600 Photo scanner and controlled by default scanning software provided with the scanner – Epson Scan (Ver. 3.83US). Resolution of 4800 dpi with 24-bit color settings was used, and all software image adjustments, with the exception of the unsharp mask option, were disabled (Figure 4-10). The area of picture scanned was always larger than the minimum area required for conventional hardened air void analysis (ASTM C457, 2012).

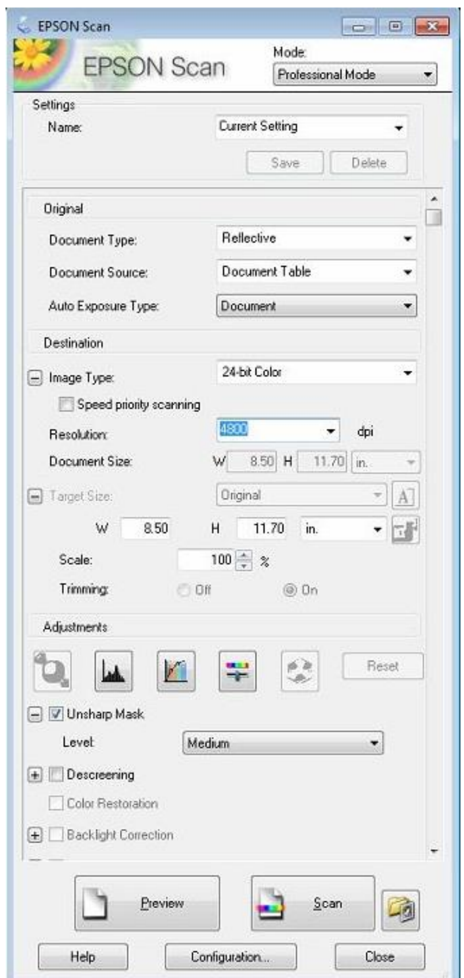

Figure 4-10: Scanner Settings

First, a dried sample was scanned (referred to as Image 1). In order to assist with future image alignment, the sample was placed on the scanning table and aligned to the bottom-right corner using glued thin glass slides, as shown in Figure 4-11. Second, the specimen was sprayed with a solution (1:1) of a 90%-phenolphthalein in alcohol and distilled water in order to color cement paste. Phenolphthalein works as a pH indicator. As long as the pH level of paste exceeded 11 (ensured by keeping the sample in vacuum before scanning), the color changed to purple-pink. Only a thin layer of solution was applied to eliminate excessive amounts of fluid coloring aggregate particles. The sample was dried using a hairdryer, pores were cleaned with compressed air to remove excess solution from air voids.

Finally, an orange powder (Strait-Line Marking Chalk) was used to fill all air voids in the investigated sample. The powder was uniformly distributed over the sample surface using a microscope slide and then pressed into pores by a rubber stopper. This process was repeated two times to ensure all voids were completely filled. A steel razorblade was used to remove excess powder from the sample and, if needed, the surface was dusted with a lightly-oiled fingertip covered by a laboratory glove. The specimen was then rescanned (referred to as Image 2). All scanned images are shown in Figure 4-12.

Figure 4-11: Scanning Setup

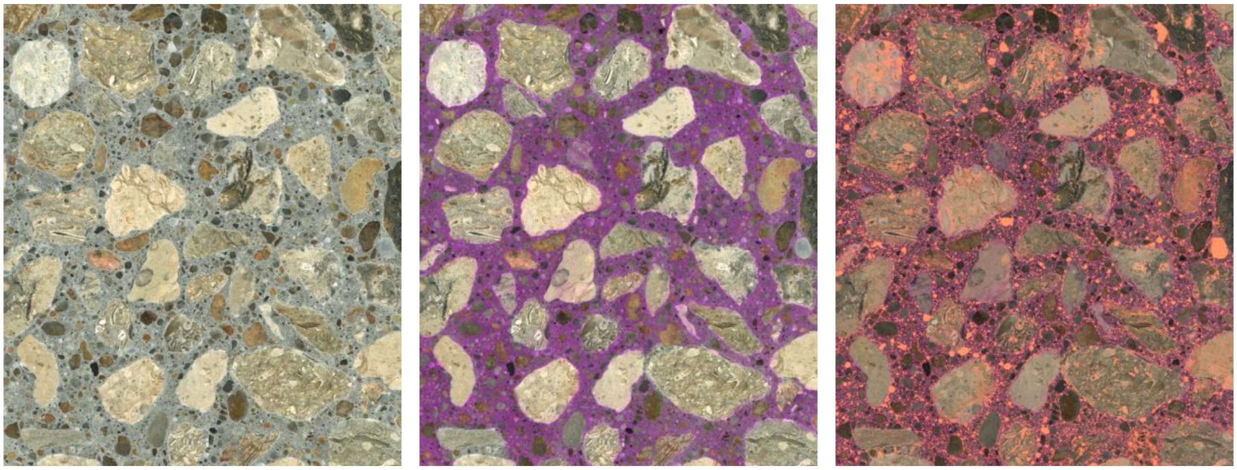

(a) (b) (c)

Figure 4-12: (a) Image 1 – No Surface Treatment, (b) Phenolphthalein-Stained Surface, (c) Image 2 – Orange Powder Pressed into Air Voids

4.6 Raw Image Alignment

All three images had to be aligned with respect to each other in order to conduct the entire analysis. As mentioned, every time the sample was scanned, it was always placed on the exact same location on the scanning table. However, since the resolution was 4800 dpi (i.e., 1 pixel is approximately 5 microns), a slight misalignment can cause error in analysis. Therefore, the determination was made that an image processing technique should be used to precisely align the three images. Adobe Photoshop software and its automatic "Load files into stack" script was utilized and eventually an alignment with a maximal error of 1-2 pixels was achieved. Once aligned, all three images were cropped to remove border image portions no longer overlapping the other two images because of a shift or rotation the image experienced during alignment.

4.7 Phase Detection

First, Image 1 and Image 3 were combined using the difference filter (Figure 4-13b). This filter subtracted respective color values from each image and used the resultant value to create a composite image; black color (value of 0) indicates no difference between two images. The black color corresponds to aggregate particles since only the paste experienced a color change. Binary threshold operation was applied to the image to extract aggregate particles. This operation caused all pixels with value higher than the selected threshold value to be white, while all pixels with lower value became black; therefore, the image's color mode was switched from 24-bit RGB (three channels and 256 possible color value in each channel) to a binary image (single channel with two possible color values, black or white, for each pixel). At the conclusion of this step, aggregate particles were detected (Figure 4-13b).

Unfortunately, this process sometimes tended to overestimate the total paste content because some aggregate particles might have not been always fully detected. Ideally, no change in color in aggregate should occur (therefore all aggregate would be colored black by the difference filter). However, especially light color aggregate (limestone, sandstone) got sometimes slightly colored by the phenolphthalein solution and therefore the colored portions of aggregate particle were missed.

Once the difference filter was applied, aggregate (black) particles with are less than 50 pixels were removed. Those particles were typically a noise created during the image processing.

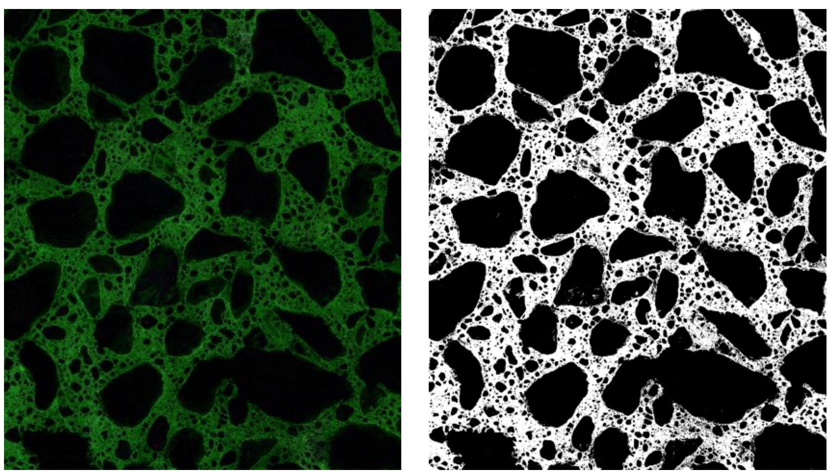

(a) (b)

Figure 4-13: Aggregate Detection: (a) Image 1 and Image 2 Combined - Difference Filter Applied, (b) Aggregate Particles Detected by Threshold Operation

Second, Image 2 was utilized to detect air voids as the applied orange powder highlighted all pores present in the sample, i.e., entrained and entrapped air voids as well as air pores present in aggregate particles. Brightness levels of the image were adjusted using Adobe Photoshop, resulting in an image with dark (black) background and red-orange air voids. Subsequently, air voids were selected based on color, extracted from the dark background, changed to a white color, and copied into a new image with a gray background. This new image utilized a single channel indexed color mode (often referred to as grayscale mode), allowing each pixel to have a color value from 0 to 255 (Figure 4-14).

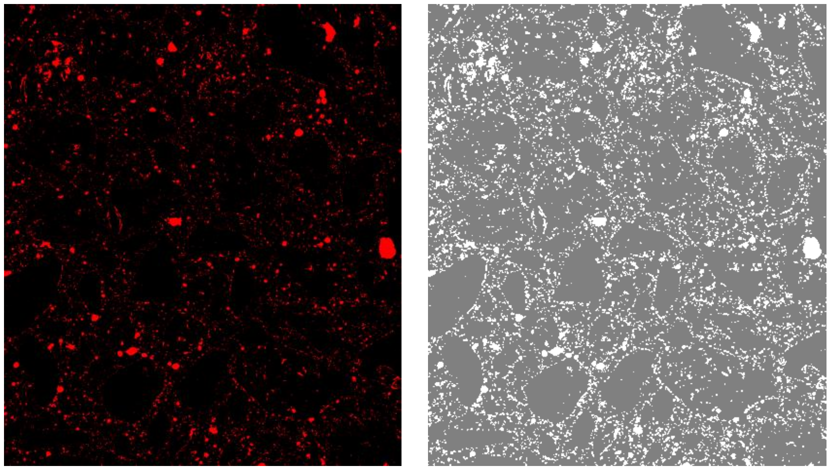

(a) (b)

Figure 4-14: Voids Detection: (a) Image 2 after Brightness Adjustments, (b) Grayscale Image with Detected Pores

False Color Image

The false color image, created using the binary image shown in Figure 4-13b and Figure 4-14, used the grayscale mode with black color representing aggregate, white color corresponding to air voids, and gray color indicating cement paste.

4.8 Air Void Analysis

A new software application, KSU Void Analyzer, was developed to facilitate air void analysis of previously generated images. .NET Framework 4.5 with 64-bit architecture, Microsoft Visual Studio 2012 and C# programing language were used to create this application. In order to perform advanced image processing tasks, AForge, EmguCV, and ClipperLibrary frameworks (all available under the GPU/GPL license) were incorporated into KSU Void Analyzer.

KSU Void Analyzer provided all information obtained using conventional analysis methods such as total air void content and spacing factor and total areas of concrete phases such as aggregate, cement paste, and air. In addition, information such as sizes, centroid locations, and other properties could be obtained from the software.

Spacing factor was obtained by performing the linear traverse method (ASTM C457, 2012) on the false color image as if it was a real hardened concrete sample. However, analysis was performed by computer software rather than a human operator. The software iterated through the sample from left to right, investigating every pixel. Total length of traverse, traverse length through air, and traverse length through paste were recorded in order to calculate the spacing factor.

4.9 Air Void Clustering Evaluation

To investigate the effect air void clustering may have on compressive strength of concrete, an evaluation method was implemented in the software that could quantify air clustering serenity. This method utilized existing false-color image and information obtained in previous steps of the analysis, particularly location of air void centroids and areas of aggregate particles. Since analysis of each aggregate would be extremely demanding computationally, only particles with area of more than 20,000,000 pixels (0.86 in^2) were investigated.

As a first step, equidistant lines derived from boundaries of selected aggregate particles were formed, creating 5 layers of uniform thickness (0.26 mm) immediately surrounding analyzed particles. Each layer was then searched for the presence of air void, and the total percentage of air voids within the investigated area was recorded for each layer. Local values of air content were then compared to the total air void content of the analyzed sample. Clustering index was defined as a ratio of air void content of the first investigated layer to the total air void content of the entire sample.

4.10 Air Void Clustering Rating

A method of clustering evaluation developed by Kozikowski et al. (2005) was also used to estimate the air void clustering extent. This method was performed by an independent operator than the person performing the hardened air void sample image analysis. Twenty or more largest aggregate particles in each sample were selected for rating. Those particles were then investigated under a microscope and assigned to a category represented with a number from 0 to 3 based on severity of void clustering. Once all particles were rated, the number of particles in each category were multiplied by a category number and then averaged over the total number of particles. Therefore, a single number indicating the air void level was generated.

Chapter 5 - Field Testing

5.1 Introduction

Two ongoing construction projects under the supervision of KDOT, with the retempering practice implemented, were visited in summer 2014.

The first site (Site I) was located in northwest Topeka, KS (Shawnee County) where a new interchange at US 24 and Menoken Road was being constructed. Site I was visited and samples were taken on June 20th, 2014, when a deck of the Bridge No. 70-44 (US-75 SB) was placed.

The second site (Site II) was located approximately 15 miles south of Topeka, KS, near Carbondale, KS (Osage County). This project, visited and sampled on July 7th, 2014, included placing a new overlay on the north bridge approach (Bridge No. 70-44 on US-75).

5.2 Methods

At both sites, fresh concrete properties (before and after water addition) were measured and recorded. Samples for compressive strength were made according to ASTM C31 (2012) were followed. Samples for hardened air void analysis were also made. After casting, samples were stored in a cooler on site for the initial 24-hour curing period and then transported to K-State laboratories and stored in the 100% moisture room at 72°F.

Similarly to mixes in the laboratory study, compressive strength was tested at 7 and 28 days (ASTM C39, 2012; ASTM C1231, 2014), and hardened air void analysis (including the automatic clustering evaluation) was carried out.

5.3 Materials, Mix Design & Retempering

The same mix design (KDOT Mix No. 1PT0835A) was used in both cases. The design specifications are presented in Table 5-1. The retempering however was different for each project. For concrete delivered at Site I, 1 gallon per cubic yard was withheld at the batching plant and later added to the concrete in the truck, while 2 gallons of water per cubic yard were withheld (and added in the truck) from concrete delivered to Site II. Transformed into water-to-cement ratios, concrete from Site I had w/c 0.38 and 0.40 before and after retempering, respectively. Ratios of water to cement on Site II were 0.37 and 0.40.

Table 5-1: Mix Design - 1PT0835A

Concrete Component	Specification	KDOT ID	Producer	Dosage
Cement (lbs/yd^3)	Type I/II	161060100	Central Plains Cement	521
Coarse Aggregate (lbs/yd^3)	SCA-3 Limestone	001270217	Mid-States Materials	1,586
Fine Aggregate (lbs/yd^3)	FA-A Natural Sand	001110008	Builders Choice	1,593
Admixture #1 (oz/yd^3)	AEA (BASF MB-90)	0410000000	BASF Construction Chemicals	3.0
Admixture #2 (oz/yd^3)	Water Reducer Type A (PolyHeed 900)	04201000A	BASF Construction Chemicals	20.0
Admixture #3 (oz/yd^3)	Water Reducer Type F (Glenium)	04204000F	BASF Construction Chemicals	20.0
Water (lbs/yd^3)				208
Designed w/c		0.4		

Chapter 6 - Results

6.1 Fresh Concrete Properties

As previously discussed in Section 0, fresh concrete properties were determined for both mixes before and after retempering as well as for all control mixes. Total air content is presented in Figure 6-1, Figure 6-2, and Figure 6-3.

Obtained values of other fresh concrete properties - slump, unit weight, and temperature - are shown in Table 6-1, Table 6-2, and Table 6-3 for mixes before retempering, after retempering, and control mixes, respectively.

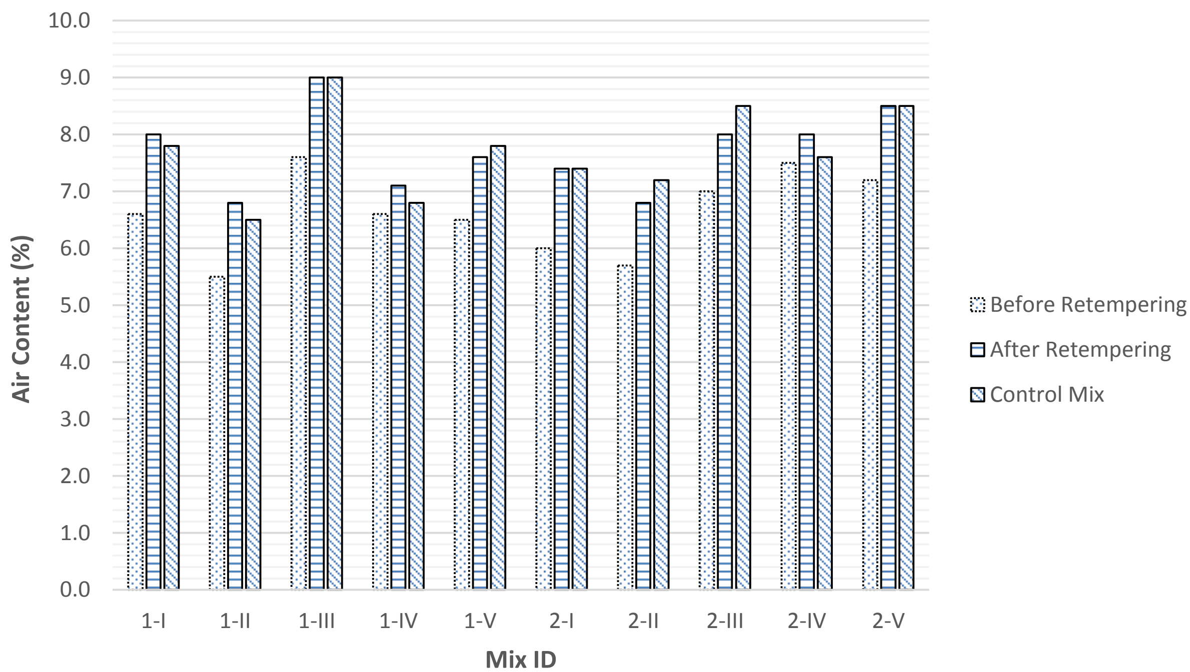

Figure 6-1: Air Content (Fresh) - Lincoln Quartzite

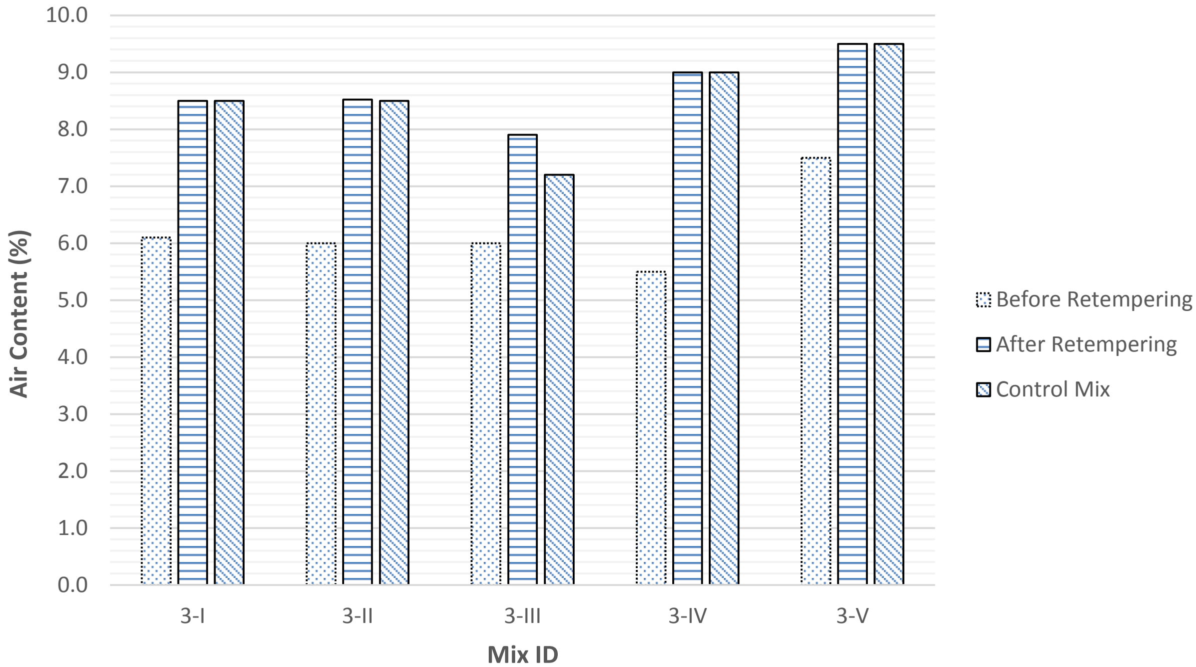

Figure 6-2: Air Content (Fresh) - Granite

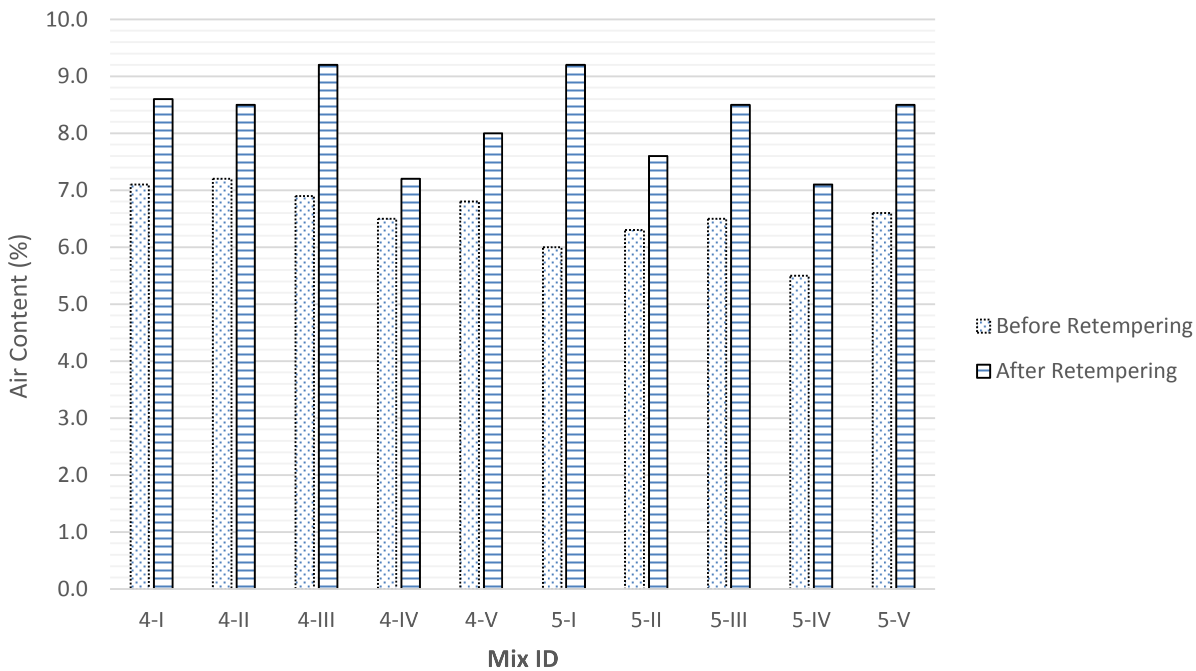

Figure 6-3: Air Content (Fresh) - Limestone and SD Quartzite

Table 6-1: Fresh Concrete Properties - Before Retempering

Mix ID	**Slump**	**Unit Weight**	**Temperature**
	in	*lb/ft³*	*°F*
1-I	2.00	144	73
1-II	2.25	145	73
1-III	2.75	140	73
1-IV	2.50	143	72
1-V	2.25	143	75
2-I	2.50	144	73
2-II	2.75	144	74
2-III	3.50	142	74
2-IV	3.00	141	73
2-V	2.75	142	74
3-I	2.25	145	75
3-II	2.25	145	74
3-III	2.25	144	78
3-IV	2.00	146	74
3-V	2.50	142	74
4-I	2.00	141	79
4-II	2.25	140	67
4-III	2.25	142	75
4-IV	2.00	142	72
4-V	2.00	141	70
5-I	1.50	143	73
5-II	1.00	143	67
5-III	1.75	144	73
5-IV	1.50	144	74
5-V	1.75	143	74

Table 6-2: Fresh Concrete Properties - After Retempering

Mix ID	**Slump**	**Unit Weight**	**Temperature**
	in	*lb/ft³*	*°F*
1-I-R	4.75	N/A	73
1-II-R	4.50	141	72
1-III-R	4.75	138	72
1-IV-R	3.75	141	70
1-V-R	3.50	140	74
2-I-R	4.25	141	72
2-II-R	4.25	141	73
2-III-R	4.50	139	73
2-IV-R	4.50	139	72
2-V-R	4.50	139	73
3-I-R	4.50	139	74
3-II-R	5.50	139	74
3-III-R	4.00	141	77
3-IV-R	5.00	139	73
3-V-R	4.75	137	73
4-I-R	3.00	137	77
4-II-R	4.50	139	66
4-III-R	3.75	139	74
4-IV-R	3.25	142	72
4-V-R	4.25	139	69
5-I-R	3.50	137	71
5-II-R	2.75	140	66
5-III-R	3.75	139	72
5-IV-R	3.00	141	74
5-V-R	3.25	139	73

Table 6-3: Fresh Concrete Properties - Control Mixes

Mix ID	**Slump**	**Unit Weight**	**Temperature**
	in	*lb/ft³*	*°F*
1-I-C	4.0	140	71
1-II-C	4.1	142	72
1-III-C	4.8	138	71
1-IV-C	4.1	142	73
1-V-C	4.2	140	71
2-I-C	4.0	141	73
2-II-C	4.1	141	72
2-III-C	4.8	139	73
2-IV-C	4.1	140	74
2-V-C	4.2	139	75
3-I-C	4.5	139	72
3-II-C	4.3	139	72
3-III-C	4.3	142	72
3-IV-C	4.0	139	73
3-V-C	4.8	138	73

6.2 Compressive Strength

Compressive strengths at 7 days are shown in Figure 6-4, Figure 6-5, and Figure 6-6, while values of compressive strength at 28 days are presented in Figure 6-7, Figure 6-8, and Figure 6-9. To recall, every testing sample consisted of three concrete cylinders (4 x 8 in) and measured values were averaged over the number of tested cylinders in order to determine the final value of compressive strength at a given time for a given mix.

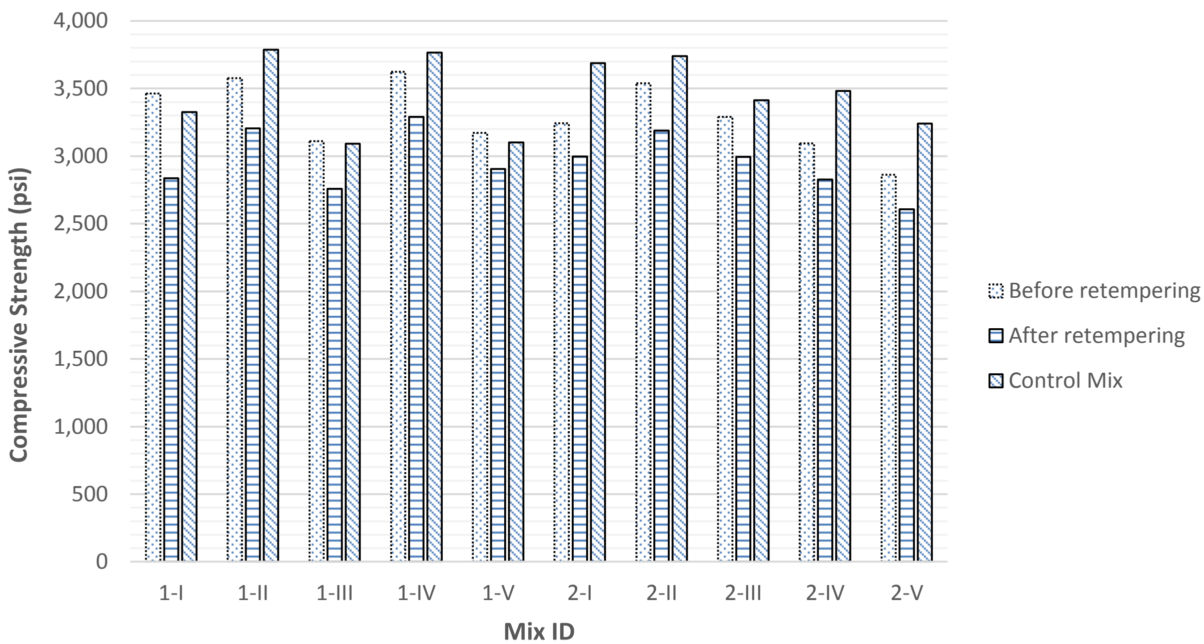

Figure 6-4: Compressive Strength at 7 days - Lincoln Quartzite

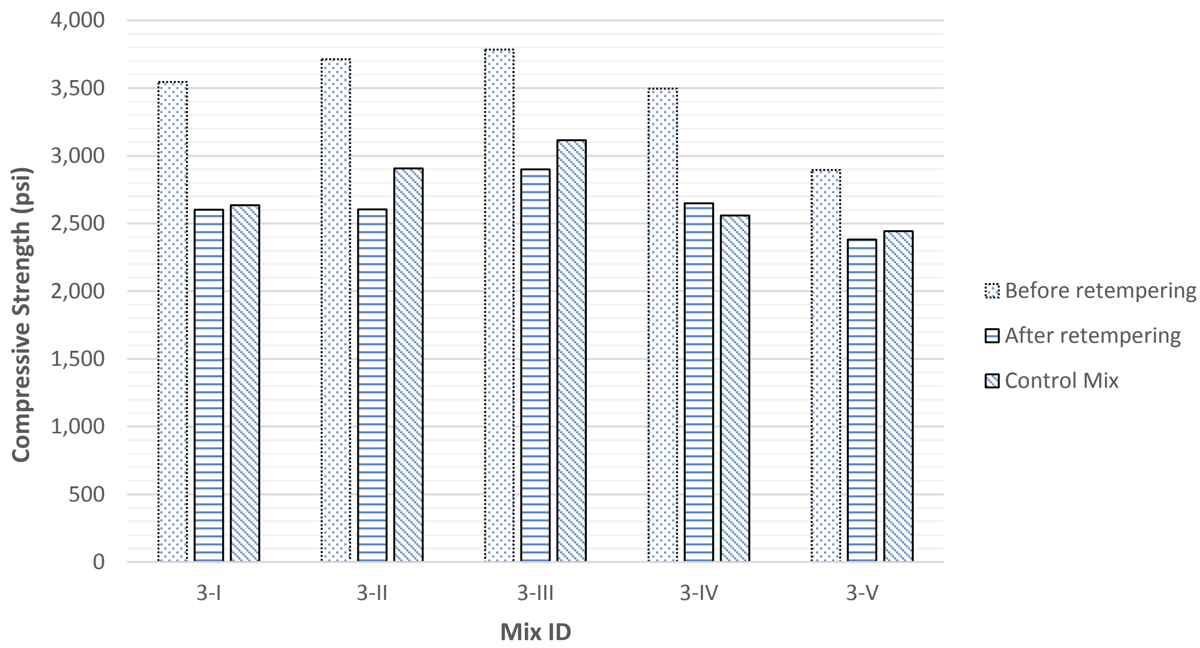

Figure 6-5: Compressive Strength at 7 days - Granite

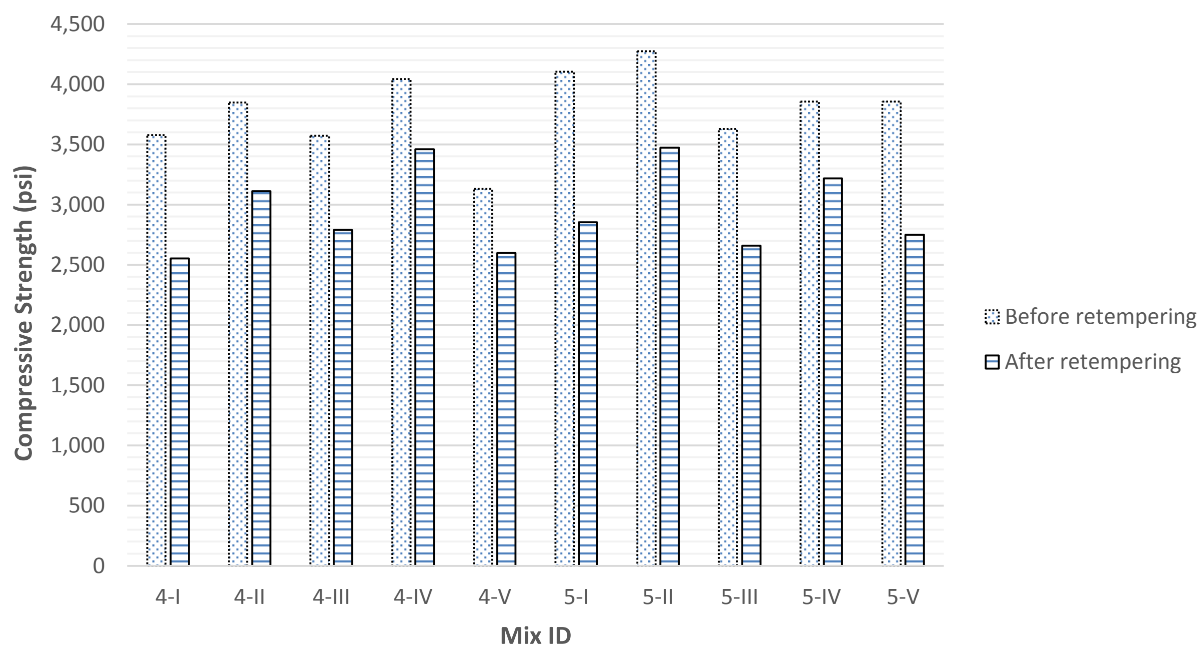

Figure 6-6: Compressive Strength at 7 days - Limestone and SD Quartzite

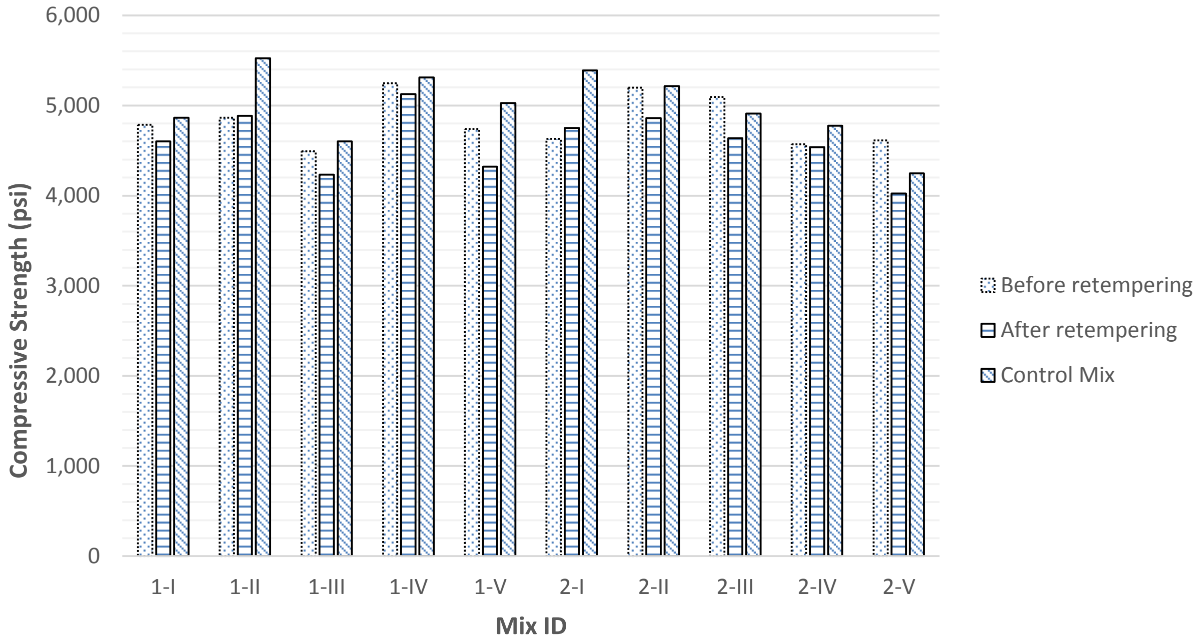

Figure 6-7: Compressive Strength at 28 days - Lincoln Quartzite

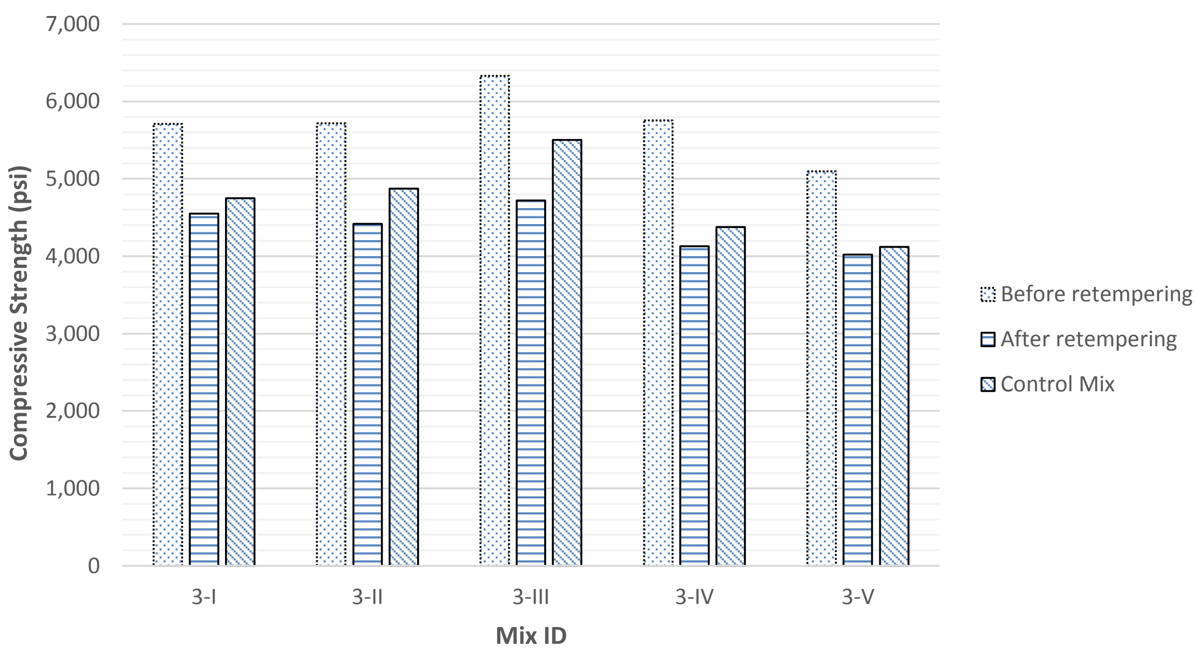

Figure 6-8: Compressive Strength at 28 days - Granite

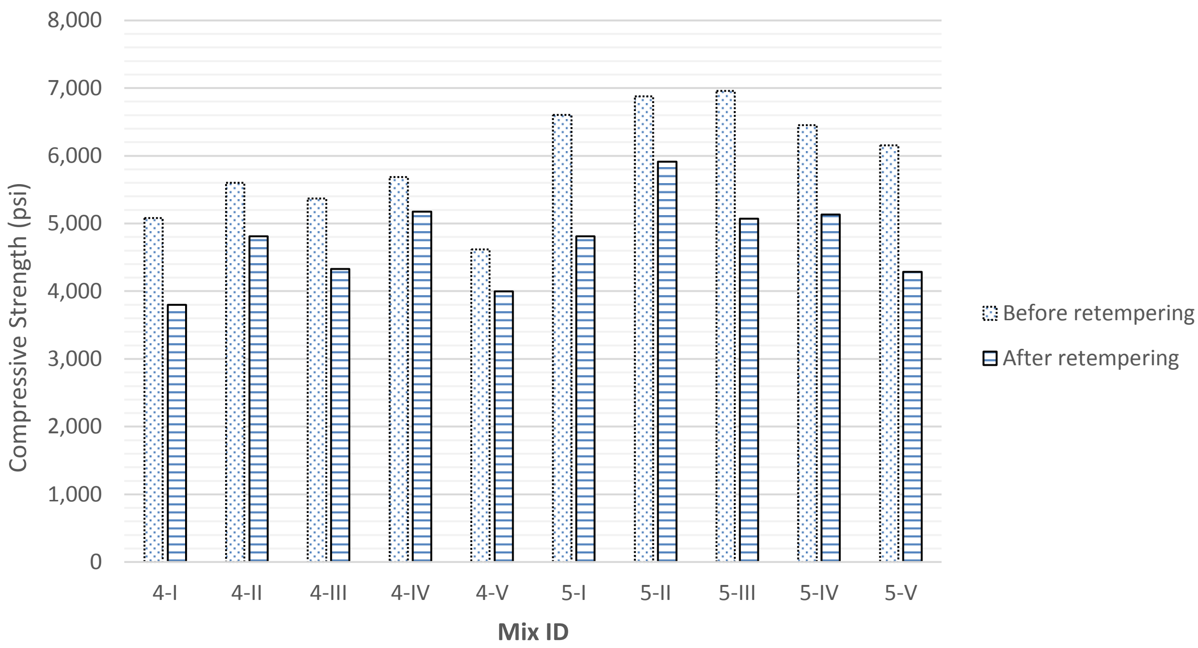

Figure 6-9: Compressive Strength at 28 days - Limestone and SD Quartzite

6.3 Air Void Content of Hardened Concrete

Total air void content obtained from the hardened concrete analysis as described in Section 0 is presented in Figure 6-10, Figure 6-11, and Figure 6-12. Corresponding spacing factors are shown in Figure 6-13, Figure 6-14, and Figure 6-15.

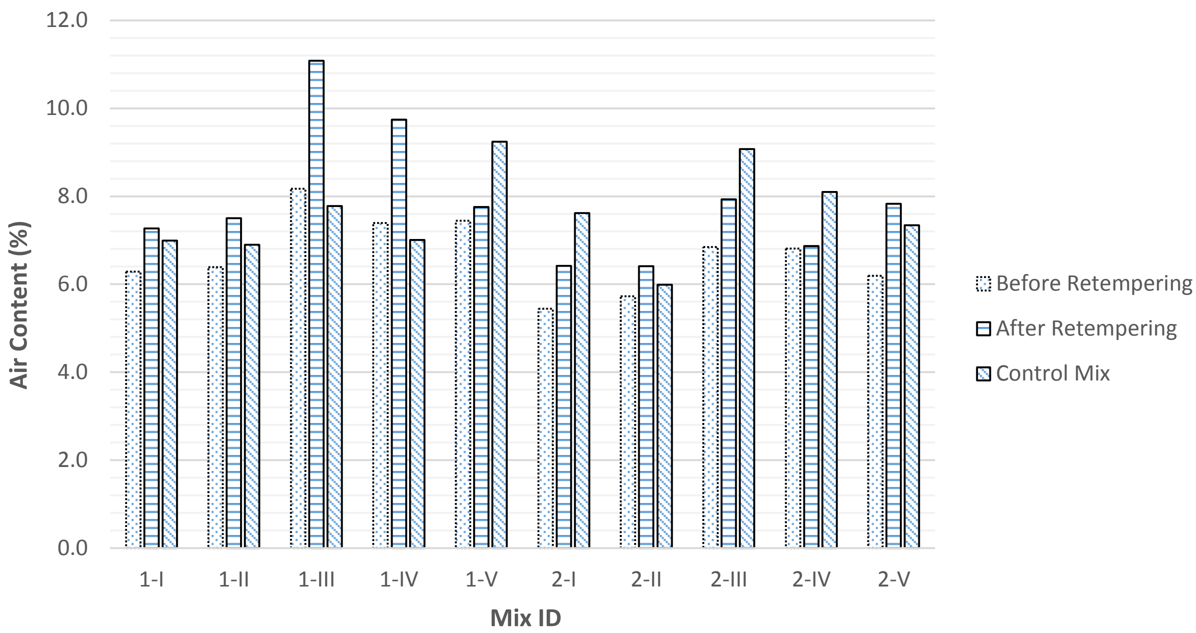

Figure 6-10: Air Content (Hardened) - Lincoln Quartzite

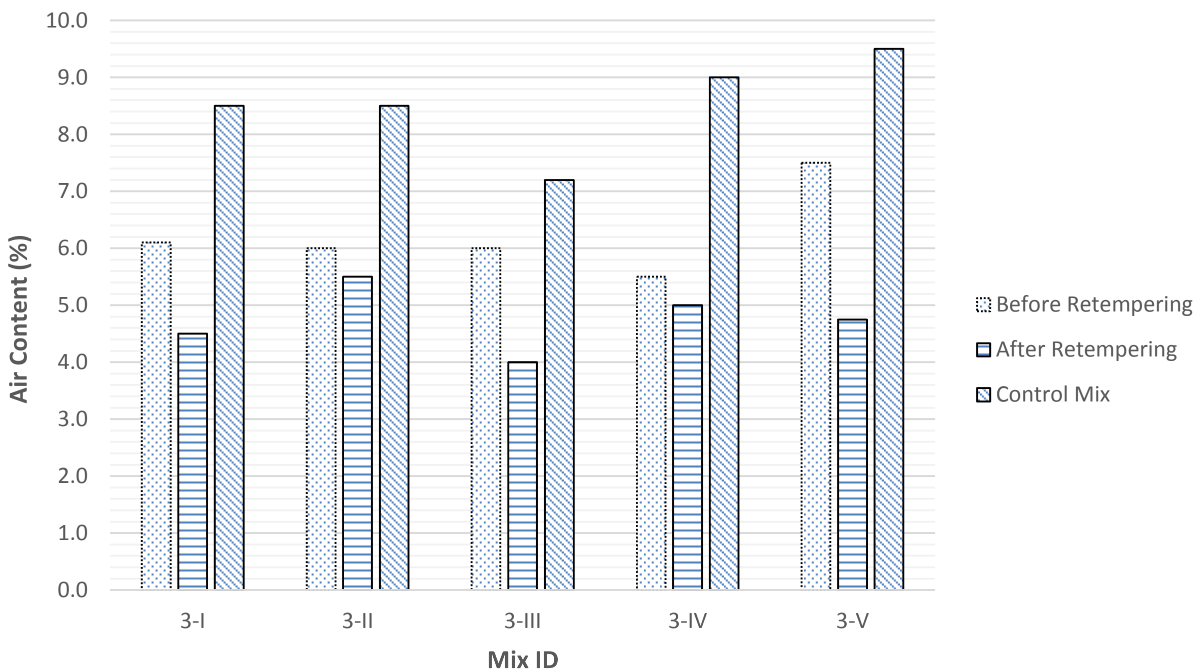

Figure 6-11: Air Content (Hardened) - Granite

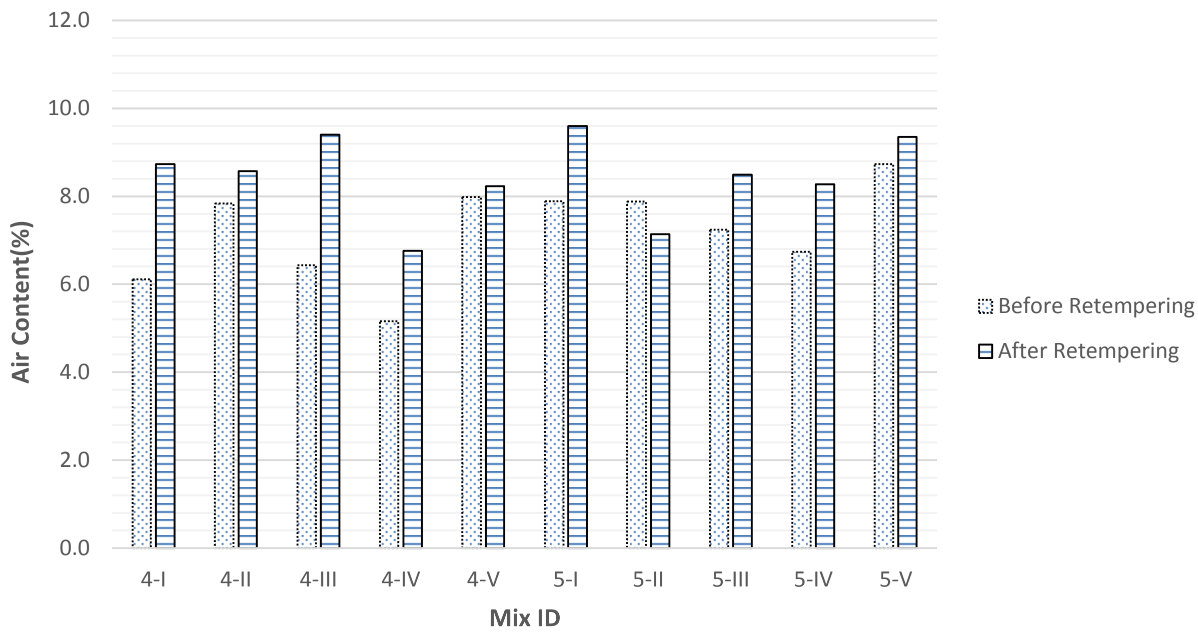

Figure 6-12: Air Content (Hardened) - Limestone and SD Quartzite

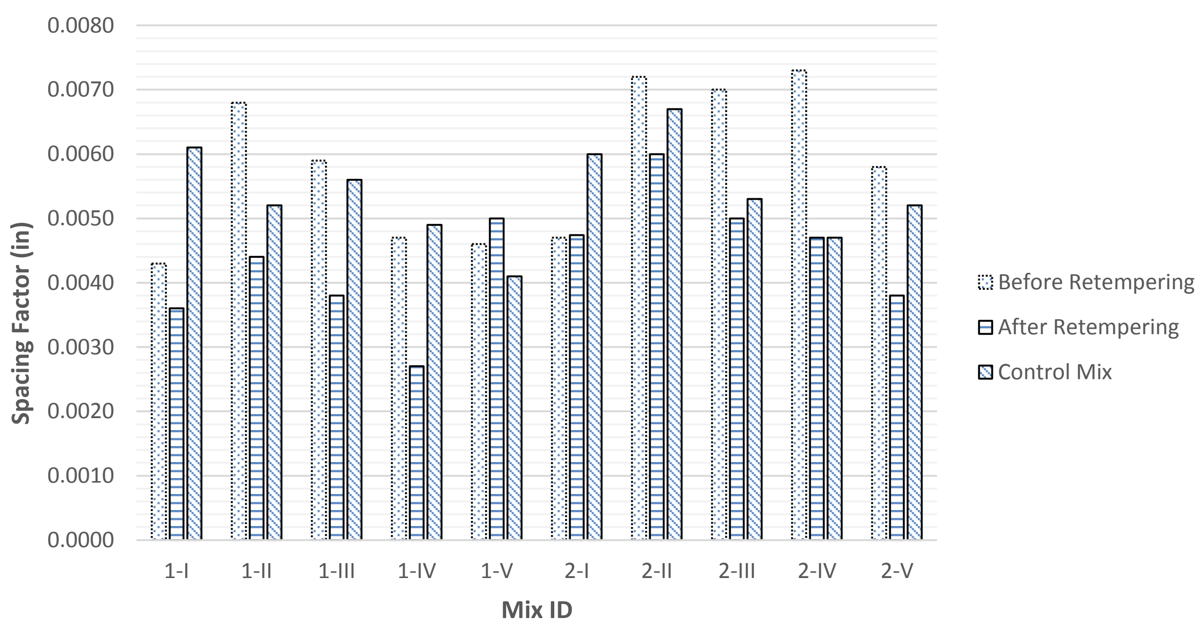

Figure 6-13: Spacing Factor - Lincoln Quartzite

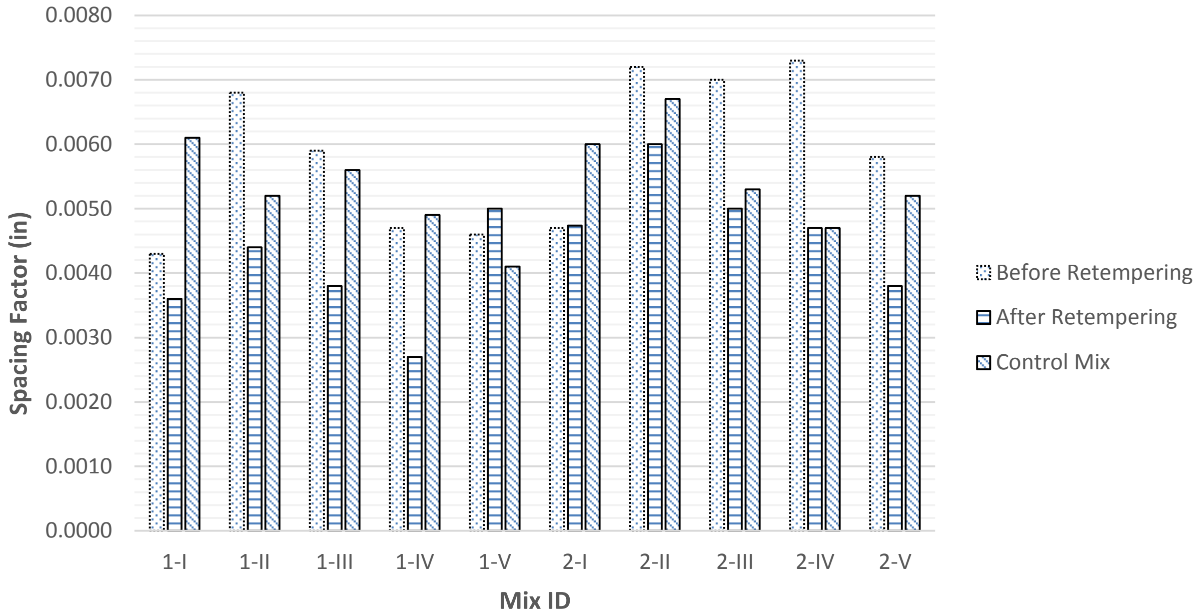

Figure 6-14: Spacing Factor - Granite

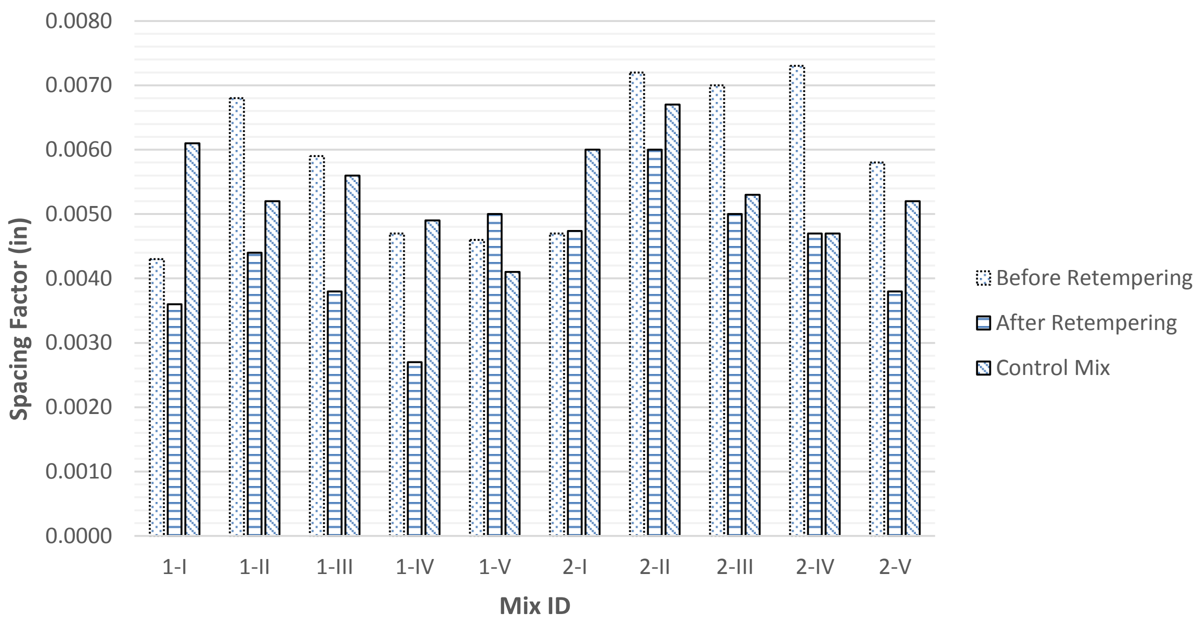

Figure 6-15: Spacing Factor - Limestone and SD Quartzite

6.4 Air Void Clustering

Results of the clustering analysis are presented in Figure 6-16, Figure 6-17, and Figure 6-18. Visual ratings of air void clustering obtained from the manual analysis are shown in Figure 6-19, Figure 6-20, and Figure 6-21.

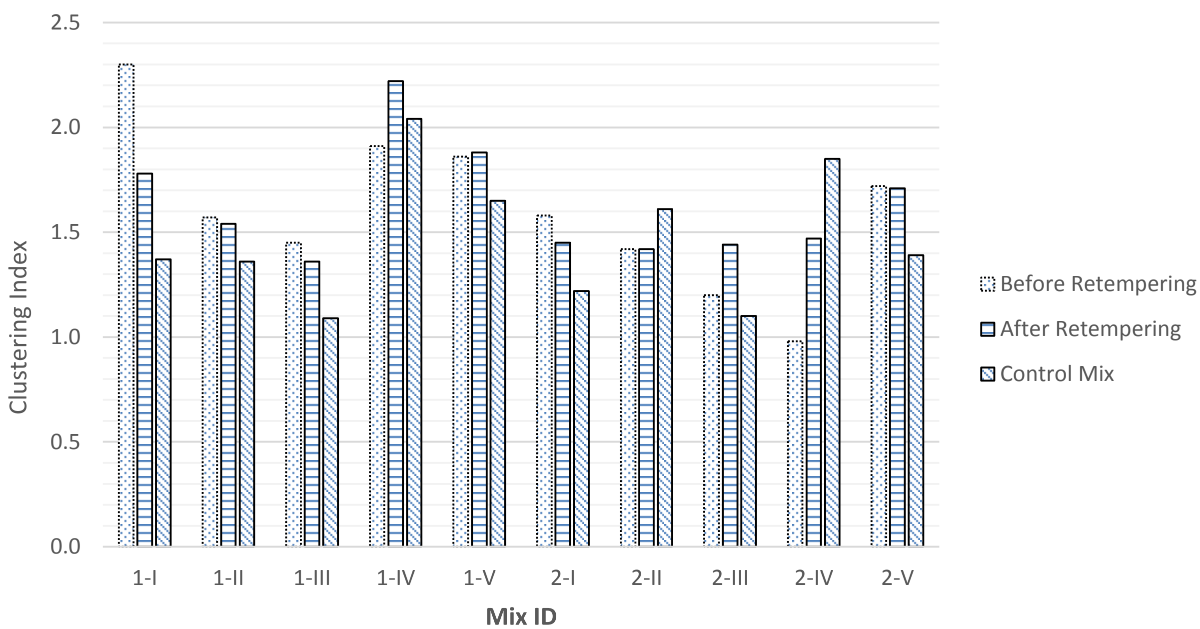

Figure 6-16: Clustering Index - Lincoln Quartzite

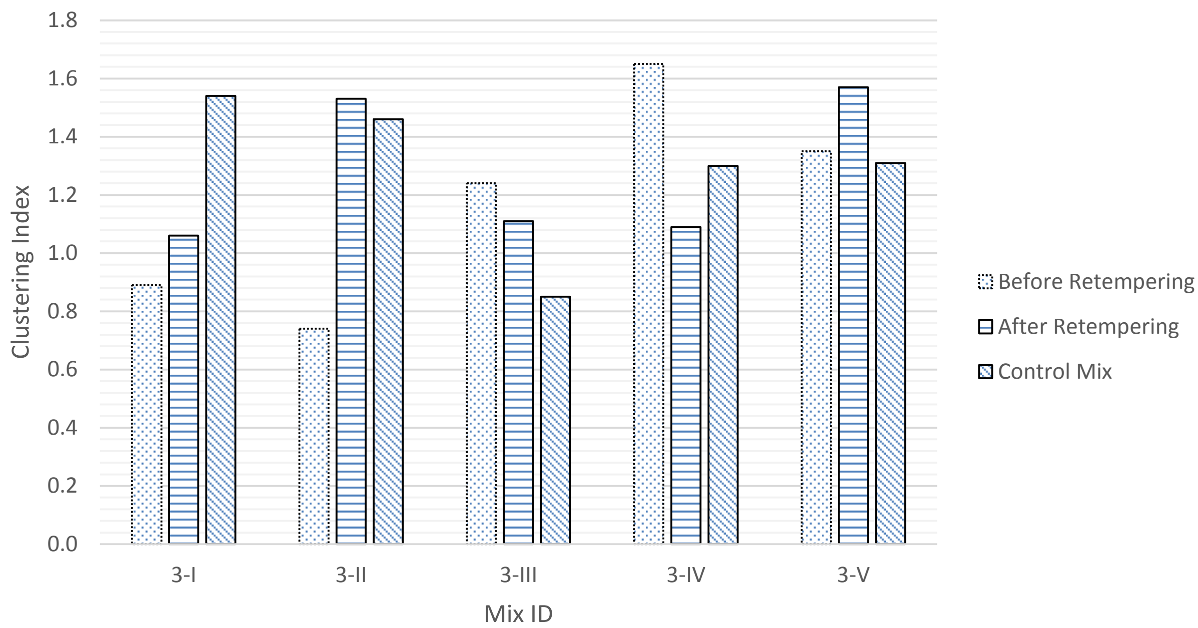

Figure 6-17: Clustering Index - Granite

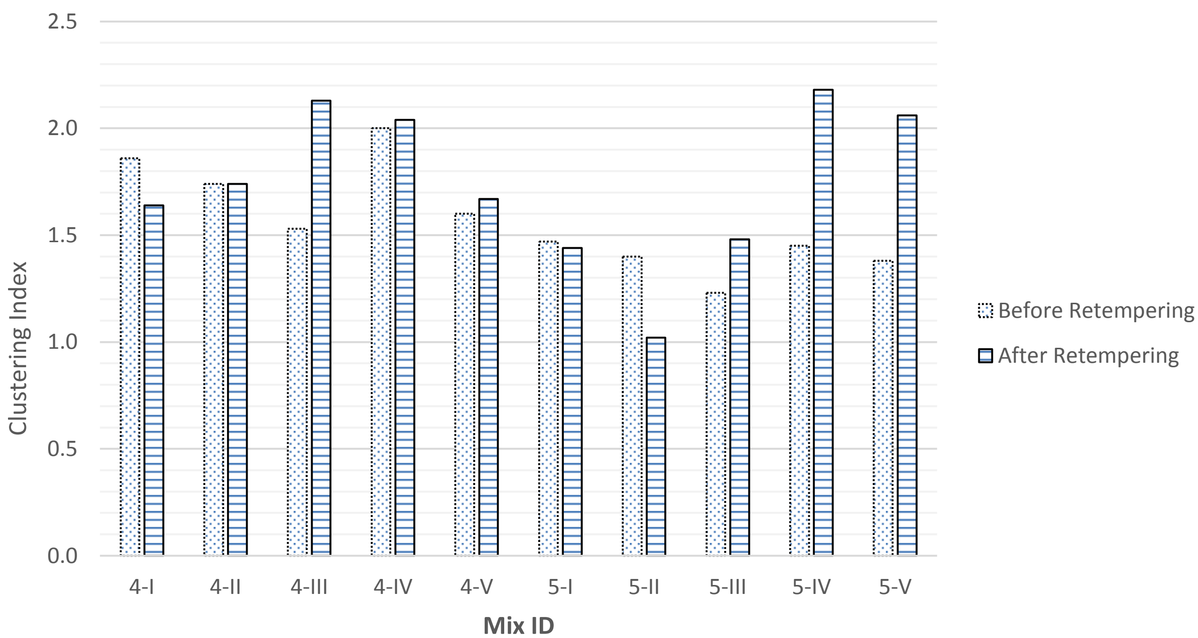

Figure 6-18: Clustering Index - Limestone and SD Quartzite

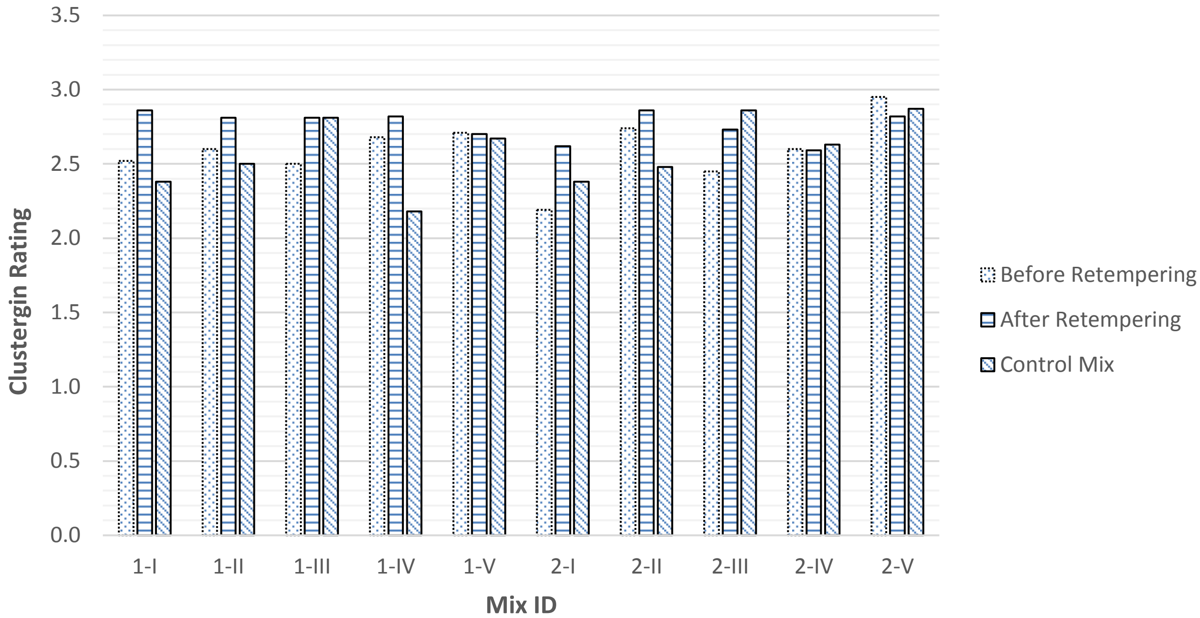

Figure 6-19: Clustering Index (Visual Rating) - Lincoln Quartzite

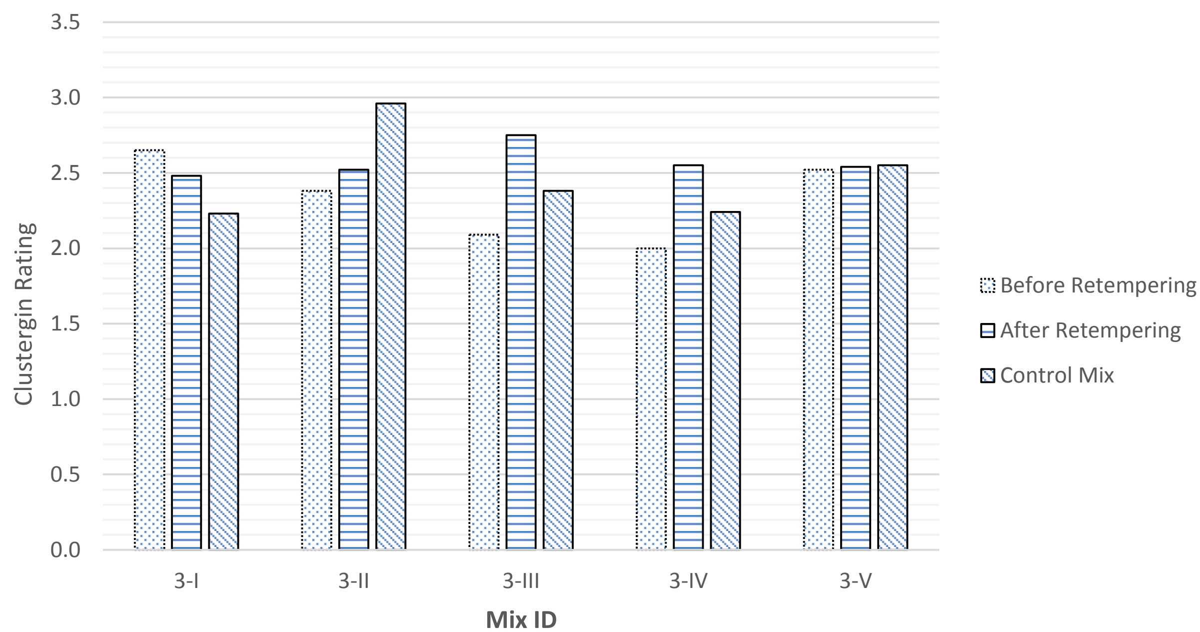

Figure 6-20: Clustering Index (Visual Rating) - Granite

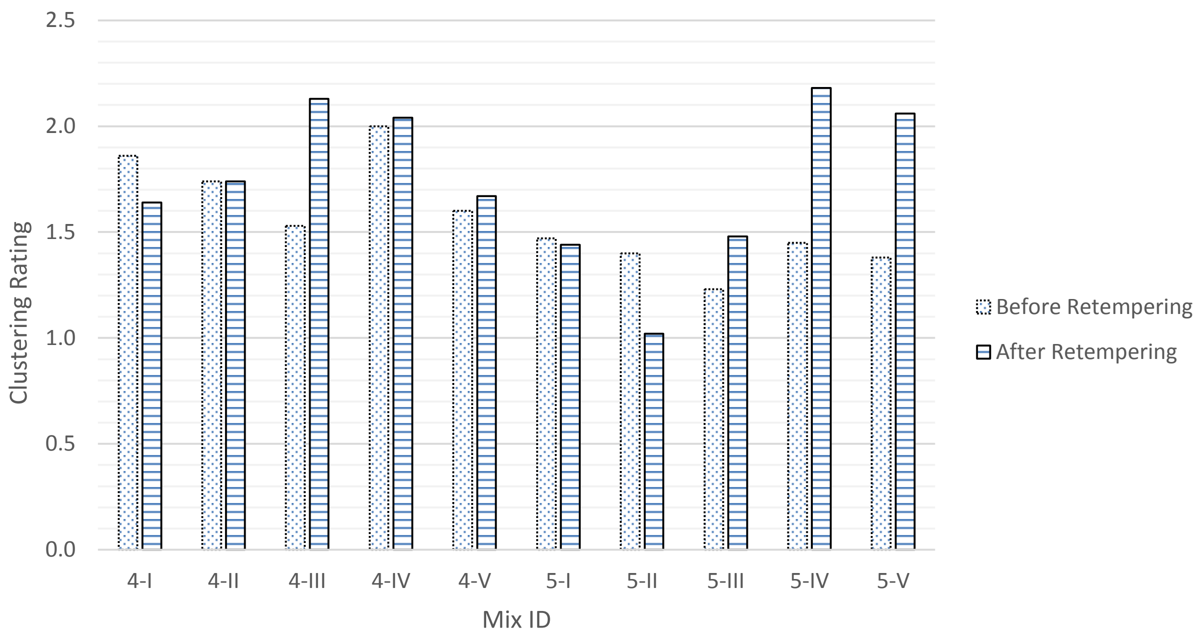

Figure 6-21: Clustering Index (Visual Rating) - Limestone and SD Quartzite

6.5 Field Samples

Fresh concrete properties of field mixes are presented in Table 6-4.

Table 6-4: Fresh Concrete Properties - Field Testing

Site	Slump	Air Content	Unit Weight	Temperature
	in	*%*	*lb/ft³*	*°F*
Site I – Before Water Addition	3.25	6.2	144	84
Site I – After Water Addition	4.00	6.6	142	85
Site II – Before Water Addition	0.50	4.5	147	79
Site II – After Water Addition	1.50	5.8	145	81

Values of concrete compressive strength at both 7 and 28 days are shown in Figure 6-22 and Figure 6-23, respectively.

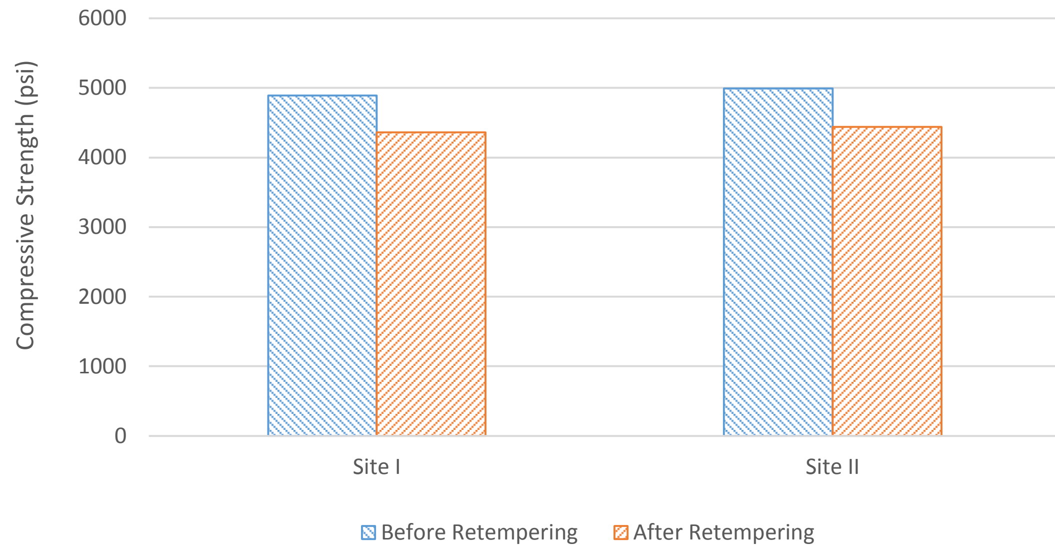

Figure 6-22: Compressive Strength at 7 days - Field Testing

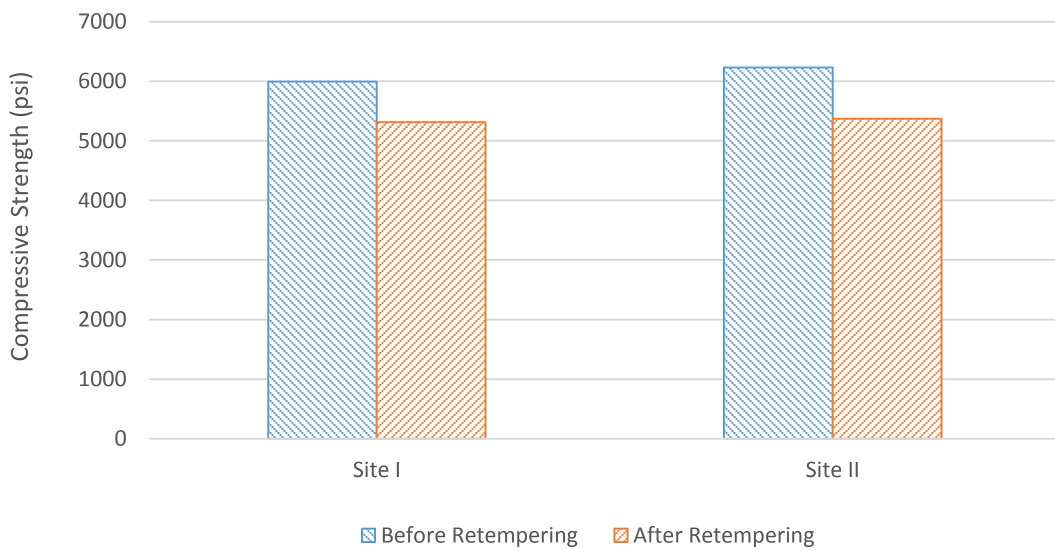

Figure 6-23: Compressive Strength at 28 days - Field Testing

Results of the hardened air void analysis – air content and Clustering Index - are presented in Figure 6-24 and Figure 6-25, respectively.

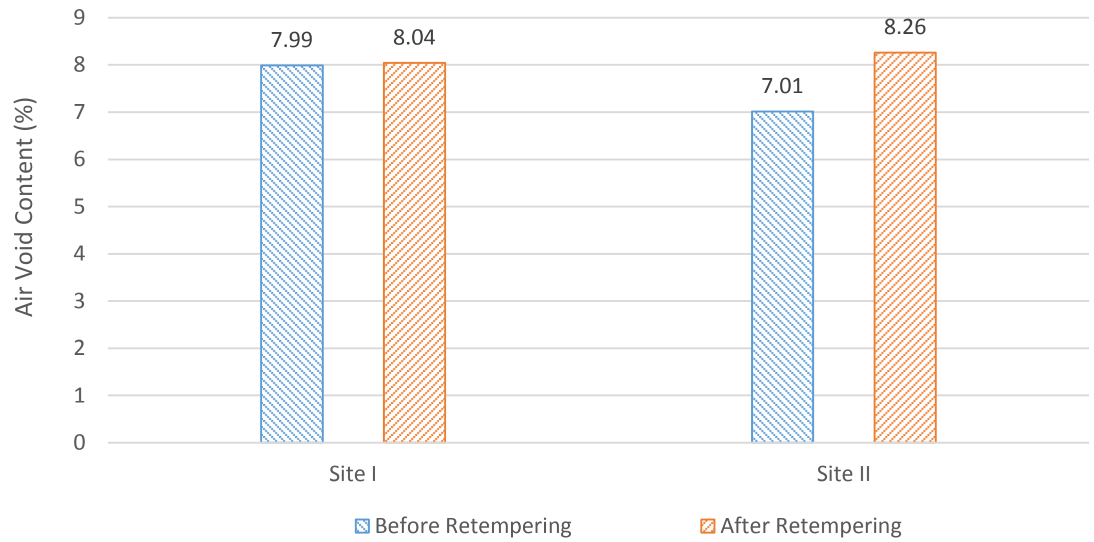

Figure 6-24: Hardened Air Void Content - Field Testing

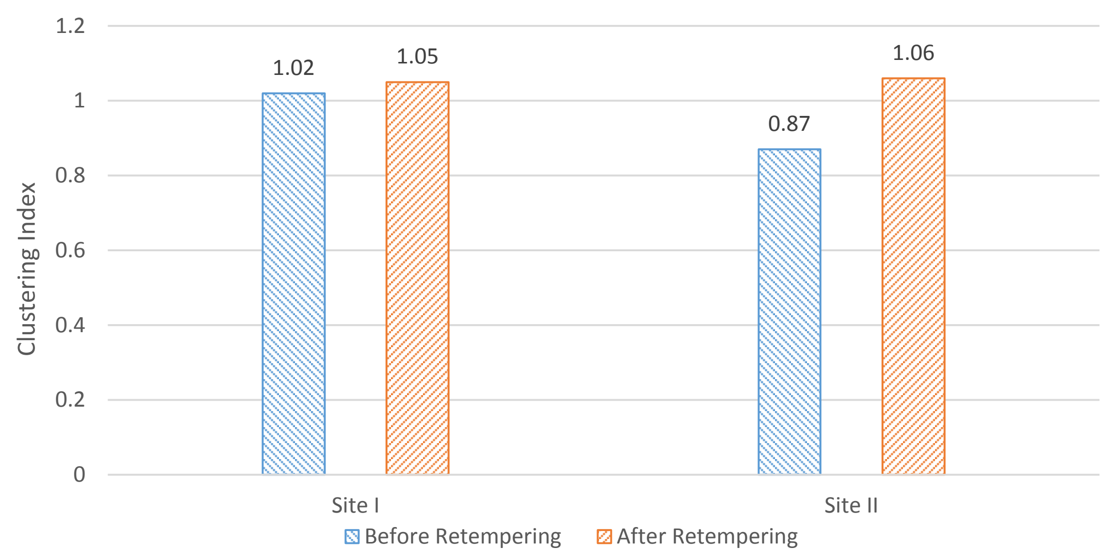

Figure 6-25: Clustering Index - Field Testing

Chapter 7 - Discussion

Three variables were examined in this study: (1) retempering, (2) aggregate type, (3) air entraining admixture type. Results with respect to all three investigated variables will be separately discussed in the following subsections.

7.1 Retempering

To recall, mixes with Lincoln Quartzite had a water-to-cement ratio equal to 0.41 and 0.43 before and after retempering, respectively. Mixes utilizing Granite, Limestone and SD Quartzite experienced change in the w/c from 0.43 to 0.45 from retempering. For both cases, the additional mixing period during retempering was 2 minutes long.

Changes in concrete fresh properties before and after retempering corresponded to what was expected. In all cases, retempered mixes experienced increase in slump and air content, as well as decrease in unit weight. Concrete slump always increased after retempering (Figure 7-1), which is not surprising as one of the main reasons why the retempering practice is utilized in the industry is to increase concrete workability. The increase in slump as a percentage ranged from 100% to 320% (average value was 178% with standard deviation of 53%). Variation in slump values for mixes after retempering and control mixes is most likely caused by the precision of retempering procedure as it is almost impossible to precisely determine the resultant water-to-cement ration of concrete after it has been retempered. Nevertheless, the difference was not found to be significant.

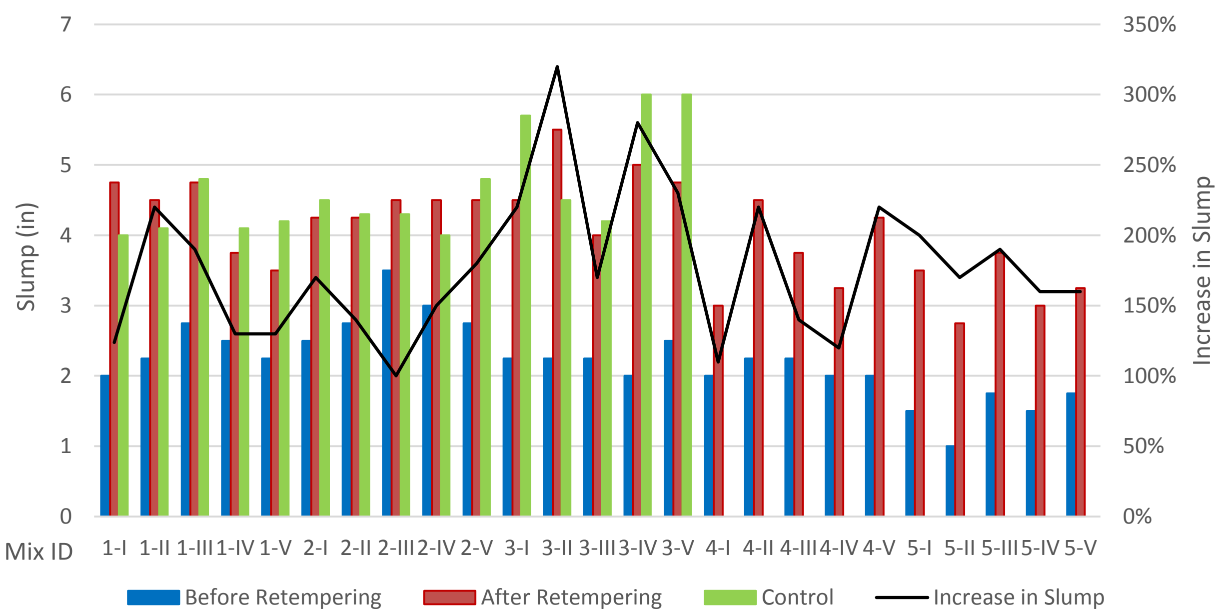

Figure 7-1: Slump Before and After Retempering

Similarly, an increase in total air content was observed in all mixes after retempering, as shown in Figure 7-2. On average, air content increased by 1.6% after retempering (standard deviation was 0.7%). The highest observed increase was 3.5% while the lowest value of air content increase was found to be 0.5%. The additional mixing action and higher concrete fluidity allowed more air to be folded into the concrete and be stabilized.

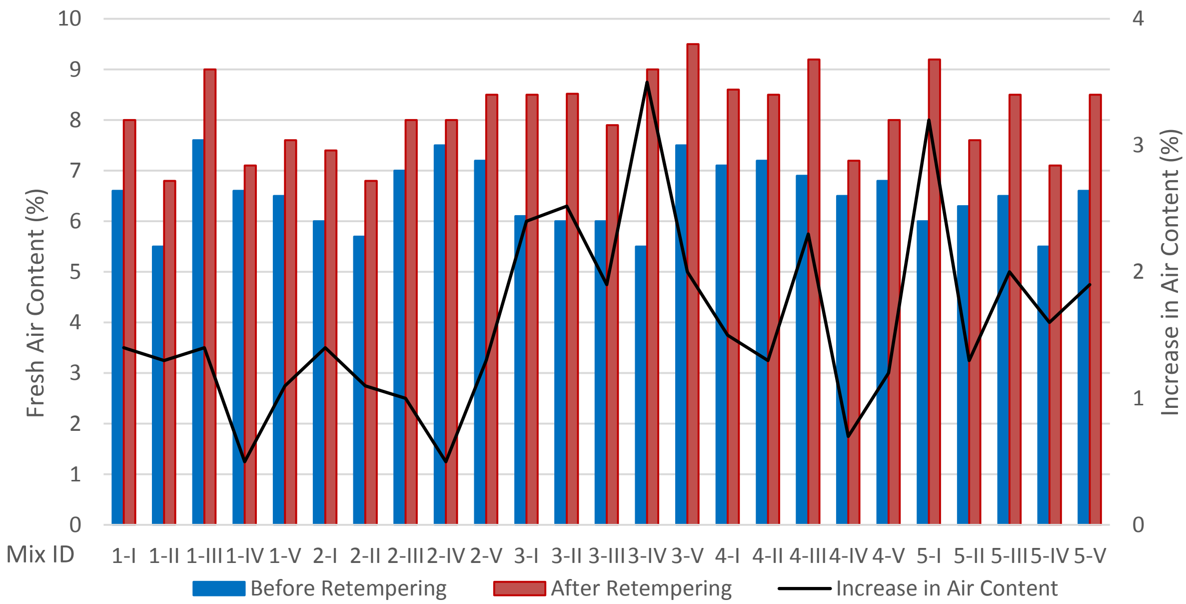

Figure 7-2: Fresh Air Content Before and After Retempering

Relationship between the air content of fresh concrete and unit weight is presented in Figure 7-3. Strong correlation can be seen between those two concrete properties as found R^2 values were 0.78, 0.69, and 0.94 for mixes before retempering, after retempering, and control mixes, respectively. Lower value of the R^2 coefficient is most likely caused by imprecision of the pressure method for high air contents and rounding the values to the nearest 0.5% for air content values above 8% as required.

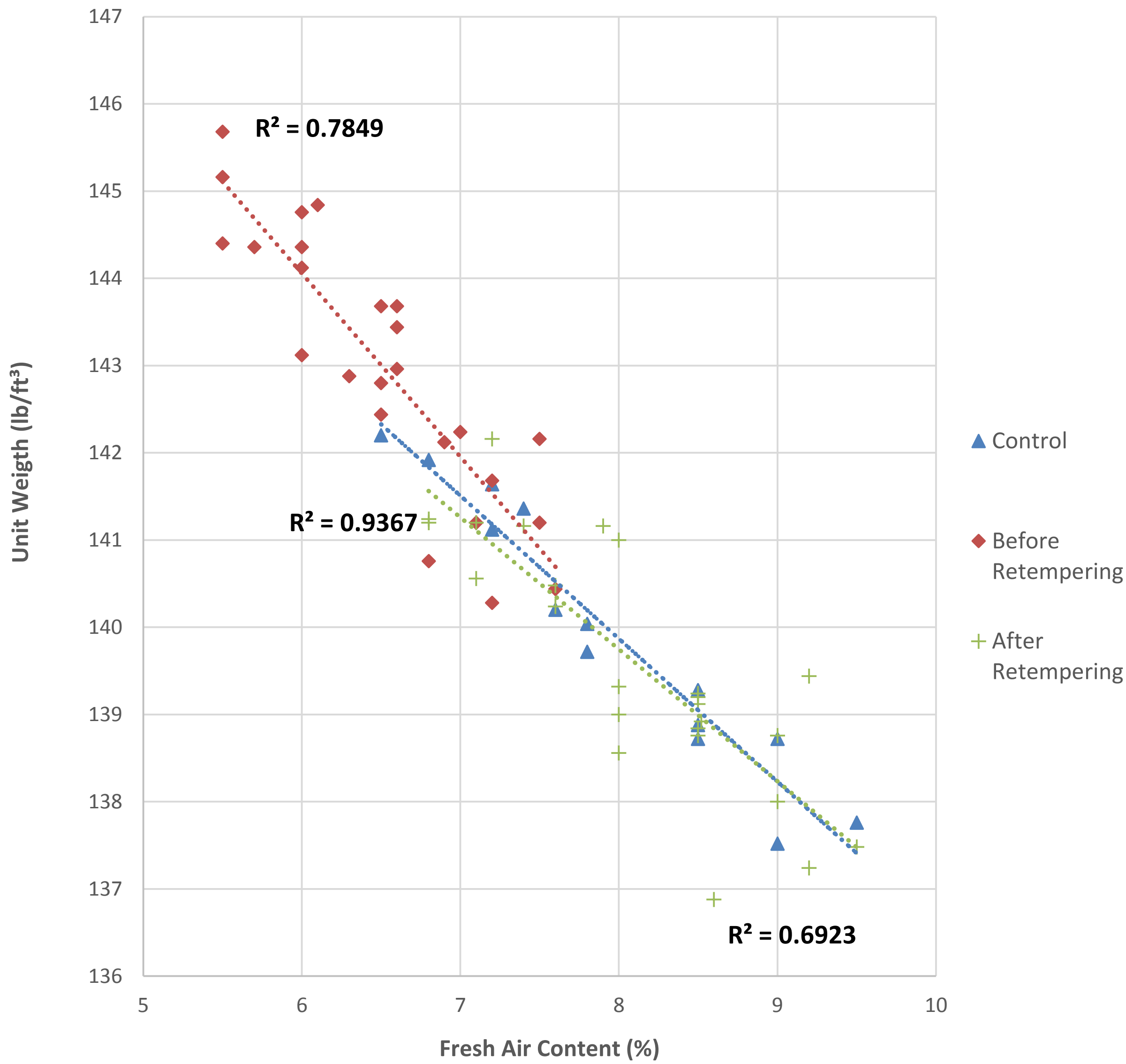

Figure 7-3: Air Content vs Unit Weight

Retempering has been previously associated with air void clustering (Naranjo, 2007; Kozikowski, David, Peter, & Steven, 2005). Therefore, it was predicted that retempered mixes should expect higher levels of air void clustering than non-retempered ones. Despite the predictions, many mixes showed less clustering activity after retempering (10 out of 25), as presented in Figure 7-4. Average change in clustering index before and after retempering was only 10% (standard deviation equaled to 31%). The maximal observed increase in clustering after retempering was 107% whereas the highest decrease was by 34%.

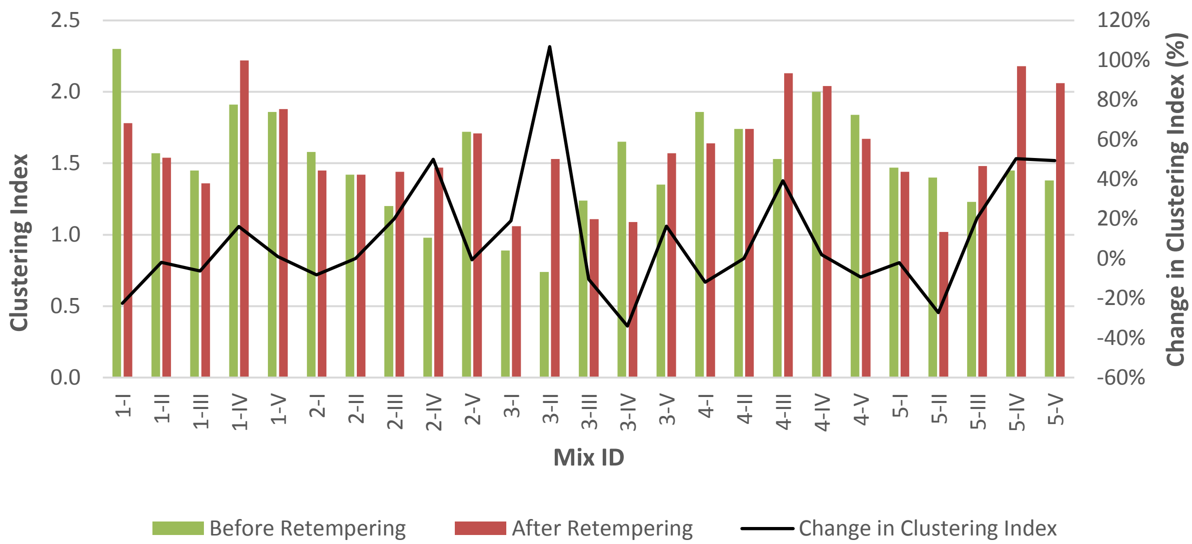

Figure 7-4: Clustering Index - Before and After Retempering

Comparison of clustering indexes of mixes after retempering and control mixes is provided in Figure 7-5. It is evident that majority of mixes after being retempered showed higher clustering rate than corresponding control mixes (11 out of 15). However, retempered mixes had clustering index increased only by 9% (standard deviation was 20%), which is believed to be insignificant, especially considering the variance in air content between tempered and control mixes.

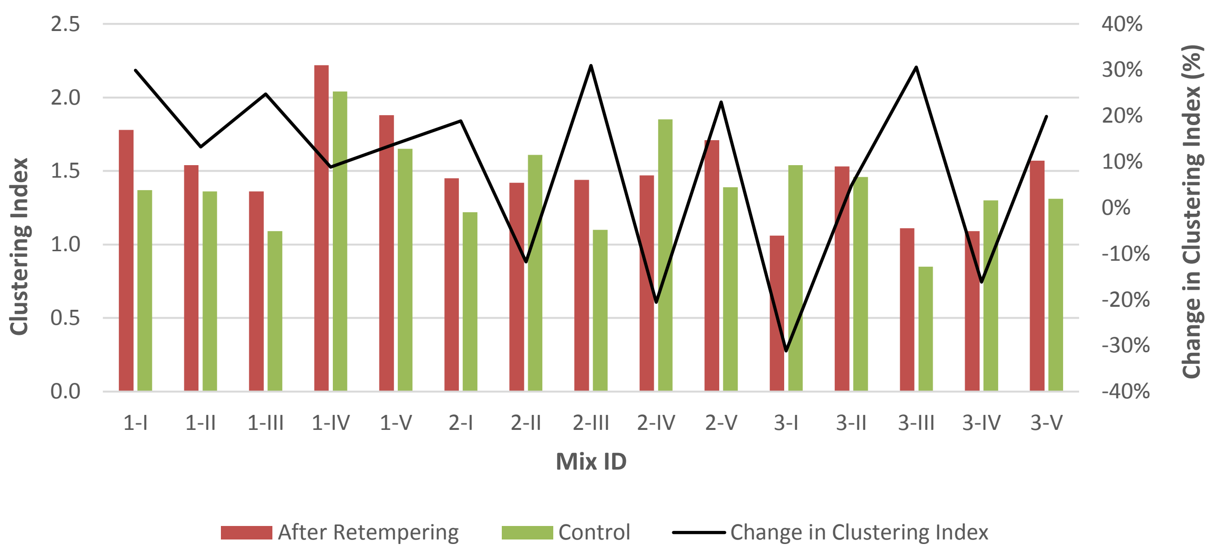

Figure 7-5: Clustering Index - After Retempering and Control Mixes

Based on the presented data, it seems that retempering has no or very little influence on formation of air void clusters around coarse aggregate, which is in opposition to what was believed. On the other hand, compressive strength at both 7 and 28 days very much corresponded to what was expected. Compressive strength in all but 2 cases (out of 50) decreased after retempering, as shown in Figure 7-6 (7 days) and Figure 7-7 (28 days). At 7 days, average decrease in strength after concrete being retempered was 15% (standard deviation 8%) while at 28 days, average decrease was 11% with standard deviation of 10%. The maximum decrease in strength was 30% and 28% for strengths at 7 and 28 days, respectively. The lowest decrease was observed to be 8% at 7 days and surprisingly, one mix showed similar compressive strength after retempering at 28 days (3% higher than the non-retempered mixture).

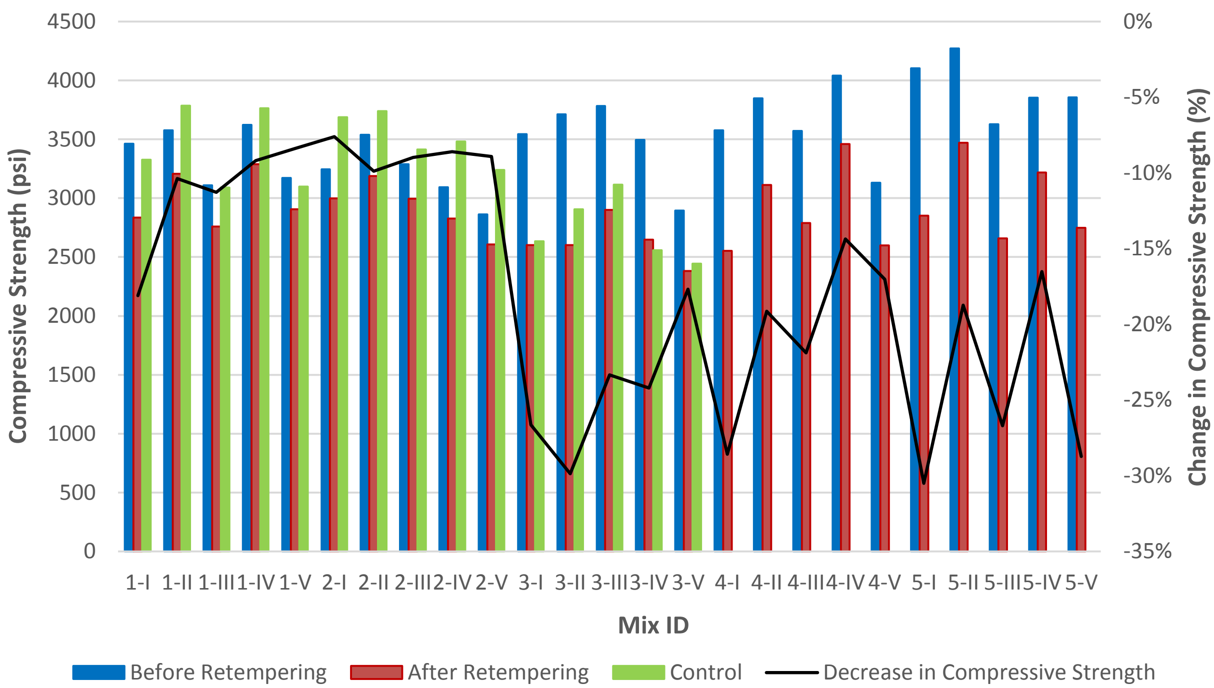

Figure 7-6: Compressive Strength at 7 days

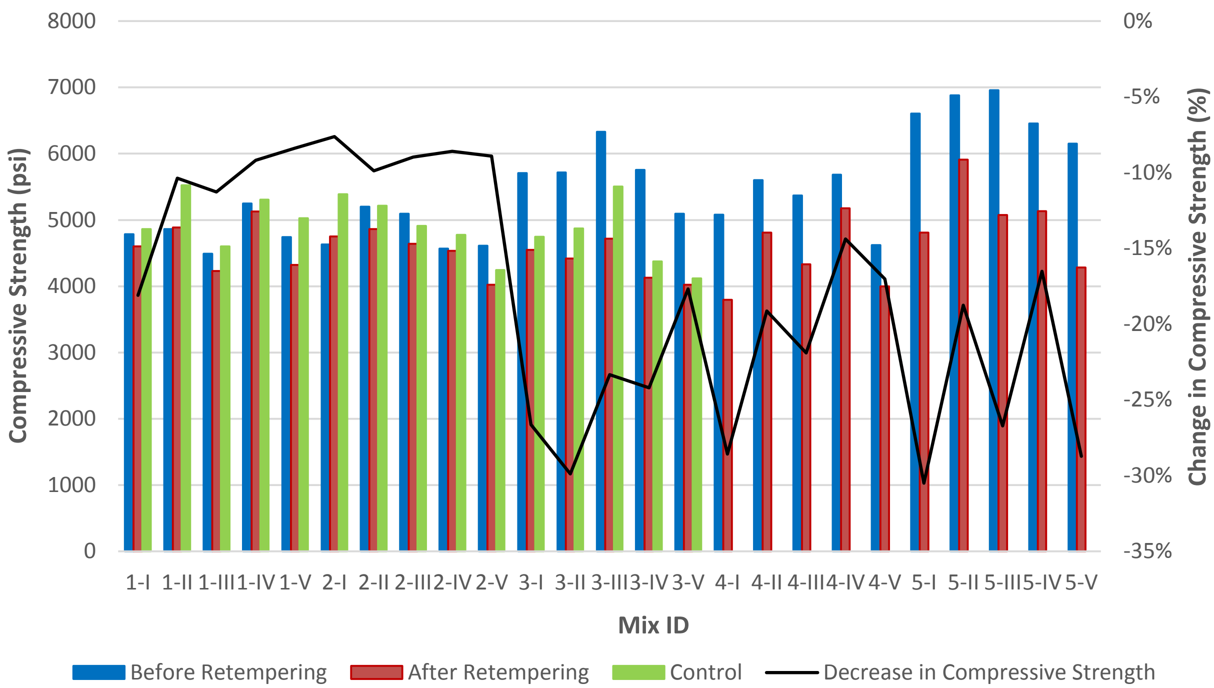

Figure 7-7: Compressive Strength at 28 days

The decrease in compressive strength can be credited to the fact that water-cement ratio increased as well as the overall air content. Moreover, suggestions has been previously made (Cross, Duke, Kellar, & Johnston, 2000; Kozikowski, David, Peter, & Steven, 2005) that air void clustering can be a factor affecting the compressive strength of retempered mixes. However, data obtained in this laboratory study does not confirm this hypothesis. As shown in Figure 7-8 and Figure 7-9, neither mixes before nor after retempering exhibit any kind of correlation between the compressive strength and the clustering index.

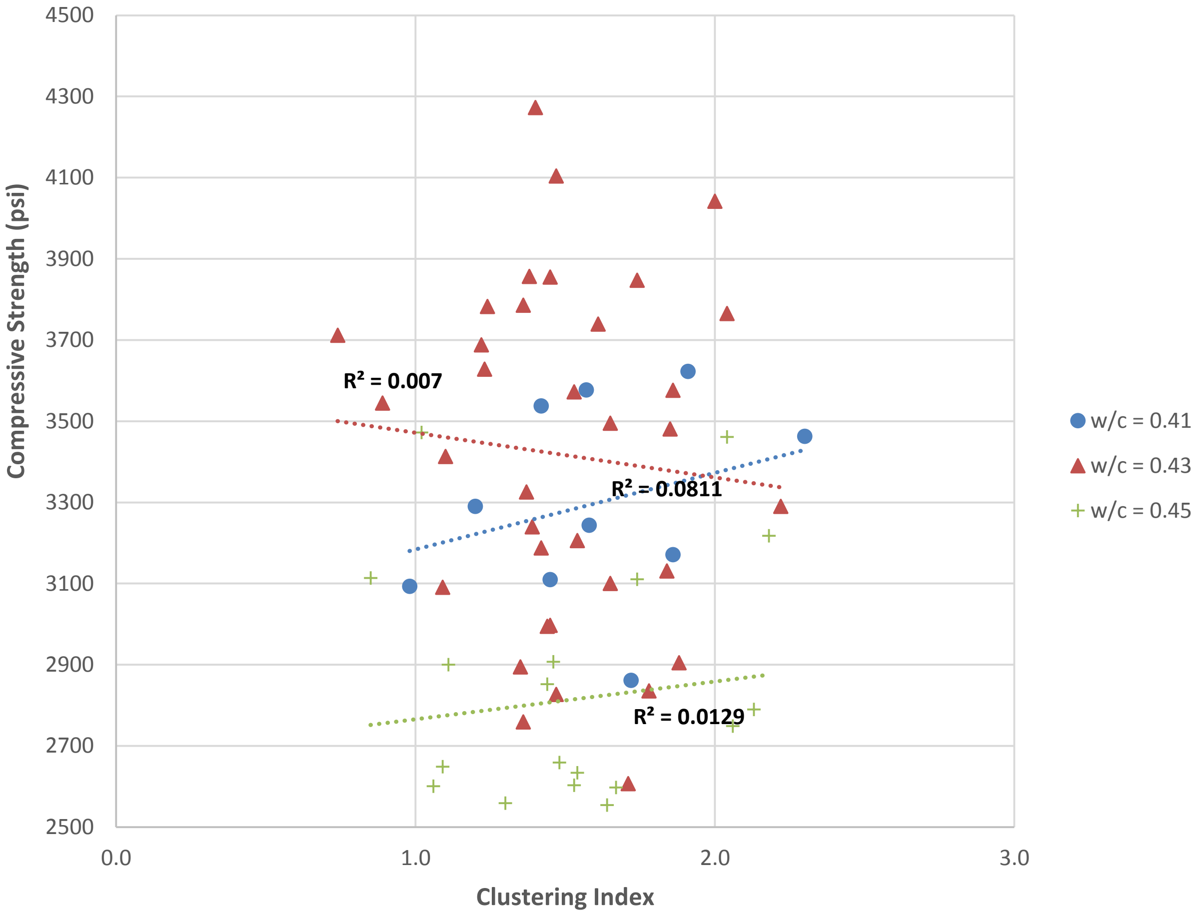

Figure 7-8: Clustering Index vs Compressive Strength at 7 days

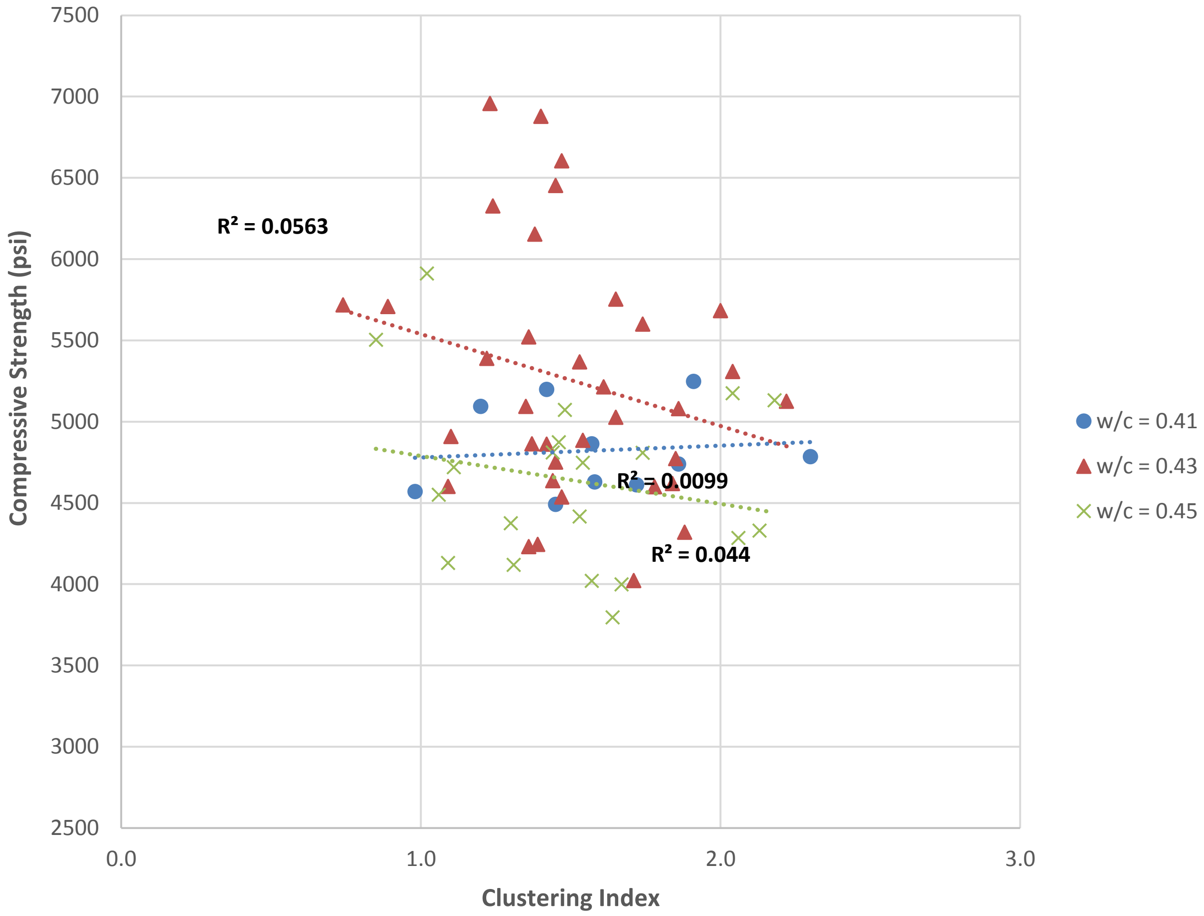

Figure 7-9: Clustering Index vs Compressive Strength at 28 days

On the other hand, a strong correlation was found between the air content and compressive strength for all mixes. Relationships are presented in Figure 7-10 and Figure 7-11 for data obtained at 7 and 28 days, respectively. The presented sample includes all mixes and considering the variability in material properties, different water-cement ratios as well as different chemical admixtures, values of the R^2 seem conclusive. Thus, it is more likely that the loss of compressive strength in mixes after retempering is rather a function of air content and water-cement ratio than the clustering rate.

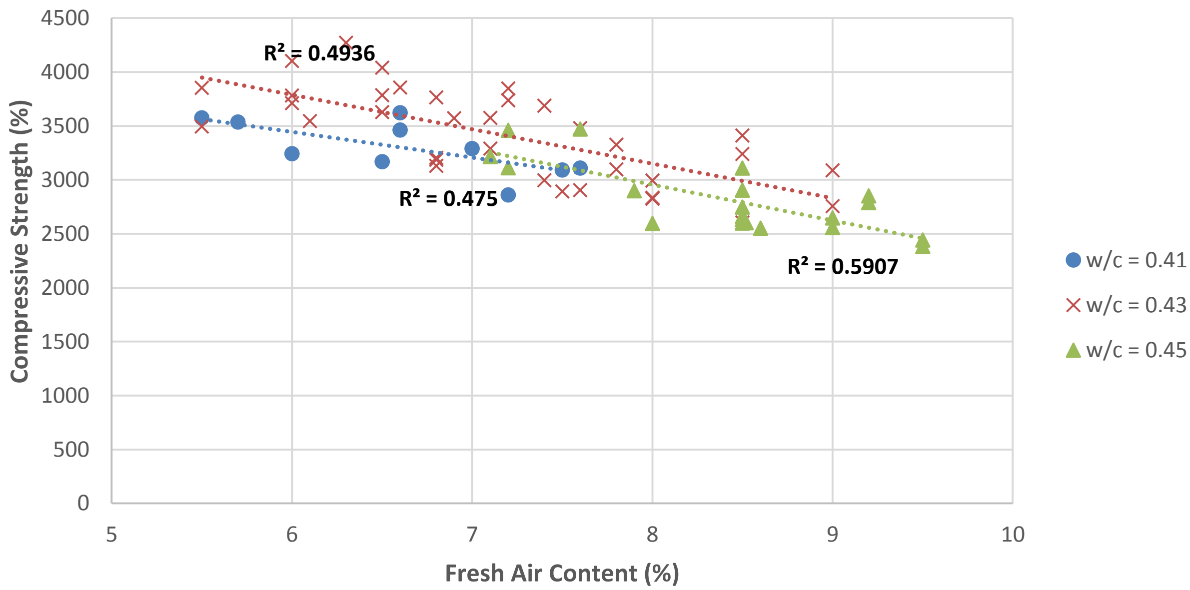

Figure 7-10: Fresh Air Content vs Compressive Strength at 7 days

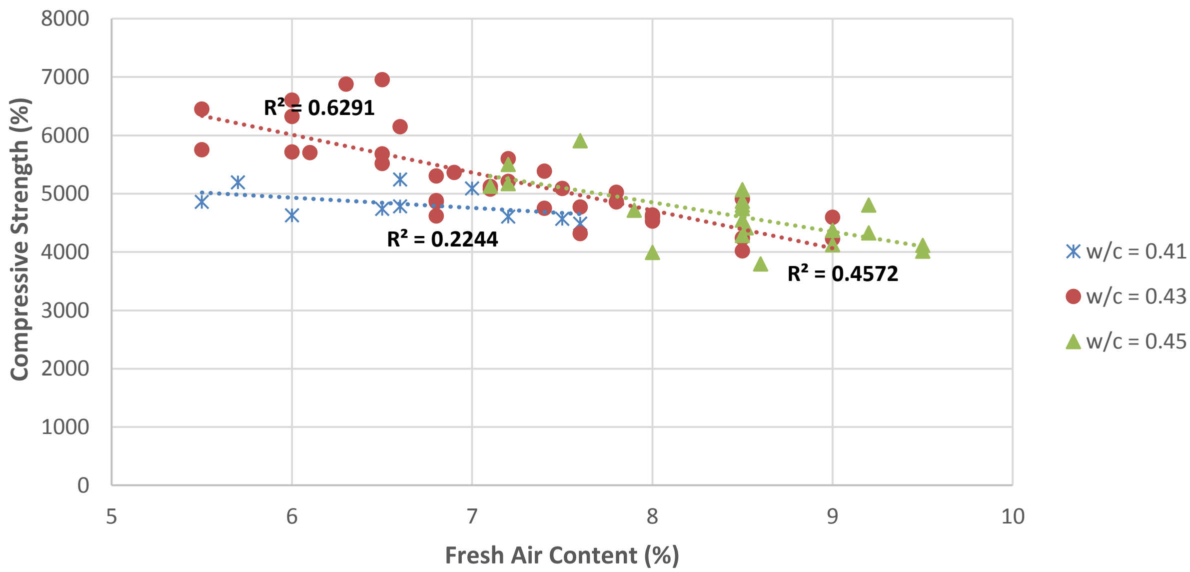

Figure 7-11: Fresh Air Content vs Compressive Strength at 28 days

7.2 Aggregate Type

Absolute difference in slump between retempered and non-retempered mixes is presented in Figure 7-12. Granite shows the highest average increase. This is not very surprising since Granite had the largest particles among tested aggregate types and it is well known that increase in aggregate size generally results in slump increase.

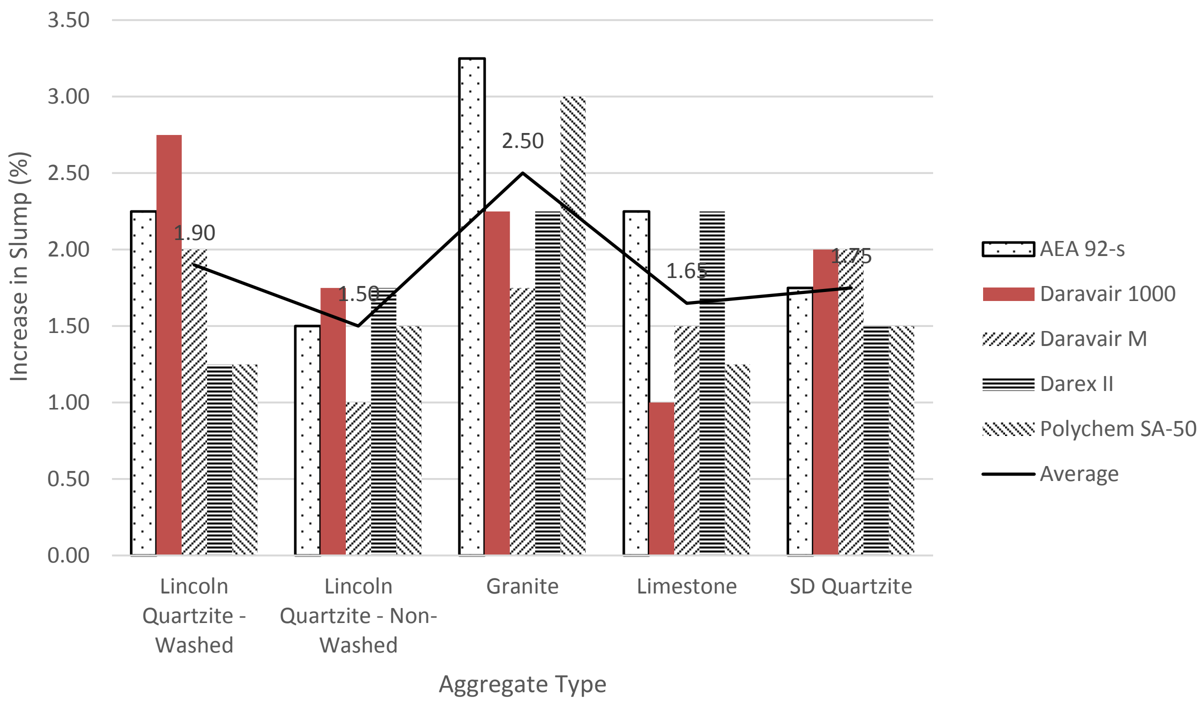

Figure 7-12: Slump Change after Retempering

Total air content is directly related to slump. Difference in the total air content before and after retempering with respect to used aggregate is shown in Figure 7-13. Results show that increase in total air content for mixes containing Lincoln Quartzite and Limestone were rather similar – in average 18%, 16%, and 20% for non-washed Quartzite, washed Quartzite and Limestone, respectively. However, mixes utilizing Granite and SD Quartzite, on the other hand, saw average increase in fresh air content of 41% and 33%, respectively.

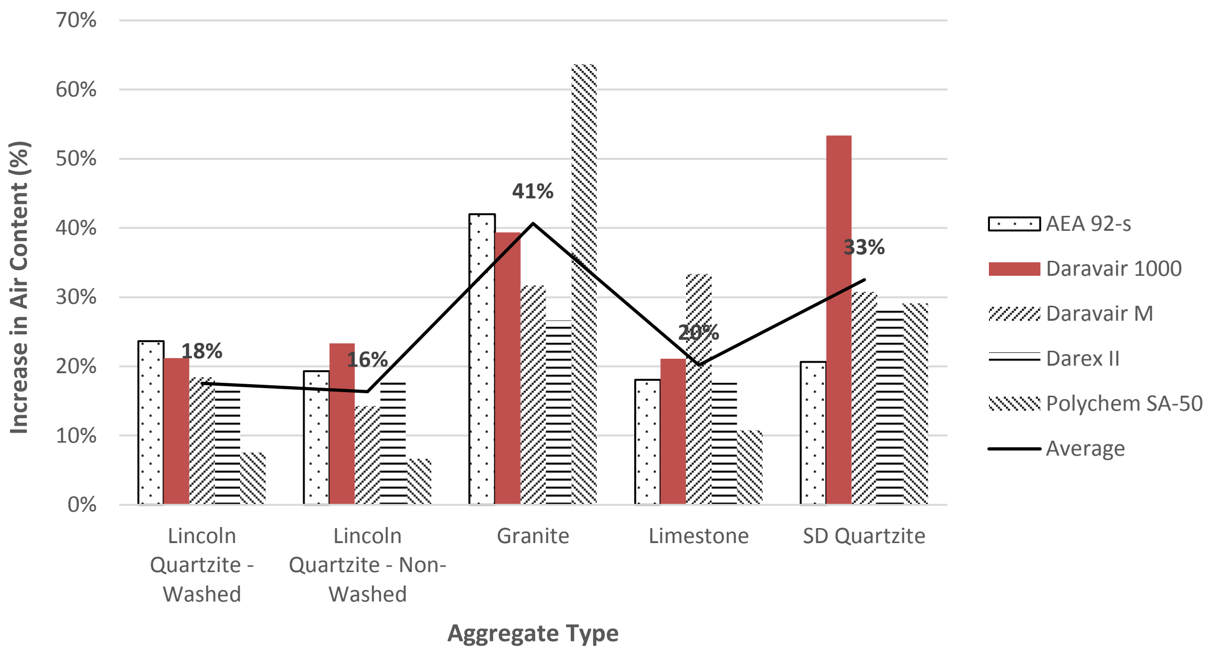

Figure 7-13: Increase in Air Content after Retempering by Aggregate Type

Clustering indexes split based on aggregate type are presented in Figure 7-14 - Figure 7-18. No particular trend on relationship in clustering that could be associated with the aggregate type was observed. This indicates that the aggregate itself has no or very little effect on formation of air void clusters around its particles.

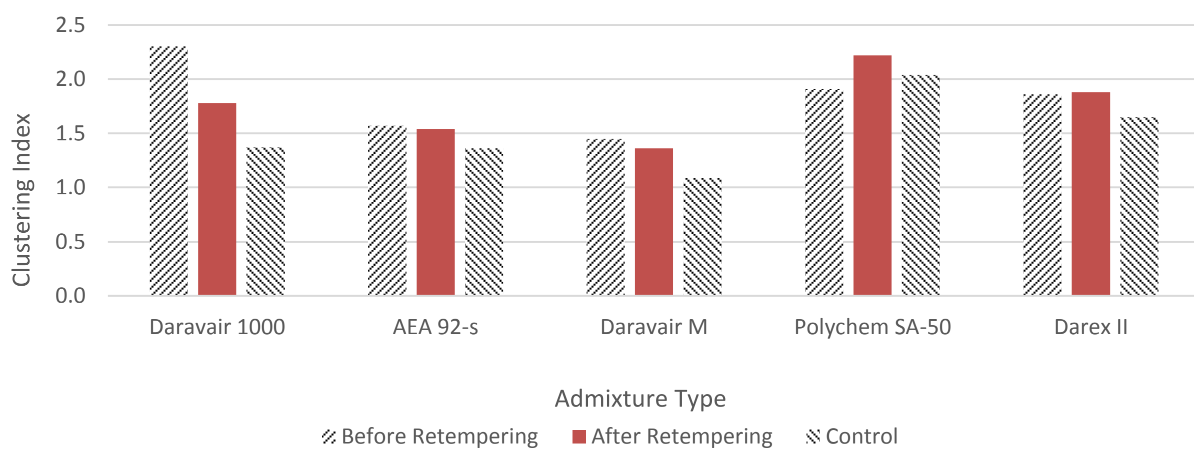

Figure 7-14: Clustering Index - Non-washed Lincoln Quartzite

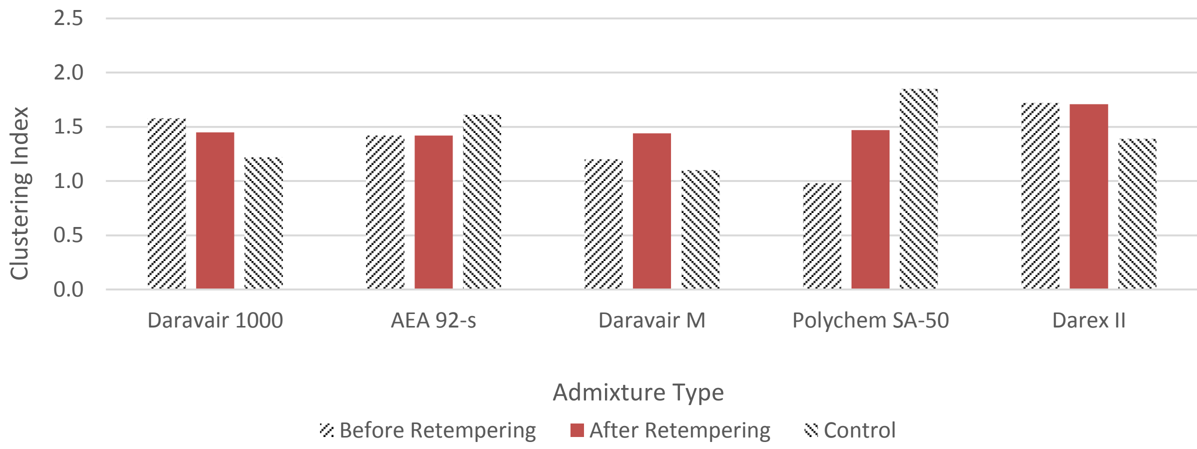

Figure 7-15: Clustering Index - Washed Lincoln Quartzite

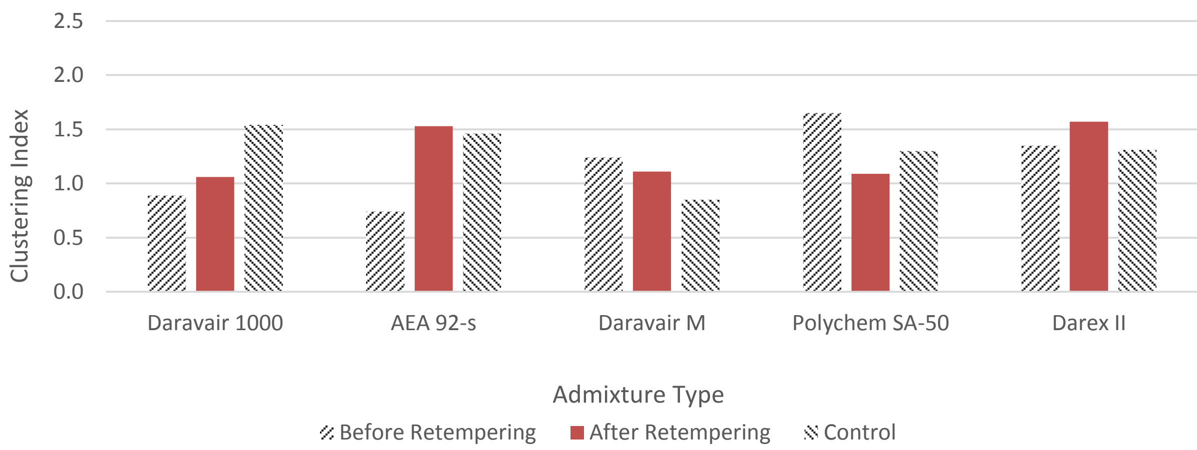

Figure 7-16: Clustering Index - Granite

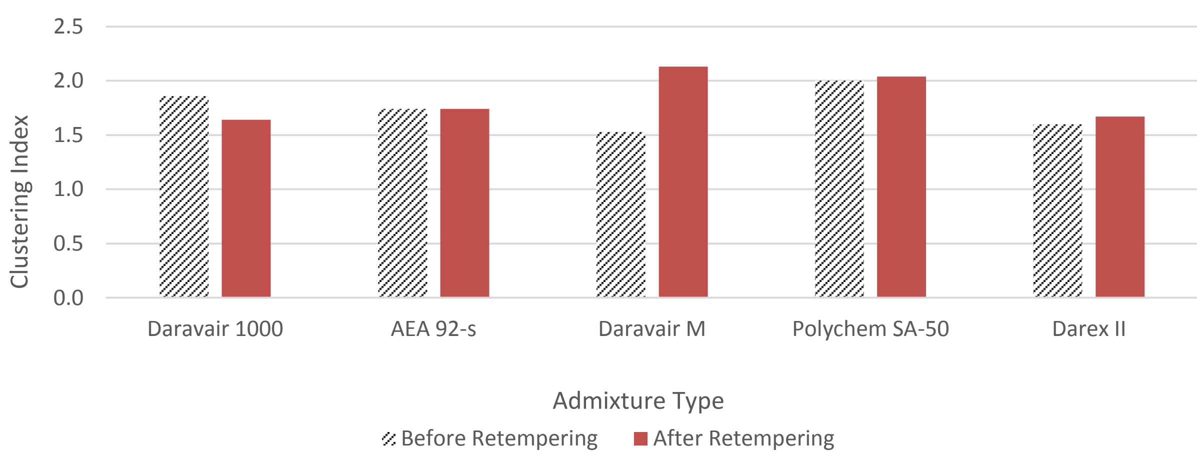

Figure 7-17: Clustering Index - Limestone

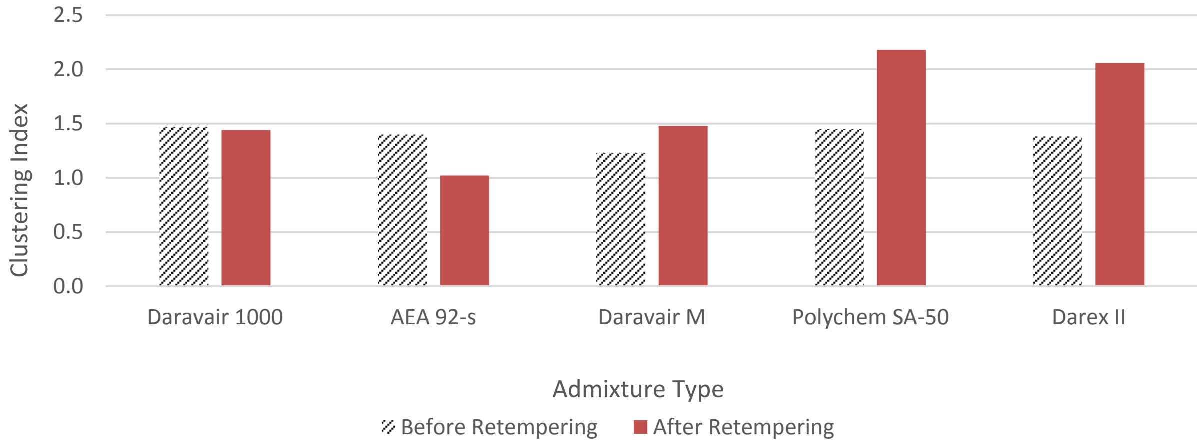

Figure 7-18: Clustering Index - SD Quartzite

Plots of changes in compressive strengths versus clustering indexes based on aggregate type are shown in Figure 7-19 - Figure 7-23. The highest R^2 value was seen for values of compressive strength at 7 days of non-washed Lincoln Quartzite (0.75). However, such a high correlation was only observed in this case, the other 9 sets of data does not indicated any significant relationship between clustering index and compressive strength values. This finding is accordance with the observation made the Subsection 0, namely that air void clustering has no effect on compressive strength. The effect the aggregate type has on the clustering rate and subsequently on the compressive strength seems to be alike.

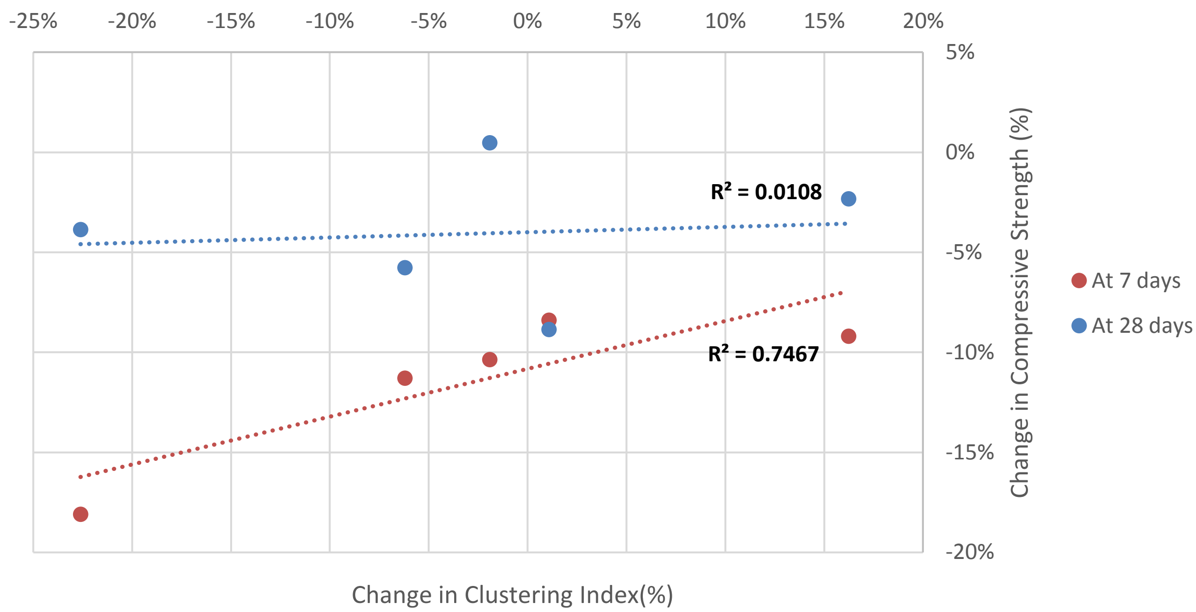

Figure 7-19: Clustering Index vs Compressive Strength - Non-washed Lincoln Quartzite

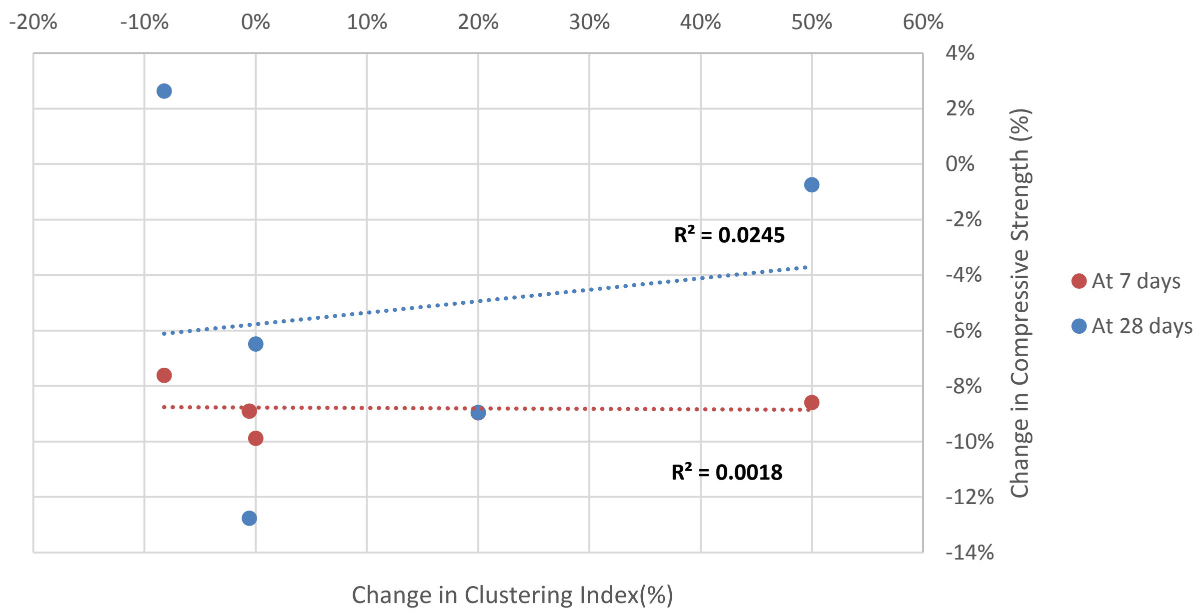

Figure 7-20: Clustering Index vs Compressive Strength - Washed Lincoln Quartzite

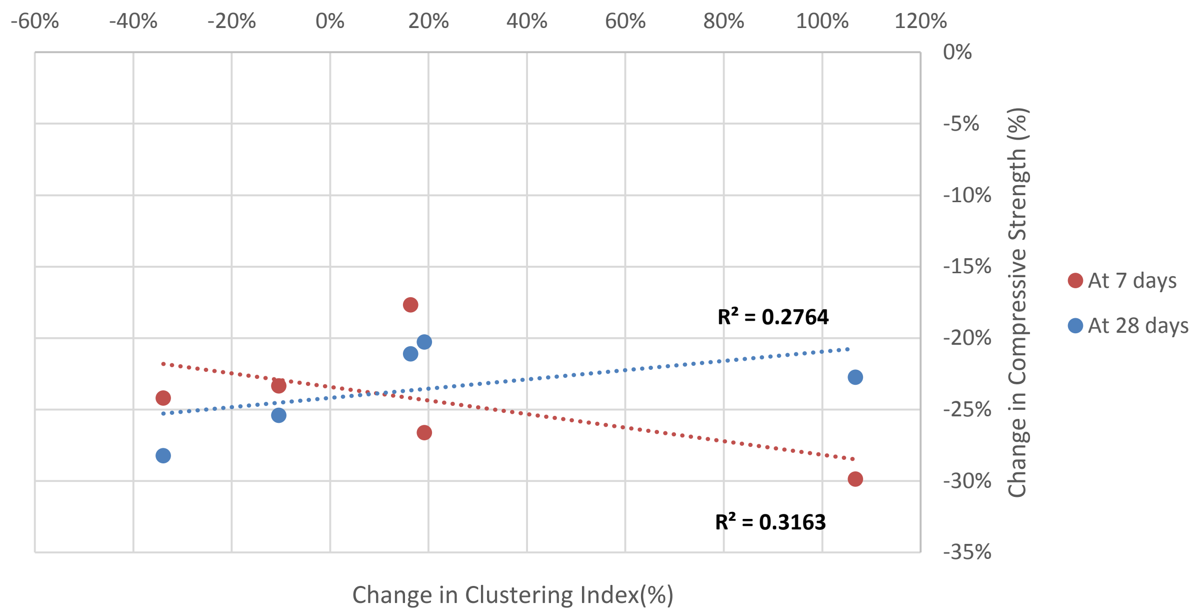

Figure 7-21: Clustering Index vs Compressive Strength - Granite

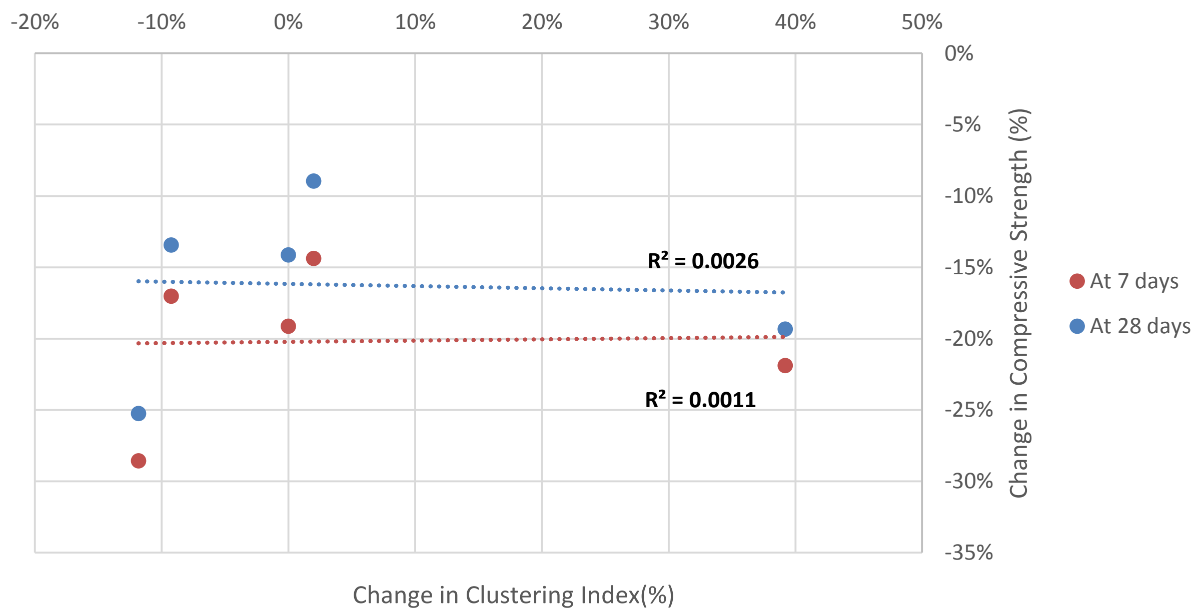

Figure 7-22: Clustering Index vs Compressive Strength - Limestone

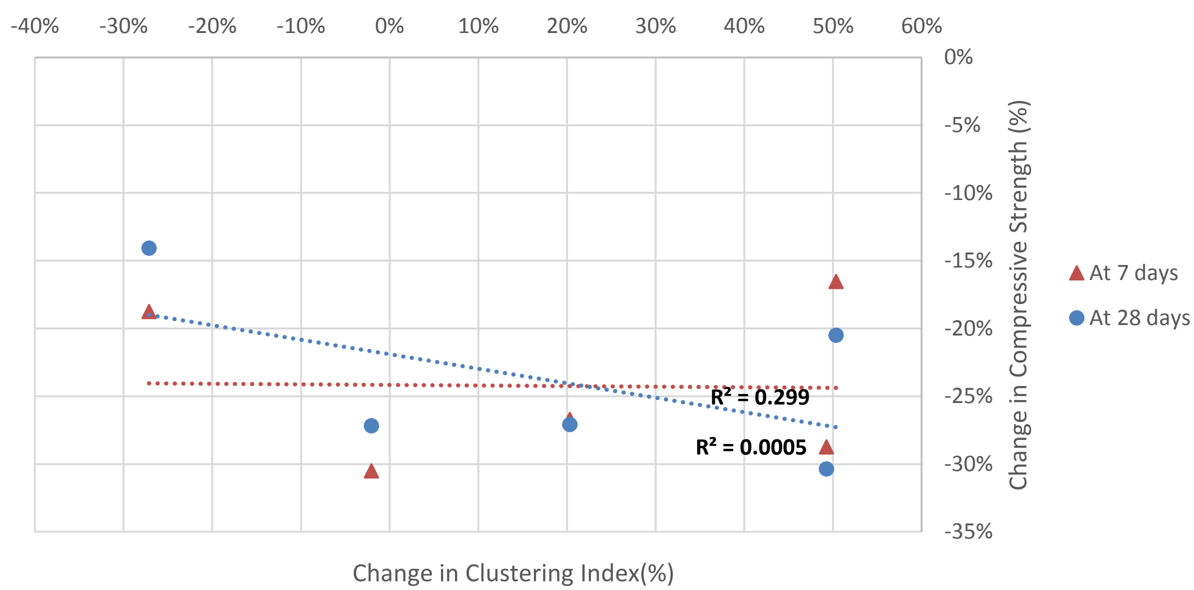

Figure 7-23: Clustering Index vs Compressive Strength - SD Quartzite

Concern with a performance of dirty Lincoln Quartzite was expressed by KDOT in the past and was one of the reasons why this study was conducted. Particularly, compressive strength samples from a pavement project in Kansas, which utilized non-washed Lincoln Quartzite, failed to meet the compressive strength requirements prescribed by KDOT. Several interesting observation regarding the behavior of washed and non-washed aggregate were made:

A lower dosage of air entraining admixture in mixes with washed aggregate was typically required to achieve the same air content as for the mixtures containing dirty rock, as shown in Figure 7-25. This was much expected as the dirty aggregate contains more fine particles and clay than washed rock, thus its specific surface is higher and potential for absorption by clay particles requires a higher dosage of AEA to achieve the same total air content.

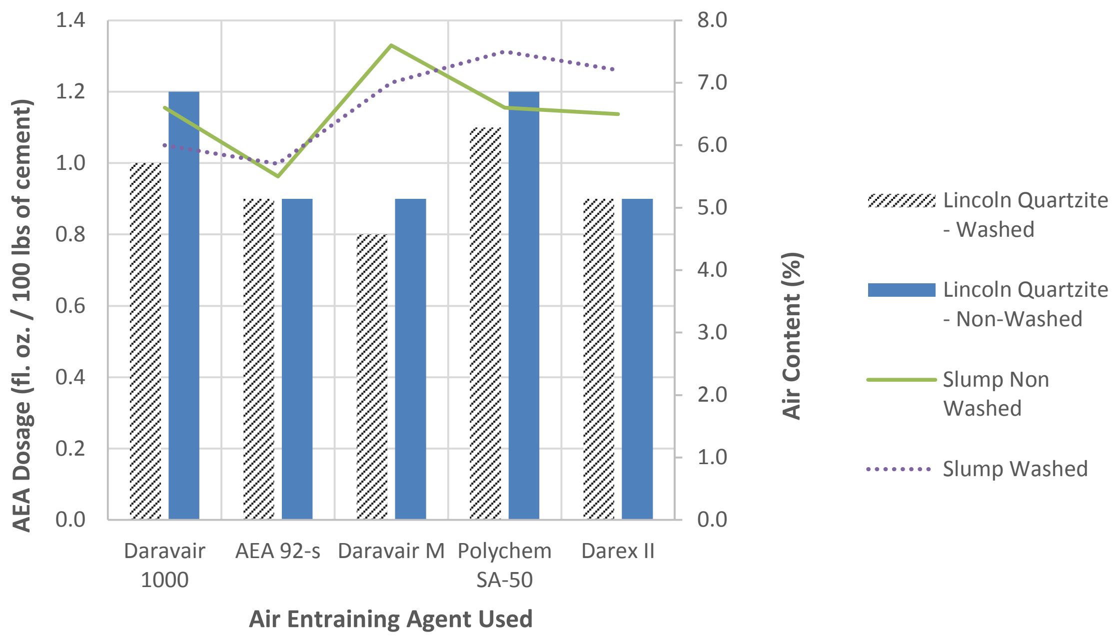

Figure 7-24: AEA Dosage vs Air Content - Lincoln Quartzite

As discussed in the Subsection 0, mixes with Lincoln Quartzite experienced lower increase in slump and air content after retempering than mixes containing the other types of coarse aggregate. This fact suggests that in order to restore the required workability of concrete with Lincoln Quartzite in the field utilizing the retempering technique, considerably higher amount of additional water would be needed. Therefore, the loss of compressive strength due to increased water to cement ratio could be higher as well.

Dark regions of higher cement paste density were observed in various mixes with Lincoln Quartzite. Those regions, typical for retempered concrete, are areas of higher cement concrete and thus lower water-to-cement ratio. If hydrated properly, these areas can be very strong. However, if dry cement particles are captured within those regions their compressive strength will be very low and the area will form a zone of weakness (Walker, Lane, & Paul, 2006). Examples of these zones observed in mixes with Lincoln Quartzite are presented in Figure 7-25 and their occurrence in particular mixes is summarized in Table 7-1.

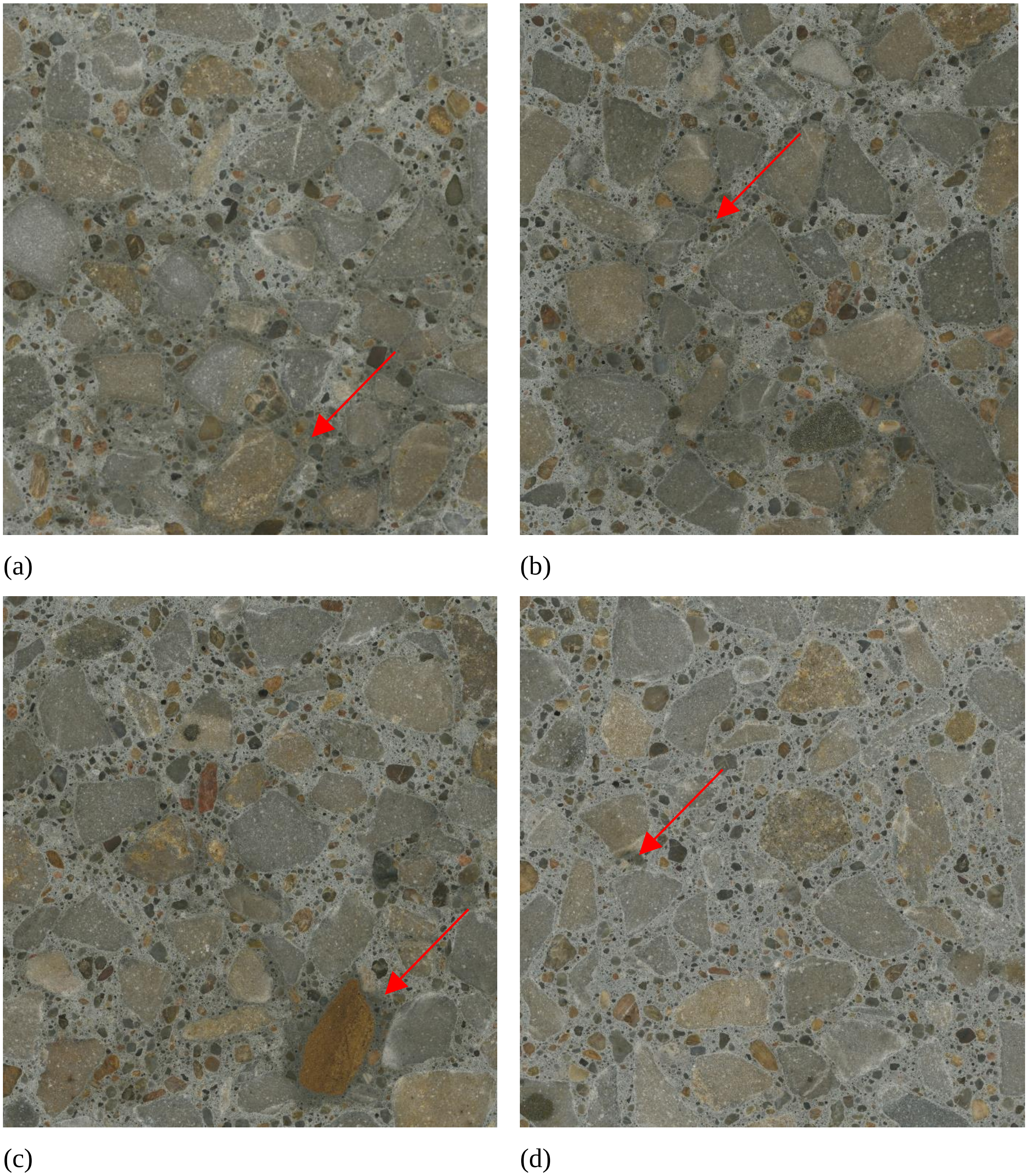

Figure 7-25: Lower Density Zones (a) 1-II-R, (b) 2-II-R, (c), 1-III-R, (d) 1-I-C.

Table 7-1: Low Density Zones in Lincoln Quartzite

Mix ID	High Density Zone	Mix ID	High Density Zone	Mix ID	High Density Zone
Before Retempering		After Retempering		Control	
1-I	Y	1-I-R	Y	1-I-C	N
1-II	N	1-II-R	N	1-II-C	Y
1-III	N	1-III-R	Y	1-III-C	N
1-IV	N	1-IV-R	Y	1-IV-C	N
1-V	N	1-V-R	N	1-V-C	Y
2-I	Y	2-I-R	Y	2-I-C	Y
2-II	Y	2-II-R	Y	2-II-C	Y
2-III	Y	2-III-R	N	2-III-C	Y
2-IV	Y	2-IV-R	Y	2-IV-C	Y
2-V	Y	2-V-R	N	2-V-C	Y

Note that high density zones were present in all non-retempered mixes with washed Lincoln Quartzite. This is very unusual as those zones are typically seen in retempered concrete and it suggests that Lincoln Quartzite as an aggregate can be generally susceptible to issues related with improper mixing. Although high density regions were observed in all control mixes with washed Lincoln Quartzite as well, their severity was significantly lower. This provides explanation for the unusual results of compressive strengths of control mixes. One would expect the compressive strength of control mixes to be lower than values of mixes before retempering as control mixes were produced with higher water-to-cement ratio. However, some of the measured values showed the opposite trend, which indicates that observed dark paste in non-retempered mixes would be those with higher amounts of non-hydrated cement particles, hence zones of weakness. This could result in lower compressive strength of those mixes and despite the fact that those zones were presented in control mixes as well, their contribution to the compressive strength of control mixes was most likely insignificant due to their lower intensity.

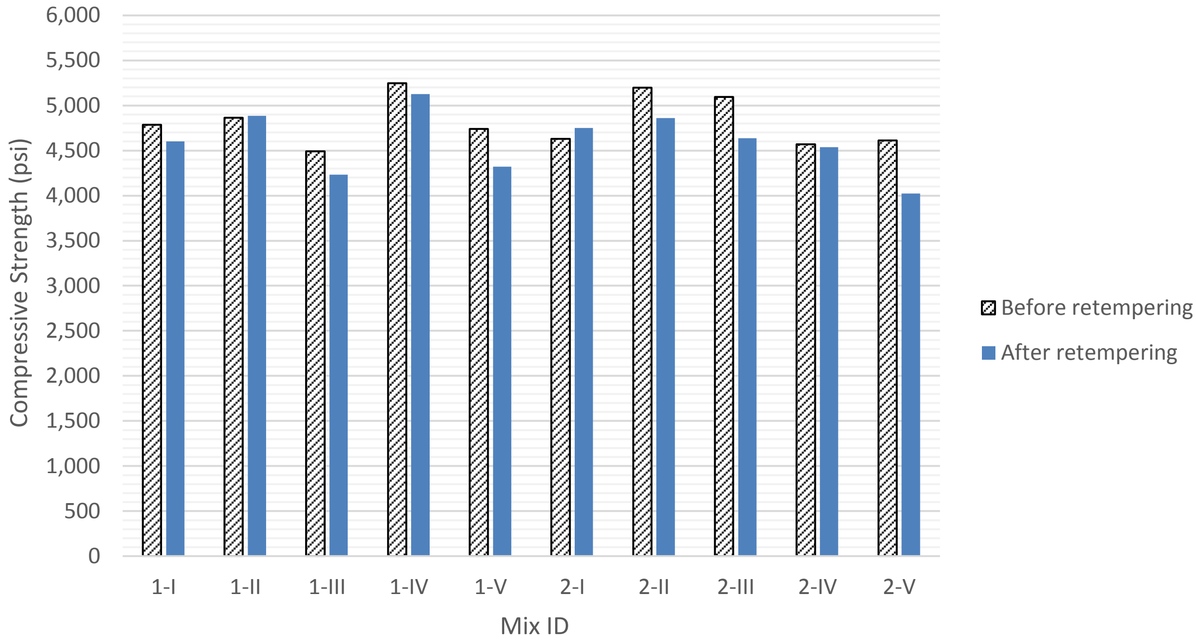

Figure 7-26: Compressive Strength - Lincoln Quartzite

Presence of low strength zones and lower dosages of AEA required to achieve similar fresh concrete properties for clean aggregate could provide explanation of low compressive strength issues experienced by KDOT. First, if the dirty aggregate is used in concrete, it is very likely that locally some of the aggregate will be cleaner than the rest of the material (for example if stored outdoors, rain can easily wash the upper layer of the aggregate pile). Those zones can then experience higher air content, hence lower compressive strength might occur.

At the same time, those "clean zones" can also experience issues related to the improper mixing of cement and water, so not only regions with higher air content, but also regions of higher cement content can be formed. Those two factor combined together could lead to the values of low compressive strengths.

7.3 Type of Air Entraining Agent

Figure 7-27 and Figure 7-28 show increase in slump and air content after retempering, respectively, with respect to the air entraining agent used. It is evident that all used AEA performed rather similarly, as the average increase in slump varied from 1.6 in to 2.1 in as well as the increase in the fresh air content after retempering ranged from approximately from 20% to 30%. Presented data suggests that the effectiveness of retempering is more dependent on type of used aggregate (as discussed in the Subsection 0), rather than on the chemical composition of air entertainer.

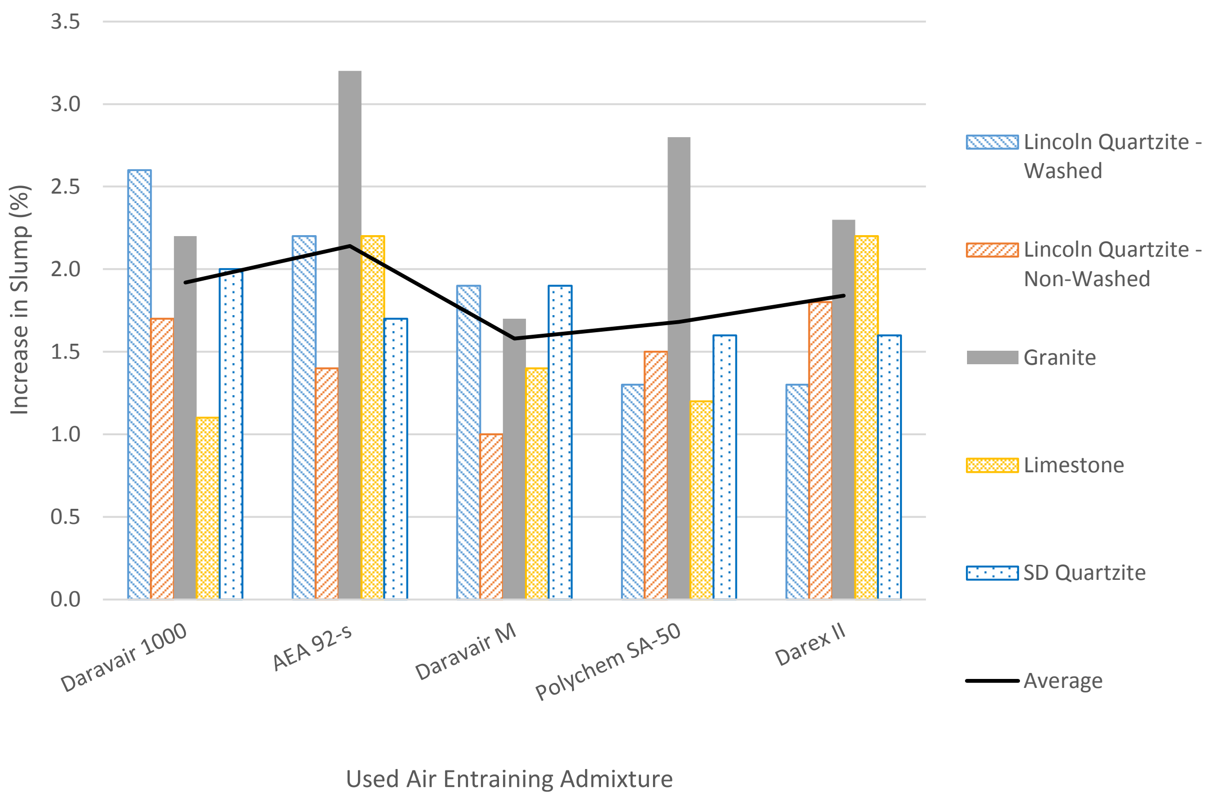

Figure 7-27: Increase in Slump After Retempering by Used AEA

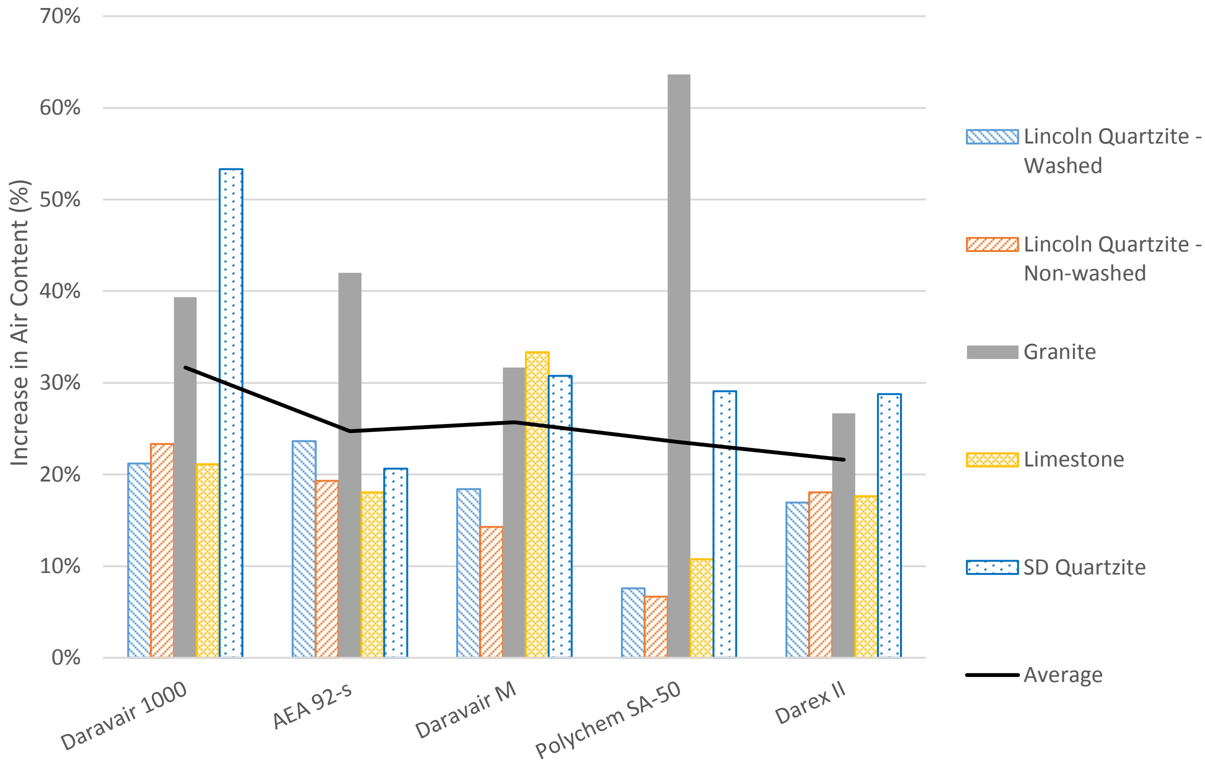

Figure 7-28: Increase in Air Content after Retempering by Used AEA

As shown in Figure 7-29 through Figure 7-33, values of clustering index were not typically affected by the type of used air entraining admixture. Polychem SA-50 showed the highest average values of the clustering index (Figure 7-34), however the difference with respect to the other air entraining admixtures was very small. Thus, it is evident that type of the AEA that is used to generate the air void system has no significant effect on the clustering rate. This is quite surprising finding since the synthetic (non-vinsol resin) air entraining agents were often blamed for air void clustering in retempered mixes. AEA-92S (*Euclid Chemical)* was chosen as a representative of the non-organic group of AEAs in this study. Contrary to the popular belief, this admixture performed rather well as it in 4 out of 5 cases the overall clustering index decreased after retempering. In fact, no other admixture showed better results than this synthetic AEA.

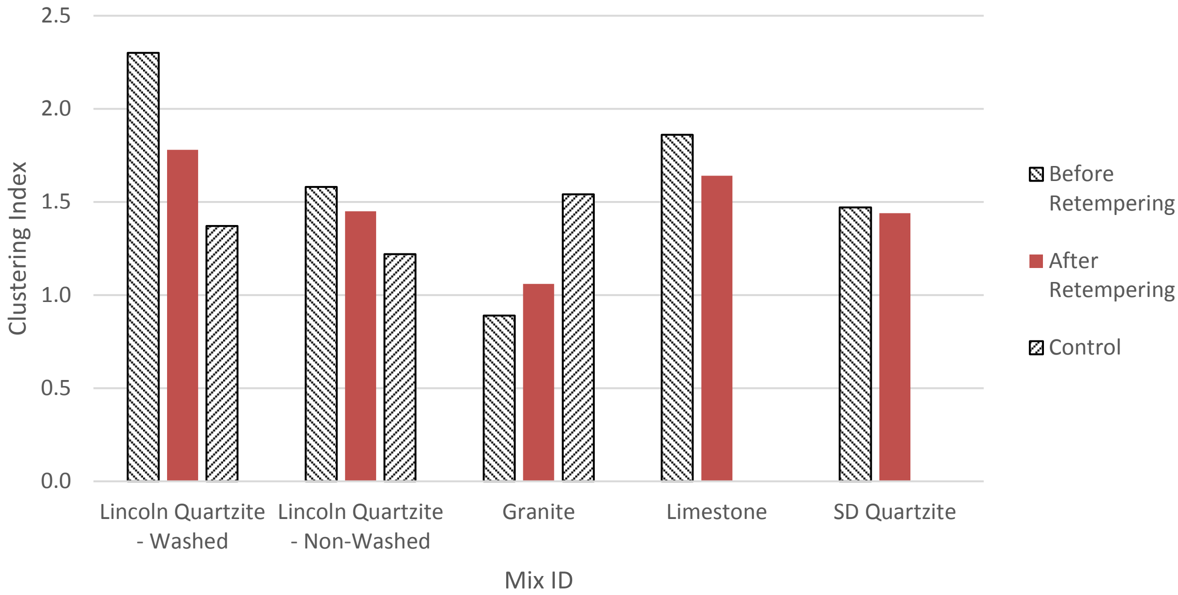

Figure 7-29: Clustering Index - Daravair 1000

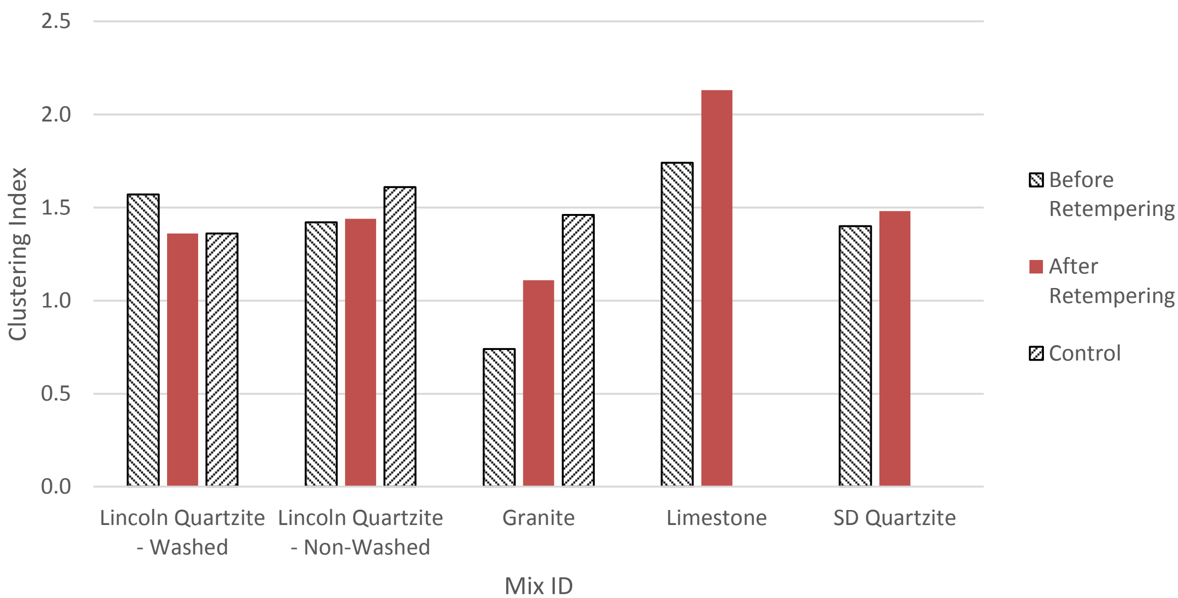

Figure 7-30: Clustering Index - AEA-92S

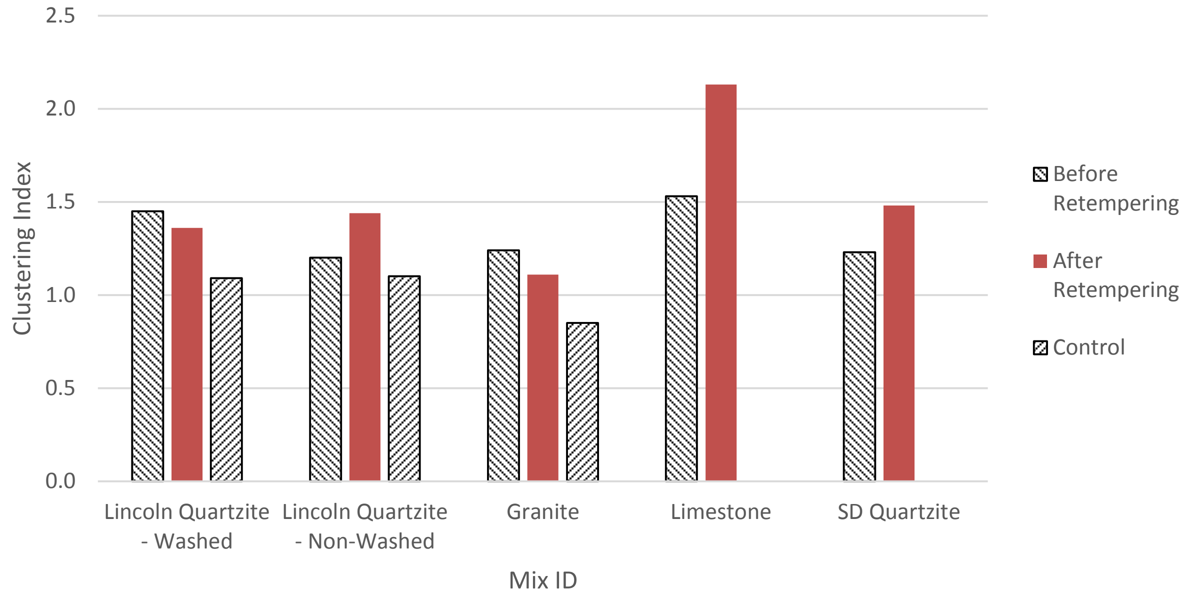

Figure 7-31: Clustering Index - Daravair M

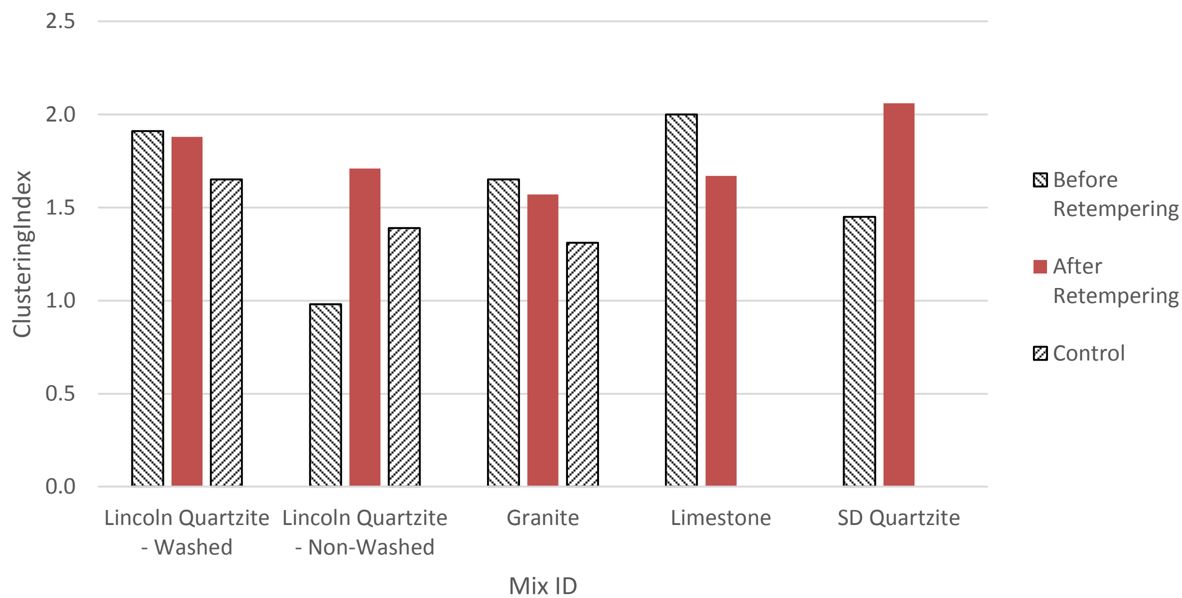

Figure 7-32: Clustering Index - Polychem SA-50

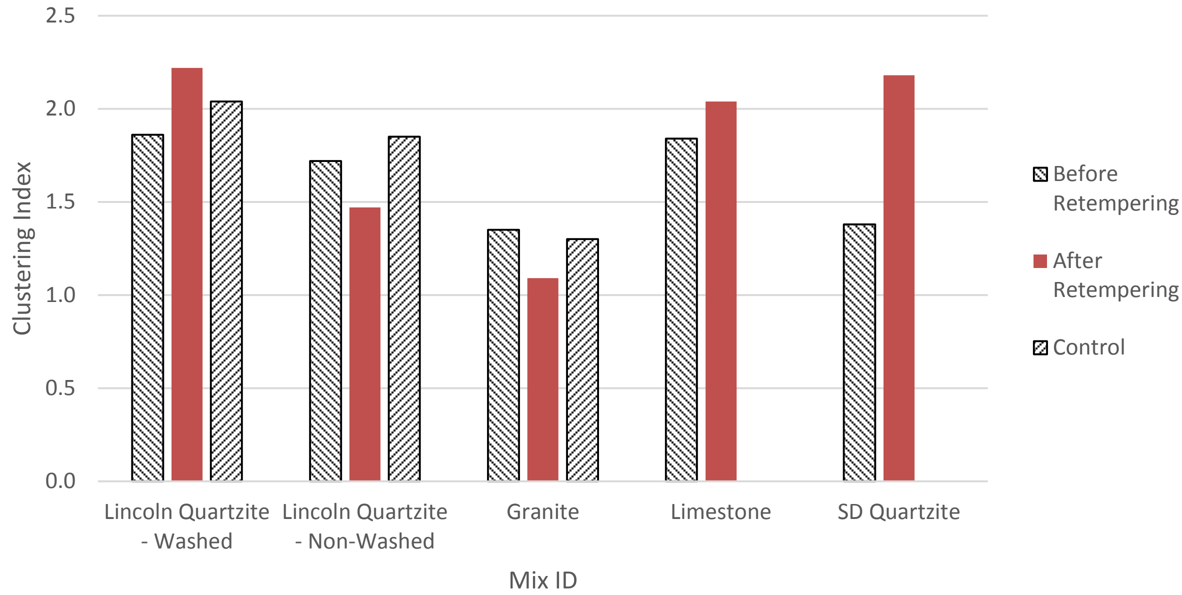

Figure 7-33: Clustering Index - Darex II

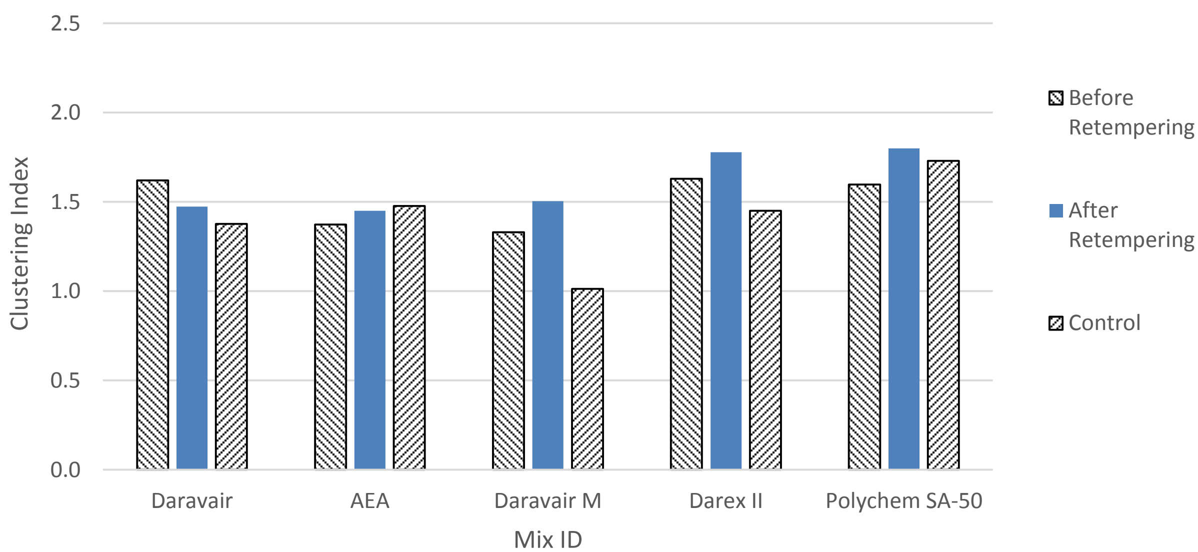

Figure 7-34: Clustering Index - Average by AEA

The relationship between change in the compressive strength at 28 days and change in the clustering index by the type of used air entraining admixture is presented in Figure 7-35 - Figure 7-39. No apparent trend was observed besides for Daravair 1000, AEA92-S, Daravair M, and Polychem SA-50. Nevertheless, value of the R^2 factor for Darex II was found to be 0.824, which could indicate there is a strong correlation between clustering and compressive strength for this particular admixture. However, since only 5 data points were available for the regression analysis, other factors were investigated as to confirm that the compressive strength is solely dependent on the clustering rate. It was found that even stronger relationship exist between the fresh air content and the compressive strength at 28 days for Darex II, as presented in Figure 7-40 This is in accordance with findings relating air content and compressive strength that were discussed in the Subsection 0 and thus it seems that the air content is really the main factor affecting the compressive strength.

Figure 7-35: Compressive Strength vs Change in Clustering Index - Daravair 1000

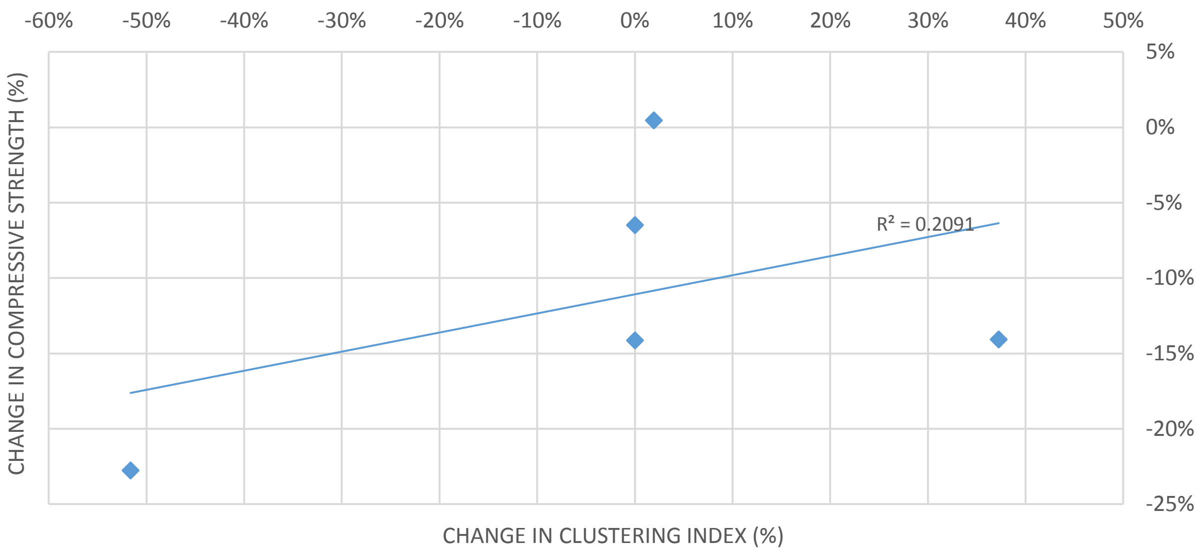

Figure 7-36: Compressive Strength vs Change in Clustering Index - AEA-92S

Figure 7-37: Compressive Strength vs Change in Clustering Index - Daravair M

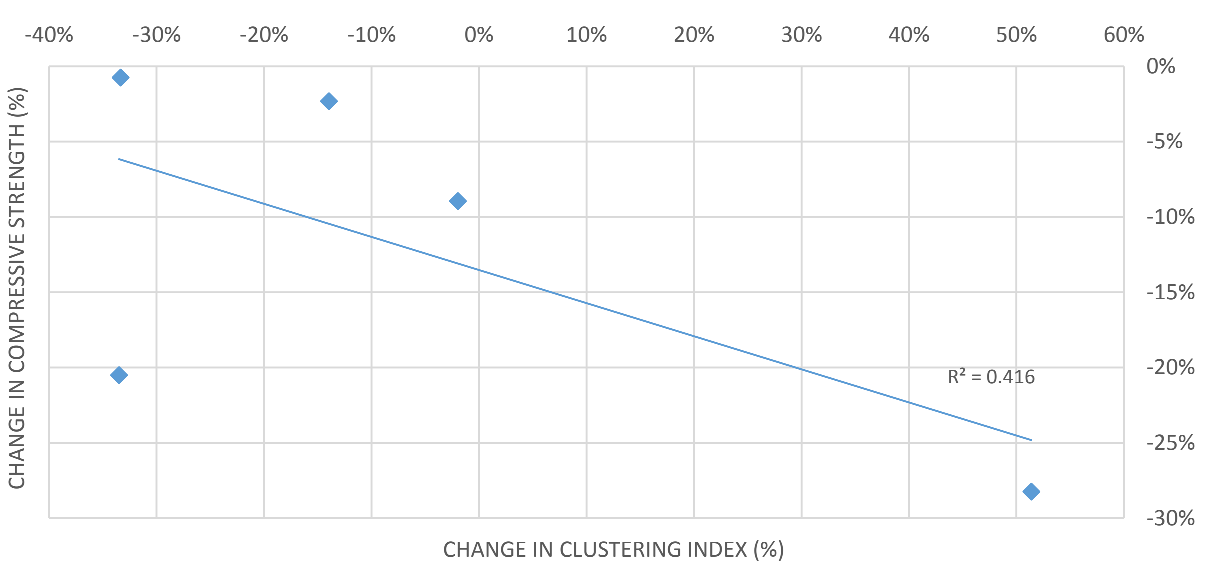

Figure 7-38: Compressive Strength vs Change in Clustering Index - Polychem SA-50

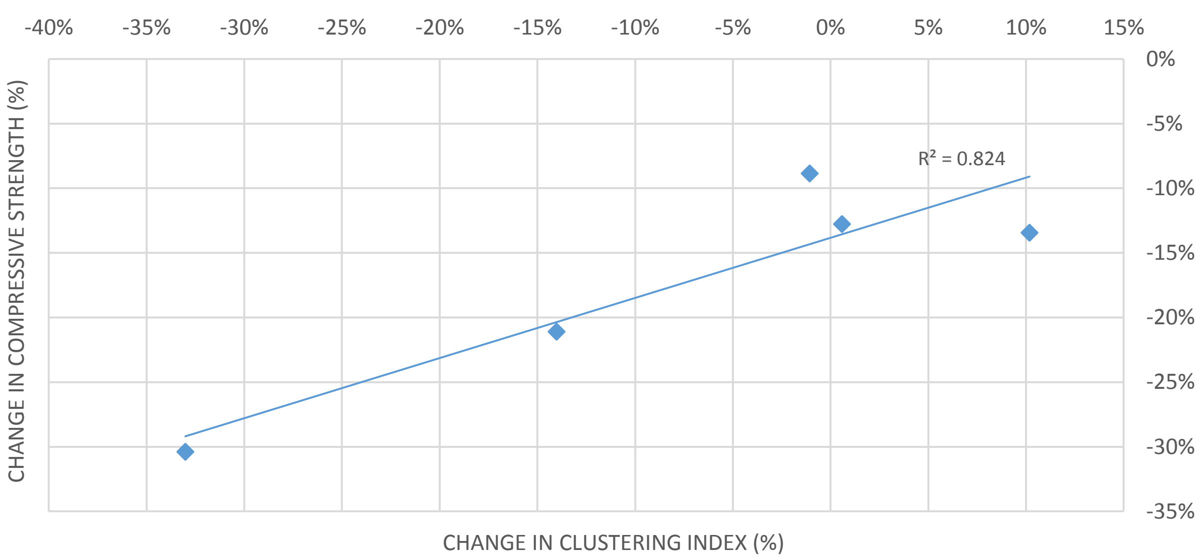

Figure 7-39: Compressive Strength vs Change in Clustering Index - Darex II

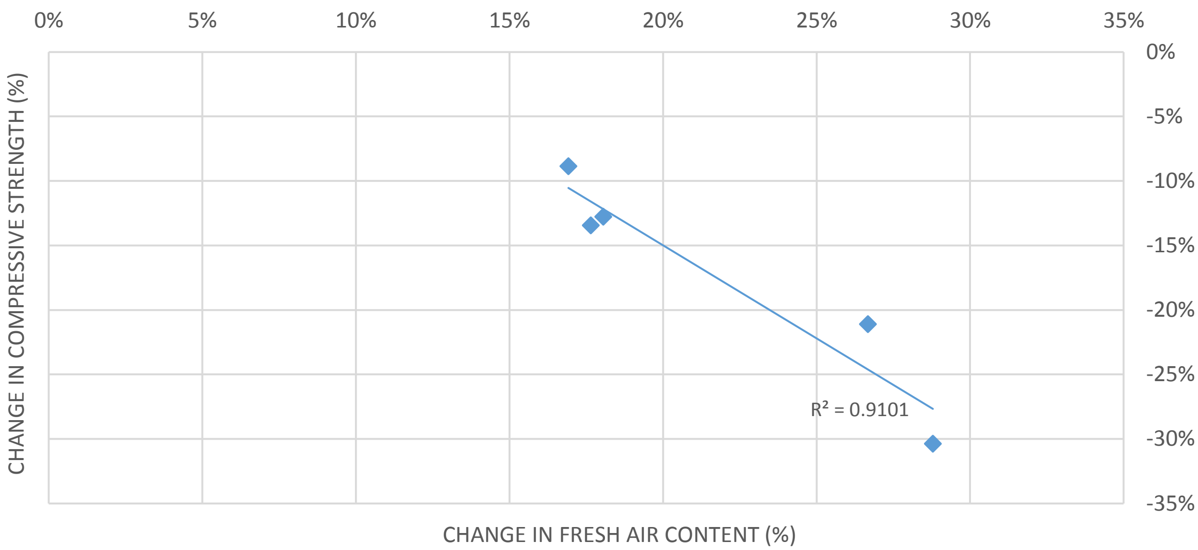

Figure 7-40: Compressive Strength vs Change in Fresh Air Content

7.4 Visual Rating of Air Void Clustering

In addition to the clustering analysis using the image processing techniques, visual evaluation following the procedure developed by Kozikowski et al. (2005) was carried out. It is evident that results of this analysis are inconsistent with the automated analysis, as shown in Figure 7-41. The results of manual evaluation followed, in most of the cases, the expected trend of higher clustering rate in retempered concrete. However, the evaluation has been assembled based on a visual investigation with a reference frame that has been not defined, thus it was found that the manual analysis is rather subjective. Furthermore, it is more likely that for systems with higher air contents, a human operator might tend to overrate the level of clustering present due to increased presence of air voids in cement paste. As all retempered samples had higher total air content that samples taken before retempering, this observation would help explain the differences in the two performed analyses.

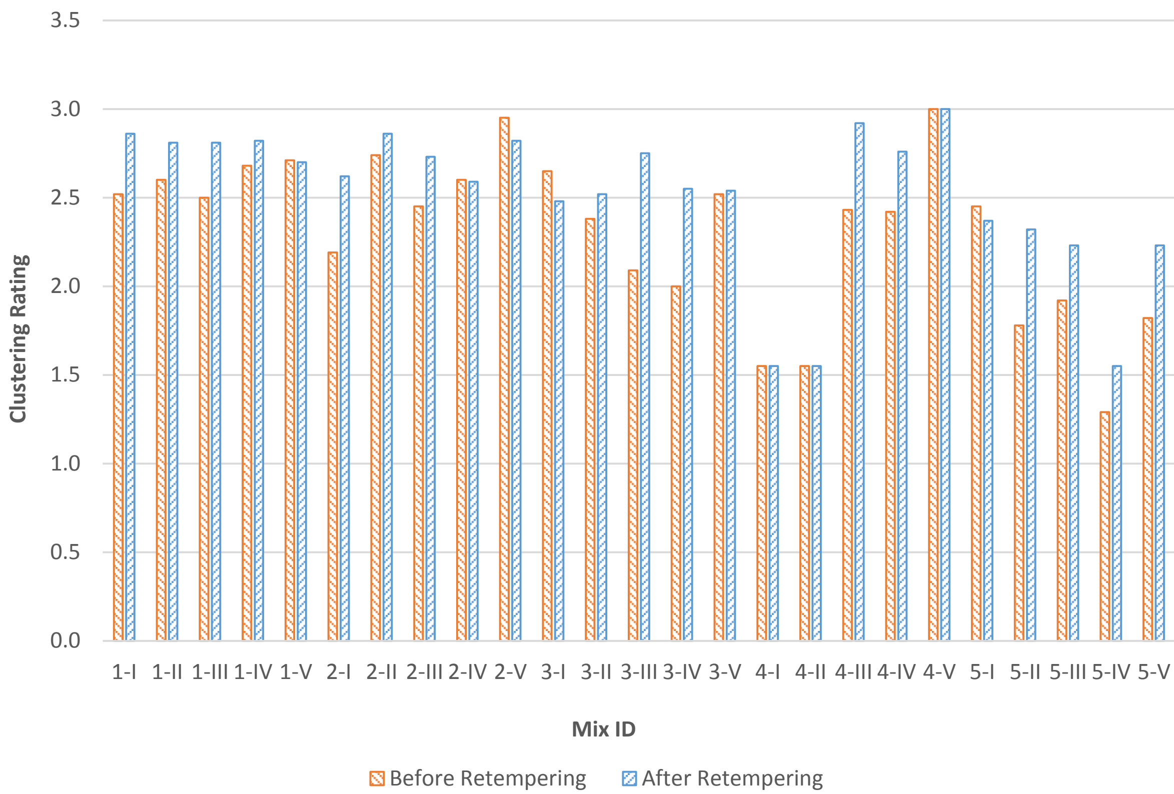

Figure 7-41: Visual Clustering Evaluation

7.5 Field Testing

Results obtained from the field testing correspond to what was found in the laboratory environment. Increases in fresh concrete properties (slump, air content) in mixes after retempering occurred in both case. Samples obtained from Site I, where concrete was retempered with only 1 gallon of mixing water per cubic yard, experienced smaller change than samples from Site II. The hardened air void content followed a similar pattern as a very small change in the air content (7.99% vs 8.04%) was observed in mixes from Site I.

As for the clustering activity, retempering in both cases did not cause any significant increase in the clustering index. Again, the change in the clustering rate before and after water addition was higher for samples from Site II, however it was still insignificant (change from 0.87 to 1.06). MasterAir AE 90 (formerly MB-AE 90) air entraining admixture was used. Although this admixture is rosin-based (organic), the manufacturer warns regarding the possibility of air void clustering in the product information sheet as some clustering concerns were raised in the past (Kozikowski, David, Peter, & Steven, 2005). However, those concerns were not found to be justified for mixes used in this study.

Compressive strength at 7 days decreased by 11% in both cases, and by 11% and 14% at 28 days for the Site I and Site II samples, respectively. These values are in the range that were observed in laboratory study and occurred because of the increase in w/c and retempering and not air void clustering. It is interesting to see almost a uniform strength drop although the amount of retempering water was different for Site I and Site II. However, caution should be exercised in drawing too strong of conclusions from this because of the small sample size (two field sites).

Chapter 8 - Conclusions and Recommendations

8.1 Conclusions

Based on the results presented and discussed in two previous sections, the following conclusions have been made:

(1) Air void clustering is reproducible in the laboratory environment as it was observed in several mixes. The highest value of the clustering index was 2.3 and 2.2 for mixes before and after retempering, respectively.

(2) A correlation between the air void clustering and compressive strength was not found. Instead, the loss in compressive strength after retempering seems to be simply a function of air void content and water-to-cement ratio.

(3) Air void clustering was not significantly affected by retempering. 10 out of 25 mixes experience decrease in clustering activity after retempering, and only a small increase was observed in the remaining 15 mixes.

(4) Granite and SD Quartzite showed higher increase in both slump and air content after retempering than other aggregates. Lincoln Quartzite, on the other hand, experienced lower increase in slump and air content after retempering than mixes containing the other types of coarse aggregate. This fact suggests that in order to restore the required workability of concrete with Lincoln Quartzite in the field utilizing the retempering technique, considerably higher amount of additional water would be needed. Therefore, the loss of compressive strength due to increased water to cement ratio could be higher as well.

(5) High density zones of cement paste were observed in mixes with Lincoln Quartzite, especially mixes that utilized washed aggregate experience occurrence of those zones. Presence of those zones could explain low compressive strengths experienced in some projects where Lincoln Quartzite was used.

(6) Lower dosage of AEA was found to be required for clean Lincoln Quartzite to achieve the same level of workability as the non-washed aggregate.

(7) The hypothesis that retempering of concrete with non-organic air entraining admixture will cause air void clustering was not confirmed. In fact, AEA-92S, synthetic air entraining agent used in the study, showed the best performance of all used AEAs as 4

out 5 mixes with this admixture experienced decrease in clustering index after retempering.

(8) Kozikowki's visual rating of air void clustering was in disagreement with the automated, analytical method developed and implemented as part of the KSU Air Void Analyzer software. Visual evaluation led to biased results, and it seems that air void clustering tends to be overrated in concrete systems with high air content if this method is used.

(9) Concrete obtained from real pavement projects shown similar behavior as concrete prepared under laboratory conditions.

8.2 Recommendations

Lincoln Quartzite showed some behavior different than other aggregates (high density paste zone, low increase in slump and air content after retempering). Retempering of concrete with Lincoln Quartzite should be avoided.

8.3 Future Research Needs

(1) The effect of temperature on the clustering of air voids is still unclear. Further research investigating this factor is needed to better understand the phenomena of air void clustering.

(2) Fine aggregate is known to have strong impact on performance of air entraining agents, thus its effect on air void clustering and retempering should be scrutinized.

(3) Further testing of Lincoln Quartzite, especially with focus on the formation of high density paste zones, is needed.

References

ASTM C1231. (2014). Standard Practice for Use of Unbonded Caps in Determination of Compressive Strength of Hardened Concrete Cylinders. West Conshohocken, PA: ASTM International.

ASTM C127. (2012). Standard Test Method for Density, Relative Density (Specific Gravity), and Absorption of Coarse Aggregate. West Conshohocken, PA: ASTM International.

ASTM C128. (2012). Standard Test Method for Density, Relative Density (Specific Gravity), and Absorption of Fine Aggregate. West Conshohocken, PA: ASTM International.

ASTM C136. (2006). Standard Test Method for Sieve Analysis of Fine and Coarse Aggregates. West Conshohocken, PA.

ASTM C138. (2012). Standard Test Method for Density (Unit Weight), Yield, and Air Content (Gravimetric) of Concrete. West Conshohocken, PA: ASTM International.

ASTM C143. (2012). Standard Test Method for Slump of Hydraulic-Cement Concrete. West Conshohocken, PA: ASTM International.

ASTM C172. (2010). Standard Practice for Sampling Freshly Mixed Concrete. West Conshohocken, PA: ASTM International.

ASTM C173. (2014). Standard Test Method for Air Content of Freshly Mixed Concrete by the Volumetric Method. West Conshohocken, PA: ASTM International.

ASTM C192. (2013). Standard Practice for Making and Curing Concrete Test Specimens in the Laboratory. West Conshohocken, PA: ASTM International.

ASTM C231. (2010). Standard Test Method for Air Content of Freshly Mixed Concrete by the Pressure Method. West Conshohocken, PA: ASTM International.

ASTM C31. (2012). Standard Practice for Making and Curing Concrete Test Specimens in the Field. West Conshohocken, PA: ASTM International.

ASTM C39. (2012). Standard Test Method for Compressive Strength of Cylindrical Concrete Specimens. West Conshohocken, PA: ASTM International.

ASTM C457. (2012). Microscopical Determination of Parameters of the Air-Void System in Hardened Concrete. West Conshohocken, PA: ASTM International.

Chatterji, S. (2003). Freezing of Air-Entrained Cement-Based Materials and Specific Actions of Air-Entraining Agents. Cement and Concrete Composites, 25(7), 759-765.

Cross, W., Duke, E., Kellar, J., & Johnston, D. (2000). Investigation of Low Compressive Strengths of Concrete Paving,. Pierre, SD: South Dakota Department of Transportation.

Distlehorst, J. (2009). Evaluation of Air-Void Clustering in Concrete Pavement from Meade, Kansas. Topeka, KS: Kansas Department of Transportation.

Du, L., & Folliard, K. J. (2005). Mechanism of Air Entrainment in Concrete. Cement and Concrete Research, 1463-1471.

Garboczi, E. J., Bentz, D. P., Snyder, K. A., Martys, N. S., Stutzman, P. E., Ferraris, F. C., & Bullard, J. W. (2014). An Electronic Monograph: Modeling and Measuring the Structure and Properties of Cement-Based Materials. Gaithersburg, MD: Materials and Structural Systems DIvision, National Institute of Standards and Technology. Retrieved from http://ciks.cbt.nist.gov/~garbocz/

Kansas Department of Transportation. (2007). Standard Specifications For State Road & Bridge Construction. Division 400 - Concrete. Topeka, KS: Kansas Department of Transportation.

Kansas Department of Transportation. (2014). List of Non-Reactive Siliceous Aggregate Sources for Concrete (Revised 04/25/14). Topeka, KS: Kansas Department of Transportation.

Kosmatka, S. H., Kerkhoff, B., & Panarese, W. C. (2003). Design and Control of Concrete Mixtures (14th ed.). Skokie, IL: Portland Cement Association.

Kozikowski, R. L., David, B. V., Peter, C. T., & Steven, H. G. (2005). Factors Affecting the Origin of Air-Void Clustering. (PCA R&D Serial No. 2789). Skokie, Illinios: Portland Cement Association.

Ley, T. (2007). The Effects of Fly Ash on the Ability to Entrain and Stabilize Air in Concrete. Dissertation, The University of Texas at Austin, Austin.

Litvan, G. (1973). Frost Action in Cement Paste. Materials and Structures, 6(4), 293-298.

Naranjo, A. (2007). Clustering of Air Voids Around Aggregates in Air Entrained Concrete. Master's Thesis, The University of Texas in Austin.

Peterson, K. (2008). Automated Air-Void System Characterization of Hardened Concrete: Helping Computers to Count Air-voids Like People Count Air-Voids – Methods for Flatbed Scanner Calibration. Dissertation, Michigan Technological University.

Pigeon, M., & Pleau, R. (1995). Durability of Concrete in Cold Climates. CRC Press.

Pomeroy, D. (1989). ACI Special Publication. Concrete Durability: From Basic Research to Practical Reality, 111-130. Farmington Hills, MI: American Concrete Institute.

Powers , T. C., & Willis, T. F. (1949). The Air Requirement of Frost Resistant Concrete. Proceedings of the Twenty-Ninth Annual Meeting of the Highway Research Board (pp. 184-211). Washington, D.C.: Highway Research Board.

Powers, T. C., & Helmuth, R. A. (1953). Theory of Volume Changes in Hardened Portland-Cement Paste During Freezing. Skokie, IL: Portland Cement Association.

Ramachandran, V. S. (1997). Concrete Admixtures Handbook (2nd ed.). William Andrew.

Torrans, P. H., & Ivey, D. L. (1968). Review of Literature on Air-Entrained Concrete. College Station, Texas: Texas Transportation Institute, Texas A&M University.

Walker, H. N., Lane, D. S., & Paul, E. S. (2006). Petrographic Methods of Examining Hardened Concrete: A Pethrographic Manual. Virginia Transportation Research Council. McLean, VA: Federal Highway Administration.

Whiting, D. A., & Nagi, M. A. (1998). Manual on Control of Air Content in Concrete. Skokie, IL: Portland Cement Association.

Appendix A - Hardened Air Void Analysis Results

1-I

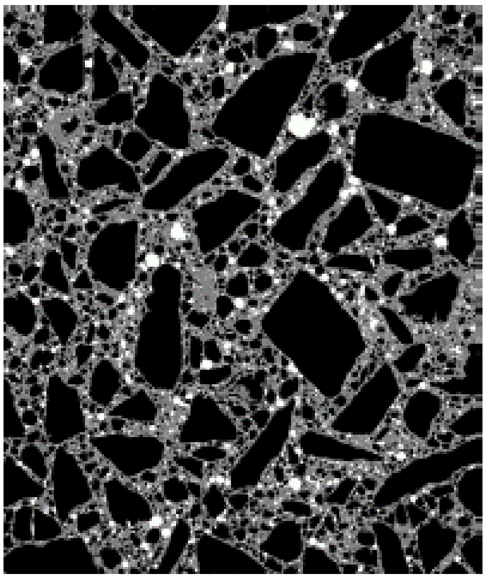

False-Color Image

Air Void Content	6.29	%
Spacing Factor	0.0043	in.
Air Void Area	0.55	in²
# of Air Voids	48724	
Paste Area	2.65	in²
Paste Content	30.12	%
Aggregate Area	5.6	in²
Clustering Index	2.3	
# Agg Analyzed	17	
Minimum Clustering Rate	5.45	%
Maximum Clustering Rate	26.98	%

1-I-R

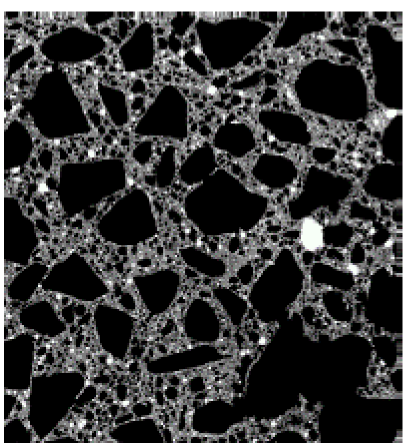

False-Color Image

Air Void Content	7.27	%
Spacing Factor	0.0036	in.
Air Void Area	0.69	in²
# of Air Voids	48380	
Paste Area	2.5	in²
Paste Content	26.48	%
Aggregate Area	6.27	in²
Clustering Index	1.78	
# Agg Analyzed	6.85	
Minimum Clustering Rate	685	%
Maximum Clustering Rate	17.8	%

1-II

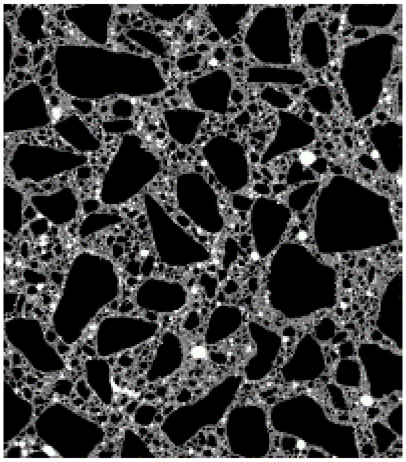

Air Void Content	6.39 %
Spacing Factor	0.0068 in.
Air Void Area	0.77 in²
# of Air Voids	28108
Paste Area	3.69 in²
Paste Content	29.59 %
Aggregate Area	7.77 in²
Clustering Index	1.57
# Agg Analyzed	24
Minimum Clustering Rate	4.27 %
Maximum Clustering Rate	17.07 %

False-Color Image

1-II-R

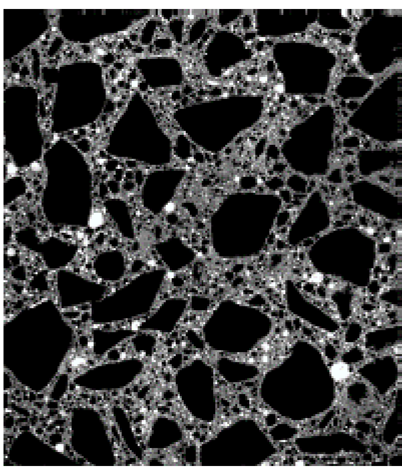

Air Void Content	7.5 %
Spacing Factor	0.0044 in.
Air Void Area	0.9 in²
# of Air Voids	46917
Paste Area	3.19 in²
Paste Content	26.52 %
Aggregate Area	7.95 in²
Clustering Index	1.54
# Agg Analyzed	25
Minimum Clustering Rate	1.85 %
Maximum Clustering Rate	19.03 %

False-Color Image

1-III

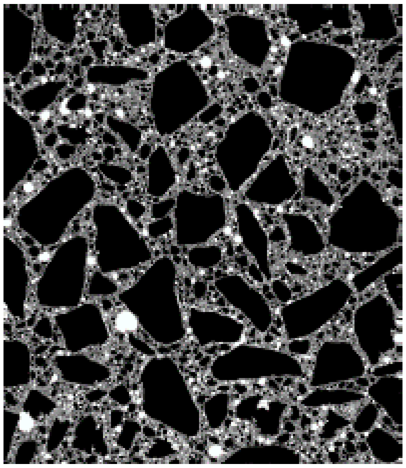

False-Color Image

Air Void Content	8.17 %
Spacing Factor	0.0059 in.
Air Void Area	0.99 in²
# of Air Voids	31833
Paste Area	3.49 in²
Paste Content	28.65 %
Aggregate Area	7.69 in²
Clustering Index	1.45
# Agg Analyzed	23
Minimum Clustering Rate	4.32 %
Maximum Clustering Rate	19.26 %

1-III-R

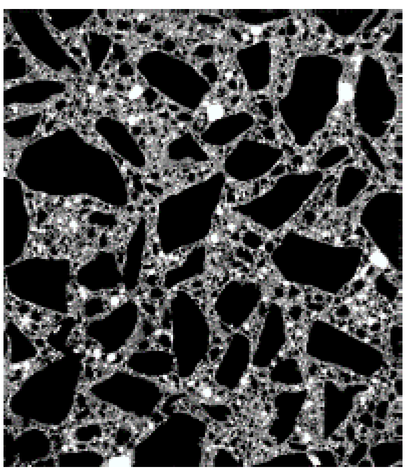

False-Color Image

Air Void Content	11.08 %
Spacing Factor	0.0038 in.
Air Void Area	1.34 in²
# of Air Voids	44843
Paste Area	3.42 in²
Paste Content	28.26 %
Aggregate Area	7.35 in²
Clustering Index	1.36
# Agg Analyzed	22
Minimum Clustering Rate	7.15 %
Maximum Clustering Rate	24.97 %

1-IV

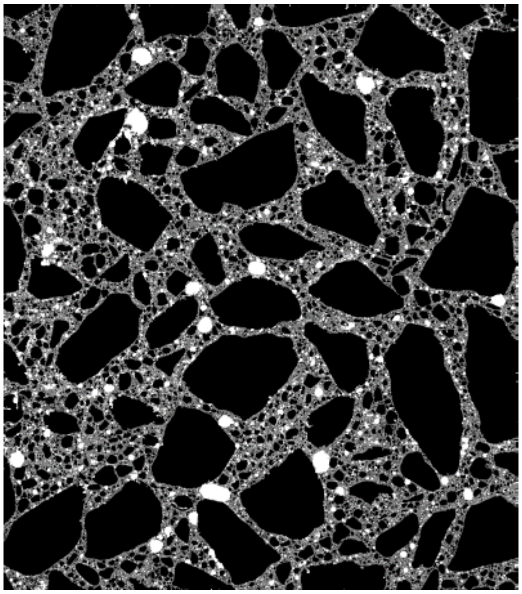

False-Color Image

Air Void Content	7.39 %
Spacing Factor	0.0047 in.
Air Void Area	0.9 in^2
# of Air Voids	38146
Paste Area	3.06 in^2
Paste Content	25.19 %
Aggregate Area	8.18 in^2
Clustering Index	1.91
# Agg Analyzed	23
Minimum Clustering Rate	7 %
Maximum Clustering Rate	23.86 %

1-IV-R

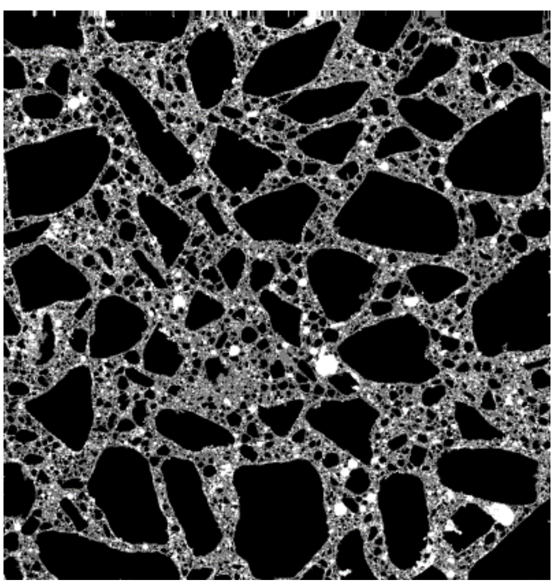

False-Color Image

Air Void Content	9.74 %
Spacing Factor	0.0027 in.
Air Void Area	0.94 in^2
# of Air Voids	48218
Paste Area	2.3 in^2
Paste Content	23.82 %
Aggregate Area	6.42 in^2
Clustering Index	2.22
# Agg Analyzed	21
Minimum Clustering Rate	36.19 %
Maximum Clustering Rate	13.53 %

1-V

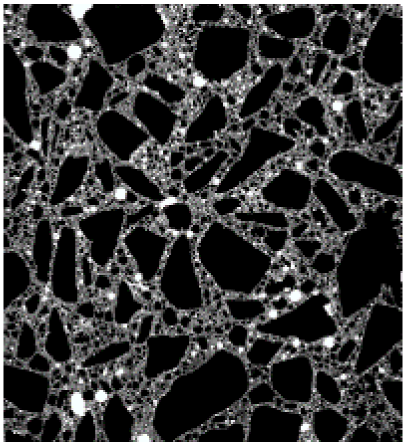

False-Color Image

Air Void Content	7.44 %
Spacing Factor	0.0046 in.
Air Void Area	0.9 in²
# of Air Voids	34349
Paste Area	2.93 in²
Paste Content	24.21 %
Aggregate Area	8.27 in²
Clustering Index	1.86
# Agg Analyzed	24
Minimum Clustering Rate	3.81 %
Maximum Clustering Rate	27.64 %

1-V-R

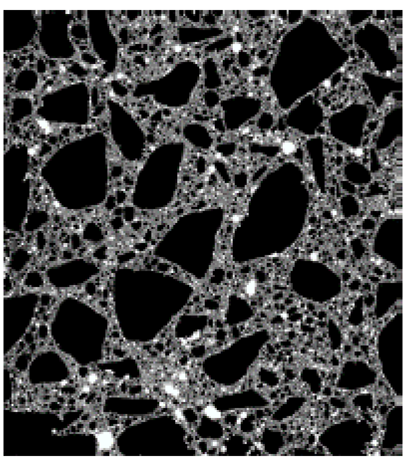

False-Color Image

Air Void Content	7.76 %
Spacing Factor	0.005 in.
Air Void Area	0.091 in²
# of Air Voids	43084
Paste Area	3.6 in²
Paste Content	30.73 %
Aggregate Area	7.21 in²
Clustering Index	18.88
# Agg Analyzed	18
Minimum Clustering Rate	8.27 %
Maximum Clustering Rate	20.24 %

2-I

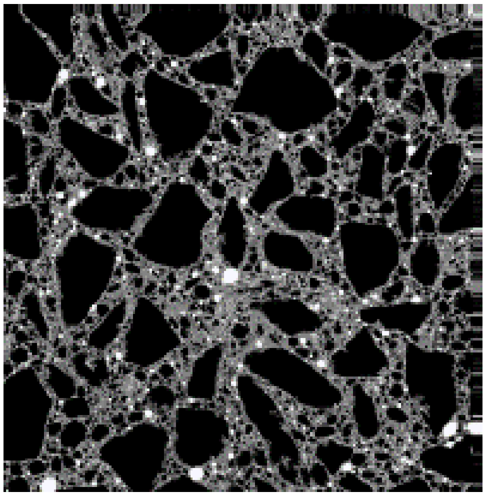

False-Color Image

Air Void Content	6	%
Spacing Factor	0.0047	in.
Air Void Area	N/A	in²
# of Air Voids	N/A	
Paste Area	N/A	in²
Paste Content	N/A	%
Aggregate Area	N/A	in²
Clustering Index	1.52	
# Agg Analyzed	22	
Minimum Clustering Rate	3.8	%
Maximum Clustering Rate	13.01	%

2-I-R

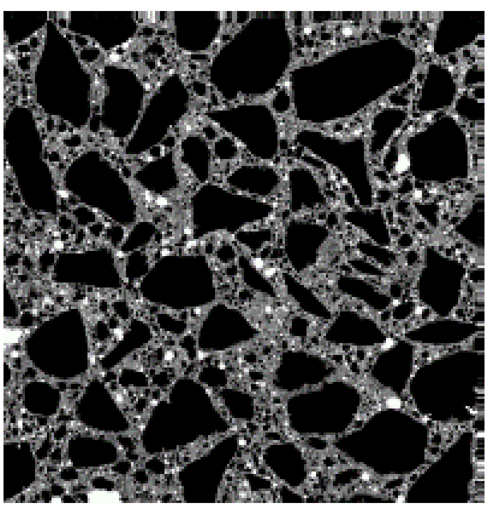

False-Color Image

Air Void Content	7.45	%
Spacing Factor	0.0047	in.
Air Void Area	N/A	in²
# of Air Voids	N/A	
Paste Area	N/A	in²
Paste Content	N/A	%
Aggregate Area	N/A	in²
Clustering Index	1.45	
# Agg Analyzed	23	
Minimum Clustering Rate	5.23	%
Maximum Clustering Rate	18.17	%

2-II

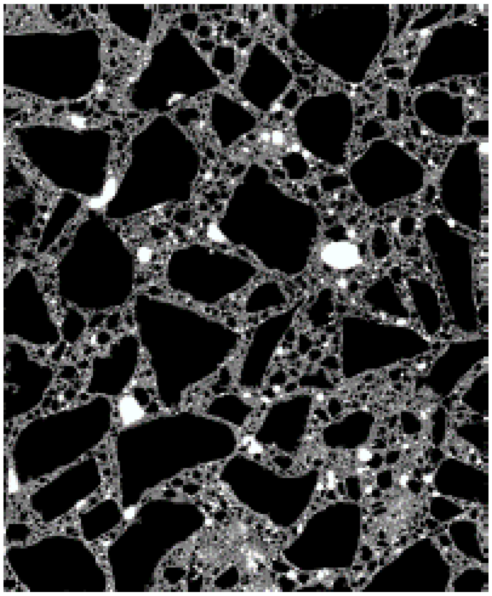

False-Color Image

Air Void Content	5.73	%
Spacing Factor	0.0072	in.
Air Void Area	0.68	in²
# of Air Voids	26386	
Paste Area	3.26	in²
Paste Content	27.42	%
Aggregate Area	7.95	in²
Clustering Index	1.42	
# Agg Analyzed	N/A	
Minimum Clustering Rate	N/A	%
Maximum Clustering Rate	N/A	%

2-II-R

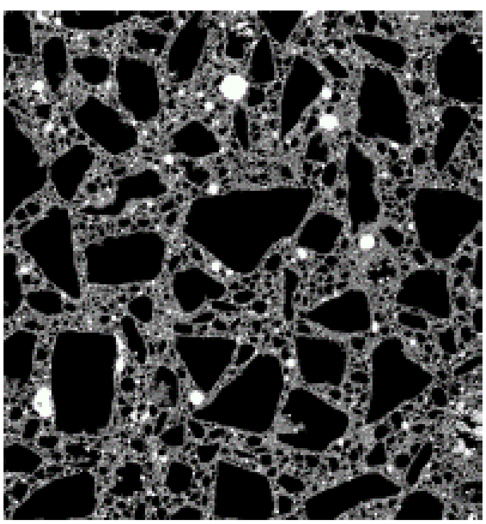

False-Color Image

Air Void Content	6.41	%
Spacing Factor	0.006	in.
Air Void Area	0.75	in²
# of Air Voids	37569	
Paste Area	3.76	in²
Paste Content	32.00	%
Aggregate Area	7.23	in²
Clustering Index	1.42	
# Agg Analyzed	22	
Minimum Clustering Rate	4.02	%
Maximum Clustering Rate	16.17	%

2-III

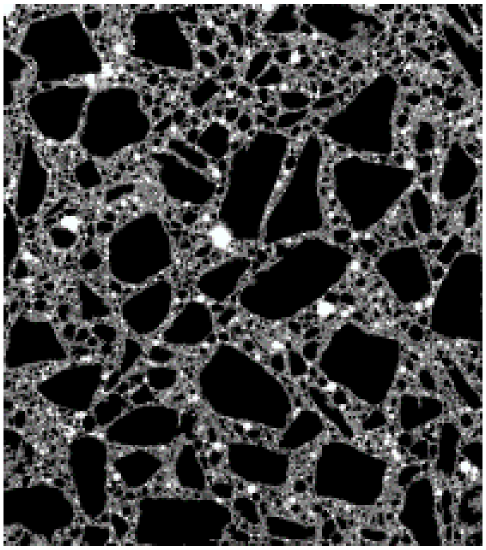

False-Color Image

Air Void Content	6.85 %
Spacing Factor	0.0070 in.
Air Void Area	0.83 in²
# of Air Voids	32564
Paste Area	3.67 in²
Paste Content	30.47 %
Aggregate Area	7.55 in²
Clustering Index	1.2
# Agg Analyzed	24
Minimum Clustering Rate	4.66 %
Maximum Clustering Rate	14.46 %

2-III-R

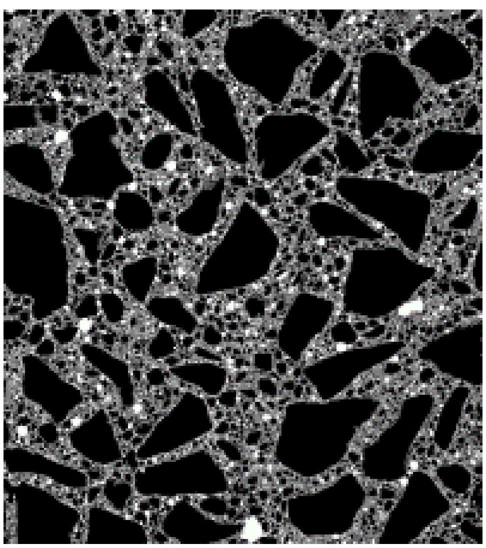

False-Color Image

Air Void Content	7.93 %
Spacing Factor	0.0050 in.
Air Void Area	0.94 in²
# of Air Voids	44094
Paste Area	3.46 in²
Paste Content	29.22 %
Aggregate Area	7.45 in²
Clustering Index	1.44
# Agg Analyzed	25
Minimum Clustering Rate	5.03 %
Maximum Clustering Rate	21.39 %

2-IV

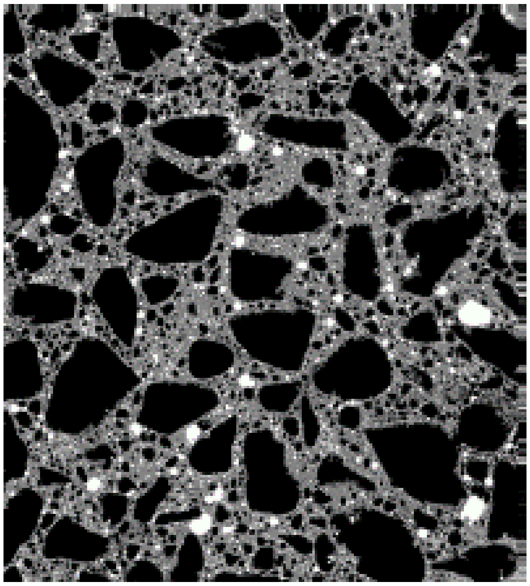

False-Color Image

Air Void Content	6.81 %
Spacing Factor	0.0073 in.
Air Void Area	0.86 in²
# of Air Voids	33397
Paste Area	4.69 in²
Paste Content	37.34 %
Aggregate Area	7.02 in²
Clustering Index	0.98
# Agg Analyzed	29
Minimum Clustering Rate	2.51 %
Maximum Clustering Rate	12.98 %

2-IV-R

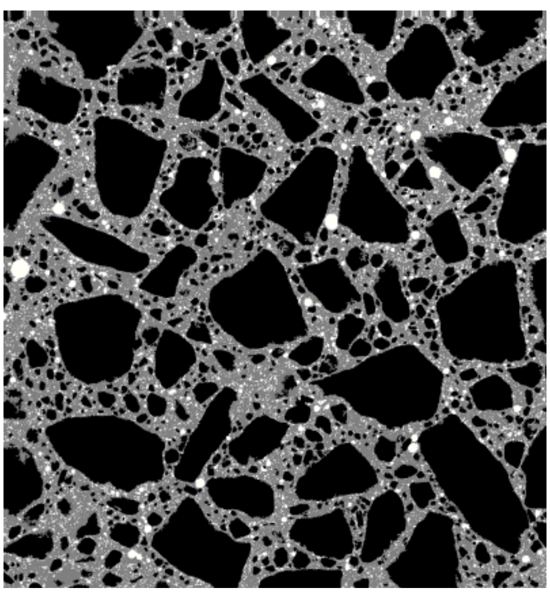

False-Color Image

Air Void Content	6.87 %
Spacing Factor	0.0047 in.
Air Void Area	0.77 in²
# of Air Voids	52171
Paste Area	4.04 in²
Paste Content	35.94 %
Aggregate Area	6.44 in²
Clustering Index	1.47
# Agg Analyzed	22
Minimum Clustering Rate	3.11 %
Maximum Clustering Rate	17.15 %

2-V

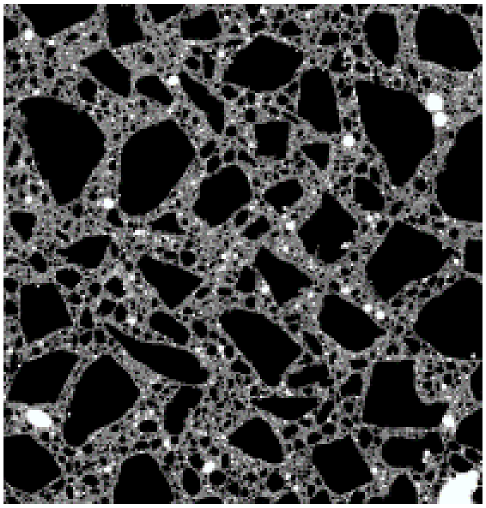

False-Color Image

Air Void Content	6.19 %
Spacing Factor	0.0058 in.
Air Void Area	0.72 in²
# of Air Voids	42512
Paste Area	3.72 in²
Paste Content	32.13 %
Aggregate Area	7.15 in²
Clustering Index	1.72
# Agg Analyzed	22
Minimum Clustering Rate	4.96 %
Maximum Clustering Rate	14.53 %

2-V-R

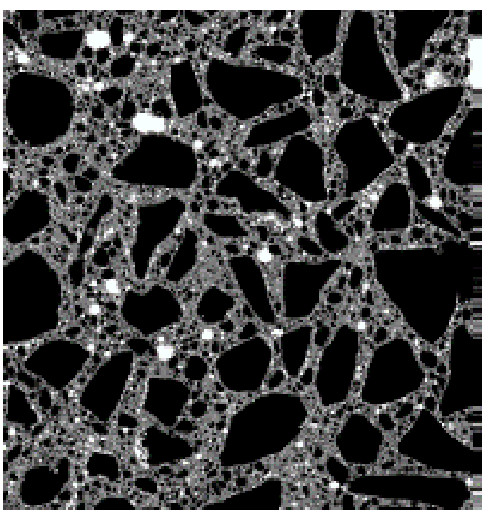

False-Color Image

Air Void Content	7.83 %
Spacing Factor	0.0038 in.
Air Void Area	0.95 in²
# of Air Voids	69076
Paste Area	3.48 in²
Paste Content	28.64 %
Aggregate Area	6.27 in²
Clustering Index	1.71
# Agg Analyzed	26
Minimum Clustering Rate	7.19 %
Maximum Clustering Rate	24.95 %

3-I

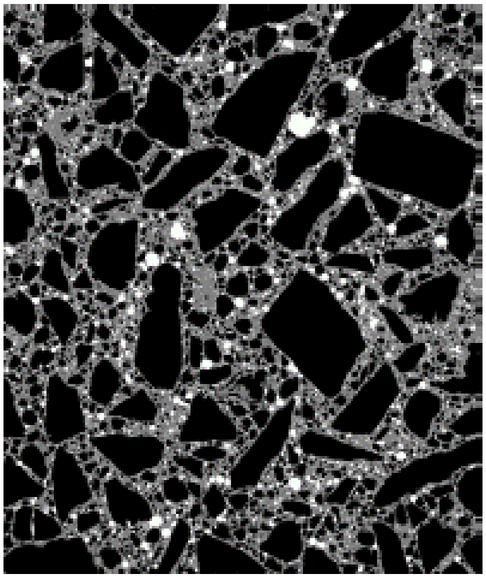

False-Color Image

Air Void Content	6.19 %
Spacing Factor	0.0091 in.
Air Void Area	0.69 in²
# of Air Voids	18329
Paste Area	3.55 in²
Paste Content	31.74 %
Aggregate Area	6.93 in²
Clustering Index	0.89
# Agg Analyzed	17
Minimum Clustering Rate	1.91 %
Maximum Clustering Rate	11.79 %

3-I-R

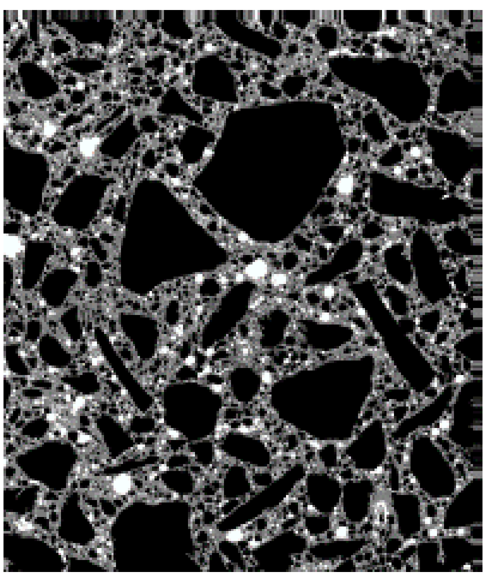

False-Color Image

Air Void Content	7.92 %
Spacing Factor	0.00637 in.
Air Void Area	0.93 in²
# of Air Voids	30489
Paste Area	3.59 in²
Paste Content	30.62 %
Aggregate Area	7.19 in²
Clustering Index	1.06
# Agg Analyzed	15
Minimum Clustering Rate	3.41 %
Maximum Clustering Rate	13.57 %

3-II

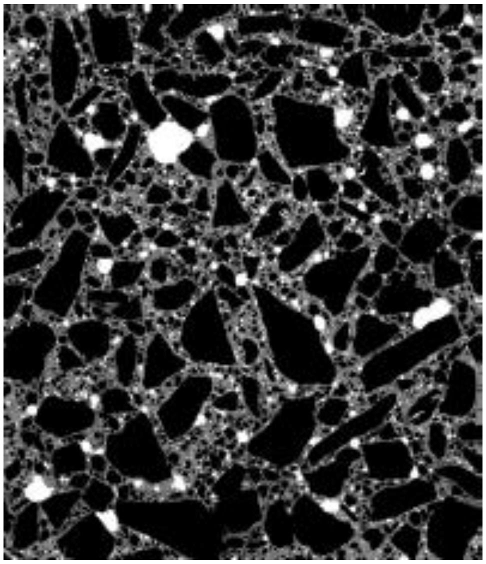

Air Void Content	6.04 %
Spacing Factor	0.0107 in.
Air Void Area	0.8 in²
# of Air Voids	18576
Paste Area	3.6 in²
Paste Content	27.22 %
Aggregate Area	8.83 in²
Clustering Index	0.76
# Agg Analyzed	28
Minimum Clustering Rate	1.36 %
Maximum Clustering Rate	8.14 %

False-Color Image

3-II-R

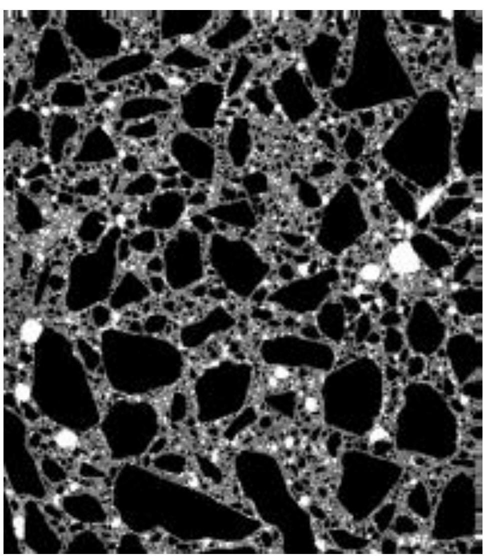

Air Void Content	8.31 %
Spacing Factor	0.0068 in.
Air Void Area	1.03 in²
# of Air Voids	31124
Paste Area	3.81 in²
Paste Content	30.80 %
Aggregate Area	7.53 in²
Clustering Index	1.26
# Agg Analyzed	19
Minimum Clustering Rate	3.49 %
Maximum Clustering Rate	24.11 %

False-Color Image

3-III

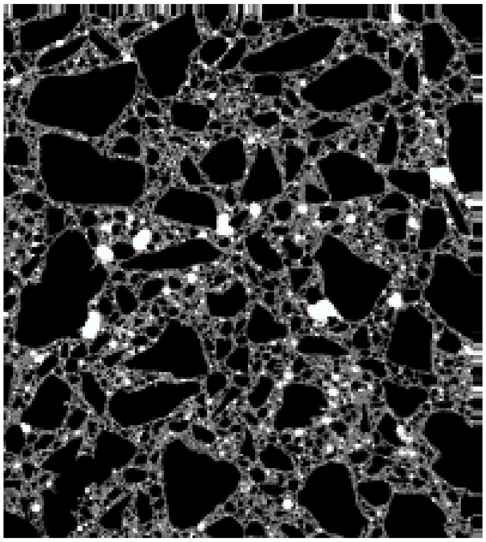

False-Color Image

Air Void Content	6.07 %
Spacing Factor	0.0078 in.
Air Void Area	0.7 in²
# of Air Voids	23396
Paste Area	3.04 in²
Paste Content	26.36 %
Aggregate Area	7.79 in²
Clustering Index	1.24
# Agg Analyzed	19
Minimum Clustering Rate	2.78 %
Maximum Clustering Rate	14.32 %

3-III-R

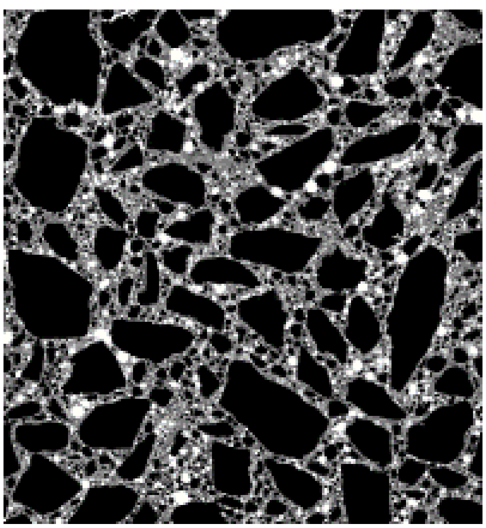

False-Color Image

Air Void Content	10.32 %
Spacing Factor	0.0052 in.
Air Void Area	1.24 in²
# of Air Voids	30705
Paste Area	3.21 in²
Paste Content	26.79 %
Aggregate Area	7.53 in²
Clustering Index	1.11
# Agg Analyzed	23
Minimum Clustering Rate	6.96 %
Maximum Clustering Rate	22.01 %

3-IV

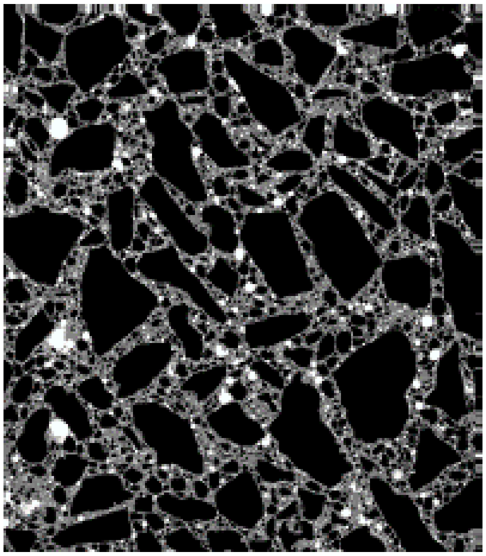

False-Color Image

Air Void Content	6.93 %
Spacing Factor	0.0056 in.
Air Void Area	0.81 in²
# of Air Voids	31097
Paste Area	2.94 in²
Paste Content	25.21 %
Aggregate Area	7.91 in²
Clustering Index	1.65
# Agg Analyzed	19
Minimum Clustering Rate	5.61 %
Maximum Clustering Rate	18.6 %

3-IV-R

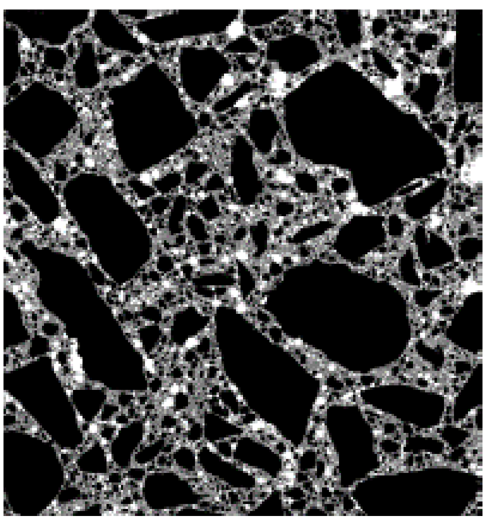

False-Color Image

Air Void Content	10.34 %
Spacing Factor	0.0048 in.
Air Void Area	1.26 in²
# of Air Voids	29004
Paste Area	2.94 in²
Paste Content	24.07 %
Aggregate Area	8.02 in²
Clustering Index	1.09
# Agg Analyzed	16
Minimum Clustering Rate	5.03 %
Maximum Clustering Rate	20.55 %

3-V

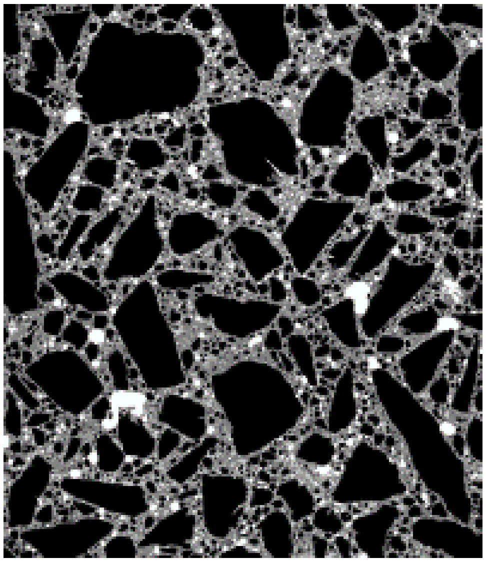

False-Color Image

Air Void Content	8.36	%
Spacing Factor	0.0053	in.
Air Void Area	1	in²
# of Air Voids	39221	
Paste Area	3.57	in²
Paste Content	29.9	%
Aggregate Area	7.36	in²
Clustering Index	1.35	
# Agg Analyzed	19	
Minimum Clustering Rate	1.67	%
Maximum Clustering Rate	20.42	%

3-V-R

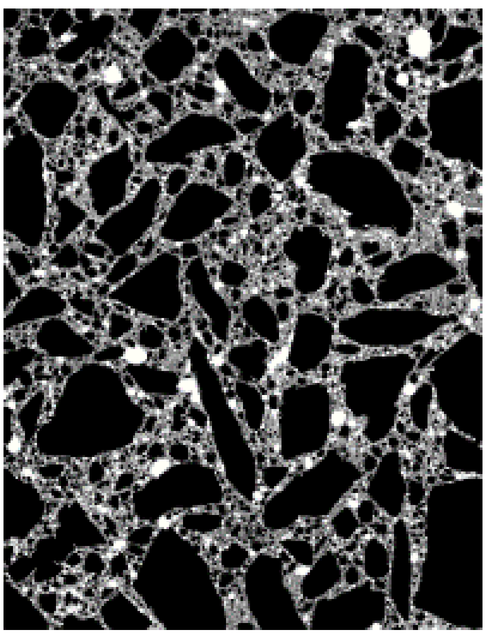

False-Color Image

Air Void Content	10.61	%
Spacing Factor	0.0037	in.
Air Void Area	1.03	in²
# of Air Voids	34758	
Paste Area	2.45	in²
Paste Content	25.16	%
Aggregate Area	6.27	in²
Clustering Index	1.57	
# Agg Analyzed	19	
Minimum Clustering Rate	11.83	%
Maximum Clustering Rate	24.82	%

4-I

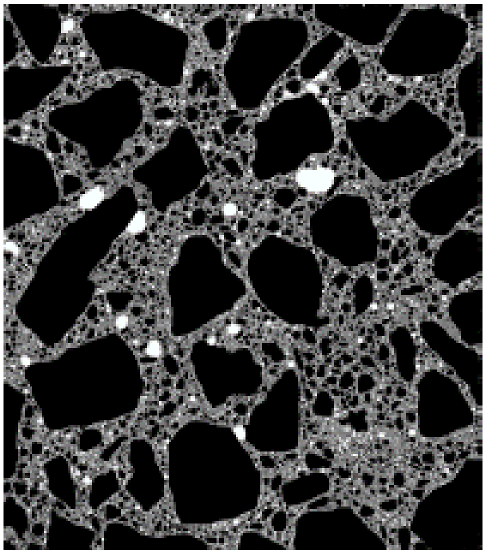

False-Color Image

Air Void Content	6.11 %
Spacing Factor	0.0054 in.
Air Void Area	0.68 in²
# of Air Voids	39329
Paste Area	3.21 in²
Paste Content	28.63 %
Aggregate Area	7.32 in²
Clustering Index	1.86
# Agg Analyzed	23
Minimum Clustering Rate	5.92 %
Maximum Clustering Rate	18.71 %

4-I-R

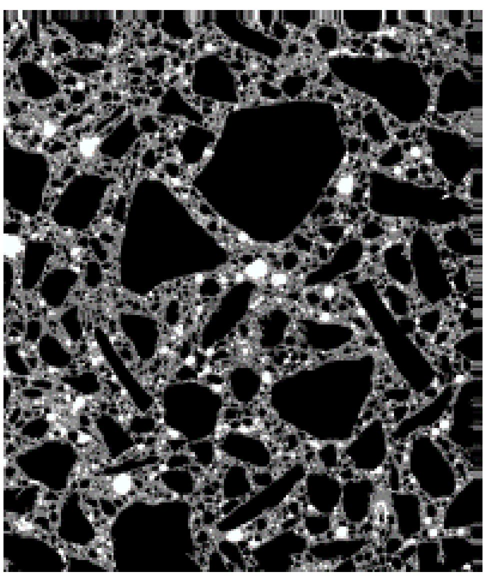

False-Color Image

Air Void Content	8.73 %
Spacing Factor	0.0042 in.
Air Void Area	1.02 in²
# of Air Voids	52614
Paste Area	3.61 in²
Paste Content	30.75 %
Aggregate Area	7.1 in²
Clustering Index	1.64
# Agg Analyzed	26
Minimum Clustering Rate	6.53 %
Maximum Clustering Rate	23.96 %

4-II

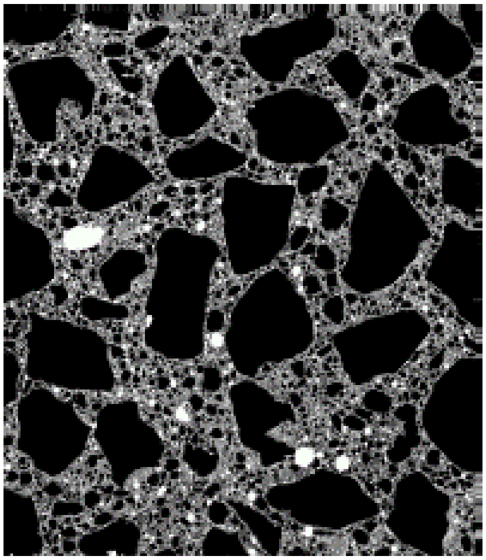

False-Color Image

Air Void Content	7.84 %
Spacing Factor	0.0045 in.
Air Void Area	0.87 in²
# of Air Voids	37124
Paste Area	3.07 in²
Paste Content	27.52 %
Aggregate Area	7.2 in²
Clustering Index	1.74
# Agg Analyzed	24
Minimum Clustering Rate	7.01 %
Maximum Clustering Rate	21.44 %

4-II-R

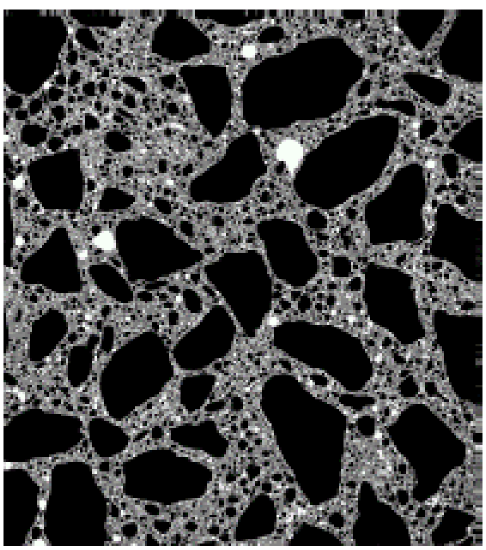

False-Color Image

Air Void Content	8.57 %
Spacing Factor	0.0037 in.
Air Void Area	1 in²
# of Air Voids	49215
Paste Area	3.21 in²
Paste Content	27.69 %
Aggregate Area	7340 in²
Clustering Index	1.74
# Agg Analyzed	23
Minimum Clustering Rate	6.87 %
Maximum Clustering Rate	20.84 %

4-III

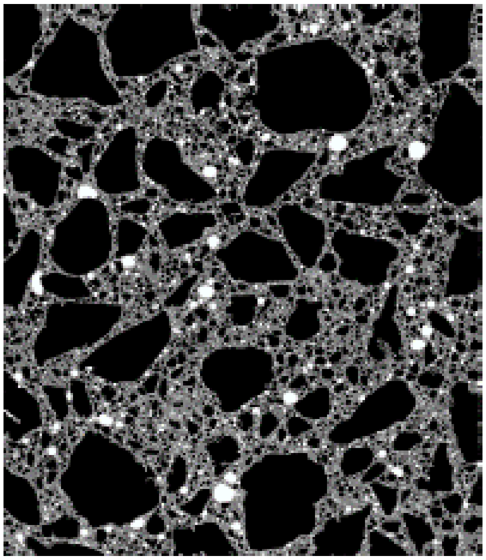

False-Color Image

Air Void Content	6.43 %
Spacing Factor	0.0063 in.
Air Void Area	0.76 in²
# of Air Voids	37145
Paste Area	3.69 in²
Paste Content	31.37 %
Aggregate Area	7.32 in²
Clustering Index	1.53
# Agg Analyzed	22
Minimum Clustering Rate	3.59 %
Maximum Clustering Rate	14.13 %

4-III-R

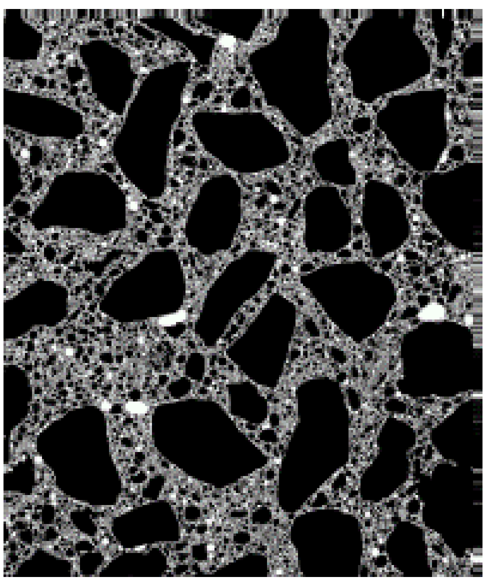

False-Color Image

Air Void Content	9.4 %
Spacing Factor	0.003 in.
Air Void Area	1.7 in²
# of Air Voids	53216
Paste Area	2.8 in²
Paste Content	24.49 %
Aggregate Area	7.55 in²
Clustering Index	2.13
# Agg Analyzed	25
Minimum Clustering Rate	12.81 %
Maximum Clustering Rate	30.16 %

4-IV

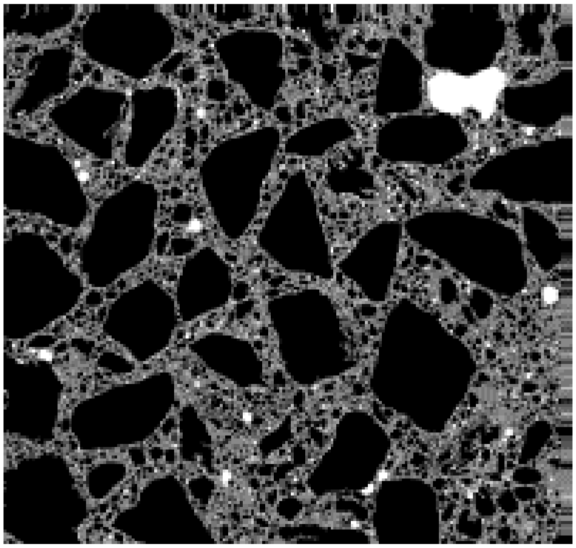

False-Color Image

Air Void Content	5.16 %
Spacing Factor	0.0061 in.
Air Void Area	0.6 in²
# of Air Voids	32849
Paste Area	3.32 in²
Paste Content	28.67 %
Aggregate Area	7.67 in²
Clustering Index	1.65
# Agg Analyzed	19
Minimum Clustering Rate	5.61 %
Maximum Clustering Rate	18.6 %

4-IV-R

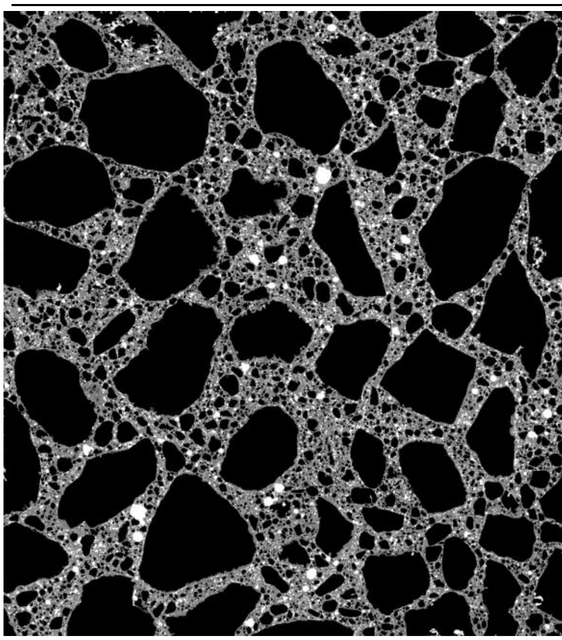

False-Color Image

Air Void Content	6.76 %
Spacing Factor	0.0039 in.
Air Void Area	0.74 in²
# of Air Voids	47246
Paste Area	2.89 in²
Paste Content	26.49 %
Aggregate Area	7.29 in²
Clustering Index	2.04
# Agg Analyzed	27
Minimum Clustering Rate	6.3 %
Maximum Clustering Rate	19.77 %

4-V

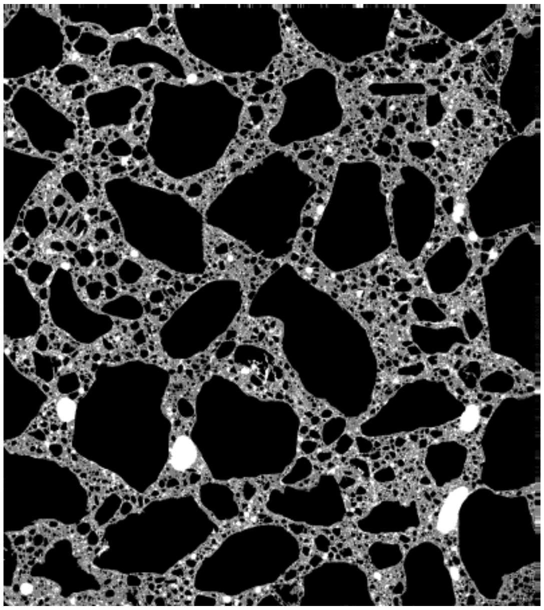

False-Color Image

Air Void Content	7.98 %
Spacing Factor	0.0036 in.
Air Void Area	0.88 in²
# of Air Voids	47304
Paste Area	2.78 in²
Paste Content	25.23 %
Aggregate Area	7.37 in²
Clustering Index	1.84
# Agg Analyzed	25
Minimum Clustering Rate	7.27 %
Maximum Clustering Rate	22.89 %

4-V-R

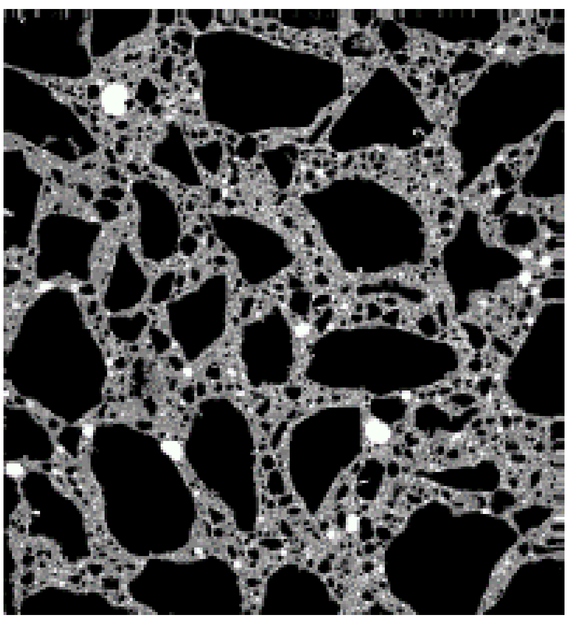

False-Color Image

Air Void Content	8.23 %
Spacing Factor	0.0042 in.
Air Void Area	0.93 in²
# of Air Voids	57293
Paste Area	3.62 in²
Paste Content	31.99 %
Aggregate Area	6.77 in²
Clustering Index	1.67
# Agg Analyzed	24
Minimum Clustering Rate	6.19 %
Maximum Clustering Rate	25.68 %

5-I

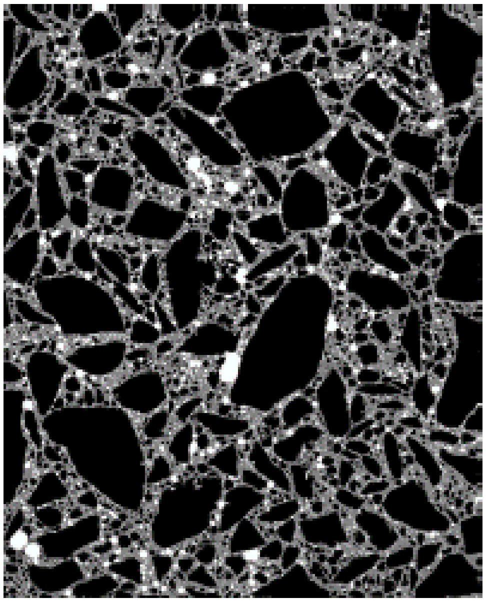

False-Color Image

Air Void Content	7.89 %
Spacing Factor	0.0057 in.
Air Void Area	0.86 in²
# of Air Voids	35336
Paste Area	3.3 in²
Paste Content	30.39 %
Aggregate Area	6.7 in²
Clustering Index	1.47
# Agg Analyzed	10
Minimum Clustering Rate	5.55 %
Maximum Clustering Rate	16.52 %

5-I-R

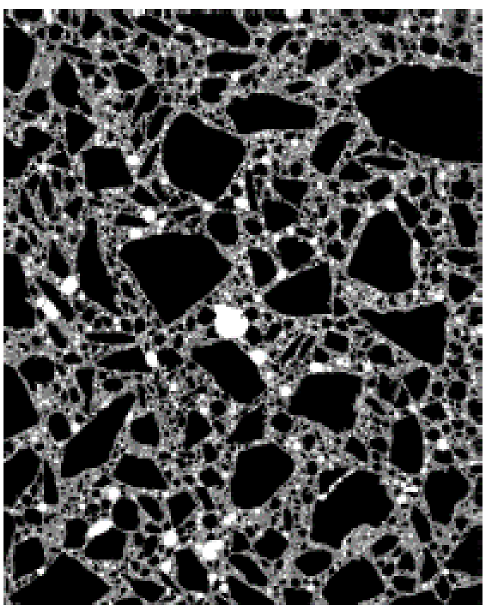

False-Color Image

Air Void Content	9.6 %
Spacing Factor	0.0045 in.
Air Void Area	0.98 in²
# of Air Voids	41733
Paste Area	3.07 in²
Paste Content	30.10 %
Aggregate Area	6.15 in²
Clustering Index	1.44
# Agg Analyzed	13
Minimum Clustering Rate	9.76 %
Maximum Clustering Rate	20.83 %

5-II

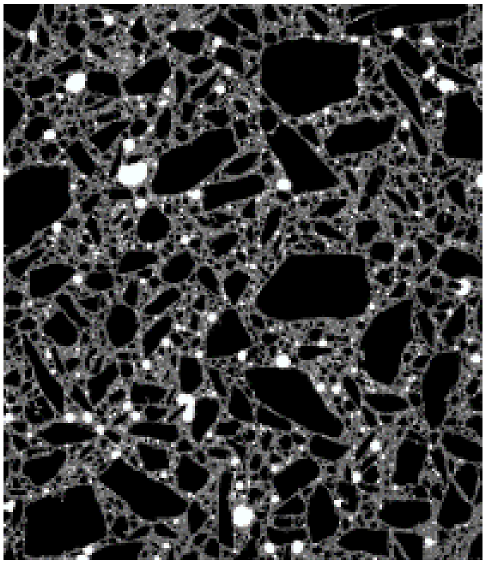

False-Color Image

Air Void Content	7.88	%
Spacing Factor	0.0061	in.
Air Void Area	0.87	in²
# of Air Voids	43098	
Paste Area	3.7	in²
Paste Content	33.39	%
Aggregate Area	6.51	in²
Clustering Index	1.4	
# Agg Analyzed	11	
Minimum Clustering Rate	8.34	%
Maximum Clustering Rate	16.34	%

5-II-R

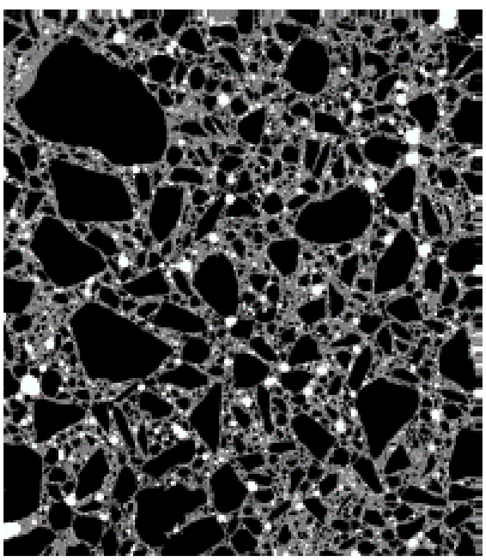

False-Color Image

Air Void Content	7.14	%
Spacing Factor	0.0078	in.
Air Void Area	0.82	in²
# of Air Voids	28196	
Paste Area	3.73	in²
Paste Content	32.52	%
Aggregate Area	6.92	in²
Clustering Index	1.02	
# Agg Analyzed	10	
Minimum Clustering Rate	5.23	%
Maximum Clustering Rate	12.3	%

5-III

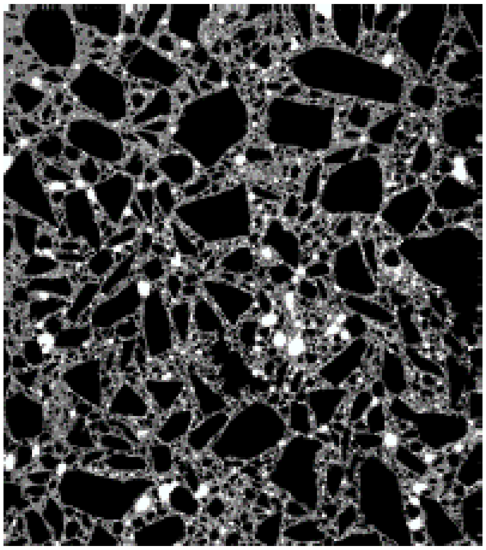

False-Color Image

Air Void Content	7.24 %
Spacing Factor	0.0058 in.
Air Void Area	0.93 in²
# of Air Voids	48254
Paste Area	3.76 in²
Paste Content	29.29 %
Aggregate Area	8.15 in²
Clustering Index	1.23
# Agg Analyzed	18
Minimum Clustering Rate	1 %
Maximum Clustering Rate	13.34 %

5-III-R

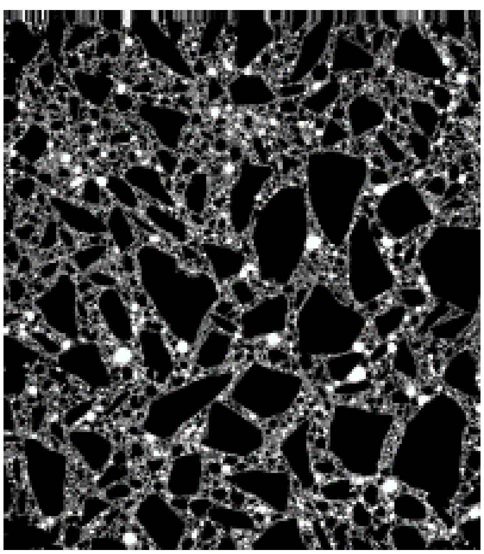

False-Color Image

Air Void Content	8.49 %
Spacing Factor	0.0047 in.
Air Void Area	1.06 in²
# of Air Voids	37359
Paste Area	3.02 in²
Paste Content	24.07 %
Aggregate Area	8.46 in²
Clustering Index	1.48
# Agg Analyzed	21
Minimum Clustering Rate	9.28 %
Maximum Clustering Rate	17.77 %

5-IV

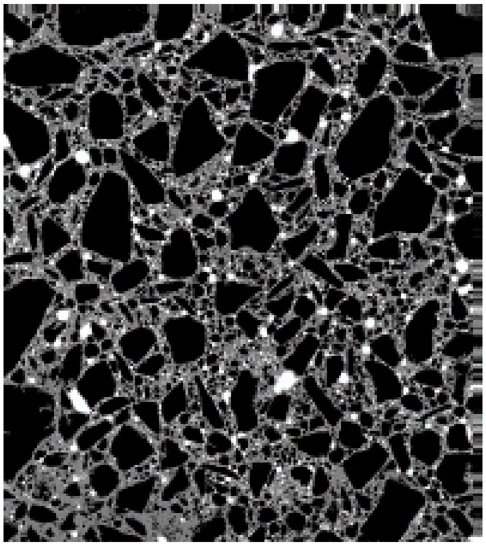

False-Color Image

Air Void Content	6.74 %
Spacing Factor	0.0064 in.
Air Void Area	0.85 in²
# of Air Voids	38733
Paste Area	3.92 in²
Paste Content	31.15 %
Aggregate Area	7.82 in²
Clustering Index	1.45
# Agg Analyzed	15
Minimum Clustering Rate	1.65 %
Maximum Clustering Rate	15.43 %

5-IV-R

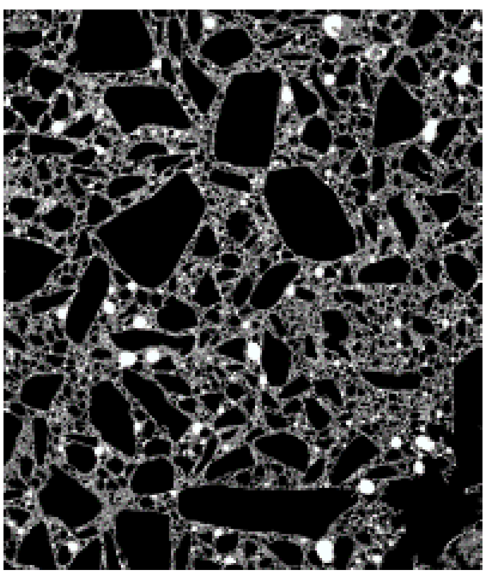

False-Color Image

Air Void Content	8.27 %
Spacing Factor	0.0039 in.
Air Void Area	0.95 in²
# of Air Voids	46475
Paste Area	2.84 in²
Paste Content	24.72 %
Aggregate Area	7.7 in²
Clustering Index	2.18
# Agg Analyzed	14
Minimum Clustering Rate	11.57 %
Maximum Clustering Rate	26.1 %

5-V

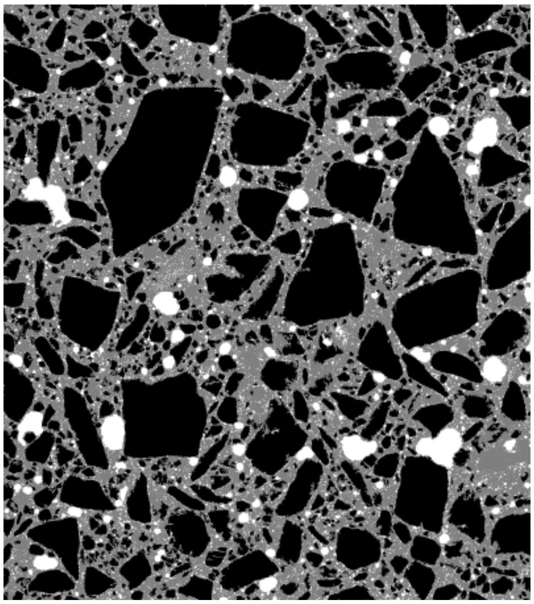

False-Color Image

Air Void Content	8.73 %
Spacing Factor	0.0054 in.
Air Void Area	0.91 in²
# of Air Voids	64138
Paste Area	3.98 in²
Paste Content	38.06 %
Aggregate Area	5.57 in²
Clustering Index	1.38
# Agg Analyzed	10
Minimum Clustering Rate	9.64 %
Maximum Clustering Rate	15.47 %

5-V-R

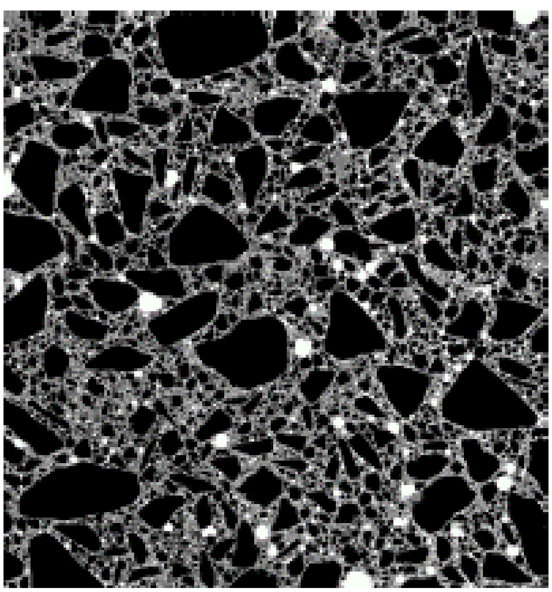

False-Color Image

Air Void Content	9.35 %
Spacing Factor	0.0031 in.
Air Void Area	1.02 in²
# of Air Voids	76475
Paste Area	3.17 in²
Paste Content	29.14 %
Aggregate Area	6.69 in²
Clustering Index	2.06
# Agg Analyzed	10
Minimum Clustering Rate	14.58 %
Maximum Clustering Rate	28.96 %

Appendix B - Visual Rating of Air Void Clustering

Sample ID	1-I

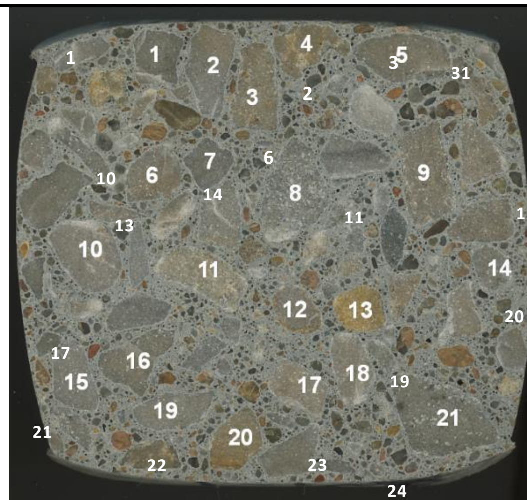

Agg. #	Rating	Agg. #	Rating	Agg. #	Rating
1	3	16	3	31	
2	3	17	2	32	
3	2	18	2	33	
4	3	19	3	34	
5	3	20	3	35	
6	2	21	3	36	
7	2	22		37	
8	2	23		38	
9	2	24		39	
10	2	25		40	
11	3	26		41	
12	2	27		42	
13	2	28		43	
14	3	29		44	
15	3	30		45	

ANALYSIS

	Total	Rating #	Total * Rating #
Rating 0	0	0	0
Rating 1	0	1	0
Rating 2	10	2	20
Rating 3	11	3	33
		Sum	**53**
		# of agg	21

RATE	**2.52**

(sum / # of agg)

Sample ID	1-II

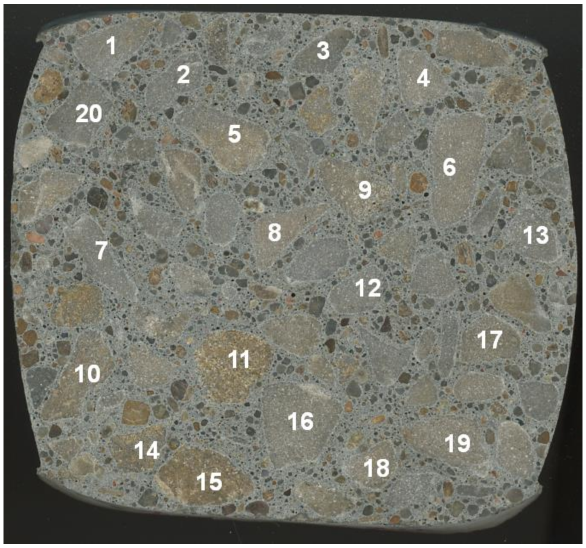

Agg. #	Rating	Agg. #	Rating	Agg. #	Rating
1	3	16	2	31	
2	2	17	2	32	
3	3	18	3	33	
4	3	19	3	34	
5	2	20	3	35	
6	2	21		36	
7	2	22		37	
8	3	23		38	
9	3	24		39	
10	3	25		40	
11	2	26		41	
12	3	27		42	
13	3	28		43	
14	3	29		44	
15	2	30		45	

ANALYSIS

	Total	**Rating #**	**Total * Rating #**
Rating 0	0	0	0
Rating 1	0	1	0
Rating 2	8	2	16
Rating 3	12	3	36
		Sum	**52**
		# of agg	20

RATE	**2.60**

(sum / # of agg)

Sample ID	1-III

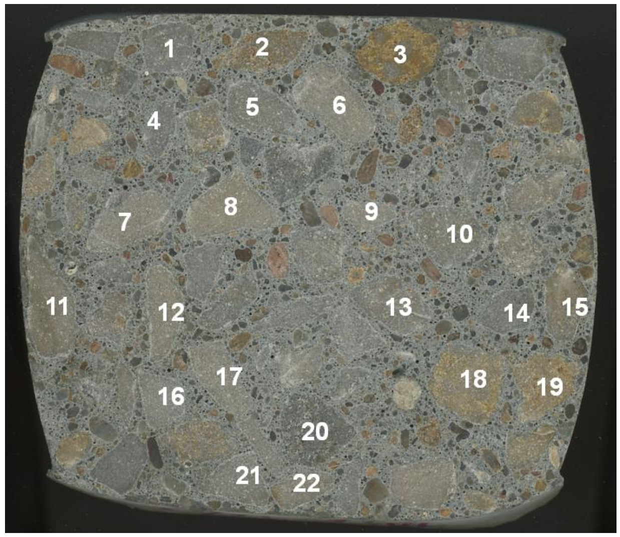

Agg. #	Rating
1	3
2	2
3	3
4	2
5	3
6	3
7	3
8	2
9	2
10	2
11	3
12	2
13	3
14	3
15	3

Agg. #	Rating
16	2
17	2
18	2
19	2
20	2
21	3
22	3
23	
24	
25	
26	
27	
28	
29	
30	

Agg. #	Rating
31	
32	
33	
34	
35	
36	
37	
38	
39	
40	
41	
42	
43	
44	
45	

ANALYSIS

	Total	Rating #	Total * Rating #
Rating 0	0	0	0
Rating 1	0	1	0
Rating 2	11	2	22
Rating 3	11	3	33
		Sum	**55**
		# of agg	22

RATE	**2.50**

(sum / # of agg)

Sample ID	**1-IV**

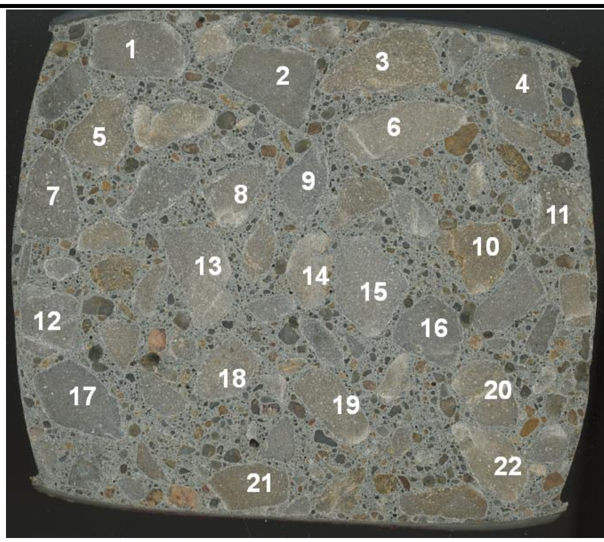

Agg. #	Rating	Agg. #	Rating	Agg. #	Rating
1	3	16	2	31	
2	3	17	3	32	
3	3	18	3	33	
4	3	19	3	34	
5	3	20	3	35	
6	2	21	3	36	
7	2	22	3	37	
8	2	23		38	
9	3	24		39	
10	3	25		40	
11	3	26		41	
12	3	27		42	
13	2	28		43	
14	2	29		44	
15	2	30		45	

ANALYSIS

	Total	**Rating #**	**Total * Rating #**
Rating 0	0	0	0
Rating 1	0	1	0
Rating 2	7	2	14
Rating 3	15	3	45
		Sum	**59**
		# of agg	22

RATE	**2.68**

(sum / # of agg)

Sample ID	**1-V**

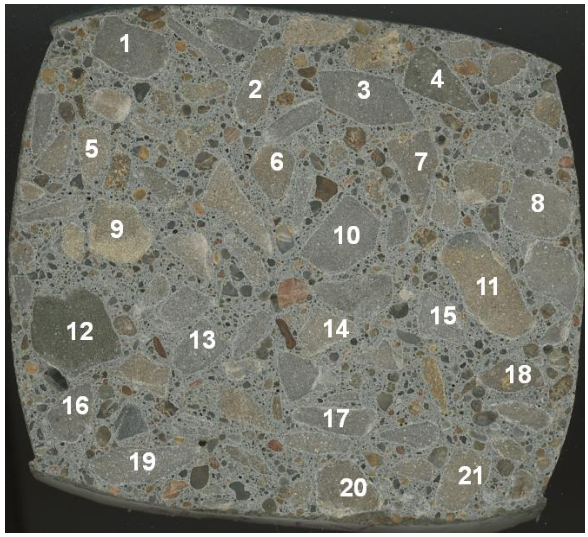

Agg. #	Rating	Agg. #	Rating	Agg. #	Rating
1	3	16	3	31	
2	2	17	3	32	
3	3	18	3	33	
4	3	19	3	34	
5	3	20	3	35	
6	2	21	3	36	
7	2	22		37	
8	3	23		38	
9	2	24		39	
10	3	25		40	
11	3	26		41	
12	2	27		42	
13	3	28		43	
14	2	29		44	
15	3	30		45	

ANALYSIS

	Total	**Rating #**	**Total * Rating #**
Rating 0	0	0	0
Rating 1	0	1	0
Rating 2	6	2	12
Rating 3	15	3	45
		Sum	**57**
		# of agg	21

RATE	**2.71**

(sum / # of agg)

Sample ID	1-I-R

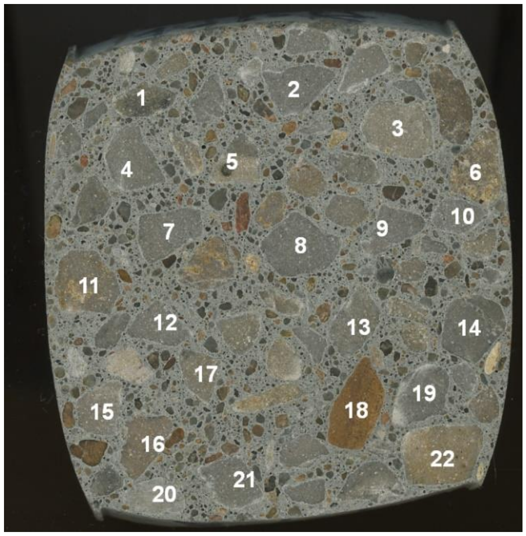

Agg. #	Rating	Agg. #	Rating	Agg. #	Rating
1	3	16	2	31	
2	2	17	3	32	
3	3	18	3	33	
4	3	19	3	34	
5	3	20	3	35	
6	3	21	3	36	
7	3	22	3	37	
8	3	23		38	
9	3	24		39	
10	3	25		40	
11	3	26		41	
12	3	27		42	
13	3	28		43	
14	3	29		44	
15	2	30		45	

ANALYSIS

	Total	**Rating #**	**Total * Rating #**
Rating 0	0	0	0
Rating 1	0	1	0
Rating 2	3	2	6
Rating 3	19	3	57
		Sum	**63**
		# of agg	22

RATE	**2.86**

(sum / # of agg)

Sample ID	**1-II-R**

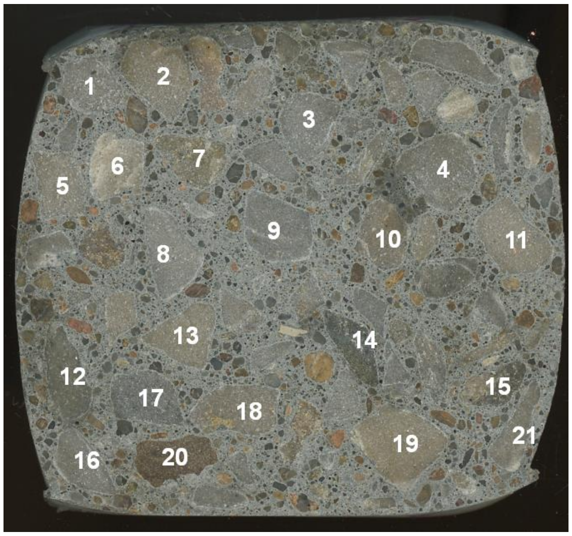

Agg. #	Rating	Agg. #	Rating	Agg. #	Rating
1	3	16	3	31	
2	3	17	2	32	
3	2	18	3	33	
4	3	19	3	34	
5	3	20	2	35	
6	3	21	3	36	
7	2	22		37	
8	3	23		38	
9	3	24		39	
10	3	25		40	
11	3	26		41	
12	3	27		42	
13	3	28		43	
14	3	29		44	
15	3	30		45	

ANALYSIS

	Total	**Rating #**	**Total * Rating #**
Rating 0	0	0	0
Rating 1	0	1	0
Rating 2	4	2	8
Rating 3	17	3	51
		Sum	**59**
		# of agg	21

RATE	**2.81**

(sum / # of agg)

Sample ID	1-III-R

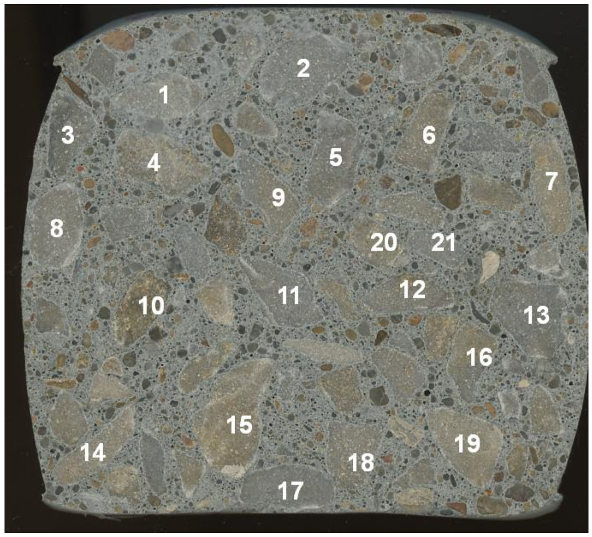

Agg. #	Rating	Agg. #	Rating	Agg. #	Rating
1	2	16	3	31	
2	3	17	3	32	
3	3	18	3	33	
4	2	19	3	34	
5	3	20	2	35	
6	2	21	3	36	
7	3	22		37	
8	3	23		38	
9	3	24		39	
10	3	25		40	
11	3	26		41	
12	3	27		42	
13	3	28		43	
14	3	29		44	
15	3	30		45	

ANALYSIS

	Total	**Rating #**	**Total * Rating #**
Rating 0	0	0	0
Rating 1	0	1	0
Rating 2	4	2	8
Rating 3	17	3	51
		Sum	**59**
		# of agg	21

RATE	**2.81**

(sum / # of agg)

Sample ID	1-IV-R

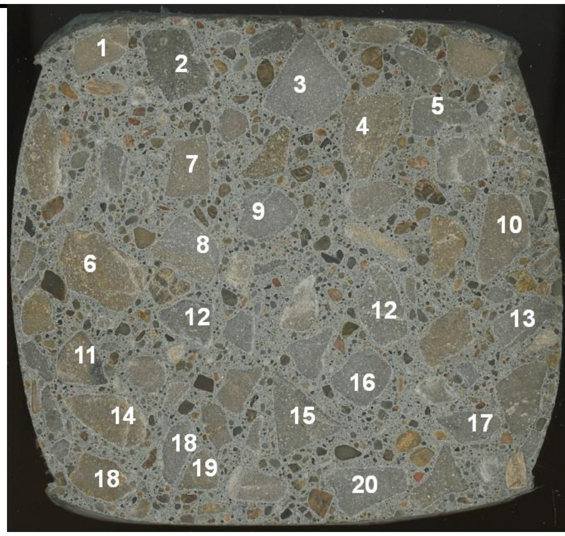

Agg. #	Rating	Agg. #	Rating	Agg. #	Rating
1	3	16	2	31	
2	3	17	3	32	
3	3	18	3	33	
4	2	19	3	34	
5	3	20	3	35	
6	3	21	2	36	
7	3	22	3	37	
8	3	23		38	
9	3	24		39	
10	3	25		40	
11	3	26		41	
12	3	27		42	
13	3	28		43	
14	3	29		44	
15	2	30		45	

ANALYSIS

	Total	**Rating #**	**Total * Rating #**
Rating 0	0	0	0
Rating 1	0	1	0
Rating 2	4	2	8
Rating 3	18	3	54
		Sum	**62**
		# of agg	22

RATE	**2.82**

(sum / # of agg)

Sample ID	1-V-R

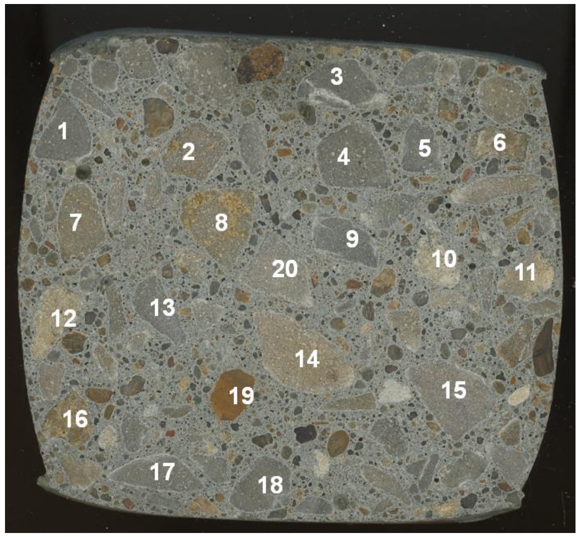

Agg. #	Rating	Agg. #	Rating	Agg. #	Rating
1	3	16	3	31	
2	3	17	3	32	
3	3	18	3	33	
4	2	19	2	34	
5	3	20	2	35	
6	3	21		36	
7	3	22		37	
8	2	23		38	
9	3	24		39	
10	3	25		40	
11	3	26		41	
12	3	27		42	
13	2	28		43	
14	2	29		44	
15	3	30		45	

ANALYSIS

	Total	**Rating #**	**Total * Rating #**
Rating 0	0	0	0
Rating 1	0	1	0
Rating 2	6	2	12
Rating 3	14	3	42
		Sum	**54**
		# of agg	20

RATE	**2.70**

(sum / # of agg)

Sample Name:	2-I

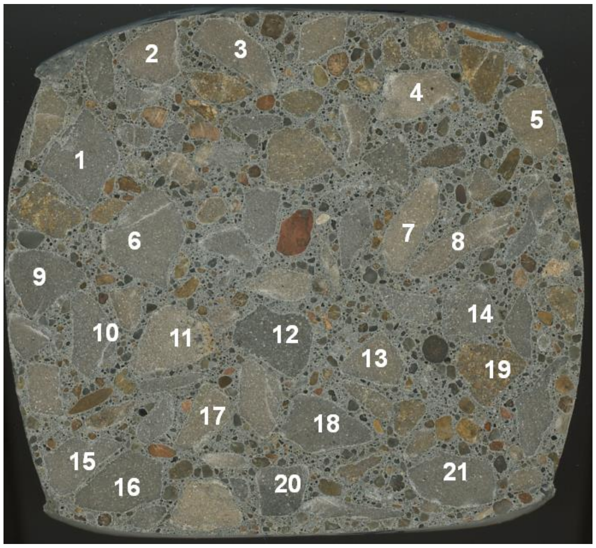

Agg. #	Rating	Agg. #	Rating	Agg. #	Rating
1	3	16	3	31	
2	2	17	2	32	
3	3	18	2	33	
4	2	19	2	34	
5	2	20	2	35	
6	2	21	3	36	
7	2	22		37	
8	2	23		38	
9	2	24		39	
10	2	25		40	
11	1	26		41	
12	2	27		42	
13	2	28		43	
14	2	29		44	
15	3	30		45	

ANALYSIS

	Total	**Rating #**	**Total * Rating #**
Rating 0	0	0	0
Rating 1	1	1	1
Rating 2	15	2	30
Rating 3	5	3	15
		Sum	**46**
		# of agg	21

RATE	**2.19**

(sum / # of agg)

Sample Name:	2-II

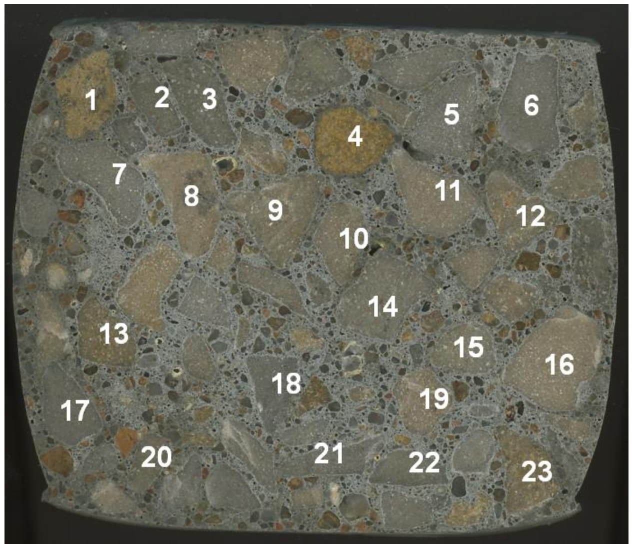

Agg. #	Rating	Agg. #	Rating	Agg. #	Rating
1	2	16	3	31	
2	3	17	3	32	
3	3	18	2	33	
4	3	19	2	34	
5	3	20	2	35	
6	3	21	3	36	
7	3	22	3	37	
8	3	23	2	38	
9	3	24		39	
10	3	25		40	
11	2	26		41	
12	3	27		42	
13	3	28		43	
14	3	29		44	
15	3	30		45	

ANALYSIS

	Total	**Rating #**	**Total * Rating #**
Rating 0	0	0	0
Rating 1	0	1	0
Rating 2	6	2	12
Rating 3	17	3	51
		Sum	**63**
		# of agg	23

RATE	**2.74**

(sum / # of agg)

Sample Name:	2-III

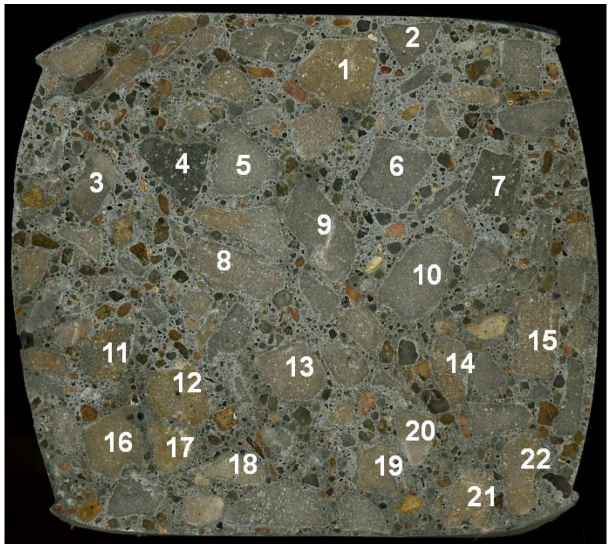

Agg. #	Rating	Agg. #	Rating	Agg. #	Rating
1	2	16	3	31	
2	2	17	3	32	
3	2	18	2	33	
4	2	19	3	34	
5	3	20	2	35	
6	2	21	3	36	
7	3	22	3	37	
8	2	23		38	
9	2	24		39	
10	2	25		40	
11	2	26		41	
12	3	27		42	
13	3	28		43	
14	2	29		44	
15	3	30		45	

ANALYSIS

	Total	**Rating #**	**Total * Rating #**
Rating 0	0	0	0
Rating 1	0	1	0
Rating 2	12	2	24
Rating 3	10	3	30
		Sum	**54**
		# of agg	22

RATE	**2.45**

(sum / # of agg)

Sample Name:	2-IV

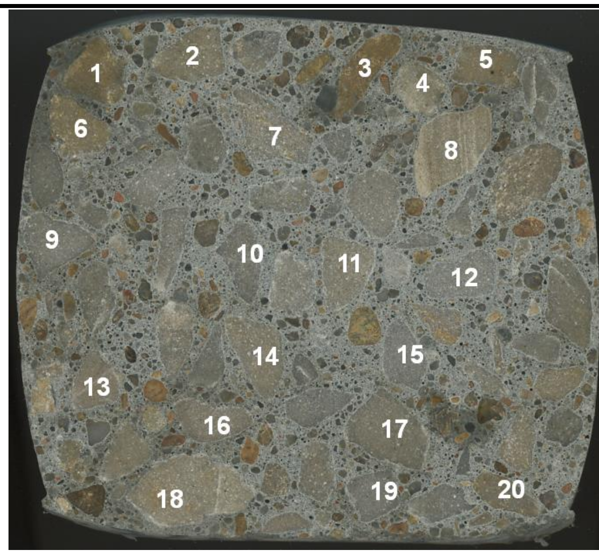

Agg. #	Rating	Agg. #	Rating	Agg. #	Rating
1	3	16	2	31	
2	3	17	2	32	
3	3	18	3	33	
4	3	19	2	34	
5	3	20	3	35	
6	3	21		36	
7	2	22		37	
8	3	23		38	
9	3	24		39	
10	3	25		40	
11	2	26		41	
12	2	27		42	
13	3	28		43	
14	2	29		44	
15	2	30		45	

ANALYSIS

	Total	**Rating #**	**Total * Rating #**
Rating 0	0	0	0
Rating 1	0	1	0
Rating 2	8	2	16
Rating 3	12	3	36
		Sum	**52**
		# of agg	20

RATE	**2.60**

(sum / # of agg)

Sample Name:	2-V

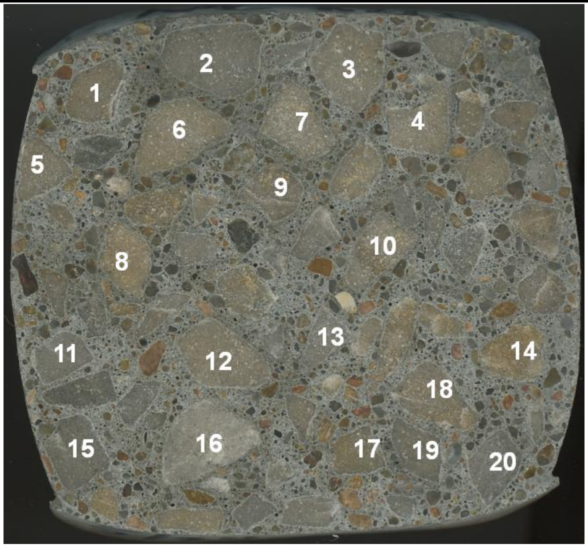

Agg. #	Rating	Agg. #	Rating	Agg. #	Rating
1	3	16	3	31	
2	3	17	3	32	
3	3	18	3	33	
4	3	19	3	34	
5	3	20	3	35	
6	2	21		36	
7	3	22		37	
8	3	23		38	
9	3	24		39	
10	3	25		40	
11	3	26		41	
12	3	27		42	
13	3	28		43	
14	3	29		44	
15	3	30		45	

ANALYSIS

	Total	Rating #	Total * Rating #
Rating 0	0	0	0
Rating 1	0	1	0
Rating 2	1	2	2
Rating 3	19	3	57
		Sum	**59**
		# of agg	20

RATE	**2.95**

(sum / # of agg)

Sample Name:	2-I-R

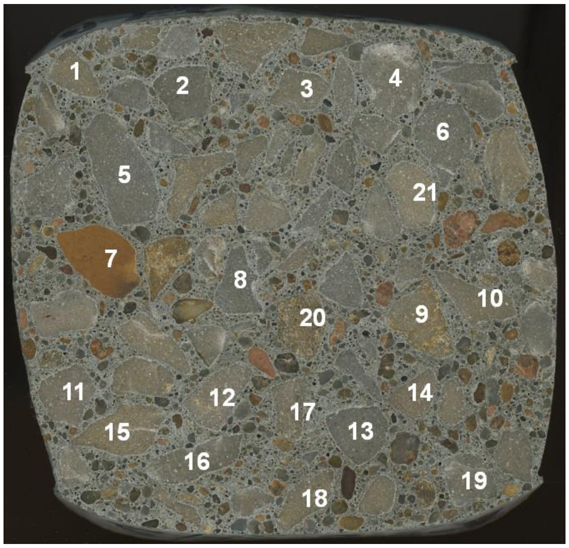

Agg. #	Rating	Agg. #	Rating	Agg. #	Rating
1	3	16	3	31	
2	2	17	3	32	
3	2	18	3	33	
4	3	19	3	34	
5	3	20	2	35	
6	2	21	2	36	
7	3	22		37	
8	3	23		38	
9	2	24		39	
10	2	25		40	
11	3	26		41	
12	3	27		42	
13	2	28		43	
14	3	29		44	
15	3	30		45	

ANALYSIS

	Total	**Rating #**	**Total * Rating #**
Rating 0	0	0	0
Rating 1	0	1	0
Rating 2	8	2	16
Rating 3	13	3	39
		Sum	**55**
		# of agg	21

RATE	**2.62**

(sum / # of agg)

Sample Name:	2-II-R

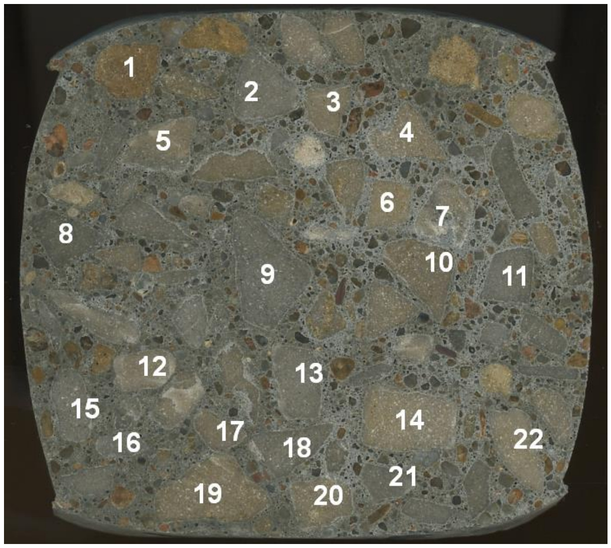

Agg. #	Rating	Agg. #	Rating	Agg. #	Rating
1	3	16	3	31	
2	3	17	3	32	
3	3	18	3	33	
4	3	19	3	34	
5	2	20	3	35	
6	3	21	3	36	
7	3	22	3	37	
8	3	23		38	
9	3	24		39	
10	3	25		40	
11	2	26		41	
12	3	27		42	
13	3	28		43	
14	2	29		44	
15	3	30		45	

ANALYSIS

	Total	**Rating #**	**Total * Rating #**
Rating 0	0	0	0
Rating 1	0	1	0
Rating 2	3	2	6
Rating 3	19	3	57
		Sum	**63**
		# of agg	22

RATE	**2.86**

(sum / # of agg)

Sample Name:	2-III-R

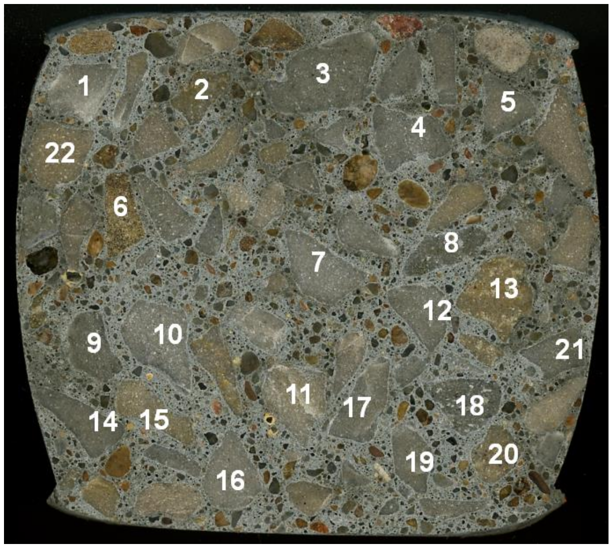

Agg. #	Rating	Agg. #	Rating	Agg. #	Rating
1	3	16	2	31	
2	3	17	3	32	
3	3	18	3	33	
4	3	19	2	34	
5	3	20	3	35	
6	2	21	3	36	
7	2	22	3	37	
8	3	23		38	
9	3	24		39	
10	3	25		40	
11	2	26		41	
12	3	27		42	
13	3	28		43	
14	3	29		44	
15	2	30		45	

ANALYSIS

	Total	**Rating #**	**Total * Rating #**
Rating 0	0	0	0
Rating 1	0	1	0
Rating 2	6	2	12
Rating 3	16	3	48
		Sum	**60**
		# of agg	22

RATE	**2.73**

(sum / # of agg)

Sample Name:	2-IV-R

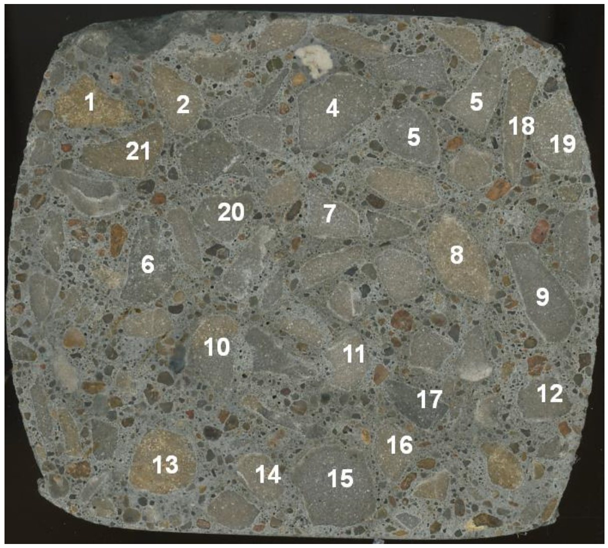

Agg. #	Rating	Agg. #	Rating	Agg. #	Rating
1	3	16	2	31	
2	3	17	3	32	
3	2	18	3	33	
4	2	19	2	34	
5	3	20	2	35	
6	3	21	3	36	
7	3	22	3	37	
8	3	23		38	
9	3	24		39	
10	2	25		40	
11	2	26		41	
12	2	27		42	
13	3	28		43	
14	3	29		44	
15	2	30		45	

ANALYSIS

	Total	**Rating #**	**Total * Rating #**
Rating 0	0	0	0
Rating 1	0	1	0
Rating 2	9	2	18
Rating 3	13	3	39
		Sum	**57**
		# of agg	22

RATE	**2.59**

(sum / # of agg)

Sample Name:	2-V-R

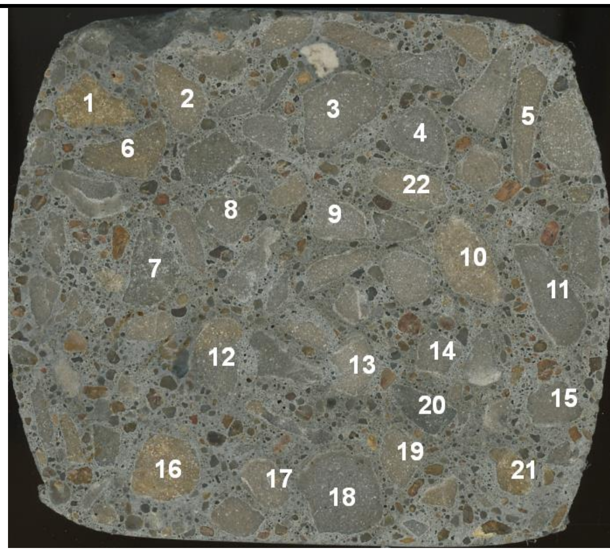

Agg. #	Rating	Agg. #	Rating	Agg. #	Rating
1	3	16	3	31	
2	3	17	3	32	
3	3	18	3	33	
4	3	19	2	34	
5	3	20	3	35	
6	3	21	3	36	
7	2	22	3	37	
8	3	23		38	
9	3	24		39	
10	3	25		40	
11	3	26		41	
12	3	27		42	
13	3	28		43	
14	2	29		44	
15	2	30		45	

ANALYSIS

	Total	**Rating #**	**Total * Rating #**
Rating 0	0	0	0
Rating 1	0	1	0
Rating 2	4	2	8
Rating 3	18	3	54
		Sum	**62**
		# of agg	22

RATE	**2.82**

(sum / # of agg)

Sample Name:	3-I

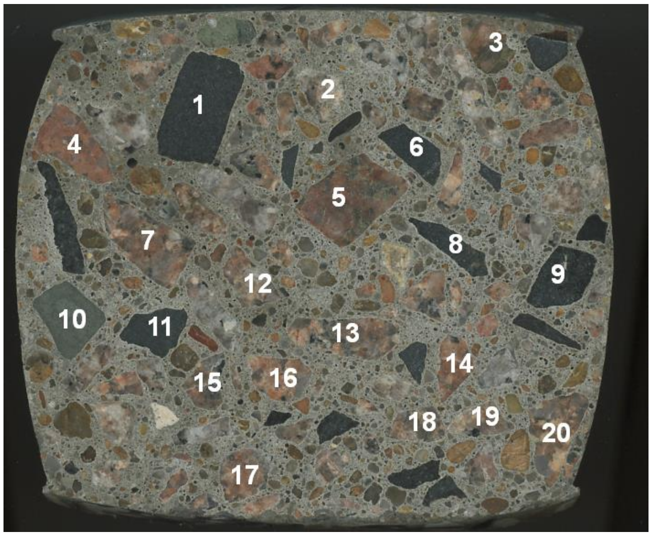

Agg. #	Rating	Agg. #	Rating	Agg. #	Rating
1	3	16	2	31	
2	3	17	3	32	
3	3	18	2	33	
4	3	19	3	34	
5	3	20	3	35	
6	3	21		36	
7	3	22		37	
8	3	23		38	
9	3	24		39	
10	3	25		40	
11	2	26		41	
12	2	27		42	
13	2	28		43	
14	2	29		44	
15	2	30		45	

ANALYSIS

	Total	Rating #	Total * Rating #
Rating 0	0	0	0
Rating 1	0	1	0
Rating 2	7	2	14
Rating 3	13	3	39
		Sum	**53**
		# of agg	20

RATE	**2.65**

(sum / # of agg)

Sample Name:	3-II

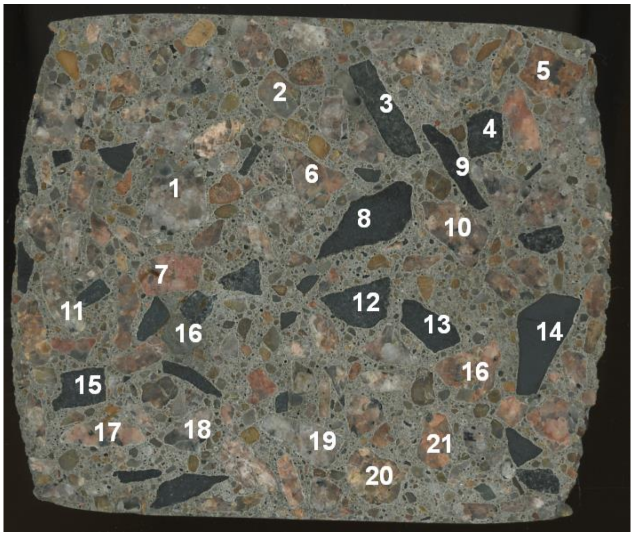

Agg. #	Rating	Agg. #	Rating	Agg. #	Rating
1	3	16	2	31	
2	3	17	3	32	
3	2	18	2	33	
4	2	19	2	34	
5	3	20	3	35	
6	2	21	2	36	
7	2	22		37	
8	2	23		38	
9	2	24		39	
10	2	25		40	
11	3	26		41	
12	3	27		42	
13	2	28		43	
14	2	29		44	
15	3	30		45	

ANALYSIS

	Total	**Rating #**	**Total * Rating #**
Rating 0	0	0	0
Rating 1	0	1	0
Rating 2	13	2	26
Rating 3	8	3	24
		Sum	**50**
		# of agg	21

RATE	**2.38**

(sum / # of agg)

Sample Name:	3-III

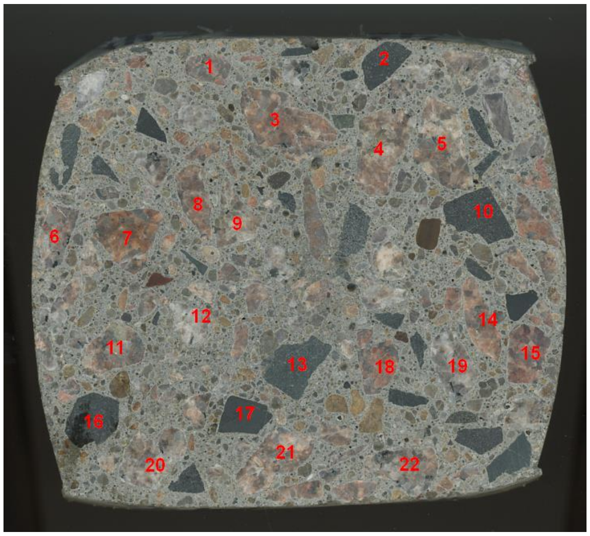

Agg. #	Rating	Agg. #	Rating	Agg. #	Rating
1	2	16	3	31	
2	2	17	2	32	
3	2	18	2	33	
4	2	19	2	34	
5	2	20	2	35	
6	3	21	2	36	
7	2	22	2	37	
8	2	23		38	
9	2	24		39	
10	2	25		40	
11	2	26		41	
12	2	27		42	
13	2	28		43	
14	2	29		44	
15	2	30		45	

ANALYSIS

	Total	Rating #	Total * Rating #
Rating 0	0	0	0
Rating 1	0	1	0
Rating 2	20	2	40
Rating 3	2	3	6
		Sum	**46**
		# of agg	22

RATE	**2.09**

(sum / # of agg)

Sample Name:	3-IV

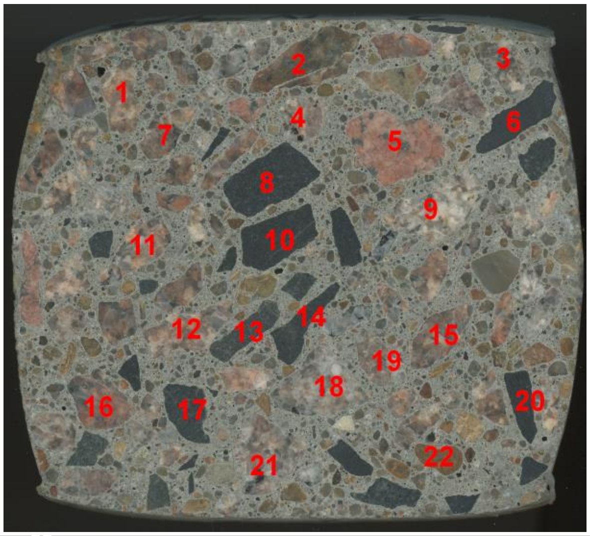

Agg. #	Rating
1	3
2	3
3	2
4	2
5	2
6	2
7	1
8	2
9	2
10	2
11	1
12	2
13	2
14	2
15	2

Agg. #	Rating
16	2
17	2
18	2
19	2
20	2
21	2
22	2
23	
24	
25	
26	
27	
28	
29	
30	

Agg. #	Rating
31	
32	
33	
34	
35	
36	
37	
38	
39	
40	
41	
42	
43	
44	
45	

ANALYSIS

	Total	Rating #	Total * Rating #
Rating 0	0	0	0
Rating 1	2	1	2
Rating 2	18	2	36
Rating 3	2	3	6
		Sum	**44**
		# of agg	22

RATE	**2.00**

(sum / # of agg)

Sample Name:	3-V

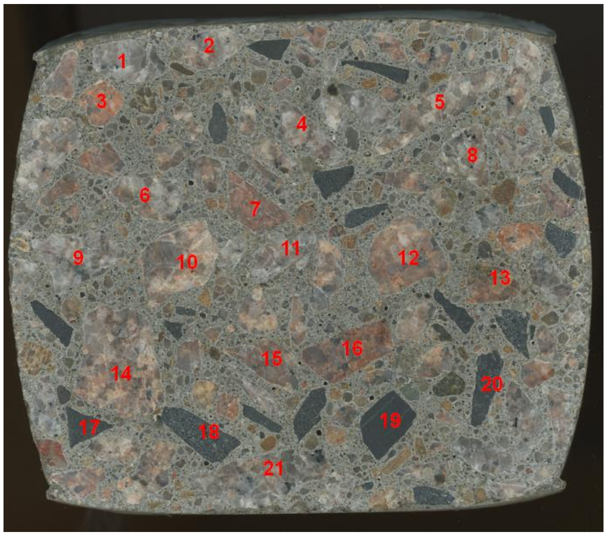

Agg. #	Rating	Agg. #	Rating	Agg. #	Rating
1	3	16	2	31	
2	3	17	3	32	
3	3	18	2	33	
4	2	19	2	34	
5	2	20	2	35	
6	3	21	3	36	
7	2	22		37	
8	3	23		38	
9	3	24		39	
10	3	25		40	
11	2	26		41	
12	2	27		42	
13	2	28		43	
14	3	29		44	
15	3	30		45	

ANALYSIS

	Total	**Rating #**	**Total * Rating #**
Rating 0	0	0	0
Rating 1	0	1	0
Rating 2	10	2	20
Rating 3	11	3	33
		Sum	**53**
		# of agg	21

RATE	**2.52**

(sum / # of agg)

Sample Name:	3-I-R

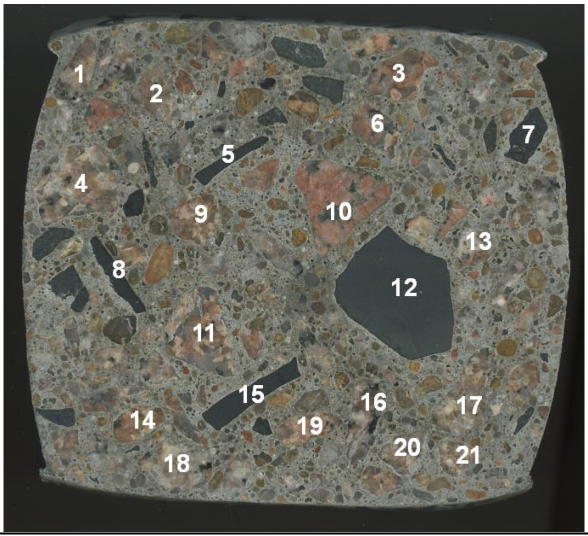

Agg. #	Rating	Agg. #	Rating	Agg. #	Rating
1	3	16	2	31	
2	3	17	3	32	
3	3	18	2	33	
4	3	19	2	34	
5	2	20	3	35	
6	3	21	3	36	
7	3	22		37	
8	2	23		38	
9	2	24		39	
10	2	25		40	
11	2	26		41	
12	2	27		42	
13	3	28		43	
14	2	29		44	
15	2	30		45	

ANALYSIS

	Total	**Rating #**	**Total * Rating #**
Rating 0	0	0	0
Rating 1	0	1	0
Rating 2	11	2	22
Rating 3	10	3	30
		Sum	**52**
		# of agg	21

RATE	**2.48**

(sum / # of agg)

Sample Name:	3-II-R

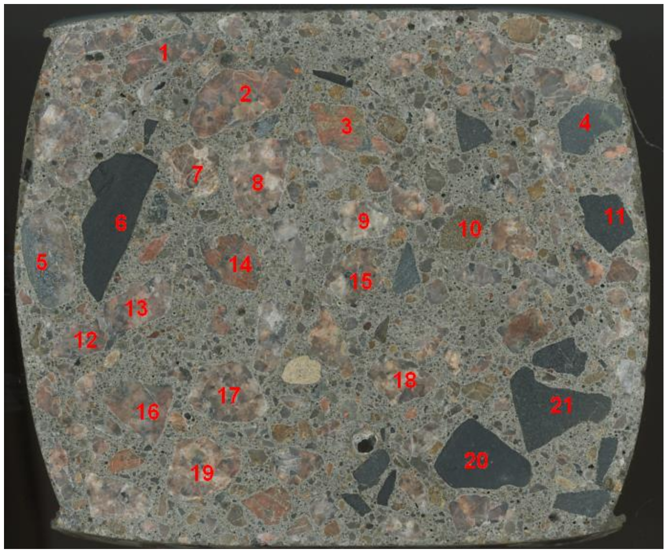

Agg. #	Rating	Agg. #	Rating	Agg. #	Rating
1	3	16	2	31	
2	3	17	2	32	
3	2	18	2	33	
4	3	19	2	34	
5	3	20	2	35	
6	2	21	3	36	
7	3	22		37	
8	3	23		38	
9	3	24		39	
10	2	25		40	
11	3	26		41	
12	3	27		42	
13	3	28		43	
14	2	29		44	
15	2	30		45	

ANALYSIS

	Total	**Rating #**	**Total * Rating #**
Rating 0	0	0	0
Rating 1	0	1	0
Rating 2	10	2	20
Rating 3	11	3	33
		Sum	**53**
		# of agg	21

RATE	**2.52**

(sum / # of agg)

Sample Name:	3-III-R

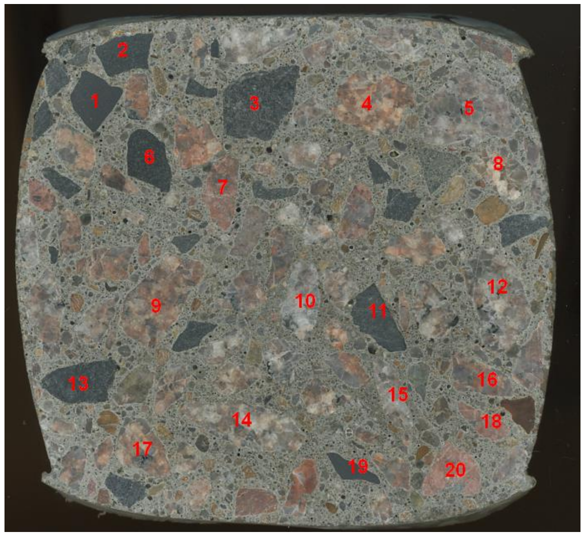

Agg. #	Rating	Agg. #	Rating	Agg. #	Rating
1	3	16	2	31	
2	3	17	3	32	
3	3	18	3	33	
4	3	19	2	34	
5	3	20	3	35	
6	3	21		36	
7	3	22		37	
8	3	23		38	
9	3	24		39	
10	2	25		40	
11	2	26		41	
12	2	27		42	
13	3	28		43	
14	3	29		44	
15	3	30		45	

ANALYSIS

	Total	**Rating #**	**Total * Rating #**
Rating 0	0	0	0
Rating 1	0	1	0
Rating 2	5	2	10
Rating 3	15	3	45
		Sum	**55**
		# of agg	20

RATE	**2.75**

(sum / # of agg)

Sample Name:	3-IV-R

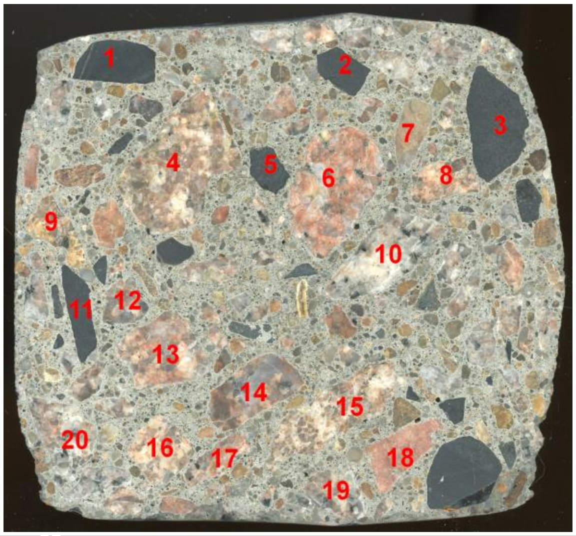

Agg. #	Rating
1	3
2	2
3	3
4	3
5	2
6	2
7	2
8	3
9	3
10	2
11	2
12	2
13	2
14	2
15	3

Agg. #	Rating
16	3
17	3
18	3
19	3
20	3
21	
22	
23	
24	
25	
26	
27	
28	
29	
30	

Agg. #	Rating
31	
32	
33	
34	
35	
36	
37	
38	
39	
40	
41	
42	
43	
44	
45	

ANALYSIS

	Total	**Rating #**	**Total * Rating #**
Rating 0	0	0	0
Rating 1	0	1	0
Rating 2	9	2	18
Rating 3	11	3	33
		Sum	**51**
		# of agg	20

RATE	**2.55**

(sum / # of agg)

Sample Name:	3-V-R

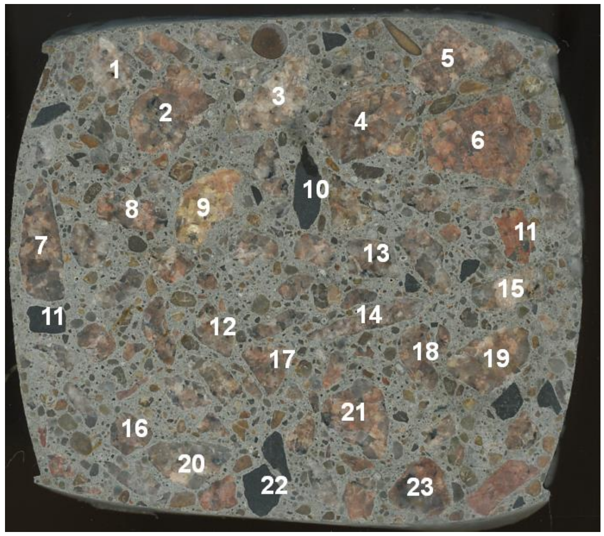

Agg. #	Rating	Agg. #	Rating	Agg. #	Rating
1	3	16	3	31	
2	2	17	2	32	
3	3	18	2	33	
4	3	19	2	34	
5	3	20	2	35	
6	3	21	2	36	
7	3	22	3	37	
8	2	23	3	38	
9	2	24	2	39	
10	3	25		40	
11	3	26		41	
12	3	27		42	
13	3	28		43	
14	2	29		44	
15	2	30		45	

ANALYSIS

	Total	Rating #	Total * Rating #
Rating 0	0	0	0
Rating 1	0	1	0
Rating 2	11	2	22
Rating 3	13	3	39
		Sum	**61**
		# of agg	24

RATE	**2.54**

(sum / # of agg)

Sample Name:	4-I

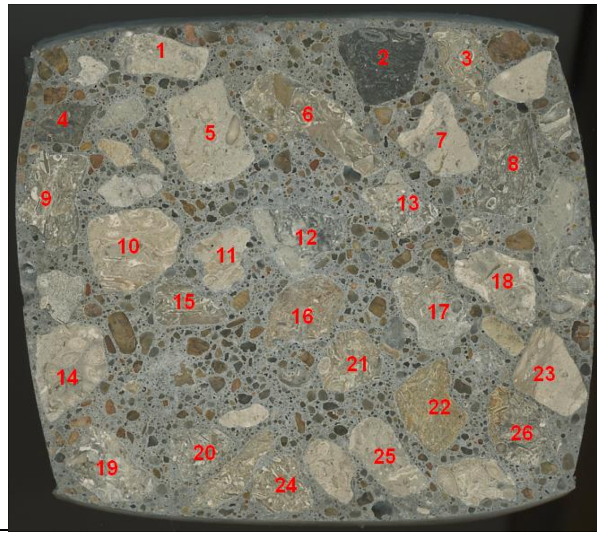

Agg. #	Rating	Agg. #	Rating	Agg. #	Rating
1	1	16	2	31	1
2	2	17	1	32	1
3	1	18	1	33	2
4	2	19	2	34	
5	2	20	2	35	
6	2	21	2	36	
7	2	22	2	37	
8	2	23	2	38	
9	2	24	1	39	
10	2	25	1	40	
11	1	26	1	41	
12	1	27	2	42	
13	2	28	1	43	
14	1	29	1	44	
15	1	30	2	45	

ANALYSIS

	Total	**Rating #**	**Total * Rating #**
Rating 0	0	0	0
Rating 1	15	1	15
Rating 2	18	2	36
Rating 3	0	3	0
		Sum	**51**
		# of agg	33

RATE	**1.55**

(sum / # of agg)

Sample Name:	4-II

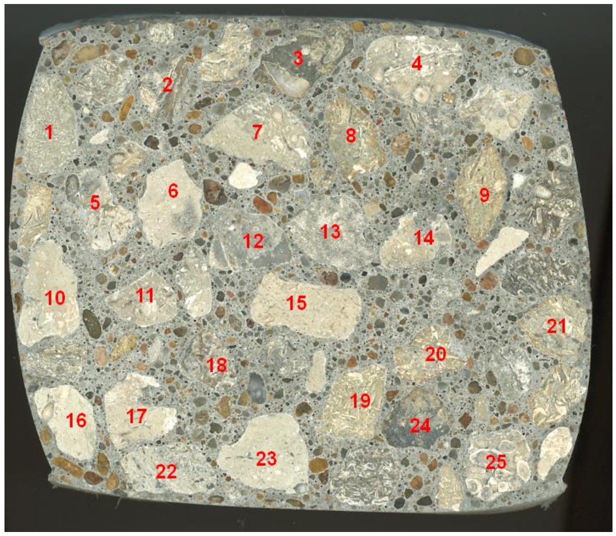

Agg. #	Rating	Agg. #	Rating	Agg. #	Rating
1	1	16	2	31	1
2	2	17	1	32	1
3	1	18	1	33	2
4	2	19	2	34	
5	2	20	2	35	
6	2	21	2	36	
7	2	22	2	37	
8	2	23	2	38	
9	2	24	1	39	
10	2	25	1	40	
11	1	26	1	41	
12	1	27	2	42	
13	2	28	1	43	
14	1	29	1	44	
15	1	30	2	45	

ANALYSIS

	Total	**Rating #**	**Total * Rating #**
Rating 0	0	0	0
Rating 1	15	1	15
Rating 2	18	2	36
Rating 3	0	3	0
		Sum	**51**
		# of agg	33

RATE	**1.55**

(sum / # of agg)

Sample Name:	4-III

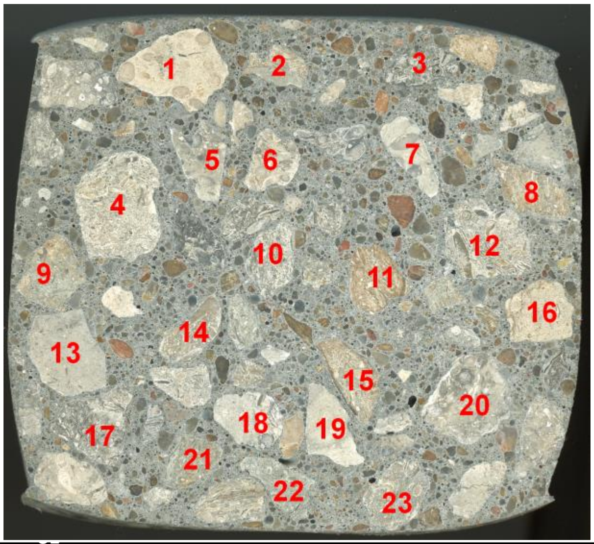

Agg. #	Rating
1	3
2	2
3	2
4	3
5	2
6	2
7	2
8	3
9	3
10	2
11	2
12	3
13	3
14	2
15	2

Agg. #	Rating
16	3
17	3
18	2
19	2
20	3
21	2
22	2
23	3
24	
25	
26	
27	
28	
29	
30	

Agg. #	Rating
31	
32	
33	
34	
35	
36	
37	
38	
39	
40	
41	
42	
43	
44	
45	

ANALYSIS

	Total	**Rating #**	**Total * Rating #**
Rating 0	0	0	0
Rating 1	0	1	0
Rating 2	13	2	26
Rating 3	10	3	30
		Sum	**56**
		# of agg	23

RATE	**2.43**

(sum / # of agg)

Sample Name:	2/19 4-IVb

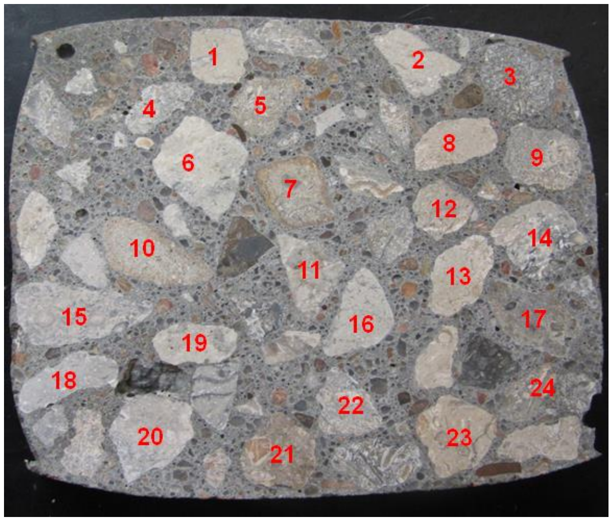

Agg. #	Rating
1	3
2	3
3	2
4	3
5	2
6	2
7	2
8	2
9	2
10	2
11	2
12	2
13	3
14	3
15	3

Agg. #	Rating
16	2
17	3
18	2
19	2
20	2
21	2
22	3
23	3
24	3
25	
26	
27	
28	
29	
30	

Agg. #	Rating
31	
32	
33	
34	
35	
36	
37	
38	
39	
40	
41	
42	
43	
44	
45	

ANALYSIS

	Total	**Rating #**	**Total * Rating #**
Rating 0	0	0	0
Rating 1	0	1	0
Rating 2	14	2	28
Rating 3	10	3	30
		Sum	**58**
		# of agg	24

RATE	**2.42**

(sum / # of agg)

Sample Name:	2/11 4-V

Agg. #	Rating	Agg. #	Rating	Agg. #	Rating
1	3	16	3	31	
2	3	17	3	32	
3	3	18	3	33	
4	3	19	3	34	
5	3	20	3	35	
6	3	21	3	36	
7	3	22	3	37	
8	3	23	3	38	
9	3	24	3	39	
10	3	25		40	
11	3	26		41	
12	3	27		42	
13	3	28		43	
14	3	29		44	
15	3	30		45	

ANALYSIS

	Total	**Rating #**	**Total * Rating #**
Rating 0	0	0	0
Rating 1	0	1	0
Rating 2	0	2	0
Rating 3	24	3	72
		Sum	**72**
		# of agg	24

RATE	**3.00**

(sum / # of agg)

Sample Name:	4-I-R

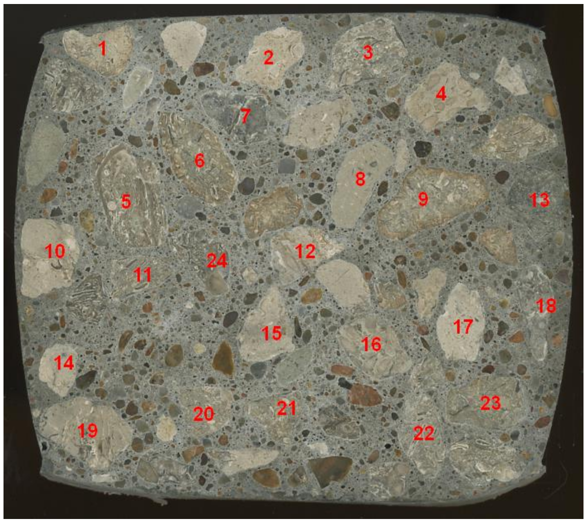

Agg. #	Rating	Agg. #	Rating	Agg. #	Rating
1	1	16	2	31	1
2	2	17	1	32	1
3	1	18	1	33	2
4	2	19	2	34	
5	2	20	2	35	
6	2	21	2	36	
7	2	22	2	37	
8	2	23	2	38	
9	2	24	1	39	
10	2	25	1	40	
11	1	26	1	41	
12	1	27	2	42	
13	2	28	1	43	
14	1	29	1	44	
15	1	30	2	45	

ANALYSIS

	Total	**Rating #**	**Total * Rating #**
Rating 0	0	0	0
Rating 1	15	1	15
Rating 2	18	2	36
Rating 3	0	3	0
		Sum	**51**
		# of agg	33

RATE	**1.55**

(sum / # of agg)

Sample Name:	4-II-R

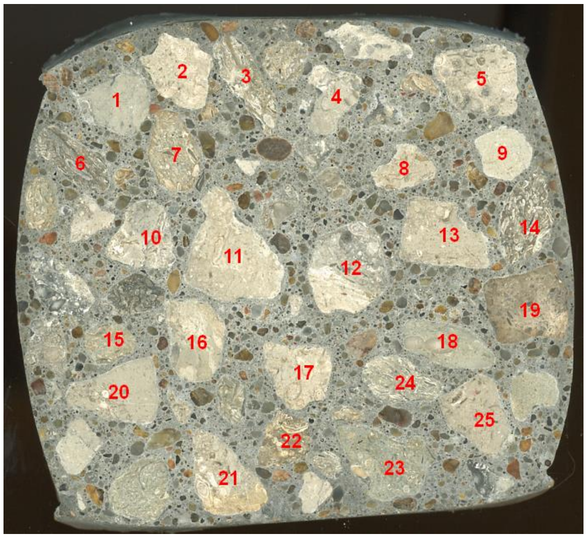

Agg. #	Rating	Agg. #	Rating	Agg. #	Rating
1	1	16	2	31	1
2	2	17	1	32	1
3	1	18	1	33	2
4	2	19	2	34	
5	2	20	2	35	
6	2	21	2	36	
7	2	22	2	37	
8	2	23	2	38	
9	2	24	1	39	
10	2	25	1	40	
11	1	26	1	41	
12	1	27	2	42	
13	2	28	1	43	
14	1	29	1	44	
15	1	30	2	45	

ANALYSIS

	Total	**Rating #**	**Total * Rating #**
Rating 0	0	0	0
Rating 1	15	1	15
Rating 2	18	2	36
Rating 3	0	3	0
		Sum	**51**
		# of agg	33

RATE	**1.55**

(sum / # of agg)

Sample Name:	4-III-R

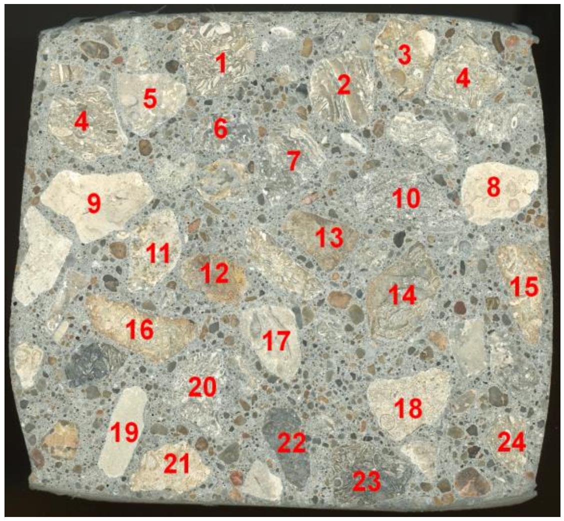

Agg. #	Rating
1	3
2	3
3	3
4	3
5	3
6	3
7	3
8	3
9	3
10	3
11	3
12	3
13	3
14	2
15	3

Agg. #	Rating
16	3
17	2
18	3
19	3
20	3
21	3
22	3
23	3
24	3
25	3
26	
27	
28	
29	
30	

Agg. #	Rating
31	
32	
33	
34	
35	
36	
37	
38	
39	
40	
41	
42	
43	
44	
45	

ANALYSIS

	Total	Rating #	Total * Rating #
Rating 0	0	0	0
Rating 1	0	1	0
Rating 2	2	2	4
Rating 3	23	3	69
		Sum	**73**
		# of agg	25

RATE	**2.92**

(sum / # of agg)

Sample Name:	4-IV-R

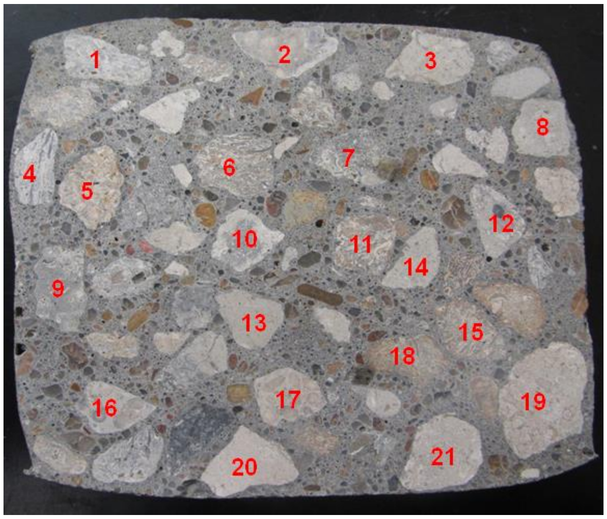

Agg. #	Rating
1	3
2	2
3	3
4	3
5	2
6	3
7	3
8	3
9	3
10	3
11	3
12	2
13	3
14	2
15	3

Agg. #	Rating
16	3
17	3
18	3
19	3
20	2
21	3
22	
23	
24	
25	
26	
27	
28	
29	
30	

Agg. #	Rating
31	
32	
33	
34	
35	
36	
37	
38	
39	
40	
41	
42	
43	
44	
45	

ANALYSIS

	Total	**Rating #**	**Total * Rating #**
Rating 0	0	0	0
Rating 1	0	1	0
Rating 2	5	2	10
Rating 3	16	3	48
		Sum	**58**
		# of agg	21

RATE	**2.76**

(sum / # of agg)

Sample Name:	4-V-R

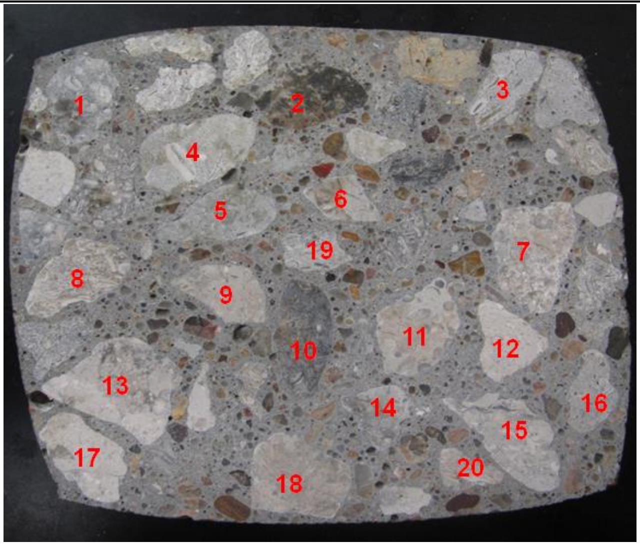

Agg. #	Rating
1	3
2	3
3	3
4	3
5	3
6	3
7	3
8	3
9	3
10	3
11	3
12	3
13	3
14	3
15	3

Agg. #	Rating
16	3
17	3
18	3
19	3
20	3
21	
22	
23	
24	
25	
26	
27	
28	
29	
30	

Agg. #	Rating
31	
32	
33	
34	
35	
36	
37	
38	
39	
40	
41	
42	
43	
44	
45	

ANALYSIS

	Total	**Rating #**	**Total * Rating #**
Rating 0	0	0	0
Rating 1	0	1	0
Rating 2	0	2	0
Rating 3	20	3	60
		Sum	**60**
		# of agg	20

RATE	**3.00**

(sum / # of agg)

Sample Name: 5-I

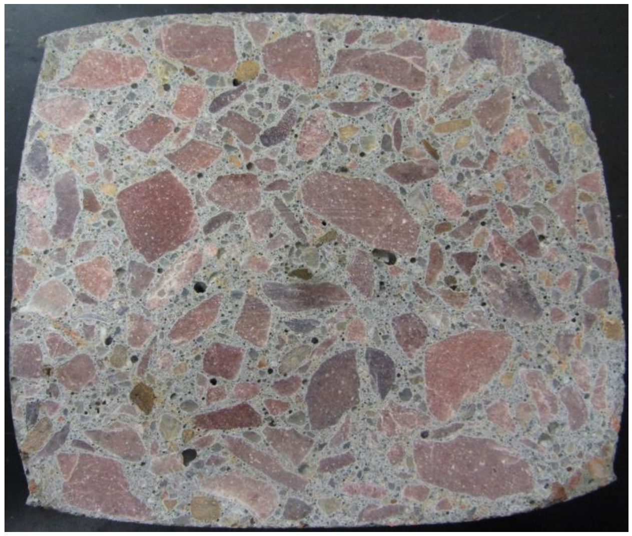

Agg. #	Rating
1	3
2	3
3	2
4	2
5	3
6	3
7	3
8	2
9	2
10	2
11	2
12	2
13	2
14	2
15	2

Agg. #	Rating
16	2
17	3
18	2
19	2
20	3
21	2
22	2
23	3
24	3
25	3
26	3
27	3
28	3
29	2
30	2

Agg. #	Rating
31	2
32	3
33	3
34	
35	
36	
37	
38	
39	
40	
41	
42	
43	
44	
45	

ANALYSIS

	Total	**Rating #**	**Total * Rating #**
Rating 0	0	0	0
Rating 1	0	1	0
Rating 2	18	2	36
Rating 3	15	3	45
		Sum	**81**
		# of agg	33

RATE	**2.45**

(sum / # of agg)

Sample Name:	5-II

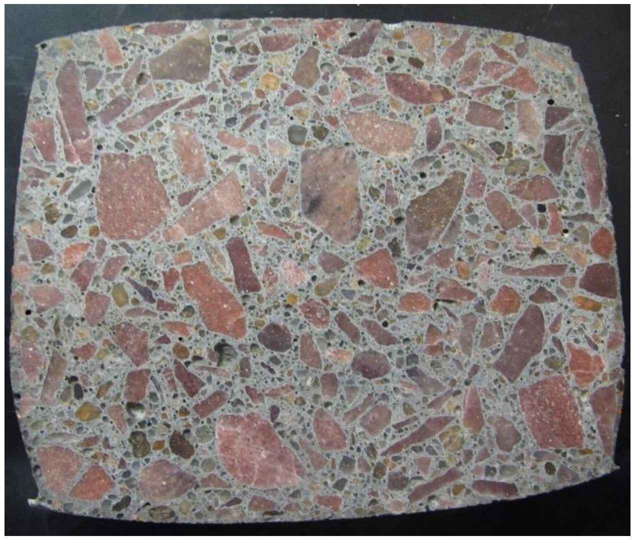

Agg. #	Rating	Agg. #	Rating	Agg. #	Rating
1	2	16	2	31	
2	2	17	2	32	
3	2	18	2	33	
4	2	19	1	34	
5	2	20	2	35	
6	2	21	2	36	
7	2	22	2	37	
8	2	23	2	38	
9	2	24	2	39	
10	2	25	2	40	
11	1	26	1	41	
12	1	27	2	42	
13	2	28		43	
14	1	29		44	
15	1	30		45	

ANALYSIS

	Total	**Rating #**	**Total * Rating #**
Rating 0	0	0	0
Rating 1	6	1	6
Rating 2	21	2	42
Rating 3	0	3	0
		Sum	**48**
		# of agg	27

RATE	**1.78**

(sum / # of agg)

Sample Name:	5-III

Agg. #	Rating	Agg. #	Rating	Agg. #	Rating
1	2	16	3	31	2
2	2	17	2	32	2
3	2	18	2	33	2
4	2	19	2	34	2
5	2	20	2	35	2
6	2	21	2	36	2
7	2	22	2	37	2
8	2	23	1	38	
9	2	24	2	39	
10	2	25	2	40	
11	2	26	1	41	
12	2	27	1	42	
13	1	28	2	43	
14	2	29	2	44	
15	2	30	2	45	

ANALYSIS

	Total	Rating #	Total * Rating #
Rating 0	0	0	0
Rating 1	4	1	4
Rating 2	32	2	64
Rating 3	1	3	3
		Sum	**71**
		# of agg	37

RATE **1.92**

(sum / # of agg)

Sample Name:	5-IV

Agg. #	Rating	Agg. #	Rating	Agg. #	Rating
1	1	16	1	31	1
2	1	17	1	32	1
3	1	18	1	33	1
4	1	19	1	34	1
5	1	20	2	35	
6	1	21	2	36	
7	2	22	2	37	
8	1	23	2	38	
9	2	24	2	39	
10	2	25	2	40	
11	1	26	1	41	
12	1	27	2	42	
13	1	28	2	43	
14	0	29	2	44	
15	0	30	1	45	

ANALYSIS

	Total	Rating #	Total * Rating #
Rating 0	2	0	0
Rating 1	20	1	20
Rating 2	12	2	24
Rating 3	0	3	0
		Sum	**44**
		# of agg	34

RATE	**1.29**

(sum / # of agg)

Sample Name:	5-V

Agg. #	Rating	Agg. #	Rating	Agg. #	Rating
1	2	16	2	31	2
2	2	17	2	32	1
3	1	18	2	33	2
4	2	19	2	34	
5	2	20	2	35	
6	2	21	2	36	
7	2	22	2	37	
8	2	23	1	38	
9	2	24	1	39	
10	2	25	2	40	
11	2	26	1	41	
12	2	27	2	42	
13	2	28	1	43	
14	2	29	2	44	
15	2	30	2	45	

ANALYSIS

	Total	**Rating #**	**Total * Rating #**
Rating 0	0	0	0
Rating 1	6	1	6
Rating 2	27	2	54
Rating 3	0	3	0
		Sum	**60**
		# of agg	33

RATE	**1.82**

(sum / # of agg)

Sample Name:	5-I-R

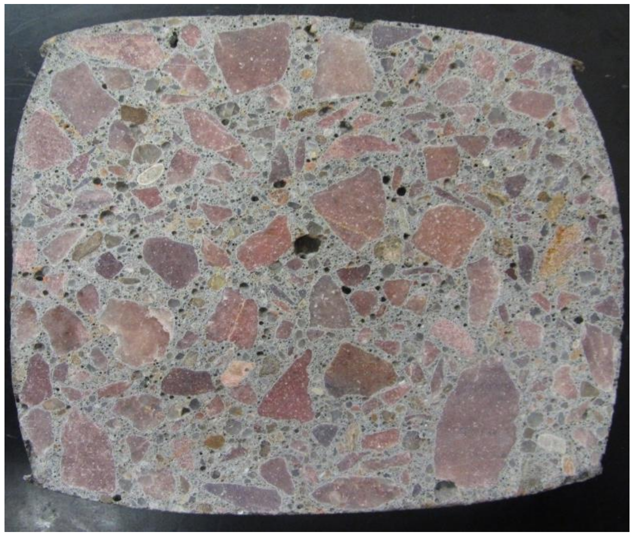

Agg. #	Rating	Agg. #	Rating	Agg. #	Rating
1	3	16	2	31	
2	2	17	2	32	
3	3	18	2	33	
4	2	19	3	34	
5	3	20	2	35	
6	3	21	2	36	
7	2	22	3	37	
8	2	23	2	38	
9	2	24	2	39	
10	3	25	2	40	
11	3	26	2	41	
12	2	27	3	42	
13	2	28	3	43	
14	2	29	2	44	
15	2	30	3	45	

ANALYSIS

	Total	**Rating #**	**Total * Rating #**
Rating 0	0	0	0
Rating 1	0	1	0
Rating 2	19	2	38
Rating 3	11	3	33
		Sum	**71**
		# of agg	30

RATE	**2.37**

(sum / # of agg)

Sample Name:	5-II-R

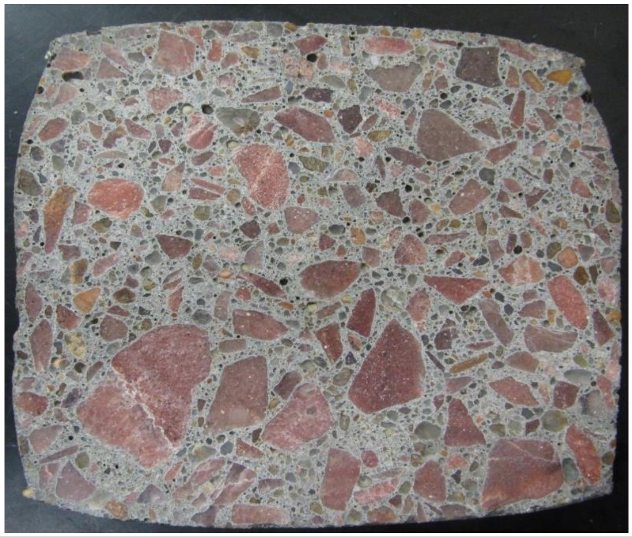

Agg. #	Rating	Agg. #	Rating	Agg. #	Rating
1	2	16	2	31	
2	2	17	3	32	
3	2	18	3	33	
4	2	19	3	34	
5	1	20	3	35	
6	2	21	3	36	
7	2	22	3	37	
8	1	23	3	38	
9	1	24	3	39	
10	2	25	3	40	
11	2	26	3	41	
12	2	27	3	42	
13	3	28	3	43	
14	2	29		44	
15	1	30		45	

ANALYSIS

	Total	**Rating #**	**Total * Rating #**
Rating 0	0	0	0
Rating 1	4	1	4
Rating 2	11	2	22
Rating 3	13	3	39
		Sum	**65**
		# of agg	28

RATE	**2.32**

(sum / # of agg)

Sample Name:	5-III-R

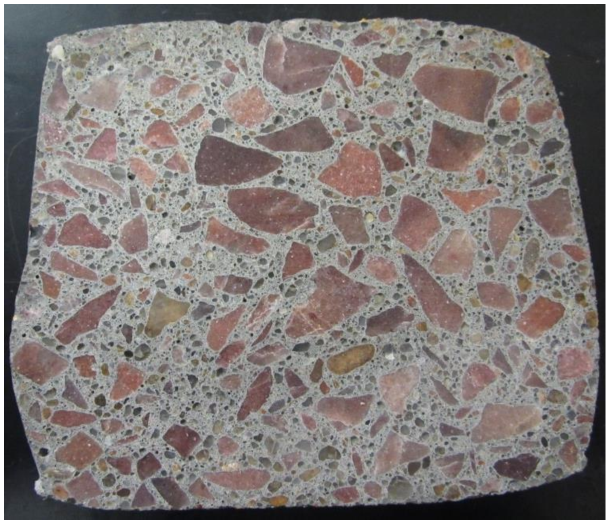

Agg. #	Rating
1	2
2	2
3	2
4	2
5	2
6	3
7	2
8	2
9	2
10	2
11	2
12	3
13	3
14	2
15	2

Agg. #	Rating
16	2
17	2
18	3
19	2
20	3
21	2
22	2
23	2
24	2
25	2
26	3
27	3
28	3
29	2
30	2

Agg. #	Rating
31	2
32	2
33	2
34	2
35	2
36	
37	
38	
39	
40	
41	
42	
43	
44	
45	

ANALYSIS

	Total	**Rating #**	**Total * Rating #**
Rating 0	0	0	0
Rating 1	0	1	0
Rating 2	27	2	54
Rating 3	8	3	24
		Sum	**78**
		# of agg	35

RATE	**2.23**

(sum / # of agg)

Sample Name:	5-IV-R

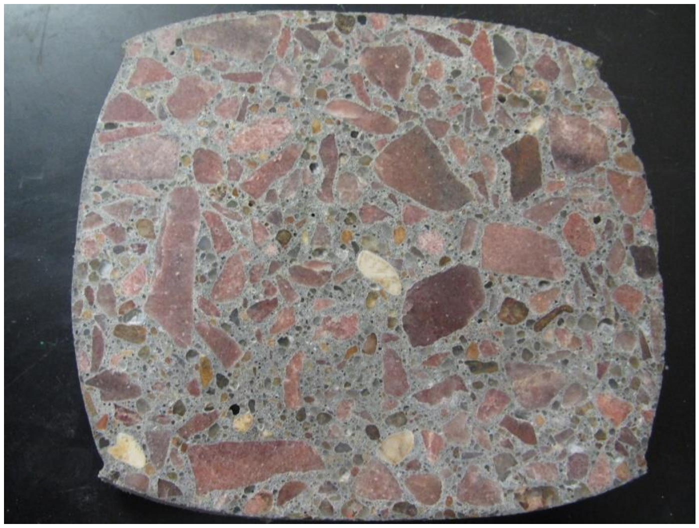

Agg. #	Rating	Agg. #	Rating	Agg. #	Rating
1	1	16	2	31	1
2	2	17	1	32	1
3	1	18	1	33	2
4	2	19	2	34	
5	2	20	2	35	
6	2	21	2	36	
7	2	22	2	37	
8	2	23	2	38	
9	2	24	1	39	
10	2	25	1	40	
11	1	26	1	41	
12	1	27	2	42	
13	2	28	1	43	
14	1	29	1	44	
15	1	30	2	45	

ANALYSIS

	Total	**Rating #**	**Total * Rating #**
Rating 0	0	0	0
Rating 1	15	1	15
Rating 2	18	2	36
Rating 3	0	3	0
		Sum	**51**
		# of agg	33

RATE	**1.55**

(sum / # of agg)

Sample Name:	5-V-R

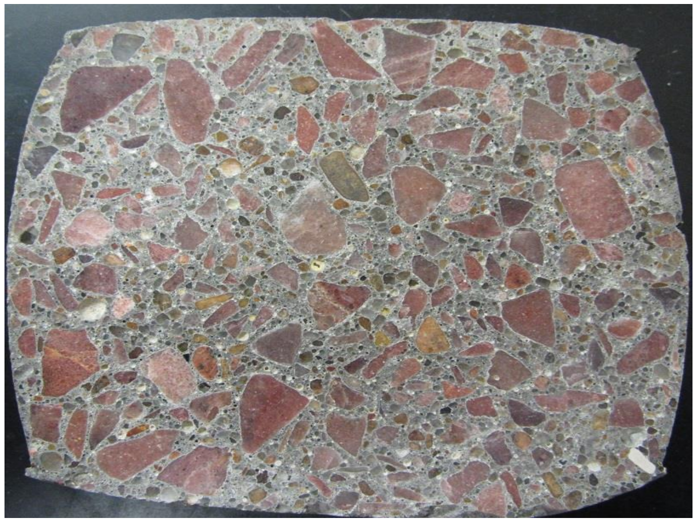

Agg. #	Rating	Agg. #	Rating	Agg. #	Rating
1	2	16	2	31	
2	1	17	2	32	
3	2	18	2	33	
4	2	19	2	34	
5	3	20	3	35	
6	3	21	2	36	
7	3	22	2	37	
8	2	23	2	38	
9	3	24	3	39	
10	3	25	2	40	
11	2	26	3	41	
12	2	27	1	42	
13	3	28	3	43	
14	2	29	2	44	
15	2	30	1	45	

ANALYSIS

	Total	Rating #	Total * Rating #
Rating 0	0	0	0
Rating 1	3	1	3
Rating 2	17	2	34
Rating 3	10	3	30
		Sum	**67**
		# of agg	30

RATE	**2.23**

(sum / # of agg)

Sample Name:	1-I-C

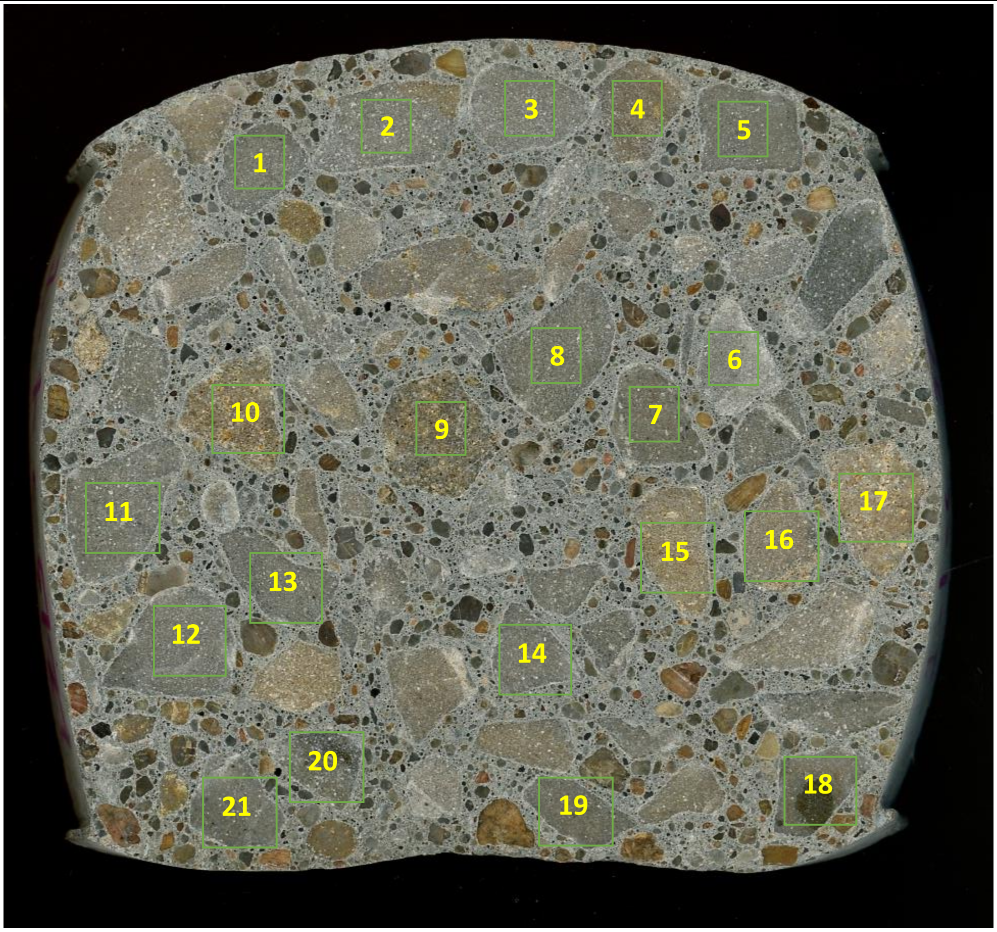

Agg. #	Rating
1	2
2	3
3	2
4	2
5	2
6	3
7	3
8	3
9	3
10	3
11	3
12	2
13	2
14	2
15	3

Agg. #	Rating
16	2
17	2
18	2
19	2
20	2
21	2
22	
23	
24	
25	
26	
27	
28	
29	
30	

Agg. #	Rating
31	
32	
33	
34	
35	
36	
37	
38	
39	
40	
41	
42	
43	
44	
45	

ANALYSIS

Rating 0	0	0	0	Sum	50
Rating 1	0	1	0	# of agg	21
Rating 2	13	2	26	**RATE**	**2.38**
Rating 3	8	3	24		

Sample Name:	1-II-C

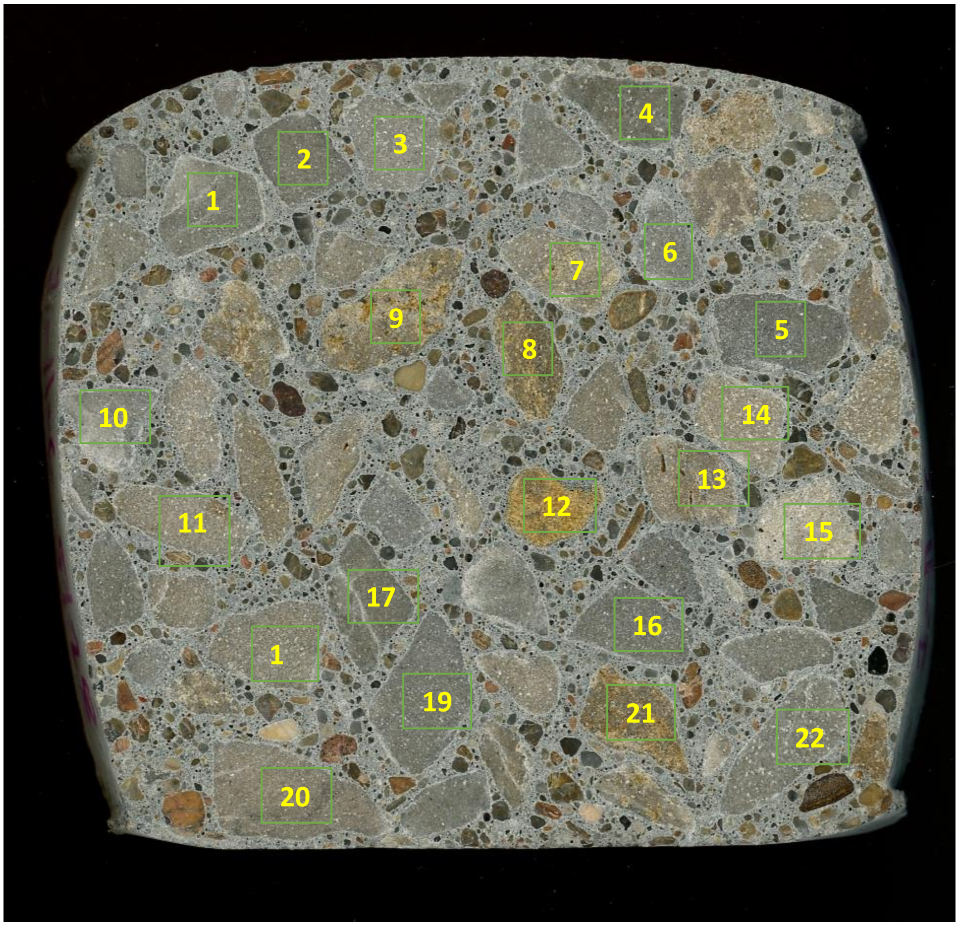

Agg. #	Rating
1	3
2	2
3	3
4	2
5	2
6	3
7	3
8	2
9	3
10	3
11	2
12	2
13	2
14	3
15	2

Agg. #	Rating
16	3
17	2
18	2
19	3
20	2
21	3
22	3
23	
24	
25	
26	
27	
28	
29	
30	

Agg. #	Rating
31	
32	
33	
34	
35	
36	
37	
38	
39	
40	
41	
42	
43	
44	
45	

ANALYSIS

Rating 0	0	0	0	Sum	55
Rating 1	0	1	0	# of agg	22
Rating 2	11	2	22	**RATE**	**2.50**
Rating 3	11	3	33		

Sample Name:	1-III-C

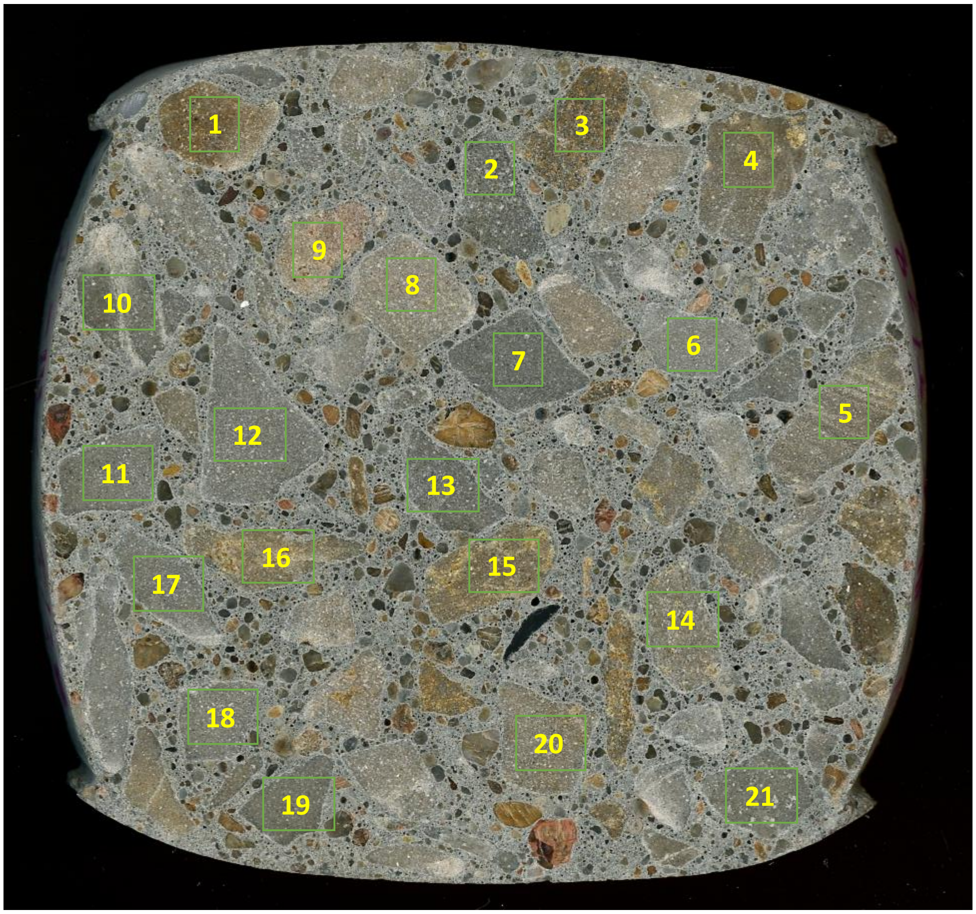

Agg. #	Rating	Agg. #	Rating	Agg. #	Rating
1	2	16	3	31	
2	3	17	3	32	
3	3	18	3	33	
4	3	19	2	34	
5	3	20	3	35	
6	3	21	2	36	
7	3	22		37	
8	3	23		38	
9	3	24		39	
10	3	25		40	
11	3	26		41	
12	3	27		42	
13	2	28		43	
14	3	29		44	
15	3	30		45	

ANALYSIS

Rating 0	0	0	0	Sum	59
Rating 1	0	1	0	# of agg	21
Rating 2	4	2	8	**RATE**	**2.81**
Rating 3	17	3	51		

Sample Name:	1-IV-C

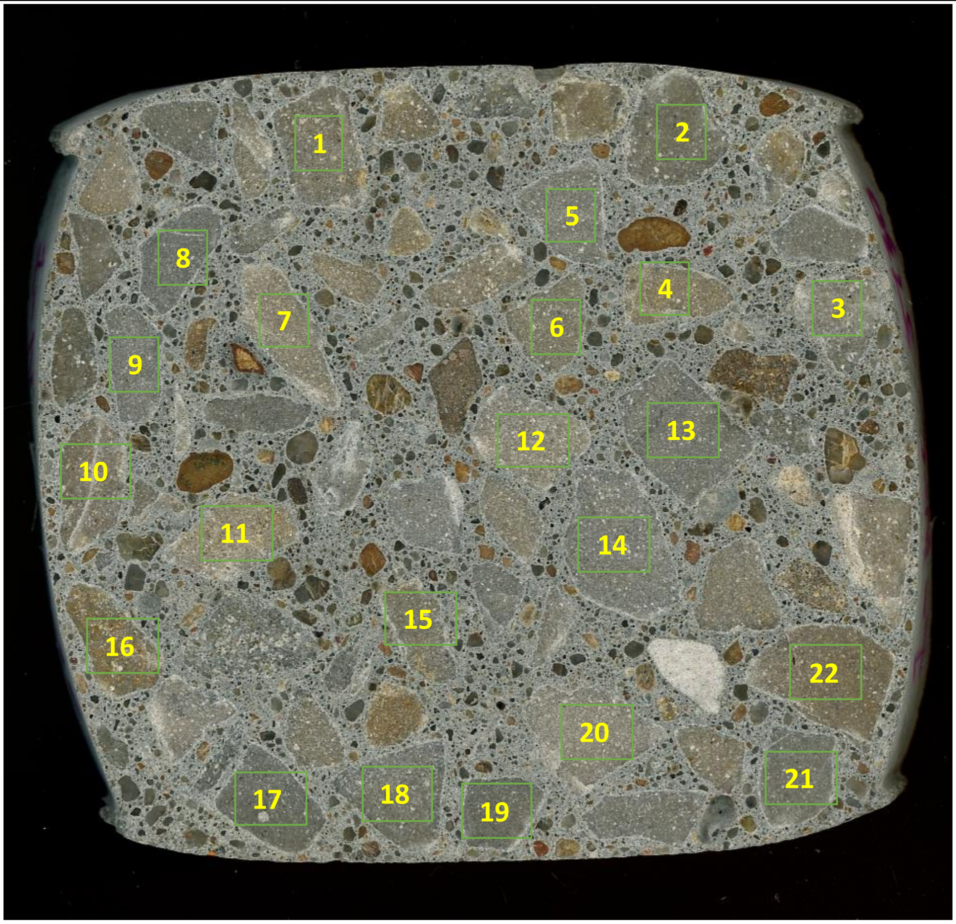

Agg. #	Rating	Agg. #	Rating	Agg. #	Rating
1	3	16	2	31	
2	2	17	2	32	
3	2	18	2	33	
4	2	19	2	34	
5	2	20	3	35	
6	2	21	2	36	
7	2	22	2	37	
8	2	23		38	
9	2	24		39	
10	2	25		40	
11	2	26		41	
12	3	27		42	
13	2	28		43	
14	2	29		44	
15	3	30		45	

ANALYSIS

Rating 0	0	0	0	Sum	48
Rating 1	0	1	0	# of agg	22
Rating 2	18	2	36	**RATE**	**2.18**
Rating 3	4	3	12		

Sample Name:	1-V-C

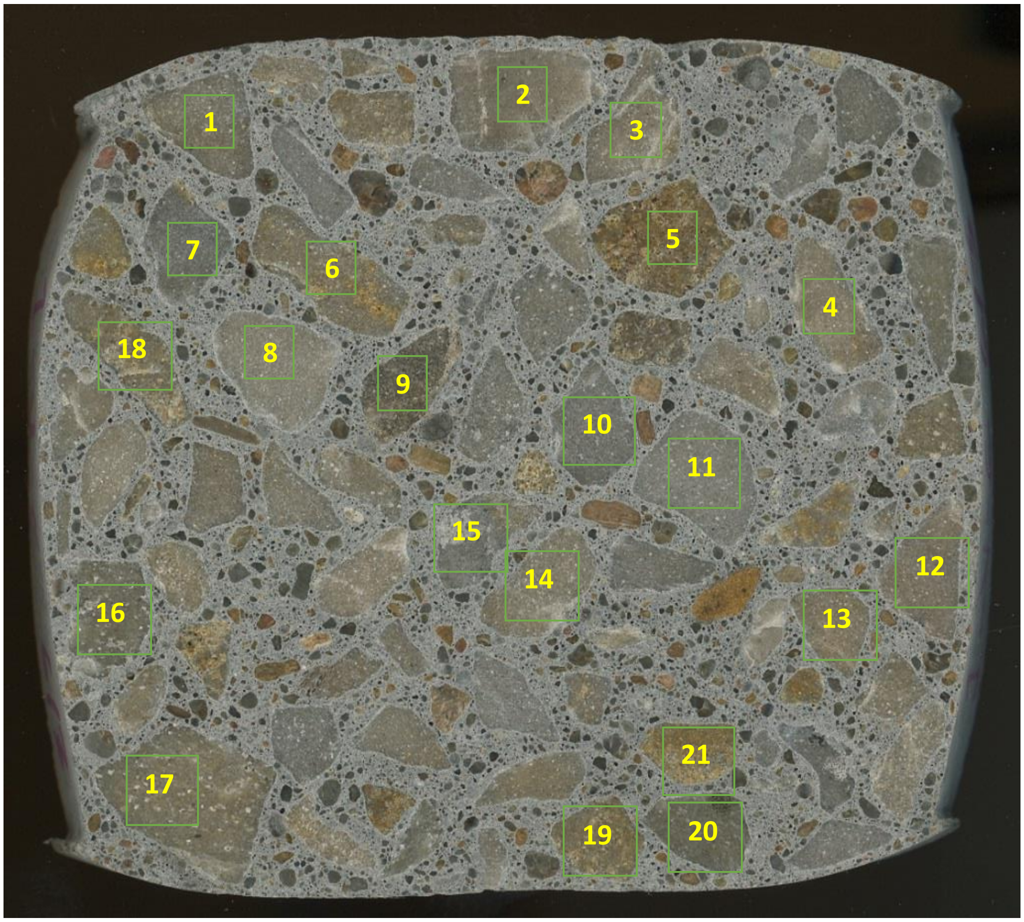

Agg. #	Rating	Agg. #	Rating	Agg. #	Rating
1	3	16	3	31	
2	3	17	3	32	
3	3	18	3	33	
4	3	19	3	34	
5	2	20	3	35	
6	3	21	2	36	
7	3	22		37	
8	3	23		38	
9	2	24		39	
10	2	25		40	
11	3	26		41	
12	3	27		42	
13	2	28		43	
14	2	29		44	
15	2	30		45	

ANALYSIS

Rating 0	0	0	0	Sum	56
Rating 1	0	1	0	# of agg	21
Rating 2	7	2	14	**RATE**	**2.67**
Rating 3	14	3	42		

Sample Name:	2-I-C

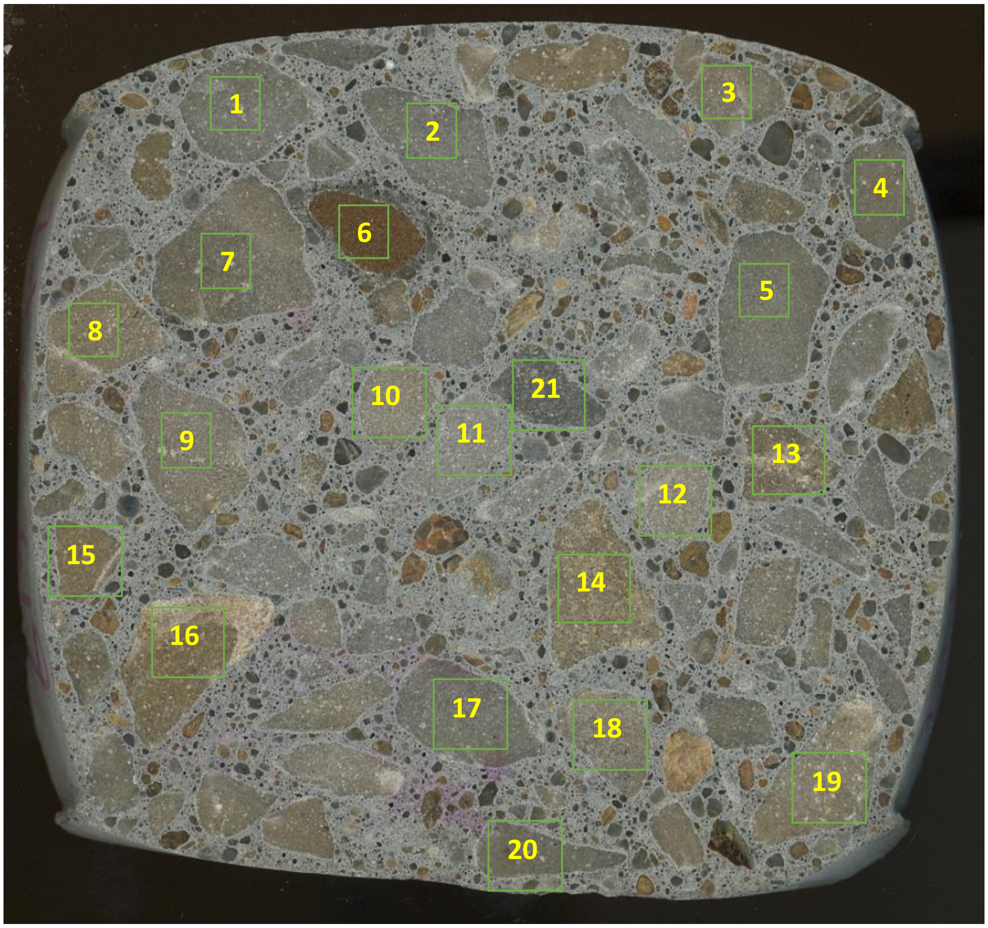

Agg. #	Rating	Agg. #	Rating	Agg. #	Rating
1	3	16	3	31	
2	3	17	2	32	
3	2	18	2	33	
4	2	19	3	34	
5	2	20	3	35	
6	3	21	2	36	
7	3	22		37	
8	2	23		38	
9	2	24		39	
10	2	25		40	
11	2	26		41	
12	3	27		42	
13	2	28		43	
14	2	29		44	
15	2	30		45	

ANALYSIS

Rating 0	0	0	0	Sum	50
Rating 1	0	1	0	# of agg	21
Rating 2	13	2	26	**RATE**	**2.38**
Rating 3	8	3	24		

Sample Name:	2-II-C

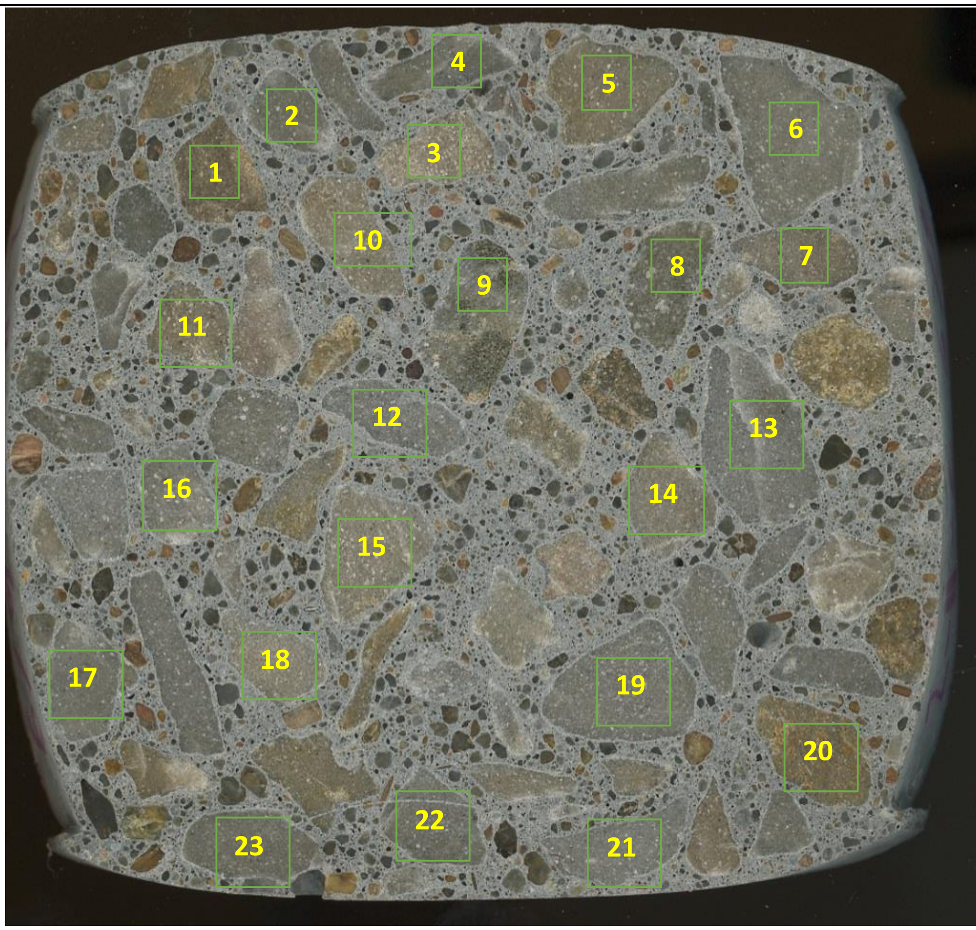

Agg. #	Rating	Agg. #	Rating	Agg. #	Rating
1	2	16	3	31	
2	2	17	3	32	
3	2	18	2	33	
4	2	19	2	34	
5	3	20	3	35	
6	2	21	3	36	
7	3	22	2	37	
8	3	23	3	38	
9	2	24		39	
10	2	25		40	
11	3	26		41	
12	2	27		42	
13	3	28		43	
14	3	29		44	
15	2	30		45	

ANALYSIS

Rating 0	0	0	0	Sum	57
Rating 1	0	1	0	# of agg	23
Rating 2	12	2	24	**RATE**	**2.48**
Rating 3	11	3	33		

Sample Name:	2-III-C

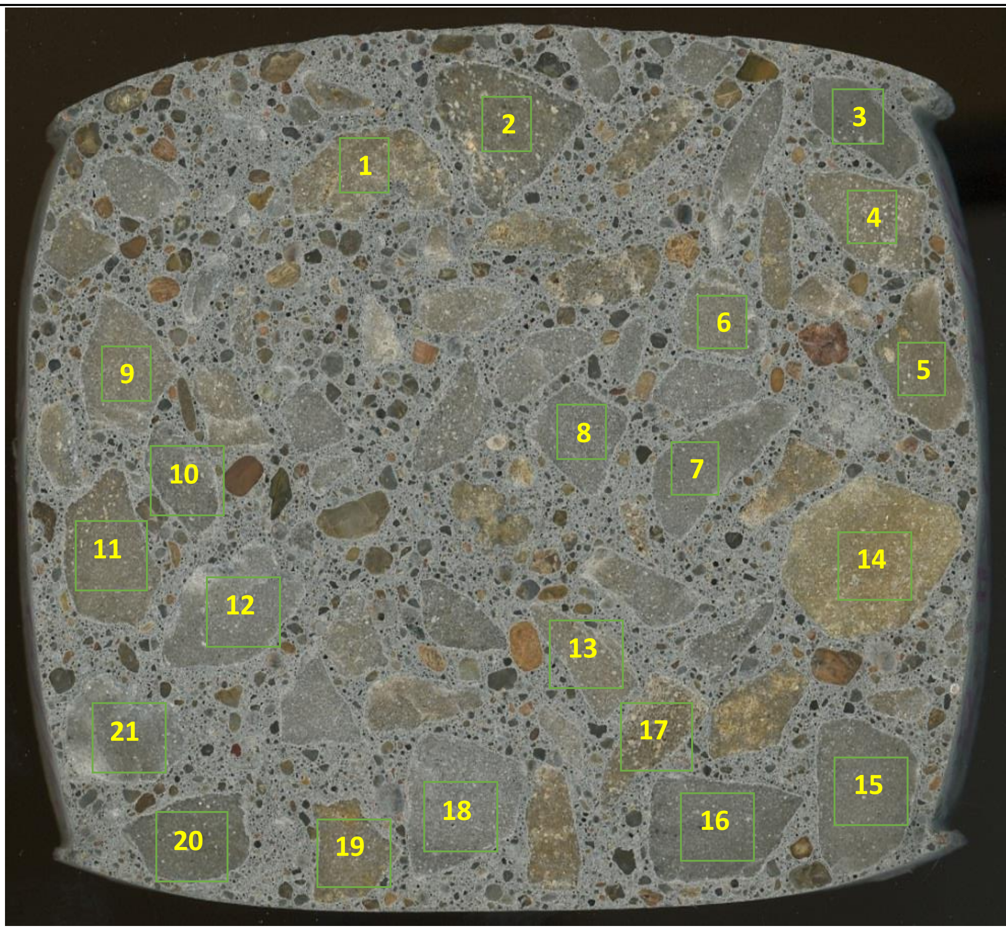

Agg. #	Rating	Agg. #	Rating	Agg. #	Rating
1	3	16	3	31	
2	3	17	2	32	
3	3	18	3	33	
4	3	19	3	34	
5	3	20	2	35	
6	3	21	3	36	
7	3	22		37	
8	3	23		38	
9	3	24		39	
10	2	25		40	
11	3	26		41	
12	3	27		42	
13	3	28		43	
14	3	29		44	
15	3	30		45	

ANALYSIS

Rating 0	0	0	0	Sum	60
Rating 1	0	1	0	# of agg	21
Rating 2	3	2	6	**RATE**	**2.86**
Rating 3	18	3	54		

Sample Name:	2-IV-C

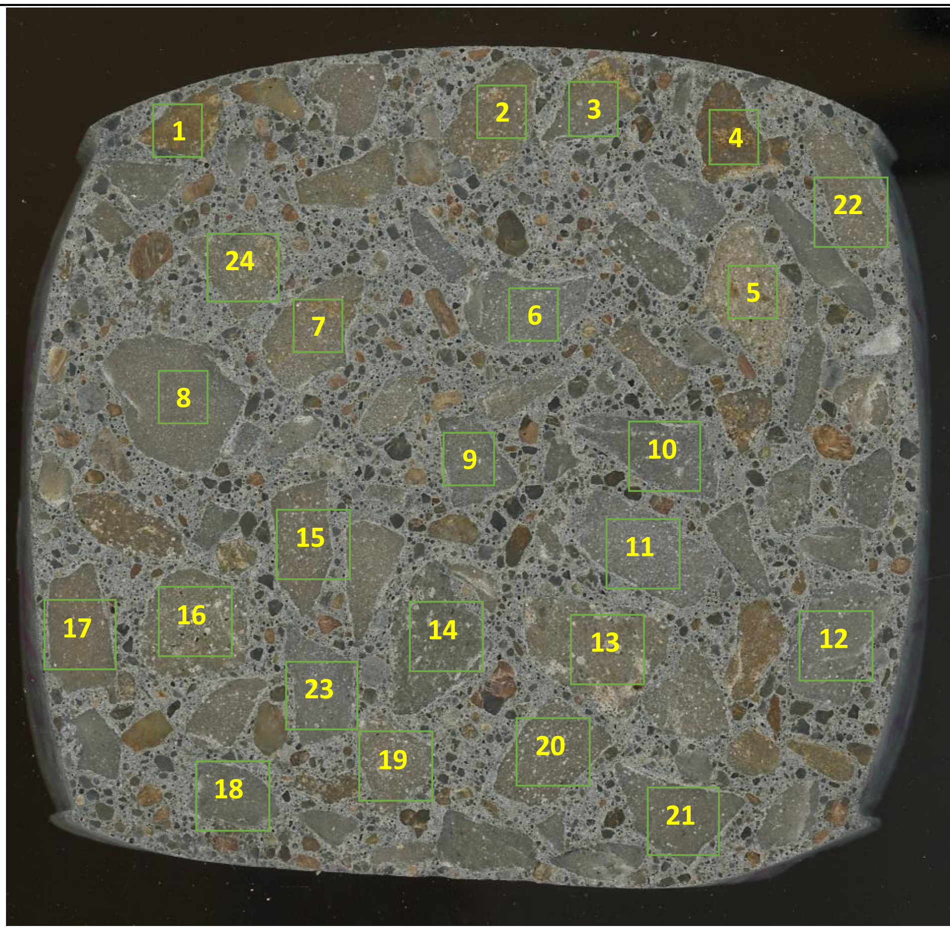

Agg. #	Rating
1	3
2	3
3	3
4	3
5	2
6	3
7	3
8	3
9	2
10	3
11	3
12	3
13	2
14	2
15	2

Agg. #	Rating
16	2
17	2
18	3
19	3
20	2
21	3
22	3
23	2
24	3
25	
26	
27	
28	
29	
30	

Agg. #	Rating
31	
32	
33	
34	
35	
36	
37	
38	
39	
40	
41	
42	
43	
44	
45	

ANALYSIS

Rating 0	0	0	0	Sum	63
Rating 1	0	1	0	# of agg	24
Rating 2	9	2	18	**RATE**	**2.63**
Rating 3	15	3	45		

Sample Name:	2-V-C

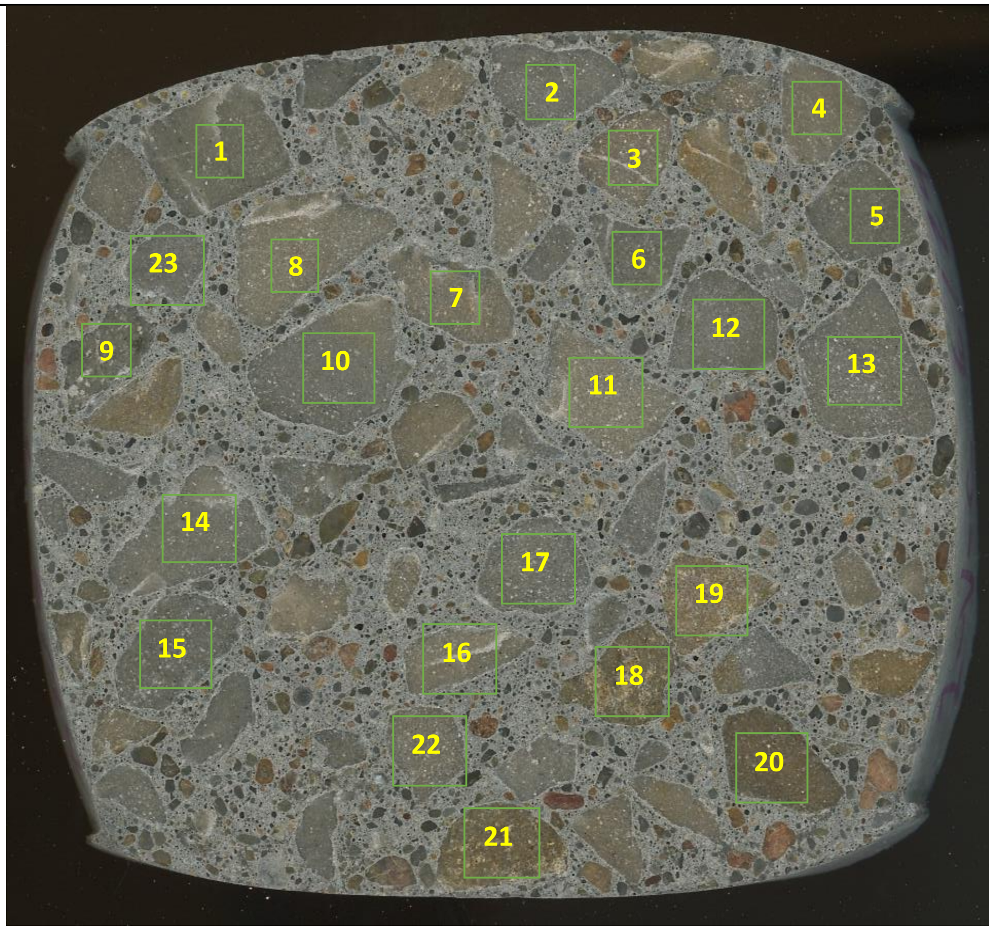

Agg. #	Rating	Agg. #	Rating	Agg. #	Rating
1	3	16	3	31	
2	3	17	3	32	
3	3	18	3	33	
4	3	19	2	34	
5	3	20	3	35	
6	3	21	3	36	
7	3	22	3	37	
8	3	23	3	38	
9	3	24		39	
10	3	25		40	
11	3	26		41	
12	2	27		42	
13	2	28		43	
14	3	29		44	
15	3	30		45	

ANALYSIS

Rating 0	0	0	0	Sum	66
Rating 1	0	1	0	# of agg	23
Rating 2	3	2	6	**RATE**	**2.87**
Rating 3	20	3	60		

Sample Name:	3-I-C

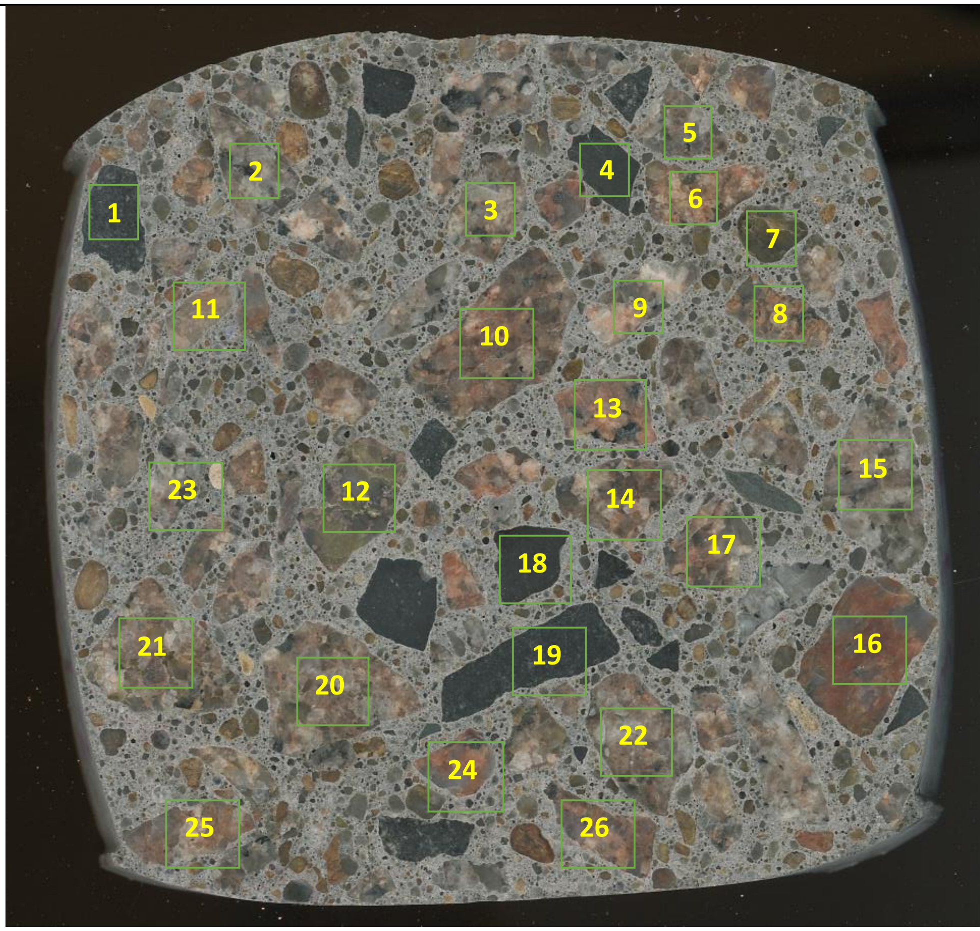

Agg. #	Rating	Agg. #	Rating	Agg. #	Rating
1	2	16	2	31	
2	2	17	2	32	
3	2	18	2	33	
4	2	19	2	34	
5	3	20	2	35	
6	2	21	2	36	
7	2	22	3	37	
8	2	23	2	38	
9	2	24	3	39	
10	2	25	2	40	
11	2	26	3	41	
12	2	27		42	
13	3	28		43	
14	2	29		44	
15	3	30		45	

ANALYSIS

Rating 0	0	0	0	Sum	58
Rating 1	0	1	0	# of agg	26
Rating 2	20	2	40	**RATE**	**2.23**
Rating 3	6	3	18		

Sample Name:	3-II-C

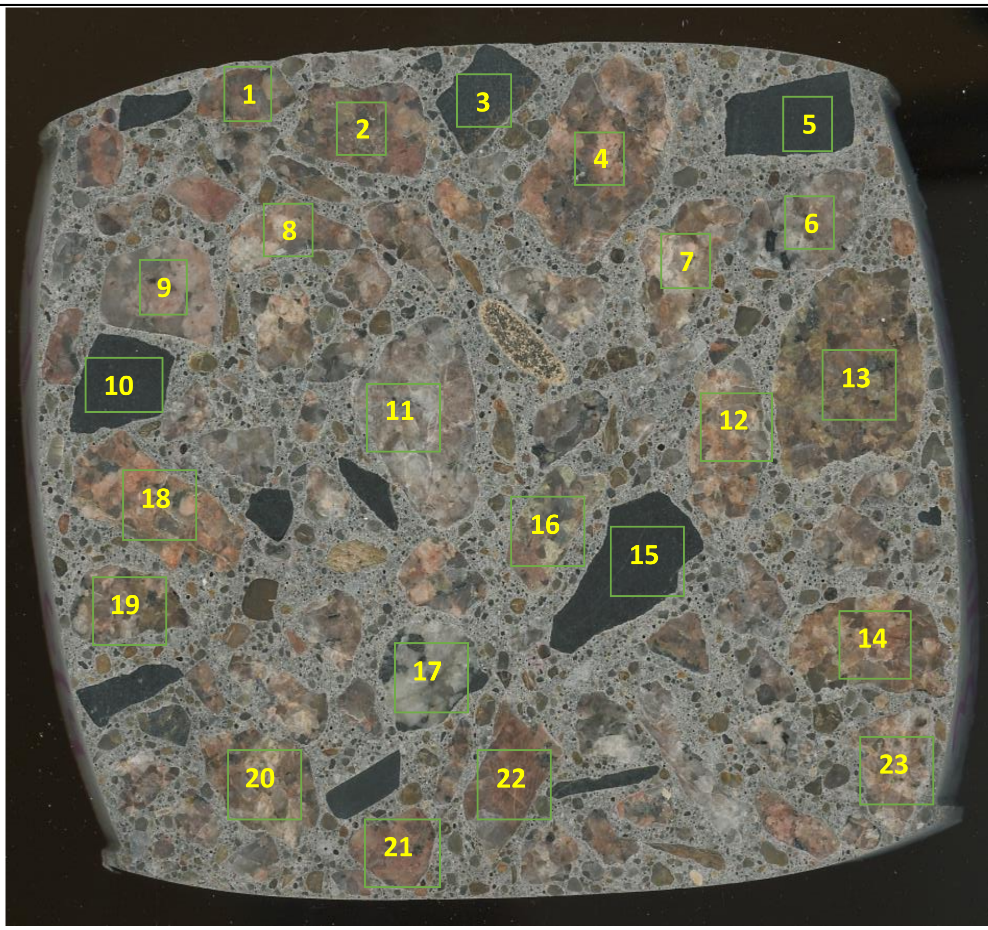

Agg. #	Rating	Agg. #	Rating	Agg. #	Rating
1	3	16	3	31	
2	3	17	3	32	
3	3	18	3	33	
4	3	19	3	34	
5	3	20	3	35	
6	3	21	3	36	
7	3	22	3	37	
8	3	23	3	38	
9	3	24		39	
10	3	25		40	
11	3	26		41	
12	3	27		42	
13	3	28		43	
14	2	29		44	
15	3	30		45	

ANALYSIS

Rating 0	0	0	0	Sum	68
Rating 1	0	1	0	# of agg	23
Rating 2	1	2	2	**RATE**	**2.96**
Rating 3	22	3	66		

Sample Name:	3-III-C

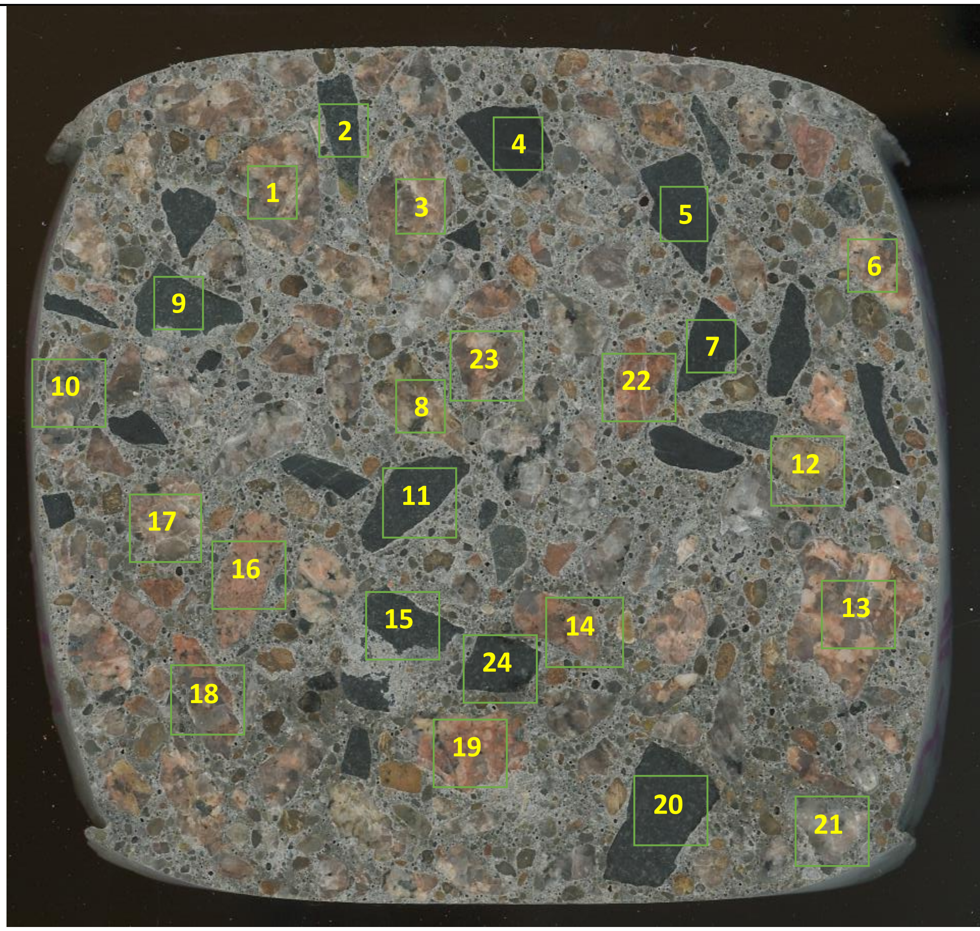

Agg. #	Rating	Agg. #	Rating	Agg. #	Rating
1	3	16	3	31	
2	2	17	2	32	
3	3	18	3	33	
4	2	19	3	34	
5	2	20	2	35	
6	2	21	2	36	
7	2	22	2	37	
8	2	23	2	38	
9	3	24	2	39	
10	3	25		40	
11	2	26		41	
12	2	27		42	
13	2	28		43	
14	3	29		44	
15	3	30		45	

ANALYSIS

Rating 0	0	0	0	Sum	57
Rating 1	0	1	0	# of agg	24
Rating 2	15	2	30	**RATE**	**2.38**
Rating 3	9	3	27		

Sample Name:	3-IV-C

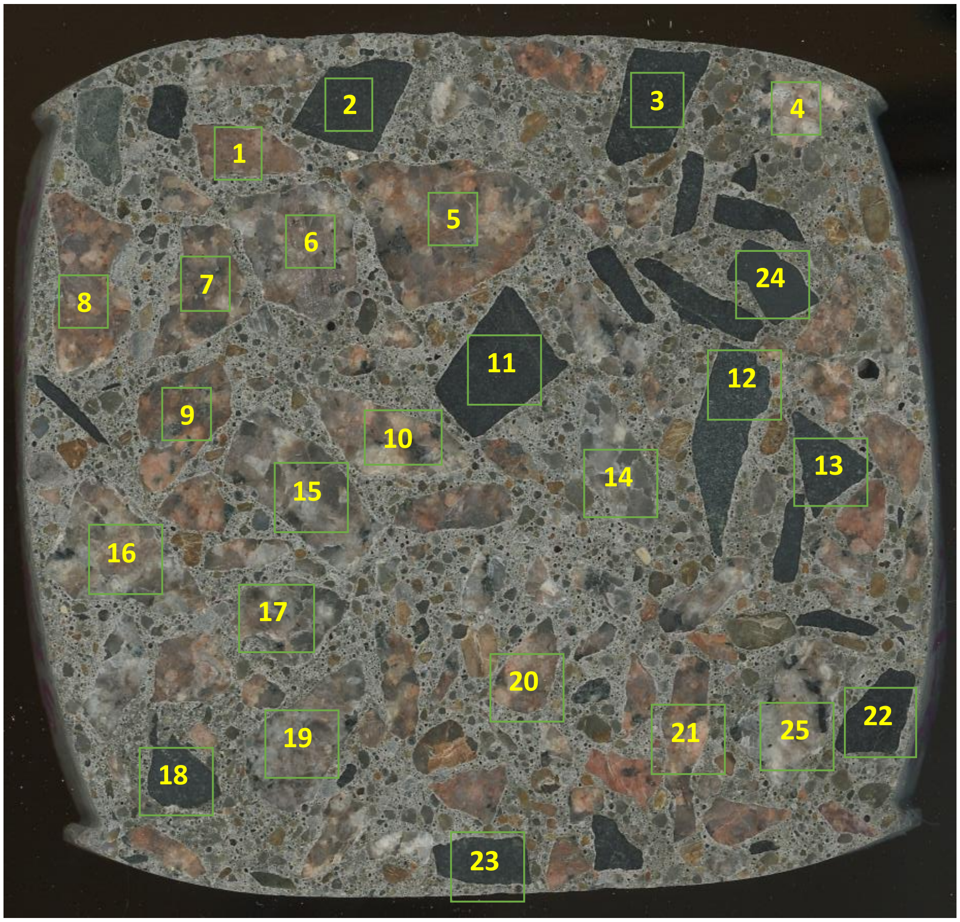

Agg. #	Rating	Agg. #	Rating	Agg. #	Rating
1	2	16	2	31	
2	2	17	3	32	
3	2	18	2	33	
4	3	19	3	34	
5	2	20	2	35	
6	2	21	2	36	
7	2	22	2	37	
8	3	23	2	38	
9	2	24	2	39	
10	3	25	2	40	
11	2	26		41	
12	2	27		42	
13	2	28		43	
14	3	29		44	
15	2	30		45	

ANALYSIS

Rating 0	0	0	0	Sum	56
Rating 1	0	1	0	# of agg	25
Rating 2	19	2	38	**RATE**	**2.24**
Rating 3	6	3	18		

Sample Name:	3-V-C

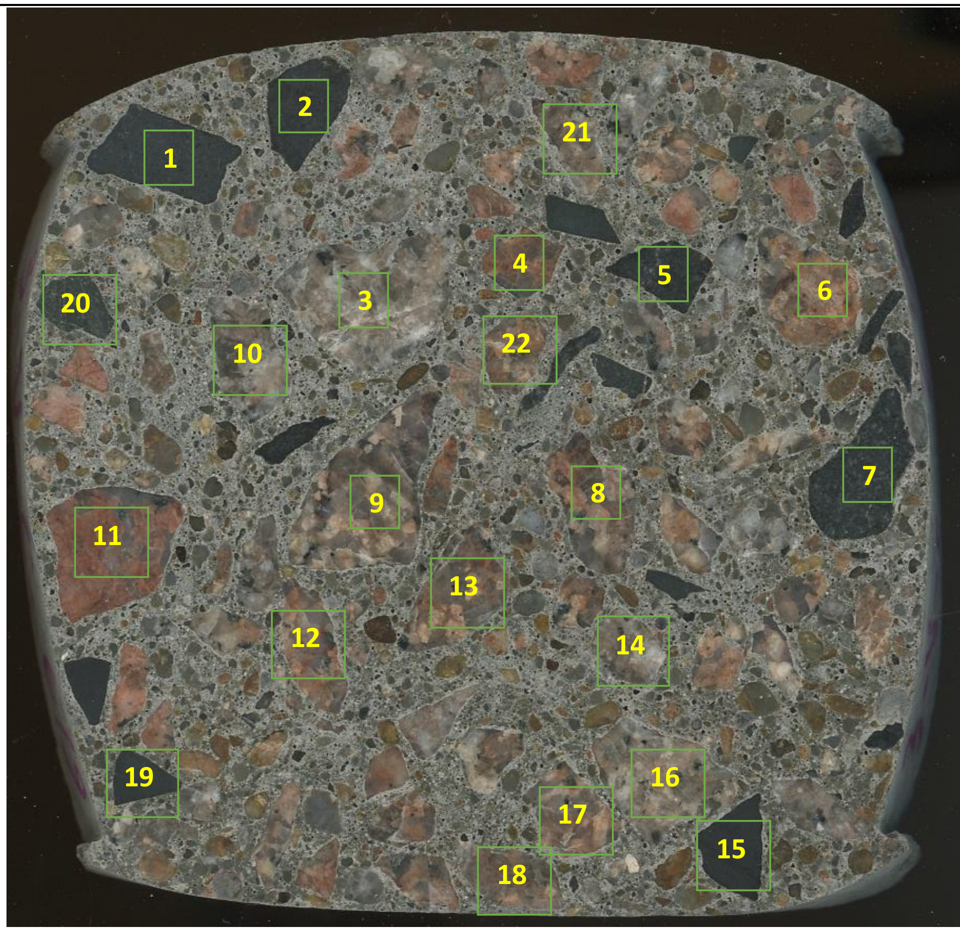

Agg. #	Rating	Agg. #	Rating	Agg. #	Rating
1	3	16	3	31	
2	3	17	2	32	
3	3	18	2	33	
4	3	19	2	34	
5	3	20	2	35	
6	3	21	3	36	
7	2	22	3	37	
8	2	23		38	
9	3	24		39	
10	3	25		40	
11	2	26		41	
12	2	27		42	
13	3	28		43	
14	2	29		44	
15	2	30		45	

ANALYSIS

Rating 0	0	0	0	Sum	56
Rating 1	0	1	0	# of agg	22
Rating 2	10	2	20	**RATE**	**2.55**
Rating 3	12	3	36		

Appendix C - Hardened Air Void Analysis Procedure

This appendix describes the procedure of air void analysis of hardened concrete that was implemented in this study. Sample polishing is always required prior to hardened void analysis itself, however this is not presented in this appendix as there are many guidelines available in the literature discussing this topic.

Part A: Material and Equipment Needed

- Flatbed scanner allowing scanning in color (sometimes referred to as the “photo mode”) and in high resolution (minimum of 4800 dpi is recommended)
- The newest version of the scanning software
- Solution of Phenolphthalein (1.0% in 95% Alcohol, Macron Fine Chemicals) in distilled water (1:1)
- Plastic bottle with sprayer (for phenolphthalein application)
- Orange chalk powder (Irwin Strait-Line Marking Chalk)
- Rubber stopper
- Thin microscope slides (1 mm thickens)
- Steel razorblade
- Scanner glass cleaning cloth
- Paper towels
- Adobe Photoshop (or equivalent image processing software)
- K-State Air Void Analyzer software

Part B: Image Scanning

1. All software image enhancement should be disabled. However, functions automatically adjusting scanning exposure can be used. The scanning resolution should be at least 4800 dpi, the minimum recommended color mode is 24-bit. TIFF image format (with no compression) should be used to save images.

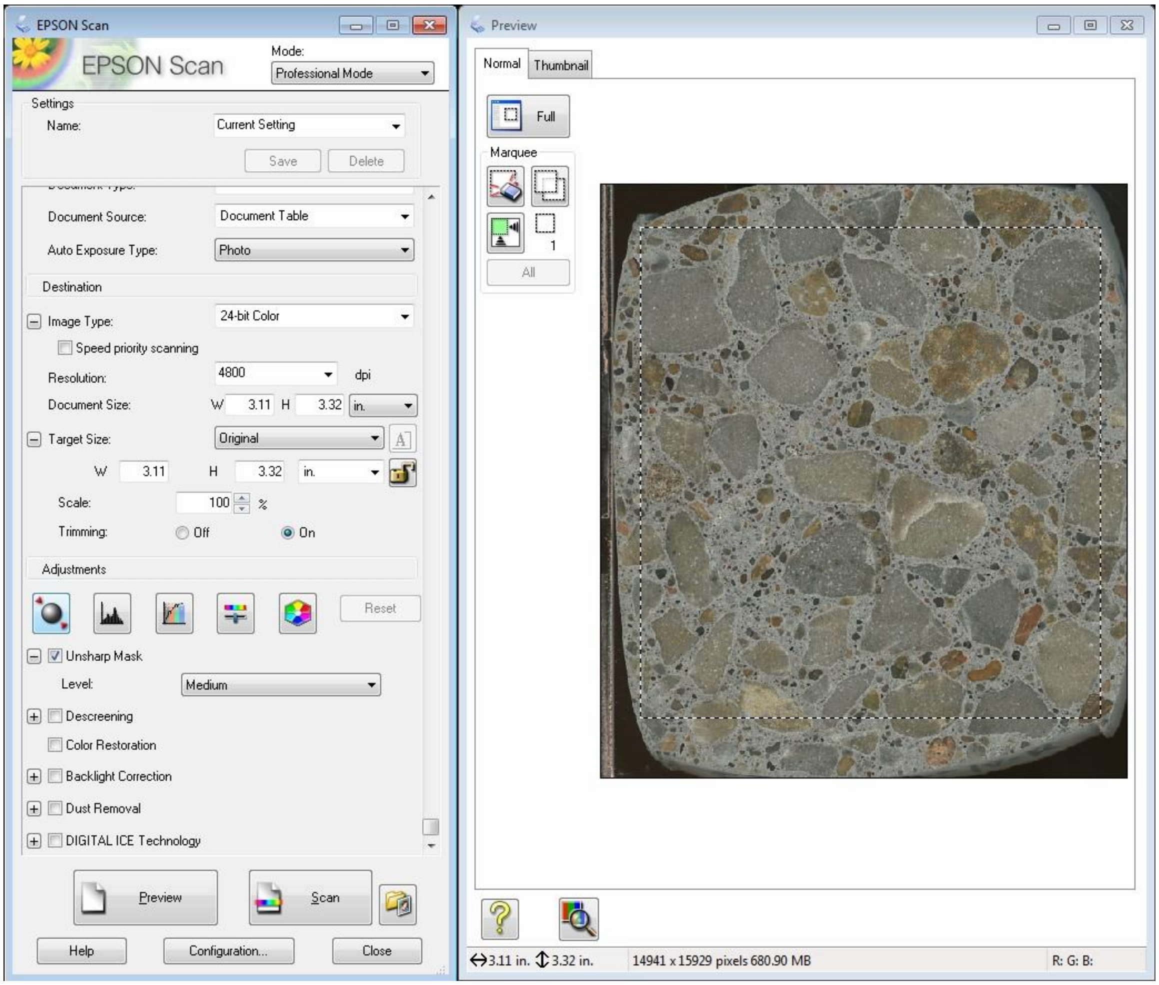

2. In order to make the future image alignment easier, an effort should be made to place the sample always on the same place on the scanning table. The scanning area selection should not be changed.

3. Not scanner glass protection against scratching is required as long as samples are placed on the scanning table with the upmost care. The scanning table should be cleaned often as the finer dust particles as well as the chalk powder could scratch the glass.

4. Sample shall be scanned twice:
   (1) First, a dried polished sample should be scanned.
   (2) Sample sprayed with a phenolphthalein solution and with pores filled with an orange powder should be scanned. Spray the sample with a phenolphthalein solution. Only a thin layer of solution shall be applied to eliminate excessive amounts of fluid coloring aggregate particles. The sample should be dried using a hairdryer. Finally, fill all air voids with the orange powder. The powder should be uniformly distributed over the sample surface using a microscope slide and then pressed into pores by a rubber stopper. This process should be repeated two times to ensure all voids were completely filled. A steel razorblade can be used to remove excess powder from the sample and, if needed, the surface can be dusted with a lightly-oiled fingertip covered by a laboratory glove.

Part C: Image Alignment (using Adobe Photoshop)

1. "Load Files into Stack" function of the Adobe Photoshop should be used.

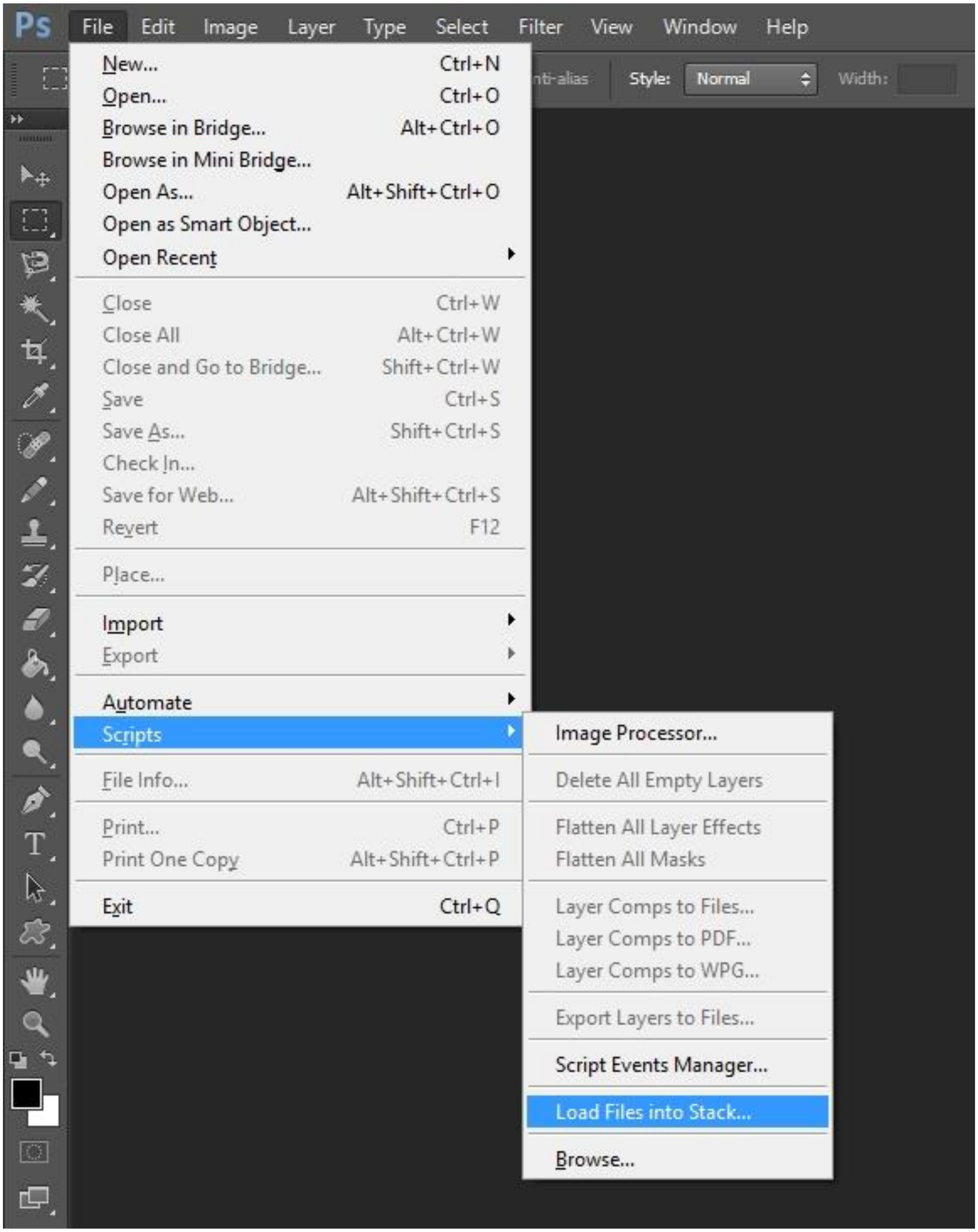

2. In the dialog window of this function, it is important that “Attempt to Automatically Align Source Images” checkbox is checked.

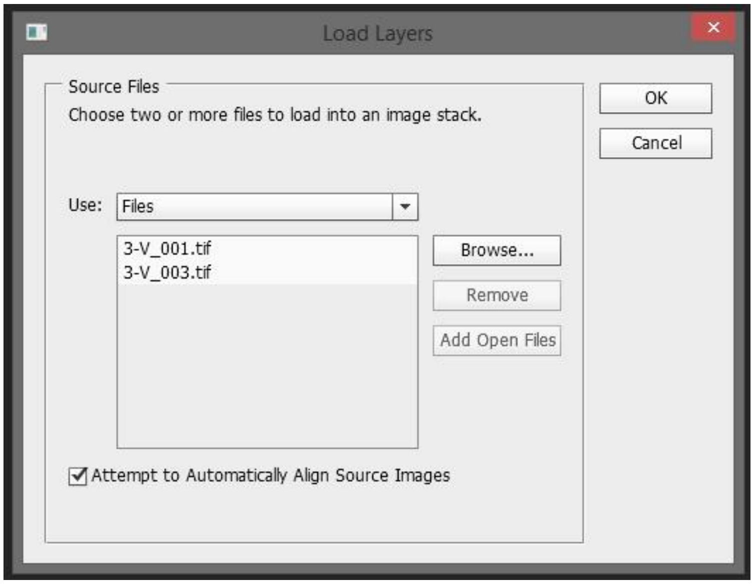

3. Once the aligning process is finished, two layers with aligned images are created. Make a selection containing overlapping areas of both images for every layer and create a new image containing the overlapping (aligned) layers.

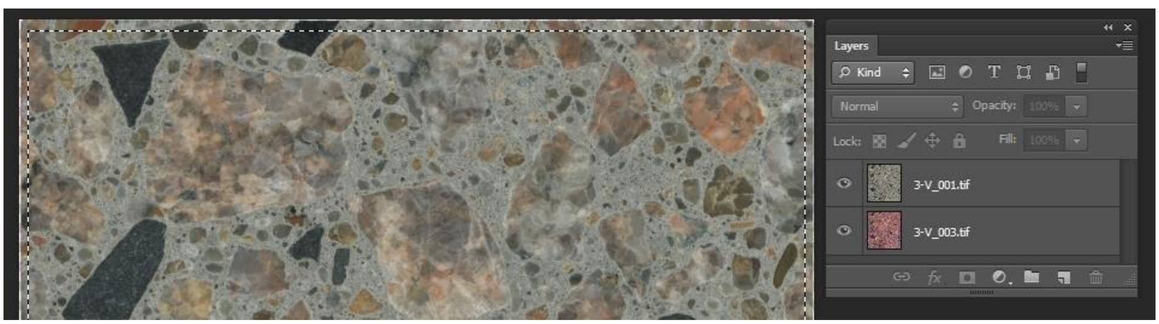

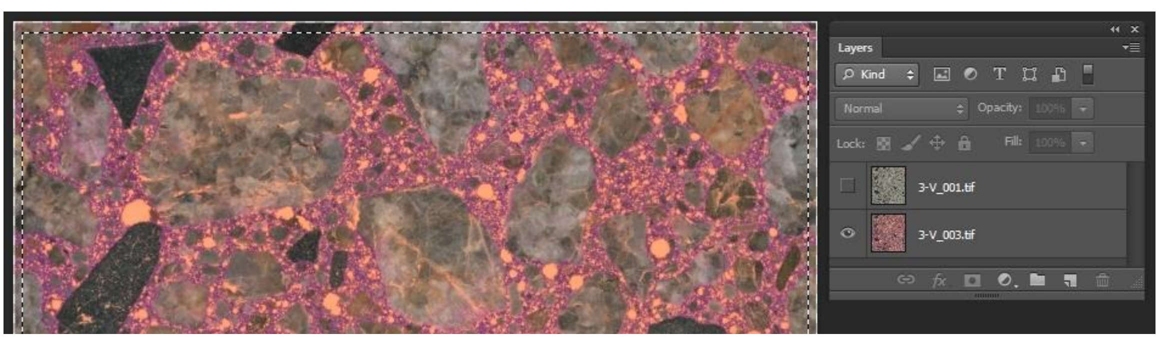

Part D: False Color Image

1. In the newly created image with two aligned layers, choose "Difference" in the blending layer drop box.

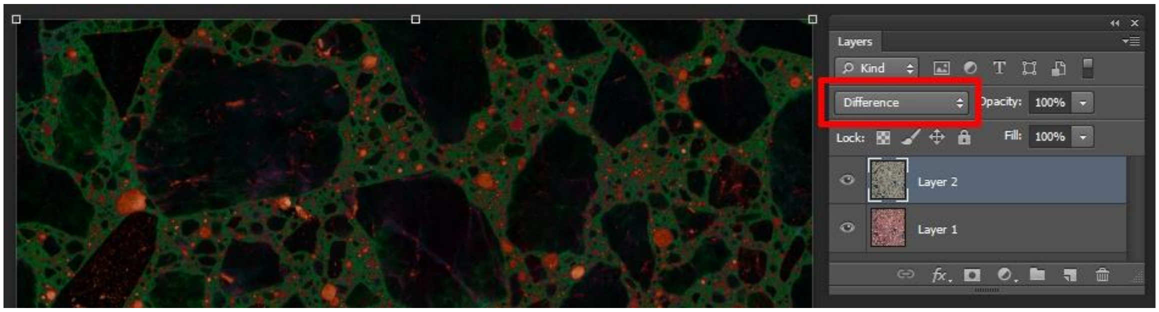

2. Apply the threshold operation on the image (Image → Adjustments → Threshold). The threshold value should be selected so the aggregate particles are detected as accurately as possible. However, it is always better to "underestimate" the aggregate particles as the white spaces in the aggregate will be filled later and the small noise particles will be deleted. If high threshold value is selected, a lot of noise particles is detected and the cleaning procedure will not be successful. Typically a threshold level corresponding to the valley bottom between two peaks in the image histogram is the appropriate value.

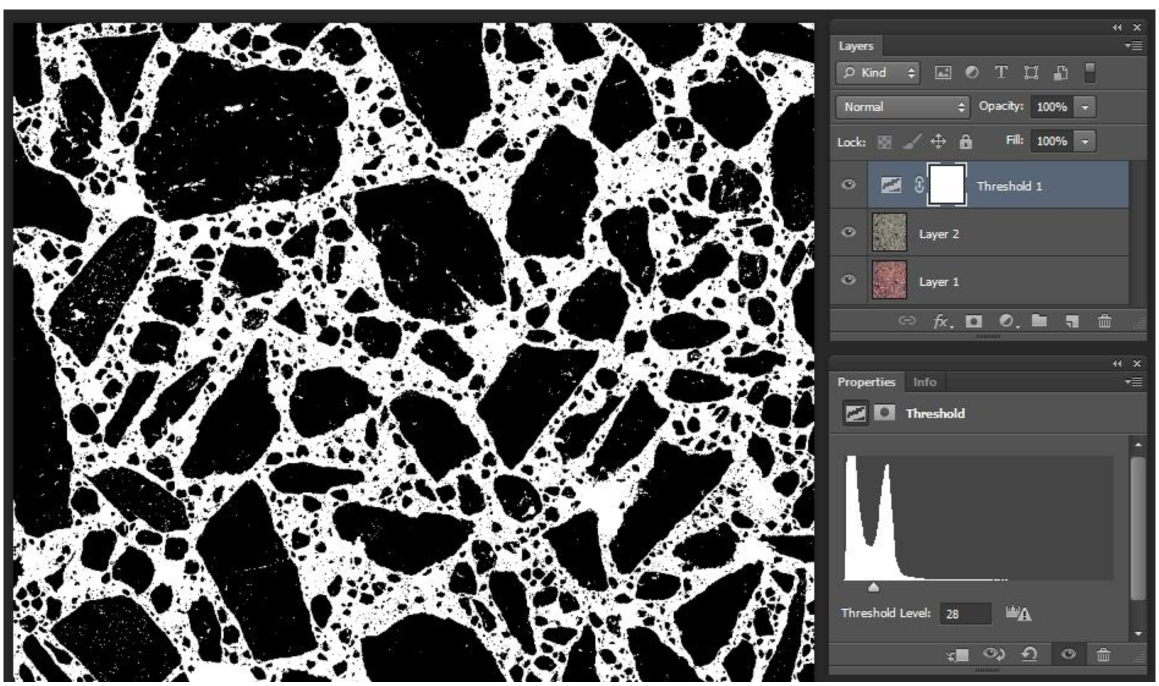

3. Duplicate all layers into a new document and merge them. Change the image mode to "Grayscale" once merged (Image → Mode → Grayscale). Save the image (use the uncompressed TIFF format with discarded layers).

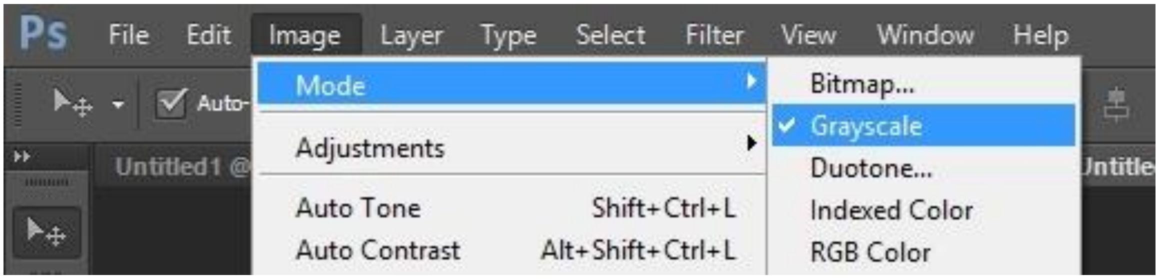

4. Use the "Aggregate Cleaner" module of KSU Void Analyzer to remove the noise particles and fill the air voids inside aggregates. The output image is automatically generated in the program folder (output.tif).

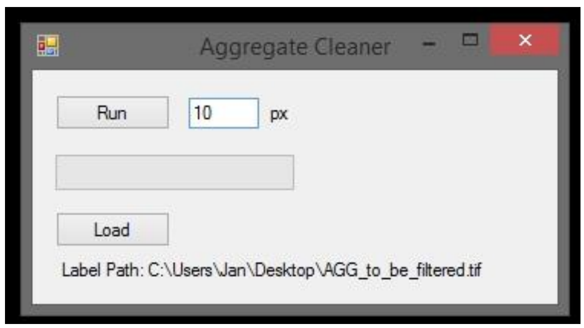

5. Open the output image in Adobe Photoshop and change the color mode again back to grayscale. Subsequently, use the Magic Wand Tool (keyboard shortcut "W") to select all white areas. Once selected, fill these areas with 50% gray color (Edit → Fill).

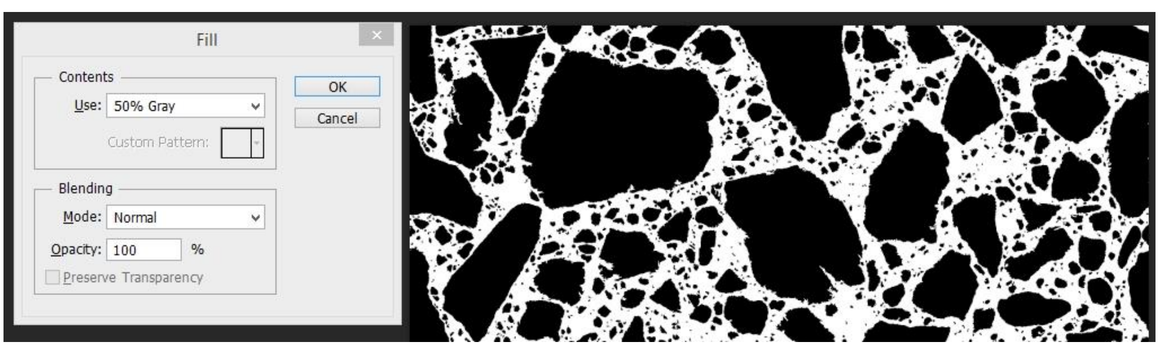

6. Get back to the document from step 2. All layers besides the layer containing the image with powder pressed into the air voids can be removed. Use the “Curves” function to detect air voids (Image → Adjustments → Curves) on the powdered image. The “Input” value depends on the quality of contrast between the paste and air voids and typically ranges from 185 to 225. Visual comparison of detected voids to the original image needs to be made when choosing the value.

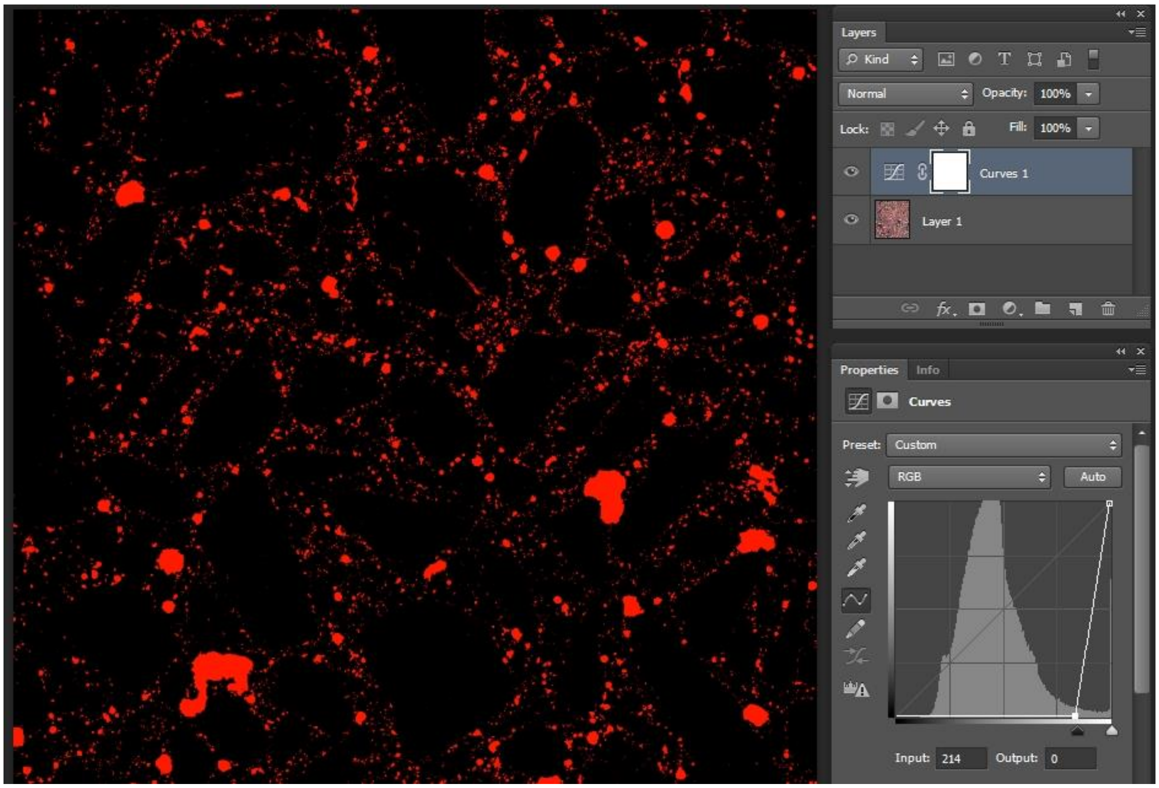

7. Create a new, empty layer and place it on top of all layers. Use the Magic Wand Tool (keyboard shortcut “W”) to color select all black areas (the “curves” layer must be selected).

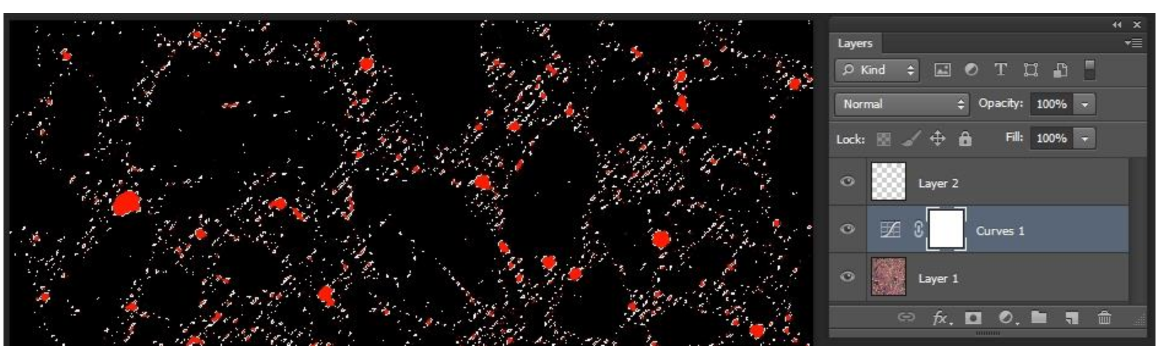

8. Select the new layer, invert the selection (Ctrl + Shift + I) and fill the selection with white color (Ctrl + Shift + F5 or Edit → Fill). Thus, a new layer containing only the air voids is created.

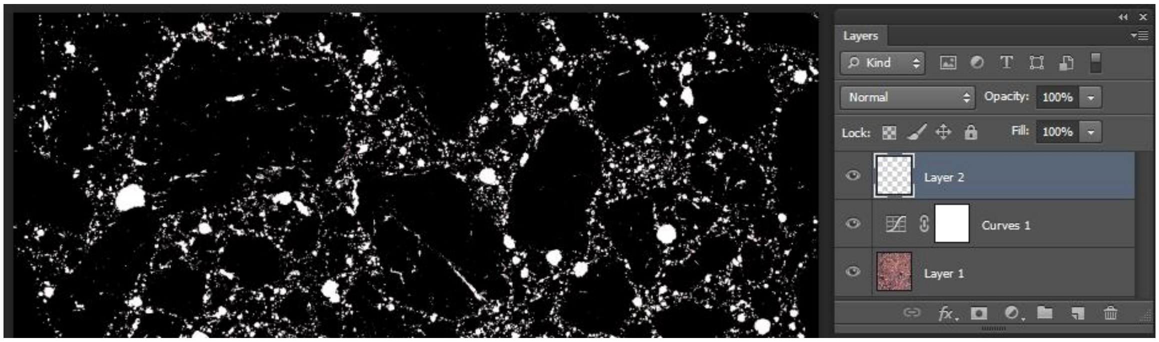

9. Duplicate this layer into the document containing the filtered aggregate image (most probably named output.tif). Select "Hard Mix" in layer blending options drop box. This is the final step as the false color image is generated. Optionally, manual corrections can be performed on this image.

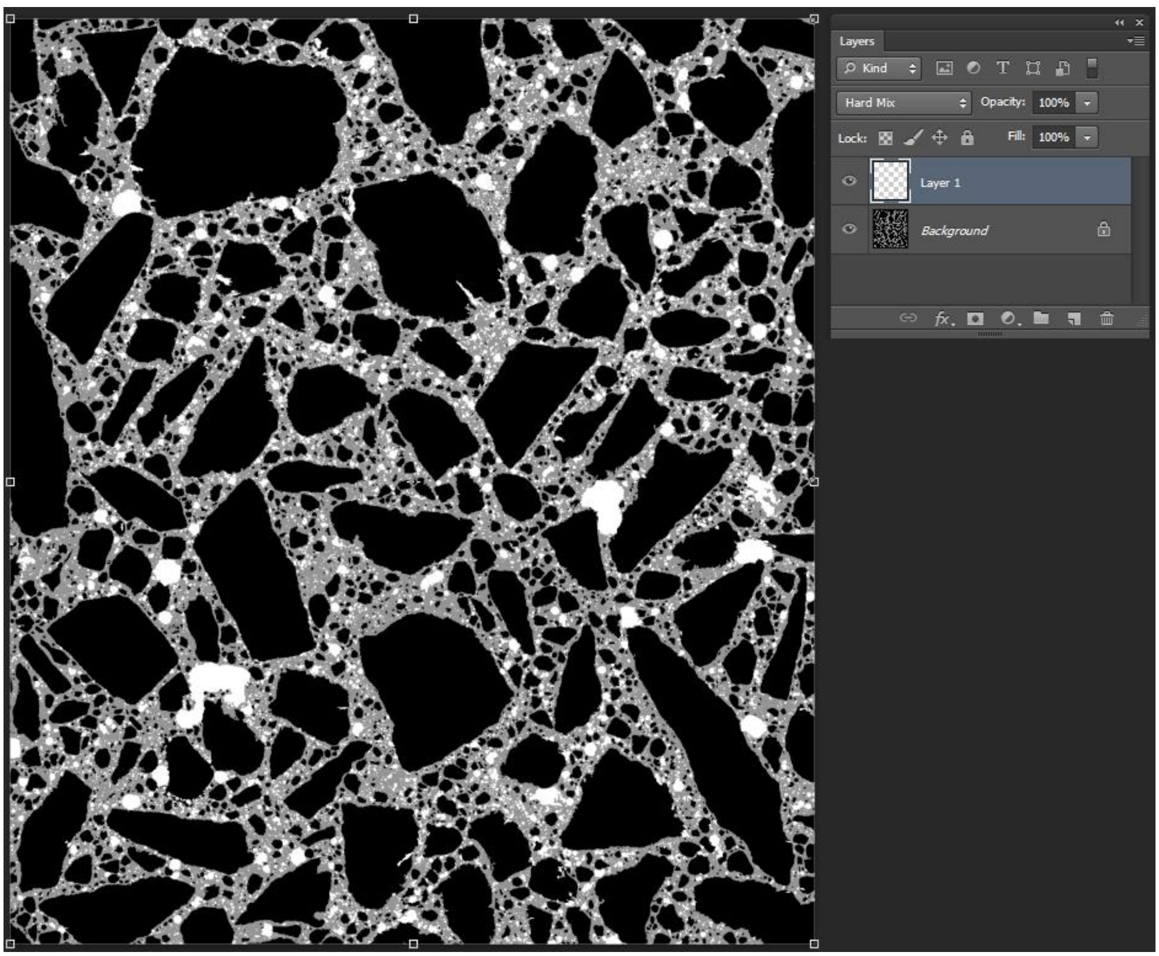

Part E: Analysis

1. K-State Air Void Analyzer is used to perform analysis of the false color image. It can be chosen whether use multiple threads (i.e. multiple processors) or if the image analysis will be performed in the single-thread mode. Using multiple threads is naturally faster, however it requires larger amount of RAM available (typically at least 4 GB for images over 700 MB). Software incorporates EmguCV library (version 2.4.9), which is a .Net wrapper to the OpenCV image processing library. During the analysis, three main tasks are executed:
   (1) Air void detection. EmguCV BlobDetector class is utilized to detect all air voids.
   (2) Aggregate detection. Identical algorithm as in the previous task in used, this time aggregate particles are targeted.
   (3) Linear Traverse Count. The linear traverse count as described in ASTM C457 is implemented. The used algorithm iterates through every pixels and the data described in the Section 11.1.2 of ASTM C457 are recorded (total length of traverse, traverse length through air, and traverse length through paste).

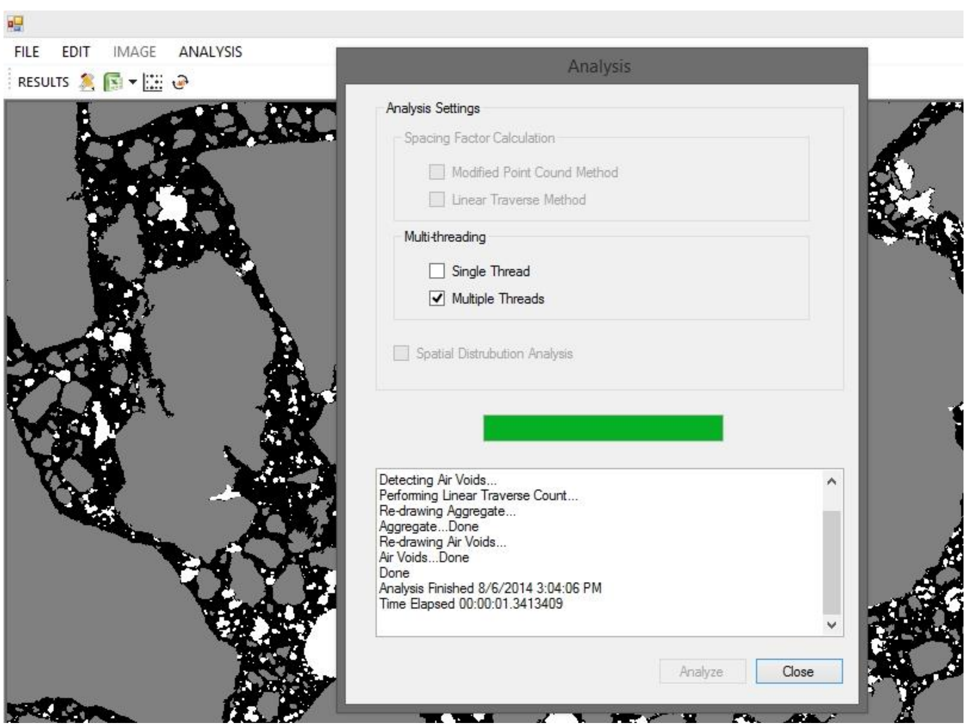

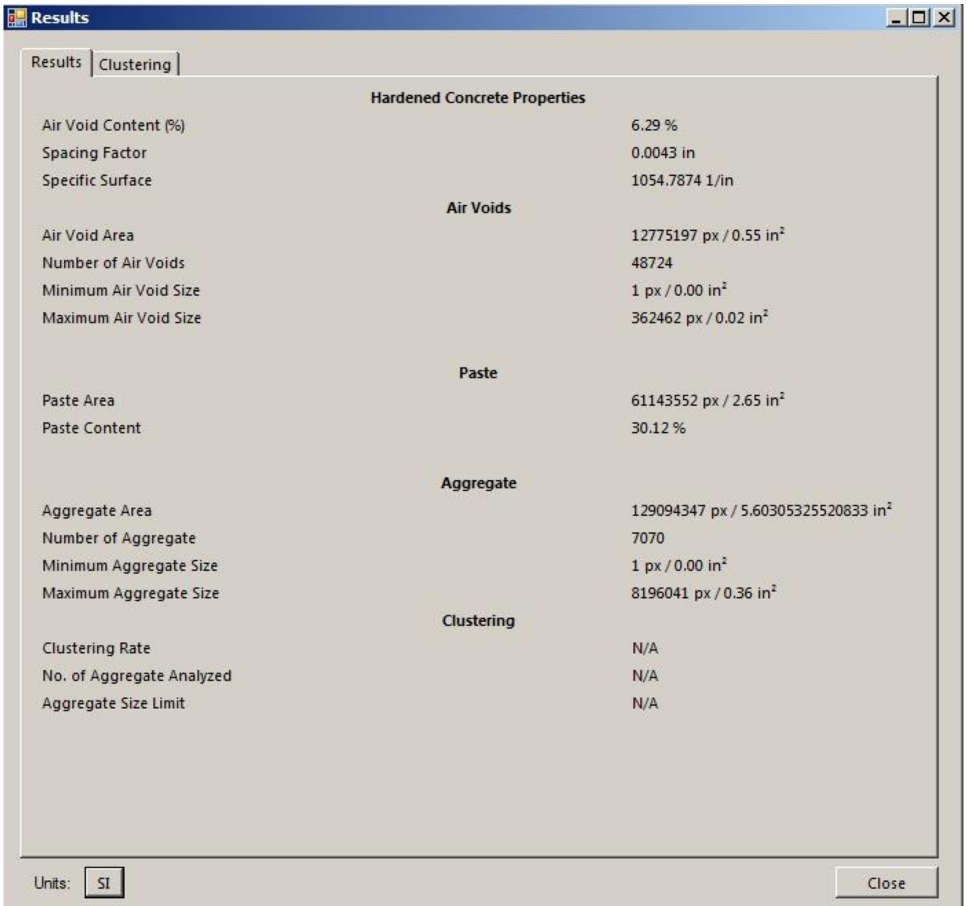

2. If desired, clustering analysis can be performed as well. Since performing clustering analysis on every single aggregate particle would be ineffective and computationally expensive, minimum aggregate size can be specified. Also, the width of the clustering zone can be defined before the analysis is carried out.

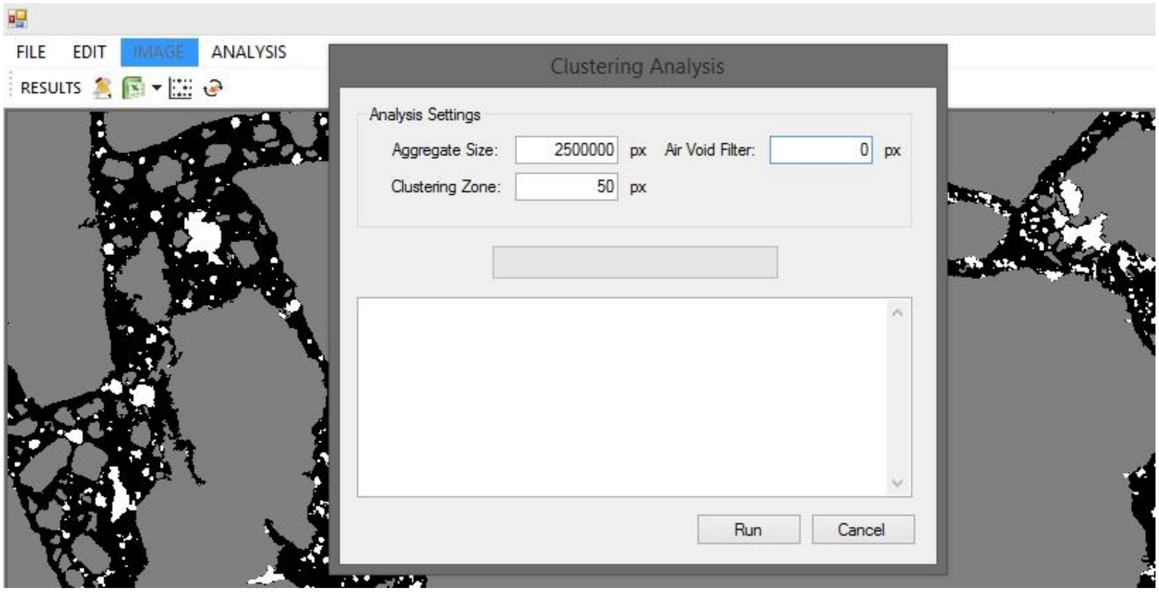
FILE
EDIT
IMAGE
ANALYSIS
RESULTS
Clustering Analysis
Analysis Settings
Aggregate Size: 2500000 px
Air Void Filter: 0 px
Clustering Zone: 50 px
Run
Cancel

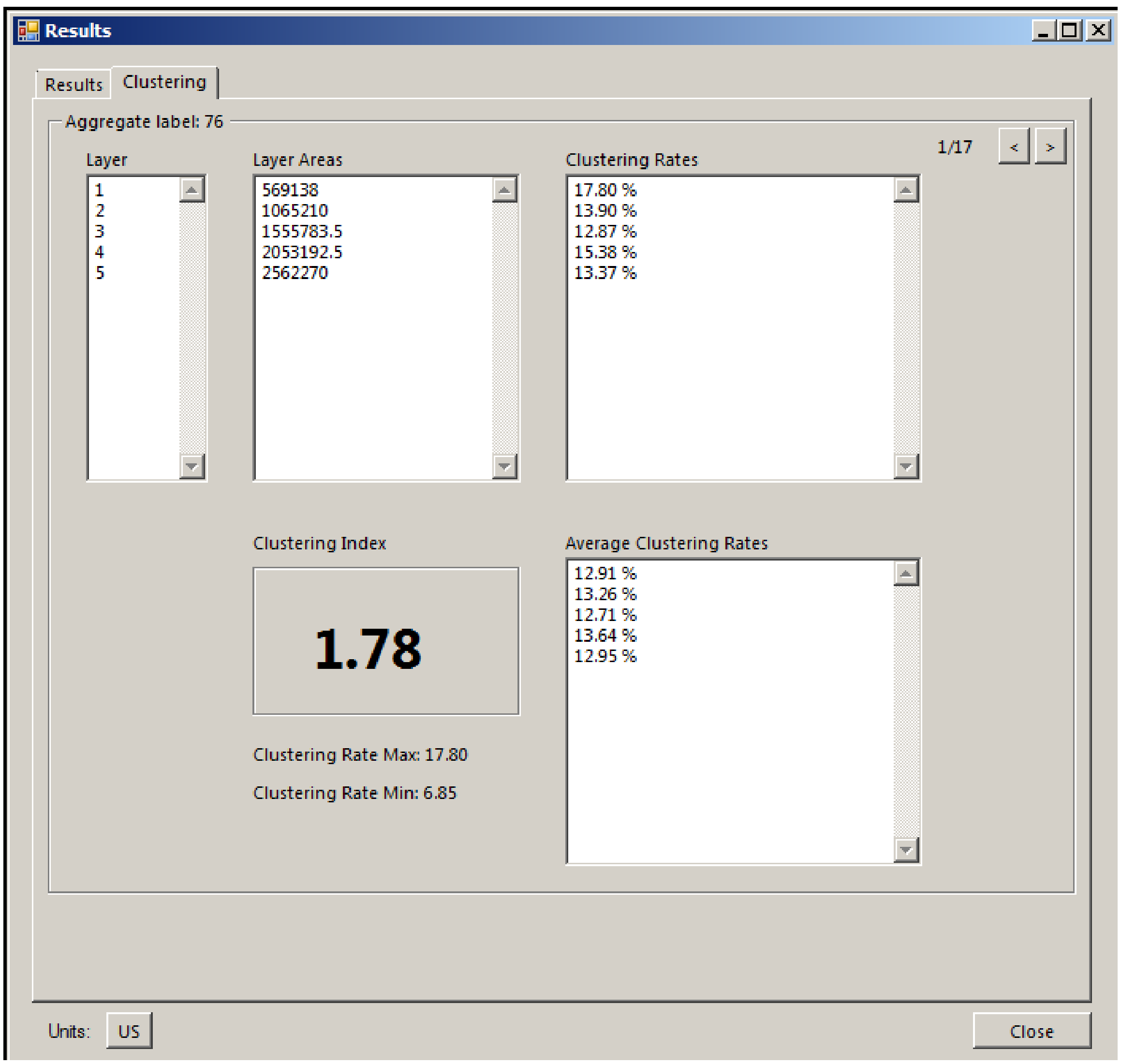
Results
Results
Clustering
Aggregate label: 76
1/17
Layer
1
2
3
4
5
Layer Areas
569138
1065210
1555783.5
2053192.5
2562270
Clustering Rates
17.80 %
13.90 %
12.87 %
15.38 %
13.37 %
Clustering Index
1.78
Clustering Rate Max: 17.80
Clustering Rate Min: 6.85
Average Clustering Rates
12.91 %
13.26 %
12.71 %
13.64 %
12.95 %
Units:
US
Close